



**Università
degli Studi
di Ferrara**

Department of Life Sciences and Biotechnology

**DOCTORAL COURSE IN
BIOMEDICAL SCIENCES AND BIOTECHNOLOGY**

DIRECTOR: Prof. Paolo Pinton

CYCLE XXXI

**Genomic, Vessel Wall Transcriptomic, and
Plasma Proteomic Approaches to Investigate
Multiple Sclerosis**

Scientific/Disciplinary Sector (SDS): BIO/10

Candidate
Ziliotto Nicole

(signature)

Supervisor
Prof. Bernardi Francesco

(signature)

Co-Supervisor
Prof. Marchetti Giovanna

(signature)

Years 2015/2018

TABLE OF CONTENTS

Main abbreviations	I
Abstract	III
1. General introduction	1
1.1 Multiple sclerosis.....	2
1.2 Hemostasis factors in multiple sclerosis	6
1.3 Coagulation and hemostasis findings in multiple sclerosis patients.....	15
2. Aims of the present work.....	29
3. Study populations	33
3.1 Italian study populations.....	34
3.2 US study population	37
4. Coagulation Factor XII Levels and Intrinsic Thrombin Generation in Multiple Sclerosis	41
4.1 Background and rationale	42
4.2 Materials and methods	44
4.3 Results and discussion.....	46
5. Hemostasis Biomarkers in Multiple Sclerosis	54
5.1 Background and rationale	55
5.2 Materials and methods	56
5.3 Results and discussion.....	57
6. Changes in expression profiles of internal jugular vein wall and plasma protein levels in multiple sclerosis	64
6.1 Background and rationale	65
6.2 Materials and methods	66
6.3 Results and discussion.....	67
7. Increased CCL18 plasma levels are associated with neurodegenerative MRI outcomes in multiple sclerosis patients.....	81
7.1 Background and rationale	82
7.2 Materials and methods	83
7.3 Results and discussion.....	84

8. Plasma levels of soluble NCAM in multiple sclerosis	90
8.1 Background and rationale	91
8.2 Materials and methods	92
8.3 Results and discussion	93
9. Are plasma levels of VAP-1 associated both with cerebral microbleeds in multiple sclerosis and intracerebral hemorrhages in stroke?.....	98
9.1 Background and rationale	99
9.2 Materials and methods	100
9.3 Results and discussion	101
10. C6orf10 low-frequency and rare variants in Italian multiple sclerosis patients	104
10.1 Background and rationale	105
10.2 Materials and methods	106
10.3 Results and discussion	115
11. General discussion and conclusions	125
Bibliography	136

MAIN ABBREVIATIONS

ADAMTS13: A disintegrin-like and metalloprotease with thrombospondin type 1 motif 13

aPTT: activated partial thromboplastin time

BMI: body mass index

BK: bradykinin

C1INH: C1 inhibitor

CCL18: C-C motif ligand 18

CCL5: C-C motif ligand 5

CCSVI: chronic cerebrospinal venous insufficiency

CD86: cluster of differentiation 86

CMBs: cerebral microbleeds

CNS: central nervous system

CV: cortical volumes

DCs: dendritic cells

DGM: deep gray matter

DMT: disease-modifying treatment

EAE: experimental autoimmune encephalomyelitis

EBV: Epstein-Barr virus

EDSS: Expanded Disability Status Scale

ELISA: enzyme-linked immunosorbent assay

EPCR: endothelial protein C receptor

ETP: endogenous thrombin potential

F: factor

FXII:Ag : FXII antigen

FXII:c : FXII activity

GA: Glatiramer acetate

GAGs: glycosaminoglycans

GM: gray matter

GWAS: genome-wide association studies

HCII: heparin cofactor II

HI: healthy individual

HLA: human leukocyte antigen

HK: high molecular weight kininogen

HS: Healthy Subjects

ICAM-1: intercellular adhesion molecule-1

ICH: intracerebral hemorrhages
IFN- β : interferon-beta
KAL: kallikrein
LVV: lateral ventricular volume
LV: lesion volume
MAF: minor allele frequency
MRI: magnetic resonance imaging
MS: multiple sclerosis
NAWM: normal appearing white matter
NBV: normalized brain volume
NCAM: neural cell adhesion molecule
PAI-1: plasminogen activator inhibitor 1
PC: protein C
PCI: protein C inhibitor
PCR: polymerase chain reaction
PK: prekallikrein
PP-MS: Primary Progressive Multiple Sclerosis
QSM: magnetic susceptibility mapping
RFU: relative fluorescence units
ROS: reactive oxygen species
RR-MS: Relapsing-Remitting Multiple Sclerosis
SNP: single nucleotide polymorphism
SP-MS: Secondary Progressive Multiple Sclerosis
TF: tissue factor
TFPI: tissue factor pathway inhibitor
TG: thrombin generation
Th17: T helper 17 lymphocyte
TM: thrombomodulin
tPA: tissue-type plasminogen activator
TTP: time to peak
uPA: urokinase-type plasminogen activator
uPAR: urokinase plasminogen activator receptor
VCAM-1: vascular adhesion molecule-1
vWF: von Willebrand Factor
WES: whole exome sequencing
WM: white matter

ABSTRACT

This study was designed to investigate, by several experimental approaches, genes, and proteins associated with multiple sclerosis (MS), an inflammatory and demyelinating disease of the central nervous system (CNS). The study design was aimed to prioritize, by the investigation in patients, potential targets and biomarkers for future mechanistic studies.

Through the genomic approach (chpt.10), selected families were investigated by WES for candidate genes from GWAS. The identified low-frequency variants were further investigated in unrelated MS patients. A number of rare and novel mutations were detected, and particularly null variants in the *C6orf10* 3' region, in combination with both intra and extra locus low-frequency SNPs. These findings provide the bases for expression studies.

The transcriptomic approach (chpt.6) was focused on the internal jugular vein wall, supported by the interaction between vascular and neurodegenerative mechanisms in MS. This original investigation produced a wealth of information on several biological pathways and permitted the combined transcriptome-protein analysis, which provided intriguing biological and clinical hints.

Analysis at protein level was conducted in plasma by multiplex assays in relation to clinical MS phenotypes and brain MRI measures, as quantitative and “intermediate” phenotypes evaluating disease progression. Higher CCL18 plasma levels were associated with more severe neurodegenerative features, a noticeable finding (chpt.7). The contribution of adhesion molecules, suggested by the transcriptomic analysis, was similarly explored (chpt.8 and 9). Correlation between plasma levels of specific adhesion molecules in MS patients highlights the leukocyte adhesion process in disease.

Increased blood-brain-barrier permeability, a key event in the MS pathophysiology, leads to the irruption of coagulation and hemostasis factors into the CNS, potentially causing an inflammatory response and immune activation. We investigated hemostasis components with main open questions in relation to MS.

FXII, the key protease of the coagulation contact activation found deposited in patients' brain, might participate in adaptive immunity during neuroinflammation. In plasma of MS patients (chpt.4), FXII protein levels were higher than activity, causing a decreased activity/antigen ratio. These findings, corroborated by specifically designed intrinsic thrombin generation assays, might support that FXII contribution in MS is not directly correlated with its “intrinsic” pro-coagulant activity.

Negative regulators of hemostasis (TFPI, ADAMTS13, HCII, TM) with anti-inflammatory properties were also studied, which detected specific patterns of correlations (chpt.5 and 11). Positive association of TFPI with TM, observed in MS patients and not in healthy subjects, would imply that endothelium perturbation acts on multiple release mechanisms. In patients, PAI-1, the key fibrinolysis inhibitor, was positively associated with FXII, and negatively associated with HCII, which suggest disease mechanisms influencing their expression in different tissues with implications in fibrin generation/impaired fibrinolysis, important contributors to neuro-inflammation/degeneration.

Correlations observed between hemostasis components plasma levels and MRI measures, of interest for brain disease mechanisms, did not overcome correction for multiple comparisons.

Extravascular leakage of blood components in MS patients, measured as cerebral microbleeds (CMBs) by MRI, was investigated in relation to plasma levels of hemostasis components. Interestingly, lower ADAMTS13 levels were detected in the MS cohort, in particular in patients with CMBs (chpt.5), who also showed higher VAP-1 levels (chpt.9). These novel findings support the investigation of two enzymes, the vWF plasma protease ADAMTS13, and the amino oxidase/adhesion protein VAP-1, in relation to CMBs.

This study provides novel MS disease biomarkers as well as potential drug targets.

Chapter 1 General Introduction

1.1 MULTIPLE SCLEROSIS

Multiple sclerosis (MS) is a chronic, inflammatory, demyelinating disease of the central nervous system (CNS) that causes irreversible and progressive accumulation of physical and cognitive disability (1, 2). In the most of the cases, the onset occurs between 20 and 40 years, which makes the MS the main cause of physical and neurological disability in young adults, affecting around 2.3 million of people in the world (3, 4).

In Italy, there is an average of 1-2 MS cases for every 1000 inhabitants, with a higher prevalence in Sardinia (3/1000 MS cases), whose population is particularly studied for the genetic components of the disease (5, 6). In fact, despite the cause of MS is still unknown, some evidence support the idea that the etiology is the consequence of several environmental factors that disturb a genetically susceptible individual (7, 8).

Epidemiological data show that there is a predominance in women compared to men, highlighting the contribution of sex-related factors to the disease susceptibility (9). Moreover, several other environmental and lifestyle risk factors seem to contribute to the susceptibility of MS, among which: vitamin D deficiency, obesity, cigarette smoking and Epstein-Barr virus infection (10, 11).

The pathogenesis of MS involves blood-brain barrier (BBB) breakdown, extravasation of immune cells, inflammation and neurodegeneration in the CNS, which results in the formation of the multifocal demyelinated lesions and development of brain atrophy (8, 12, 13).

Neurological symptoms of MS are very different, according to the damaged area of CNS. Symptoms may be intermittent attacks which can bring to complete or partial remission or they may persist and worsen over time. From the clinical point of view, four main phenotypes of MS have been defined, which take into account the onset and evolution of symptoms, and the lesions visible at the radiological level (14, 15). Very briefly:

- Clinically isolated syndrome: represent the first episode of relapse (symptomatic neurological attack), where the patient does not meet the criteria for being diagnosed with MS yet. According to the clinical evolution, the patient will enter in a different clinical phase.
- Relapsing-remitting MS (RR-MS): is the most common disease course, with defined relapses followed by periods of remission. The recovery may be partial or complete.
- Secondary progressive MS (SP-MS): most of the patients diagnosed with RR-MS evolve within 20 years from disease onset into SP-MS. It is characterized by progressive worsening of the condition that is not relapse related.

- Primary progressive MS (PP-MS): is characterized by the lack of defined attacks with the disease worsening from the onset of the symptoms.

Several disease-modifying treatments (DMTs) are currently on the market for treating RR-MS and clinically isolated syndrome. In general, these DMTs showed to reduce the neuroinflammation, in term of clinical and radiological disease activity (13, 15). In summary:

- Injectable therapies include i) interferon beta (IFN- β), the first released drug that reduces antigen presentation, T cell proliferation, and alters cytokine expression and ii) glatiramer acetate (GA) a synthetic polymer composed of 4 amino acids that alters T cell differentiation inducing proliferation of anti-inflammatory lymphocytes (13, 15).
- Monoclonal antibodies as natalizumab with an action against the α -4 subunit of the adhesion molecule VLA-4 expressed on the leukocytes surface, thus preventing leukocytes migration into the CNS through the BBB.
- Oral therapies among which the first was fingolimod an antagonist of the sphingosine 1-phosphate receptors, which blocks lymphocytes egression from lymph nodes (13, 15).
- Off-label therapies to treat MS are drugs approved for other diseases, like intravenous immunoglobulin, methotrexate, mitoxantrone (16).

The mechanism underlying the cascade of events leading to MS is still under debate (17). The long-standing outside-in hypothesis involves the migration of T lymphocytes in CNS through a disrupted BBB, setting the stage for the multifocal autoimmune plaques (8, 18). Activation of myelin-reactive T lymphocytes is mediated by antigen presenting cells (for example, microglia or dendritic cells) through human leukocyte antigen (HLA) class II presentation of myelin antigens. Interestingly, genome-wide association studies (GWAS) identified HLA locus to be associated with the greatest risk for genetic susceptibility in MS (19). The immunoreactive processes are sustained by the activated T lymphocytes that secrete cytokines and chemokines which can feed the inflammatory response. These molecules regulate also the recruitment and migration of other lymphocytes, B cells included, and monocytes/macrophages to the damaged CNS regions and in turn the production of other pro-inflammatory mediators (18). The concomitant production of matrix metalloproteinases and radical oxygen species by immune cells increases the permeability of the BBB (20). Moreover, the pro-inflammatory cytokines induce up-regulation of adhesion molecules, as well as their cognate ligands, on BBB endothelial cells, lymphocytes and other inflammatory cells (21, 22), thus favoring the immune cells migration through BBB (20). Indeed, various disease-modifying therapies (DMTs) have

been developed to inhibit adhesion molecule-mediated trafficking of T-cells through the BBB (23).

On the other hand, the importance of B cells in MS pathology has been recently reconsidered, based on the beneficial immune-modulatory effects of therapies against them (17). The new CNS-compartmentalized inflammation hypothesis suggests an ongoing antigen-specific stimulation, expansion, and maturation of B lymphocytes within the CNS (17, 24). To note, B lymphocytes may act as antigen presenting cells for T lymphocytes and their efficiency is higher when antigen levels are low (25). Little is still known about the mechanisms involved in B cell trafficking both in and out of the CNS, however, their presence into the meninges is in line with recent findings regarding the entrance of lymphatic system into CNS (26, 27).

In parallel to the lymphocytes mediated process, the development of neurodegeneration in the brain is sustained by the microglia activation, oxidative injury, accumulation of mitochondrial damage in axons, and age-related iron accumulation (28, 29). Brain atrophy assessment has become important for the evaluation of neurodegeneration and MS disease progression. Magnetic resonance imaging (MRI) provides a sensitive and selective clinical instrument capable of quantitating both the lesions and the atrophy accumulation in MS patients. The extent of brain atrophy can be assessed by measurement of the whole brain volume, cortical volume or lateral ventricular volume (LVV), which reflect regional axonal loss as well as demyelination in white and gray matter tissue structures (30). Moreover, atrophy of the deep gray matter (DGM) and particularly of the thalamus, which has a prominent role in integrating signals of complex cognitive and motor functions, is associated to physical and cognitive disability in MS (31).

Regardless of the cause, BBB disruption and vascular changes, including cerebral hypoperfusion and tissue hypoxia, are important factors in MS pathogenesis, which interact in a vicious cycle favoring the altered immune trafficking and the inflammatory events (32-34). Several pathological and histological studies showed that most of the MS lesions had a perivascular development around small cerebral veins, a feature called “central vein sign“ (35). The presence of central vein sign inside the MS lesions is a well-established finding also through in vivo imaging studies and spreads across all MS clinical phenotypes (RRMS, SPMS, and PPMS) (36, 37). Interestingly, taken into account the overlap between genetic associations for MS and cardiovascular disease (38), the synergic action of genetic and environmental factors could also influence the vasculature changes and the BBB disruption. However, to date, no genetic influence on the vasculature and BBB has been shown in MS.

The progressive failure of BBB integrity leads to focal extravascular leakage of blood components, which are known to induce several inflammatory responses (39).

These pathological manifestations may have the features of microscopic hemorrhages or radiologically measurable cerebral microbleeds (CMBs) (40). It is known that different processes may induce CMBs providing evidence for heterogeneity among them, indeed their radiographic appearance may suggest a different etiology (41). Recently CMBs have been associated with aging and with worsening of physical and cognitive disability in MS (42).

HEMOSTASIS FACTORS IN MULTIPLE SCLEROSIS

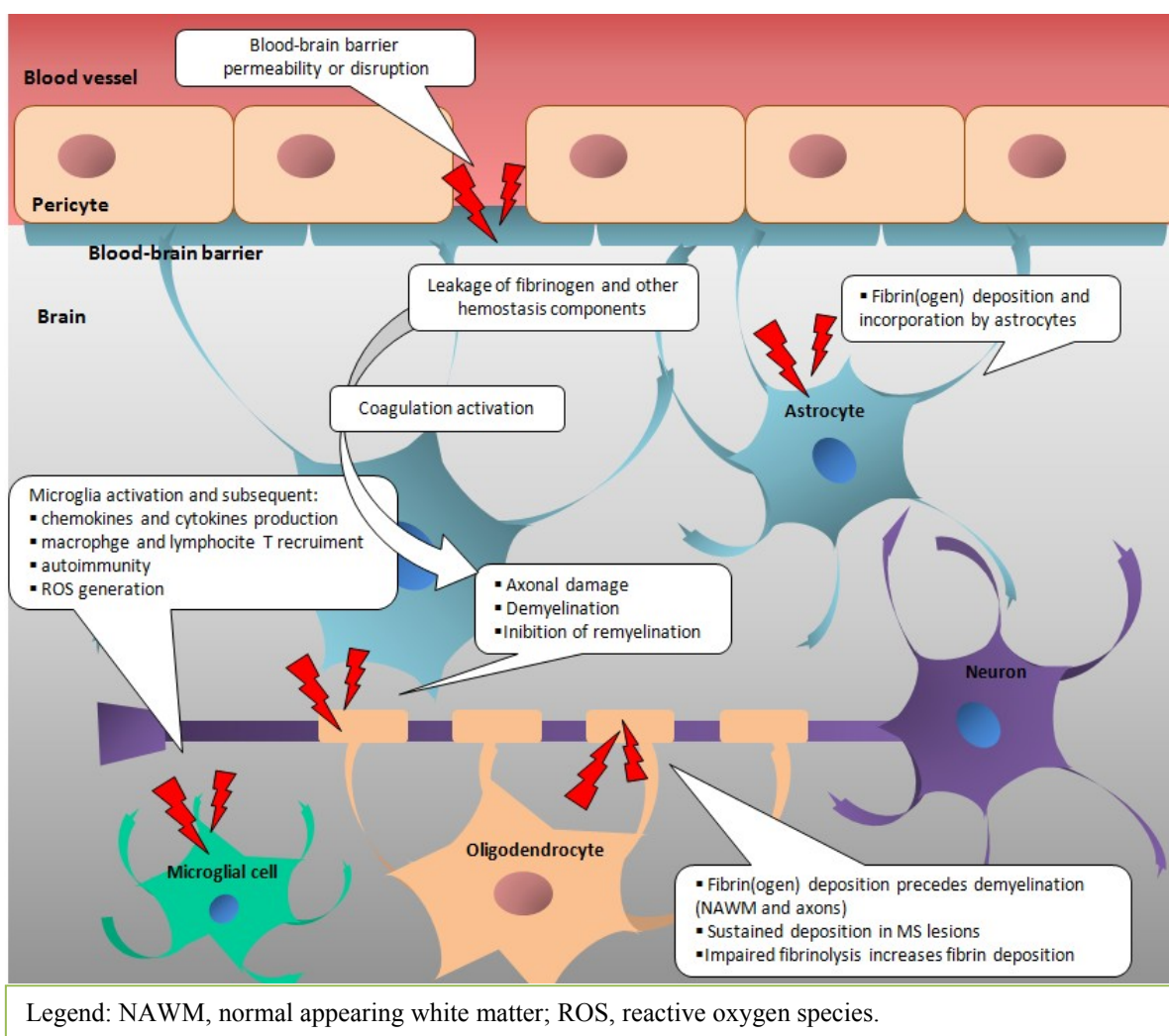
Ziliotto N, Bernardi F, Jakimovski D,
Zivadinov R.

1.2 HEMOSTASIS FACTORS IN MULTIPLE SCLEROSIS

The sophisticated physiological process of hemostasis embraces several pathways, in which procoagulant and anticoagulant forces are maintained in a constant equilibrium by fine regulation. In fact, hemostasis allows the vascular wall to act as an anticoagulant blood container until damage causes significant activation of coagulation, the confined formation of blood clot with hemorrhage cessation, and removal of the blood clot after the restoration of vascular integrity (43).

Increased BBB permeability is a feature of several neurological diseases, and one of the first events that characterizes MS pathogenesis (44-47), leading to the irruption of blood components, coagulation/hemostasis factors included, into the central nervous system (CNS) (48). In fact, BBB damage leads to leakage of hemostasis components into the brain parenchyma which potentially triggers coagulation cascade. Beside their cytotoxic deposition, hemostasis components cause inflammatory response and immune activation, sustaining neurodegenerative events in MS (Figure 1.1) (48-54).

Figure 1.1. Changes in the neurovascular interface are involved in inflammatory, immune and neurodegenerative responses in multiple sclerosis.



Worth noting, coagulation, and inflammation are characterized by multiple links, and coagulation proteins and their fragments may favor neurodegeneration (54, 55). Preclinical models represent, even though with some limitations, an informative way to investigate the pathophysiology of human diseases, and those mimicking MS have received attention in the last 3 decades. As a matter of fact, an increasing number of studies, particularly in animal models (recently reviewed in (56)), are providing insights into the tight relationship among vasculature alterations, neuroinflammation, neuroimmunology and neurodegeneration. Nevertheless, they only partially contribute to the relation between hemostasis components and experimental evidence in MS patients.

Here I will review current knowledge of how coagulation factors, coagulation inhibitors, and components of the fibrinolytic pathway are (dys)regulated in MS patients, and try to identify missing pieces of the research puzzle.

Extrinsic coagulation activation and implication for damage within the CNS

The initiation of the “extrinsic” coagulation pathway requires the “extravascular” TF, also known as Factor (F)III, thromboplastin or CD142. TF is highly expressed on the surfaces of medial and adventitial cells, acting as the trigger for arresting bleeding under damaging circumstances (43).

Surprisingly, low levels of TF in an inactive configuration may be found on endothelial cells and blood cells including platelets, lymphocytes, monocytes, macrophages, granulocytes, and neutrophils (57-59). Additionally, TF has been found as circulating in TF-bearing microparticles that are released from cells or as a soluble protein generated by alternative splicing of TF mRNA (60). Overall induction of circulating/soluble TF is stimulated during sepsis in response to bacteria, or during various chemokines- and cytokine-induced inflammatory states (39).

It has been suggested that decryption, which leads to the procoagulant activity of circulating TF, may depend on different mechanisms including change in phospholipid environment, TF oxidation/reduction modifications and TF dimerization (57, 61-63). Circulating microparticles may contribute to the formation of micro-thrombi (64). This has been suggested as one of the physiological defense strategies against bacteria, promoting so-called immunothrombosis in which the coagulation traps the pathogens, thereby preventing its spreading and supporting the immune response (65). Uncontrolled activation of immunothrombosis, related to sepsis, cancer or inflammatory states causes pathological conditions with undesired intravascular clotting contributing to pro-thrombotic risk (66).

Based on this premise, the tight relation between coagulation, inflammation, and immunity can already be appreciated in the vascular compartment.

Prominent expression of TF is known to occur in the human brain (67, 68), and studies in mice have demonstrated that astrocytes are the primary cellular source of TF, suggesting their role in cerebral hemostasis (69).

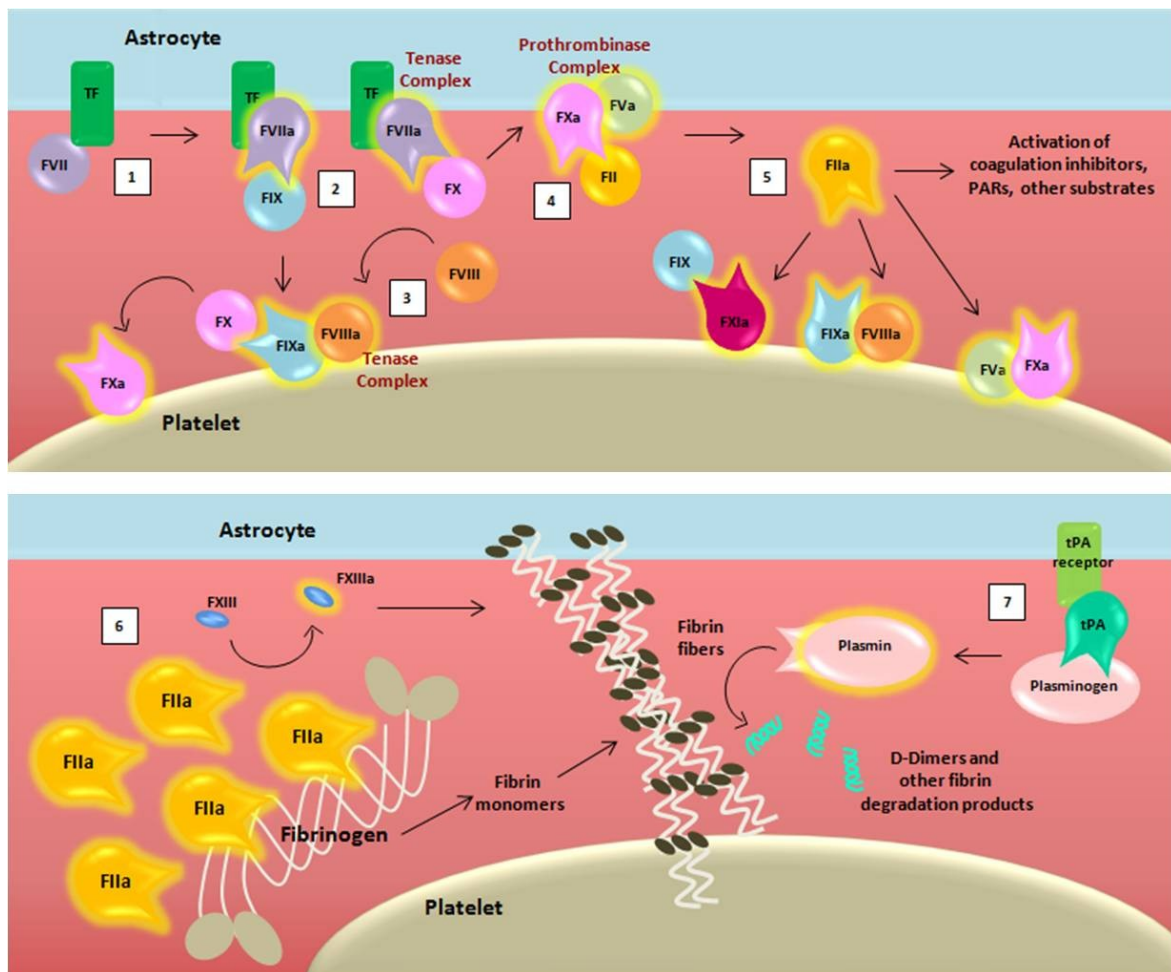
The breakdown of BBB, that characterizes the MS disease process, exposes the TF of astrocytes, which can promote the activation of coagulation cascade which requires, to support biochemical reactions, activated membranes canonically provided by platelets (70), and in addition by activated membranes from various cells. Thus, at the neurovascular interface platelets are expected to be involved in the promotion of coagulation aimed at restoring the vascular integrity (Figure 1.2) together with membranes from astrocytes. Platelets aggregation, via a complex multi-step process, involves the interaction of platelet adhesion receptors with their cognate ligands within the injury site, such as von Willebrand Factor (vWF), collagen, and fibrin (43). The “A Disintegrin-like And Metalloprotease with ThromboSpondin type 1 motif 13” (ADAMTS13), a main inhibitor of hemostasis, cleaves the ultra-large vWF in vWF multimers with lower size, decreasing the propensity of vWF to support platelet adhesion and aggregation (71, 72) (Figure 1.3).

Several cellular/tissue activities under different pathophysiological conditions (including inflammation, apoptosis, cell migration, angiogenesis and tissue remodeling (73)) are modulated by hemostasis components via the cleavage and activation of proteinase-activated receptors (PARs) (43). Noticeably, hemostasis components can elicit opposite signaling responses through activation of the same PAR, as provided by in vitro evidence, where PAR-1 may induce pro-inflammatory and anti-inflammatory signaling under activation by thrombin or the anticoagulant activated protein C (aPC), respectively (74, 75). It has been demonstrated that under coagulant conditions, FXa binds PARs (PAR-1 and PAR-2) at the vascular endothelial cells level, evoking the production of proinflammatory cytokines IL-6 and IL-8 (76), and the monocyte chemotactic protein-1 (77).

The thrombin production reinforces the signal already started by FXa, sustaining the production of the proinflammatory cytokine IL-8 through PAR-1 (76). In addition, FXa triggers a series of Ca²⁺ oscillations (76), which could have a function in the Ca²⁺-dependent activation of proinflammatory transcription factors (78). Moreover, FXa induces expression of adhesion molecules promoting the leukocyte adhesion (77), which in turn, may be sustained also by the co-localized presence of thrombin and fibrinogen (79, 80). Based on these findings, it can be hypothesized that coagulation activation at the neurovascular interface should particularly contribute towards eliciting the inflammatory

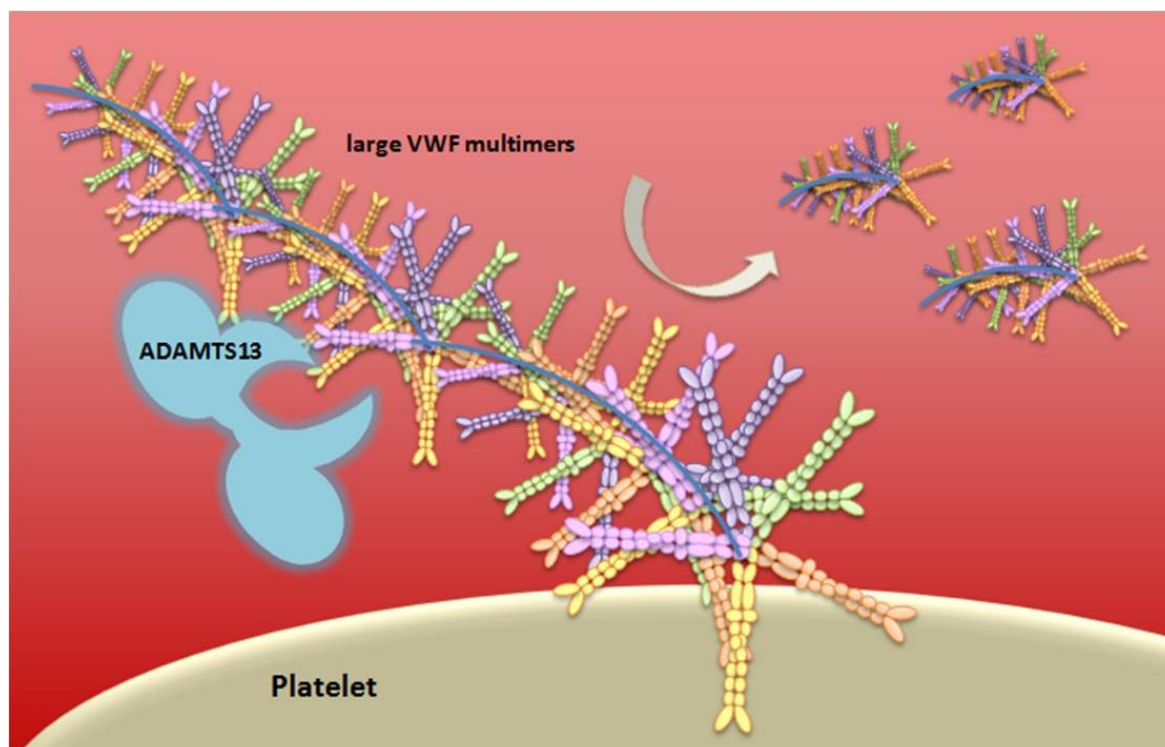
phenomenon and sustain some processes of MS pathophysiology, albeit insufficiently defined. It is known that some coagulation factors are expressed in the CNS, including FX and FII (81-84). However, the physiological functions in CNS are mostly unknown. Depending on BBB damage size, it can lead to the entrance in CNS of circulating blood components, like the high molecular weight fibrinogen as well FV (85), thus providing the complete repertory of factors able to trigger coagulation.

Figure 1.2. Schematic representation of coagulation cascade and fibrinolytic pathway after blood-brain barrier damage.



For the sake of simplicity, the intermediate cleaved forms of clotting factors, as well as their isoforms, are omitted. The coagulation cascade is activated [1] when the TF binds to its ligand, (activated) factor (F)VII, thus forming, together with membranes, a mature active binary complex (TF:FVIIa). The TF:FVIIa complex allow to cleave and activate on one side FIX and on another FX [2]. TF:FVIIa:FXa is able to activate the cofactor FVIII [3] which forms a complex with the FIXa (FIXa:FVIIIa) providing a feedback loop for FX activation. The assembly FXa:FVa, converts prothrombin (FII) into thrombin (FIIa) [4]. The initial amount of thrombin exerts its proteolytic action on FXI, FV, FVIII and other substrates [5]. Then the massive thrombin generation reaches a sufficient concentration to convert fibrinogen (FI) into fibrin monomers [6]. The organized three-dimensional assembly of monomers in protofibrils and fibrin fibers produces the blood clot. Cross-linking stabilization of fibrin clot requires FXIII activated (FXIIIa) by thrombin activity. The dissolution of the fibrin fibers are mediated by the fibrinolytic system [7]. Tissue-type plasminogen activator (tPA) converts plasminogen into plasmin which cleaves fibrin to soluble degradation products among those the D-dimers.

Figure 1.3. Schematic representation of vWF multimer size regulation by ADAMTS13



von Willebrand Factor (vWF) is stored in the Weibel-Palade bodies of endothelial cells or in the α -granules of platelets and it is released in an ultra-large form, a long multimeric string. The vWF serves as an adhesion surface to which platelets adhere and aggregate, and form a plug. The regulation of platelets adhesion depends upon cleavage of vWF in different size of multimeric string by ADAMTS13.

Nevertheless, in order to form fibrin, a sufficient amount of thrombin is needed, and in addition, an activated surface that sustains the coagulation process. Up to now, the exact sequence of events that supports coagulation in the CNS and fibrin formation, in particular in MS patients, is adapted from the general coagulation pathway and does not consider a number of bed-specific components. The key event in the CNS is represented by the presence of fibrin, which has been shown to cause the undesired activation of microglia, subsequently inducing the recruitment and activation of macrophages, thus promoting inflammatory responses (49).

Several findings in mice, and particularly in the experimental autoimmune encephalomyelitis (EAE) model, support the importance of coagulation factors in MS, either procoagulant in the extrinsic and intrinsic pathways, or anticoagulant. Intriguingly, treatment of this animal model with recombinant thrombin (depleted of pro-coagulant function) significantly ameliorates the pathological condition, reducing inflammatory cell infiltration and demyelination, decreasing activation of CD11b⁺ macrophages and reducing

accumulation of fibrin(ogen) in CNS (86). This supports the idea that the pro-coagulant function of thrombin is involved in microglia activation (87).

Other experimental findings support the role of fibrinogen in suppressing remyelination by the inhibition of oligodendrocyte progenitor cells differentiation into myelinating oligodendrocytes (51). Interestingly in the EAE marmoset model, fibrinogen was proposed to derive from the central vein in early lesions, and its deposition preceded demyelination and visible gadolinium enhancing lesions on MRI (88). The peak of fibrinogen deposition corresponded with the beginning of demyelination and axonal loss. Afterward, fibrinogen was found inside microglia/macrophages, suggesting its phagocytosis. Moreover, a positive correlation of fibrinogen deposition with an accumulation of microglia/macrophages and T cells was detected (88). Overall, fibrinogen leakage is one of the earliest detectable events in lesion pathogenesis. Very recent promising data in EAE mice have shown that a monoclonal antibody targeting fibrin, without interfering with the coagulant activity, avoids the microglia activation and monocytes infiltration into the CNS (89). Moreover, it decreases the neurotoxicity through the inhibition of reactive oxygen species (ROS) production mediated by NADPH oxidase in the innate immune cells, which has been demonstrated to be fibrin induced during the neurodegeneration process (89).

The dissolution of the fibrin clot is mediated by the fibrinolytic system (Figure 1.2). Tissue-type plasminogen activator (tPA) was found to be the most abundant plasminogen activator in control brains, with antigen concentration and enzyme activity several orders of magnitude higher than those of urokinase-type plasminogen activator (uPA) (90). Strikingly, components of the fibrinolytic system present in CNS participate in a wealth of physiological roles (91). The tPA has been involved in regulating cerebrovascular integrity (92), neuronal activity through its action on the N-methyl-D-aspartate (NMDA)-receptor, neuronal calcium signaling, axonal regeneration and microglial activation/inflammation (91). uPA exerts proteolytic and intracellular signaling functions by binding its receptor (urokinase plasminogen activator receptor, uPAR) on the cell surface, including microglia activation and axonal regeneration (93-95).

The activity of both tPA and uPA is regulated by specific plasminogen activator inhibitors (PAIs), of which the principal is PAI type 1 (PAI-1), a member of the serine protease inhibitor superfamily (SERPINS) (96). Tight connection of fibrinolysis with coagulation is further provided by thrombin, which enhances fibrinolysis through induction of expression and activity of tPA, and inactivation of PAI-1 by complex formation with it. Interestingly, under pathological conditions high PAI-1 expression may be induced by inflammatory cytokines (97).

Experimental evidence in mice showed that PAI-1 may be released by microglia and astrocytes under inflammatory conditions, increasing microglia migration into the brain and inhibiting microglia phagocytosis (98). Accordingly, in EAE mice, the inhibition of PAI-1 has been shown to decrease axonal degeneration and demyelination (99). On the contrary, tPA deficiency in EAE mice induced a more severe disease progression and CNS fibrin deposition. The uPAR depletion delayed the disease onset, acting only in the initial phase by reducing the adhesion and migration of inflammatory mononuclear cells into the CNS (100). In fact, EAE mice without uPAR subsequently develop chronic disease (100). Thus, data in animal models suggest that an impaired fibrinolytic pathway supports the inflammatory and neurodegenerative processes of the disease.

The eclectic nature of Factor XII: the crossroad between coagulation (intrinsic/ contact pathway), inflammation, and immunity

Recently, albeit only in animal model, FXII was found to be involved in adaptive immune responses via uPAR (CD87)-mediated modulation of dendritic cells (DCs) (52).

Coagulation cascade may be triggered by the circulating protein FXII, also called Hageman factor (101), activated (FXIIa) by contact with negatively charged surfaces that induce a conformational change. The contact activation system is usually identified with the intrinsic coagulation cascade pathway (102, 103). The FXIIa-initiated intrinsic coagulation pathway proceeds through activation of FXI (FXIa) and subsequent FIX activation (FIXa) (Figure 1.4), hence reaching the common pathway (Figure 1.2). Despite its contribution to fibrin formation in coagulation assays, the role of factor FXII “in vivo” has long been debated, because FXII deficiency does not exhibit a clinically relevant bleeding phenotype (104). Considering that FXII is located at the crossroad of several other pathways, this feature makes FXII a target to be inhibited without concomitant bleeding complications (105, 106).

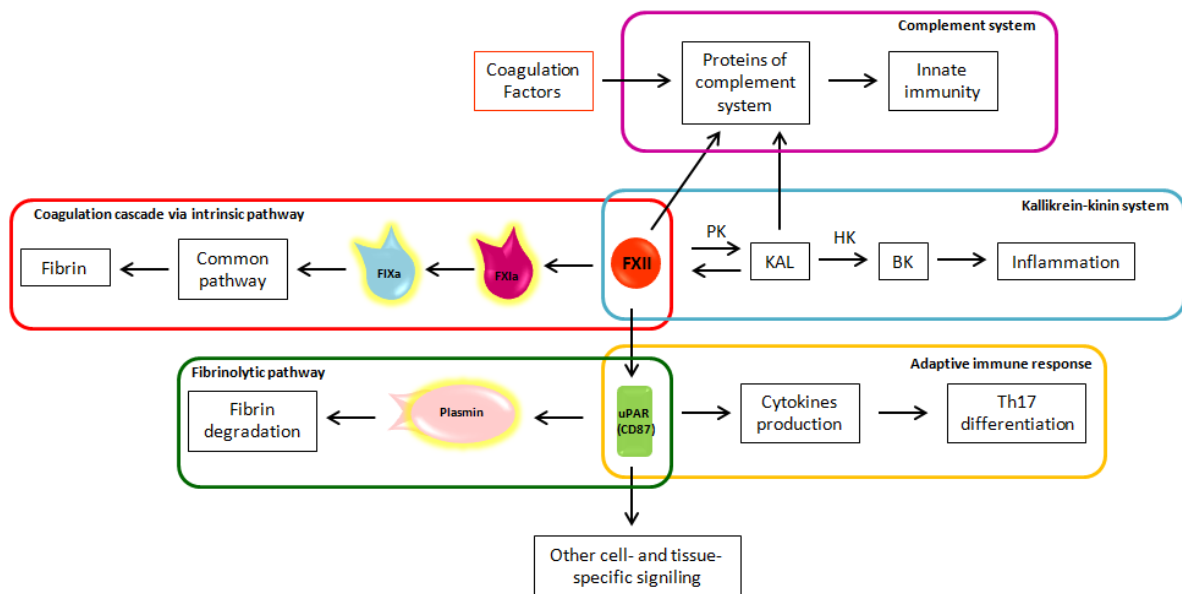
As matter of fact, FXIIa converts prekallikrein (PK) to kallikrein (KAL) (102), starting the proinflammatory kallikrein-kinin system (Figure 3). KAL acts on high molecular weight kininogen (HK), releasing the active peptide bradykinin (BK), which through bradykinin receptors mediates: 1) vasodilation induced by nitric oxide formation, 2) prostacyclin release which reduces vessel-wall exposure of TF, 3) platelet inhibition, and 4) tPA release (102). The kallikrein-kinin system is further linked to the fibrinolytic pathway by KAL, which is able to convert plasminogen to plasmin (107). Thus, from one side the kallikrein-kinin system through BK promotes inflammation and from the other the inhibition of coagulation and promotion of fibrinolysis. In the EAE animal model, the blocking of a BK receptor (B1R), mainly expressed close to the plaques, prevented the infiltration of T

lymphocytes into the CNS and restored BBB decreasing its permeability, thus avoiding inflammatory actions of BK on the tissue (108).

Interestingly, FXIIa itself has the capacity to cleave several proteins of the complement system, driving activation of innate immunity against foreign pathogens (Figure 1.4) (109). The complement cleavage products (C3a and C5a) have also been shown to exhibit robust chemo-attractive properties to human mast cells and neutrophils, highlighting the pro-inflammatory effects of the coagulation-complement interplay (110).

An example of selective pathway activation is given by mast cells (111) that, when activated, rapidly secrete granules of which heparin is one of the major constituents. Although heparin is primarily an anticoagulant, it provides a negatively charged surface that activates FXII, thus selectively promoting the inflammatory kallikrein-kinin system and possible consequent vascular leakage and BK-driven leukocytes infiltration (111).

Figure 1.4. The eclectic nature of Factor XII: the crossroad between coagulation, inflammation, and immunity.



Legend: a, activated; BK, bradykinin; F, factor; HK, high molecular weight kininogen; KAL, kallikrein; PK, prekallikrein; uPAR, urokinase plasminogen activator receptor; Th17, T helper 17 lymphocytes.

Another immuno-mediated mechanism able to induce FXIIa is supported by neutrophils through the release of neutrophil extracellular traps (NETs). NETs consist of negatively charged contents such as nucleic acids together with histones, and antimicrobial proteins, which are physiologically used to trap and kill bacteria during infection. On the other side, they trigger FXIIa and, in addition, foster the recruitment and activation of platelets, promoting events of immunothrombosis (112).

In EAE, it has been demonstrated that depletion of FXII has a protective effect, delaying disease onset and decreasing disease severity (52). Of note, no differences were found in the amount of fibrin/fibrinogen in CNS of EAE-FXII depleted mice compared to those with wild-type EAE phenotype. In support of these findings, factor XI (directly activated by FXII) deficiency does not alter the clinical course, demyelination, cytokine levels or the immune cell infiltration in the EAE model. These results support the hypothesis that FXII does not participate through the activation of intrinsic coagulation pathway, which would imply that the FXII procoagulant activity “per se” is not involved in MS (52).

1.3 COAGULATION AND HEMOSTASIS FINDINGS IN MULTIPLE SCLEROSIS PATIENTS

Overall, pro-coagulant, anti-coagulant, and fibrinolytic pathways are responsible for maintaining the hemostasis balance under physiological conditions. Significant deviation from these pathways would result in hypercoagulability leading to life-threatening thrombotic or, alternatively, to acquired/inherited bleeding diseases (e.g hemophilias).

The investigation of the coagulation (un)balance in MS patients will be now reviewed.

Historical perspective

One of the first findings of hemostasis abnormalities in MS was provided by Putnam (113) who reported the presence of definite thrombi in half of the analyzed MS case (9/17). Thrombi were described as the frequent occurrence of perivascular hemorrhages within acute lesions and as a vascular obstruction in chronic lesions. Therefore, the primary abnormality of MS was suggested to reside in the alteration of the blood clotting mechanism (113). Consequently, 43 MS cases were treated with dicoumarine, ranging between 6 months and 4 years (114). Despite the side effects, Putman and colleagues concluded that anticoagulant treatment reduced relapses in the relapsing-remitting (RR) form of MS while the course of chronic progressive disease was not affected (114). This study was criticized for lack of proper statistical analysis. Soon after, Putnam interpreted venous thrombosis as a possible pathognomonic process in MS, while others reported increased capillary fragility (115) and subcutaneous hemorrhages (116).

Later on in 1955, Persson reported increased levels of plasma fibrinogen in MS patients during relapse exacerbations, which were not related to thrombus formation (117). By that time, it was already known that fibrinogen levels were higher than in controls in the majority of chronic and degenerative diseases, thus laying the foundations for later discoveries of fibrinogen levels as a marker of inflammation (117, 118). A few years later, another study investigated blood coagulation in 33 MS patients and corroborated previous findings showing no tendency towards increased blood coagulability (119). Overall, in the

majority of investigated patients, fibrinogen levels were within the normal range, despite the wide variations that were not associated with the stage of the disease (119).

A subsequent study in 10 MS patients, explored both the blood and the cerebrospinal fluid (CSF) and revealed that neither had thromboplastin activity, nor significant abnormalities in blood platelet, coagulation factors, serum platelet-like activity nor fibrinogen levels (120). Despite the lack of abnormal findings, increased capillary fragility was reported (120). The “antithrombic” activity of normal and pathological CSF was later discovered in 1961 (121). With the exception of larger proteins like fibrinogen and FV, further studies demonstrated the presence of coagulation proteins in the CSF (122) and corroborated that degradation products of fibrin were present under pathological conditions (85).

The discrepancy in results of coagulant balance of that époque needs to be interpreted in light of unstandardized examination techniques. An increase of fibrinolytic activity was also documented, which again pointed towards an altered coagulation system in MS (123). It is worth mentioning that a few studies have investigated platelet stickiness in MS (124-126), although this topic is not discussed in this work.

Fibrin(ogen) brain deposition

Direct studies on histological brain samples, aimed at addressing fibrin deposition and alteration of the fibrinolytic pathway, started in the 1980s (Tables 1.1 and 1.2). Nowadays, it is well known that one of the key events in the pathophysiology of MS is BBB breakdown, which leads to the entry of several neurotoxic blood-derived proteins (127). Thanks to histological studies on MS brains, fibrinogen, an abundant protein in plasma, has been identified as contributing to neuroinflammation in the CNS (53, 128). Since most of the antibodies used across the studies were unable to distinguish fibrin from fibrinogen the word fibrin(ogen) would be more appropriate. However, the properties of fibrin favor the formation of oligomers and protofibrils, which aggregate laterally to make fibers, and ultimately branch to yield a three-dimensional network of insoluble fibrin (129). The detection in tissues of insoluble fibrin (fibrin deposition) by antibodies is certainly enhanced as compared with the detection of fibrinogen.

The relation between hemorrhage and demyelinating plaques was first considered by an early case report of 2 MS patients who developed CNS hemorrhage. It was suggested that the demyelinating event could contribute and set the stage for focal hemorrhages (130). However, over the course of the following years, the leakage of blood protein fibrinogen into the brain parenchyma was established as a potential marker of BBB damage (44, 131), and as a contributor to neurodegenerative events. In initial reports, the presence of heavy extracellular fibrinogen was detected in demyelinated centers of acute MS plaques (132) but also in most of the examined inactive plaques, particularly close to astrocytes (133).

Moreover, the fibrinogen within the plaques was found to overlap with macrophages and axons, and even extended into the surrounding normal-appearing brain tissue. Nevertheless, fibrinogen did not co-localized with the enlarged astrocytes outside the plaques (133). Moreover, it was shown that fibrinogen leakage gradually increased through the progression of MS lesions, reaching the highest levels within the central parenchyma of those plaques with the greatest degree of activity (134). Interestingly, fibrinogen co-localized with areas of activated microglia in MS lesions (134).

Confocal microscopy confirmed the extravascular fibrinogen presence in active MS lesions, most commonly with a distinct perivascular distribution, and in a few cases widely distributed throughout the parenchyma (135). Association of such leakage with areas of microglial activation was consistent with increased tight junctions' abnormality in the same areas (135). Confocal microscopy was extensively used to confirm the perivascular distribution of the fibrinogen leakage and demonstrate varying fibrinogen levels within MS lesions (131). Hence, the severity of altered tight junctions was associated with BBB dysfunction, which in turn both was proportional to the increase in fibrinogen leakage reaching particularly high levels in active lesions (131). A threshold of tight junctions' injury might be reached before significant and visible BBB leakage of the large, high-molecular-weight protein fibrinogen (131), which could justify the lack of fibrinogen detection close to vessels with lower tight junction abnormalities.

Postmortem magnetic resonance imaging (MRI) was also applied to detect both diffuse and focal brain abnormalities, allowing targeted histopathological examination of MS lesions (44). BBB disruption was detected by increased immunopositivity for fibrinogen in the brain parenchyma as described also by previous studies (131-135). Fibrinogen leakage was found in both active and chronic MS lesions, co-localizing with astrocytic processes and occasionally with axonal processes (as demonstrated by neurofilament immunoreactivity) which suggested that astrocytic and neuronal processes may bind or incorporate extravasated fibrinogen. Moreover, fibrinogen was not limited only to demyelinating lesions, but it was seen in both reactive lesions characterized by small clusters of microglial cells without apparent loss of myelin with a variable degree of edema, and in areas with diffusely abnormal white matter (WM) (44). Nevertheless, the presence of fibrinogen was more extensive in chronic active and inactive lesions when compared to reactive lesions (44).

A recent analysis of chronic MS lesions revealed that fibrinogen extravasation was present in chronic active lesions close to the blood vessels, but not in the chronic inactive ones (88). It was also shown that fibrin deposition might occur early in MS and precede demyelination (53), since the 'pre-demyelinating' areas of activated microglia hosted fibrin

precipitates within the extracellular space of the lesions (53). The high precipitation of fibrin on the surface of microglia was suggested to be the driving force for microglial activation according to its detection in focal plaques of microglial activation with features of hypoxia-like damage but in the absence of demyelination (53). Thus, changes in the NAWM precede the formation of inflammatory demyelinating plaques, in particular in those exhibiting the hypoxia-like demyelination pattern. Such changes were suggested to settle the inflammatory response and infiltration of T-cells, B-cells, and macrophages in the brain tissue, leading to the formation of the classic inflammatory demyelinating plaque detected by MRI (53). This is in agreement with recent findings where fibrin is able to mediate microglia activation and oxidative stress with ROS production, contributing to local neurodegenerative events (89).

Table 1.1. Histopathological evidence of hemostasis components in multiple sclerosis.

Hemostasis components	Main findings (patient sample size/methodology)	Reference
Coagulation		
FXII	Deposition nearby dendritic cells positive for uPAR.	(52)
Fibrinogen	Presence within demyelinated centres (23 acute MS plaques).	(132)
	Detected in 19 inactive plaques, co-localize with astrocytes (32 inactive plaques).	(133)
	Perivascular detection in type I, II and V lesions. Leakage within central plaques parenchyma (immunohistochemistry on 155 MS lesions from 13 early cases of MS).	(134)
	Extravascular staining with perivascular distribution in association with microglial activation (active MS lesions analyzed by confocal microscopy).	(135)
	Perivascular distribution of leakage and differential degree of deposition in WM. Co-localization with astrocytes. Correlation with the grade of tight junctions' abnormality (2198 MS and 1062 control vessels analyzed by confocal microscopy).	(131)
	Leakage both in active and chronic lesions; reactivity also in NAWM and in WM. Co-localization with astrocytes and neuronal process (postmortem MRI on MS lesions).	(44)
	Extravasation close to the blood vessels only in chronic active lesions (4 chronic active lesions and 5 chronic inactive lesions from 4 MS brains).	(88)
Fibrin(ogen)	Extracellular deposition predominantly located in layers 5 and 6 of the cortex in MS. Intracellular deposition detected in neurons and astrocytes (immunohistochemistry on the cortex of 47 progressive MS and 10 controls).	(54)
Fibrin	Staining overlap with macrophages and axons, and extended into NAWM (32 inactive plaques).	(133)
	Deposition in areas of activated microglia (immunohistochemistry on 155 MS lesions from 13 early cases of MS).	(134)
	Deposition occurs in pre-demyelinating areas of activated microglia.	(53)
Inhibitors		
Protein C inhibitor (PCI)	Detected in chronic active plaques (Mass spectrometry MS plaques).	(136)
C1 inhibitor (C1INH)	Detected in MS plaques.	(137)

Finally, fibrin(ogen) was reported in the cortex of progressive (P-MS) cases. Extracellular fibrin(ogen) deposition was mostly found in the deeper cortical layers (layers 5 and 6 vs. layer 2). In contrast, its co-localization within neuritic and astrocytic processes was predominantly in the superficial cortical layers (54). The presence of intracellular fibrin(ogen) has been suggested to occur by direct synthesis of those cells or mediated by retrograde transport in damaged axons exposed to increasing amount of protein. Overall, severe fibrin(ogen) deposition was detected in areas of significantly reduced neuronal density and particularly appeared to affect the loss of layer 5 projection neurons (54). No relationships were observed between the presence of fibrin(ogen) and microglial/macrophage density. Of note, the deposition of other proteins, such as albumin, remains controversial probably because of their inability to be converted into an insoluble matrix as fibrinogen does to fibrin, precluding accurate assessment.

In summary, these data support the entrance of fibrinogen into the CNS, which sustains the pathogenesis of MS lesions. In particular, its conversion into fibrin seems to trigger the activation of microglia, and to support inflammation and the consequent development of demyelinating lesions.

Histological evidence for an altered fibrinolytic pathway in multiple sclerosis CNS

Besides fibrin(ogen), several studies have focused on the fibrinolytic pathway (Table 1.2), and the capacity of MS lesions to break down fibrin.

Initial findings were provided by histochemical techniques, showing that the amount of fibrinolytic activity was comparable between active lesions and inactive ones (138). The fibrinolytic zones in MS brains originated from areas around vessels or capillaries and the presence of lymphocytic infiltrates, gliosis, or macrophages did not change the localization and degree of fibrinolysis. Moreover, the NAWM from MS patients was not more fibrinolytically active than that of the controls, but plaques showed more fibrinolytic activity compared to adjacent NAWM (138), hence providing an attempt of combating the fibrin. Subsequently, positive infiltrating mononuclear cells stained for tPA were observed in MS lesions particularly, within the active ones (139). This pattern converted into a strong positivity of the foamy macrophages in areas of demyelination and declined in chronic lesions. Similarly, the PAI-1 expression paralleled that of tPA on foamy macrophages(139). The disappearance of immunoreactivity for tPA in chronic MS plaques supported the role of impaired fibrinolysis as contributing event to the inflammatory stage of the demyelination mediated by fibrin. Considering the increased expression of tPA on mononuclear cells in perivascular cuffs, it was suggested to be one of the earliest

detectable signs of inflammation in MS. tPA might trigger the matrix metalloproteinase (MMP) cascade and thus facilitate entry of leukocytes into the CNS (139).

Then, another study provided a partially discordant data: although quantitatively decreased in MS lesions, tPA was found to co-localize with non-phosphorylated neurofilament and fibrin(ogen) deposits on demyelinated axons (90). On the other hand, highly significant increases in uPA, uPAR, and PAI-1 were detected in acute MS lesions and uPAR in NAWM when compared with control tissue. These three proteins were immunolocalized with mononuclear cells in perivascular cuffs and with macrophages in the lesion parenchyma. The significant increase in the uPAR complex was thought to be a trigger for focal plasmin generation and for cellular infiltration, cooperating with the MMP activity in the opening of the BBB (90).

Further investigations provided evidence for the lowest fibrinolytic activity within acute lesions which was due to the formation of tPA/PAI-1 complex (140), in turn contributing to fibrin accumulation. Nevertheless, D-dimers and fibrin degradation products were mostly localized at the neurovascular interface and on foamy macrophages and axons during the chronic inflammatory stage of lesions (140). In addition, increased PAI-1 synthesis leading to defective fibrinolysis appeared to establish before lesions formation (140). However, during the progression of lesions, an increase in lower molecular weight PAI-1 peptides was detected, as result of PAI-1 intracellular degradation mediated by macrophages (140).

Table 1.2. Histopathological evidence of fibrinolytic pathway components in multiple sclerosis.

Fibrinolytic components	Main findings (patient sample size/methodology)	Reference
Fibrinolysis	Higher fibrinolytic activity in plaques than adjacent NAWM.	(138)
tPA	Staining for infiltrated mononuclear cells in MS lesions and WM. Strong positivity of foamy macrophages in areas of demyelination and decline in chronic lesions.	(139)
	Co-localization with non-phosphorylated neurofilament and fibrin deposition in demyelinated axons.	(90)
	Decreased tPA activity in acute MS lesions. Decreased fibrinolytic activity in demyelinating MS plaques due to tPA/PAI-1 complex.	(140)
tPA receptors	Localization on macrophages, astrocytes. Increased in MS lesions compared to NAWM.	(141)
uPA and uPAR	Detected in acute MS lesions, expressed by mononuclear cells in perivascular cuffs and to macrophages in the lesion parenchyma. uPAR additionally detected in NAWM.	(90)
D-dimers	Localization on foamy macrophages and demyelinating axons.	(140)
PAI-1	Detected in acute MS lesions, expressed by mononuclear cells in perivascular cuffs and to macrophages in the lesion parenchyma.	(90)
	Up-regulation in progressive MS cortex but without an efficient fibrin degradation (immunohistochemistry on the cortex of 47 progressive MS and 10 controls).	(54)

Plasma membrane tPA receptors, which may concentrate proteolytic activity on the cell surface and in turn locally enhance the fibrinolytic response, were immunolocalized in acute MS lesions on macrophages and astrocytes (141) and increased in MS lesions when compared to NAWM samples. Furthermore, a tPA receptor was found on neuronal cells within the cortex. However, the limited availability of tPA, bound to PAI-1, reduces the production of plasmin, which further decreases the fibrinolytic activity in active MS lesions and increases axonal fibrin deposition and neurodegeneration (141). Indeed, perturbed fibrinolysis was found to be a hallmark of P-MS cases with abundant cortical fibrin(ogen) deposition (54). Overall, significant upregulation of PAI-1 in the cortex where fibrin deposition was most severe, implies that dysregulation of fibrin clearance and allow for its pathological accumulation in later stages of MS (54).

Detection of protein C inhibitor (PCI), C1 inhibitor (C1INH) and FXII in multiple sclerosis plaques

An old biochemical study based on isolation of brain capillaries from human brain samples close to MS lesion showed positive staining for FVIII (142). Different insights on coagulation components and inhibitors in MS lesions (Table 1.1) have been provided by lesion-specific proteomic profiling (136), which detected TF. This is to a certain extent expected in relation to the abundance of this protein in perivascular spaces and PCI only in chronic active lesions. PCI, which inhibits activated protein C (aPC), seems to accumulate within these lesions secondary to the disruption of the BBB during neuroinflammation. The combined presence of TF and PCI suggests pro-inflammatory thrombin formation and suppression of PC pathway, supporting a mechanism that in the presence of coagulation activation suppresses the action of coagulation inhibitors involved in MS lesion formation (136).

Further evidence for the intricate connection between coagulation, inflammation, and immunity was provided by the positive reactivity of MS lesions for proteins of the complement system, and regulators as C1INH. Taken together, these findings point towards continuing local complement synthesis, activation and regulation despite the absence of evidence of ongoing inflammation (137). Interestingly, deposition of FXII, which is inhibited by C1INH and might support autoimmunity, was detected in the histological analysis of CNS tissue from MS patients, nearby DCs positive for CD87 (uPAR) (52).

Overall, impaired fibrinolysis seems to reinforce fibrin(ogen) associated damage in MS. Differently, impaired inhibition of coagulation, and the contribution of coagulation factors through inflammatory and autoimmunity pathways in CNS requires further investigation.

Activity of hemostasis factors in plasma of multiple sclerosis patients

After 80 years from the first report on altered coagulation in MS (113), findings on this pathway in MS are still controversial and the subject of intense investigation (143-146). The use of improved laboratory methodologies allowed to investigate several features characteristic of coagulation components. Antigen (:Ag) levels provide information about the protein concentration, which is independent of its ability to be intrinsically functional and does not depend on activatory or inhibitory molecules. Similarly, testing the functional activity (:C) does not provide direct information about its protein concentration but integrate the influence of activators or inhibitors. Considering the tight relation between coagulation factors and immune response (discussed at the beginning of this review) it is intriguing to speculate that the clinical manifestation of MS could also be related to an increased pro-coagulant activity. Therefore, hemostasis components activity evaluation could contribute to identifying the causes of dysregulation.

During a PT or aPTT assay, information about clotting time is obtained providing the overall functionality of the system. When alteration in clotting time is observed, it is possible to pursue the assay using a plasma depleted of a specific coagulation component (thought to be the cause of the alteration) in order to assess the specific functional activity of that component. Continuous thrombin generation, a more sensitive and flexible method, reflects well the initiation, propagation, and termination phases of coagulation (147, 148).

The summary of evidence about the activity of coagulation components is reported in Table 1.3. In the first report about fibrinogen levels, PT and aPTT times in plasma from RRMS patients did not show significant differences, despite the raised fibrinogen levels in MS, as compared with controls (143). Similarly, plasma antithrombin (AT) activity showed no MS group differences or associations with periods of relapses or remissions (149). The activity of PC, FII, FX, FXI and FXII, and propensity of fibrinogen to clot was determined in plasma samples of MS clinical phenotypes compared to healthy individuals (144). Higher FII:C and FX:C were detected in RRMS and SPMS patients when compared to controls (144). These experimental findings suggest an increase in thrombin activity and its generation through FX activity, which by definition is part of the prothrombinase complex, in MS patients. However, increased activities do not seem balanced by increased activity of the main inhibitors (AT and PC). Furthermore, the increased activities do not depict a defined pro-thrombotic risk. Additionally, higher levels of FII:C and FXII:C were associated with a shorter period between relapses (144). Noteworthy, activity for none of the analyzed factors showed alterations in PPMS when compared to controls. This study suggested that differences in coagulation factors activity could underline different pathophysiological processes, particularly within P-MS subgroups (144).

The same investigators found that FXII:C was elevated in RRMS and SPMS compared to controls, and greater activity levels were associated with higher occurrence of relapses and shorter relapse-free period, independently from the use of immune modulatory therapy (52). Evaluation of coagulation activity has been performed by thrombin generation (145), which showed enhanced generation in RRMS patients compared to PPMS and controls, pointing to a prothrombotic state within the RRMS phenotype (145).

Further, immune-modulatory function in relation to/independent from coagulation activity, particularly for FXII, still remains to be elucidated in MS as well as heterogeneity of coagulation balance.

Concerning the activity of cellular components of coagulation, unstimulated and stimulated monocytes were not found to differ in MS and controls with respect to expression of cell surface TF or production and secretion of TF (150), which would not support the presence of pro-thrombotic components. Overall, the discordant data on prothrombotic features in MS patients in the few available publications would suggest the presence of some pro-coagulant alteration during the more active phase of the disease. Patient prothrombotic heterogeneity could be approached through stratification according to coagulation balance in order to prospectively evaluate the impact of coagulation differences on disease evolution.

Protein levels of hemostasis components in plasma, serum and cerebrospinal fluid of multiple sclerosis patients

Antigen (protein) levels of hemostasis factors have been sporadically investigated in MS (Table 1.3). Starting with the promising candidate fibrinogen, its levels were found to be unaltered in both the CSF and blood of MS patients in different studies (143, 151). Increased fibrinogen beta chain concentration was detected in CSF samples from two fulminant MS cases by mass spectrometry (152). Analysis of the CSF proteomic profiles of MS patients, collected in different phases of their clinical course, showed significantly lower fibrinogen and fibrinopeptide A (a degradation product of fibrin) concentration in CIS compared to PMS patients (153). The most recent investigation in plasma, detected high fibrinogen levels in a noticeable proportion (17/58) of patients, particularly in those with active lesions on MRI (154). Globally, these studies further support the role of fibrinogen as contributor of neuroinflammation and neurodegenerative processes in the CNS, following BBB damage.

The analysis in pre-symptomatic and post-symptomatic MS pooled serum detected proteomic changes for factors involved in the complement and coagulation pathways, with a particular decrease in MS of FX, FII, and C1INH (155). FXIII B chain and plasminogen

were decreased in post-symptomatic cases compared to controls (155). Because the serum is isolated after coagulation, thus these results might be interpreted as residual coagulation factors remaining after conversion of fibrinogen into fibrin, the last step of the pathway. Concerning the complement protein, less C1INH in patients is of interest in light of its inhibitory activity against FXII through its recruitment in the CNS. Although depositions of FXII and C1INH have been reported, the demonstration of their co-localization in MS brains is still needed (52, 137).

Table 1.3. CSF, plasma, and serum evidence of altered hemostasis components in multiple sclerosis.

Hemostasis factors, inhibitors, and receptors	Main findings (patient sample size/methodology)	Reference
CSF		
Fibrinogen	Lower levels in CIS vs PMS (proteomic profile by mass spectrometer in 24 CIS, 16 RRMS, 11 PMS).	(153)
TM	Higher levels in OIND vs SPMS. 90% of TM in CSF is related to intrathecal synthesis (17 relapse, 11 remission, 11 SP, 19 OND, 15 OIND).	(156)
Plasma		
FII, FX, Fibrinogen, PC, FII, FX, FXI	Higher FII:c and FX:c in RRMS and SPMS vs controls. No differences in activity of Fibrinogen, FXI and ProC (PT in citrate plasma: 116 RRMS, 10 PPMS, 73 SPMS, 20 controls).	(144)
FXII	Higher FXII:c in RRMS and SPMS vs controls. Higher activity correlates with higher occurrence of relapses and shorter relapse-free period (aPPT in citrate plasma: 138 RRMS, 13 PPMS, 90 SPMS, 19 CIS, 130 controls).	(52)
FII	Prothrombotic state in RRMS (Thrombin generation on citrate plasma: 15 RRMS, 15 PPMS, 19 controls).	(145)
Fibrinogen	No differences in fibrinogen levels, PT and aPTT times (42 RRMS and 31 controls).	(143)
	High levels, particularly associated with active lesions on MRI (17 out 58: 45 CIS, 12 RRMS, 1 PMS).	(154)
vWF, TM	Higher vWF activity in active MS. No differences in TM:Ag (26 RRMS, 35 controls).	(157)
AT	No differences in AT:c (37 RRMS, 32 SPMS, 34 controls).	(149)
EPCR	Trend for higher levels in MS (63 MS, 20 controls).	(158)
Serum		
FX, Prothrombin, C1INH, FXIII, Plasminogen	Reduction of FX, prothrombin and C1INH levels in pre- and post-symptomatic MS serum. Reduction in FXIII and plasminogen in post-symptomatic MS (Mass spectrometry (pooled serum of 100 MS vs. pooled serum of 100 controls).	(155)
TM	Higher levels in MS during exacerbation vs. remission state, OND, and controls (17 acute relapse, 9 PMS, 13 HAM, 10 non-HAM, 10 OND, 20 controls).	(159)
	Higher levels in OIND vs SPMS (17 relapse, 11 remission, 11 SP, 19 OND, 15 OIND).	(156)
TM, aPC	No differences (100 RRMS, 22 SPMS, 122 controls).	(160)
vWF	No difference (9 RRMS, 9 SPMS, 10 PPMS).	(161)

Regarding vWF antigen levels in the serum, differences were not found among MS patient groups (161). Differently, the activity of plasma vWF was found to be higher in patients with active MS than in controls (157) and vWF has been proposed as a marker for evaluating BBB breakdown resulting from endothelial damage in MS. Further, vWF activity was significantly decreased after immunosuppressive treatment (157). Of note, vWF “activity” promotes platelets aggregation, hence these data are potentially in line with hemostasis activation at the neurovascular interface after injury.

Levels of soluble thrombomodulin (TM), shedding from damaged endothelium, which also releases vWF, were not significantly different in serum from patients with active MS and controls (157). However, in another study, TM levels appeared to be highly increased in MS during exacerbation when compared to the remission state, and were higher in patients with acute relapse and PMS than in controls (159). In another study with serum, higher TM levels were detected in patients with other inflammatory neurological diseases resulting in a significant difference only with SPMS, which showed the lowest levels (156). The authors speculated that about 90% of TM in CSF is related to intrathecal synthesis and that higher synthesis occurs during both relapses and progression of MS (156). TM levels showed an association with disability (160). The same study did not detect differences in serum levels of PC, activated by the TM-thrombin complex, in patients subgroups or during the acute relapse measurements (160). The only one study analyzing soluble levels of EPCR, the endothelial PC receptor, found a statistical trend for higher levels in MS compared to controls (158).

Plasma, serum, and cerebrospinal fluid levels of fibrinolytic pathway components

Early evidence of fibrin degradation products in the CSF of MS patients (162) paved the way for studies which provided information regarding the proteins of the fibrinolytic pathway (Table 1.4). In the CSF of MS patients, tPA activity was higher than in controls and patients with other neurologic diseases (163), and a very low uPA activity was reported (163). Total PAI-1 antigen was higher in MS patients compared to controls, and a significant inverse relation between PAI-1 levels in CSF and plasma was observed in MS patients (164). Very high PAI-1 levels were observed during relapses (reaching values 6 times higher than controls), and the follow-up indicated 2-fold decreased values 1- 2 months after the relapses. However, a correlation between PAI-1 and tPA plasma levels was not observed (165). Levels of D-dimer, tPA, and PAI-1 did not differ between patients and controls in one study (166), but significantly higher D-dimer levels were found in RRMS in another investigation (143).

Overall, data regarding increased PAI-1 antigen levels would support the notion that impaired fibrinolysis sustains the ongoing neuroinflammatory (particularly during relapse) and neurodegenerative events in the brain as evidenced by histological studies. Considering the few and discordant studies on tPA and D-dimers, further investigation is needed, which would provide a more comprehensive view of fibrinolysis in relation to the MS disease course.

Table 1.4. CSF, plasma and serum evidence of fibrinolytic pathway components in multiple sclerosis.

Hemostasis components	Main findings	Reference
PAI-1	Higher levels in MS vs controls. PAI-1 concentration has reverse relationship of tPA:c (ELISA in CSF and plasma EDTA of 19 MS, OND, controls).	(164)
PAI-1 tPA	High levels of PAI-1 during relapses. No differences for tPA. No correlation between PAI-1 CSF and plasma levels (Plasma of 12 active RRMS, 12 stable RRMS, 10 controls).	(165)
tPA	Higher activity in MS (CSF of 7 MS, 9 leukaemia, 21 encephalitis, 20 controls).	(163)
PAI-1 tPA D-dimer	No differences (Plasma of 90 MS, 250 glioma patients 270 controls).	(166)
D-dimer	Higher levels in MS (VIDAS on plasma of 42 RRMS, 31 controls).	(143)

Effect of disease-modifying treatments on coagulation pathways

Disease-modifying treatments (DMTs) are potential modifiers of coagulation factor levels. However, few studies are available on this topic. MS patients treated with steroids showed lower plasminogen and fibrinogen levels (167). Additionally, increased fibrinolytic activity was observed in treated MS patients. These abnormalities were then considered to be a consequence of a non-specific activation of coagulation in a setting of chronic immunological disease (167). Because of the aforementioned role of fibrinogen and of the potentially decreased fibrinolysis in MS, these data are of interest and deserve additional investigation.

Another study investigated RRMS patients that developed progressive multifocal leukoencephalopathy (PML) under natalizumab treatment (pre-PML) and non-PML natalizumab-treated patients (168). PAI-2, uPA, uPAR, TFPI, and TM were among the top differentially expressed genes in peripheral blood mononuclear cells collected at baseline and during PML. These genes were significantly down-regulated at baseline in pre-PML patients compared to the group that did not develop PML. Although levels of serum protein of proteins encoded by the differentially expressed genes did not show significant differences (168), their evaluation in plasma would permit better evaluation.

Because glucocorticoids induce procoagulant reactions, the effect of high-dose intravenous methylprednisolone on fibrinogen, FVIII:C, vWF:Ag, TAT, prothrombin fragments 1+2 (F1+2), tPA:Ag, PAI-1 activity and plasmin-antiplasmin complexes (PAP), was investigated using a prophylactic low dose of low molecular weight heparin, which causes an internal bias (169). Whereas the fibrinogen levels significantly decreased, factor VIII:C and vWF:Ag significantly increased in the absence of evidence for fibrinolytic system activation or suppression (169). At high-dose methylprednisolone, 5 out of 188 MS patients developed venous thrombosis, which led the authors to speculate on the synergistic effect between the treatment and MS immunopathology (170), which could predispose patients to prothrombotic risk.

In RRMS under GA treatment, TM levels were significantly increased compared to the respective drug-free group and controls, regardless of the presence of current relapse. The authors speculated about a GA-induced mechanism of neuroprotection potentially leading to the generation of aPC (171).

Considering the heterogeneity of coagulation balance in MS patients and the few studies that evaluated the effect of DMTs on coagulation, prospective investigation would be of great interest and help in understanding drug-hemostasis interactions.

Case reports of autoimmunity affecting hemostasis in multiple sclerosis

Unfortunately, very few cohort studies addressed as to whether or not coagulation unbalance was supported by the immune activity. Higher frequency of antiphospholipid antibodies, belonging to the IgM family, were observed in MS patients during exacerbation (10 out of 17 patients, 2-4 fold increase) compared to remission. Noteworthy, a significant correlation between contrast-enhancing lesions and antibodies against FVII was found (172).

Case reports of autoimmunity affecting hemostasis components in MS have to be considered in light of the acquired dysregulated coagulation, underlining those components that are mainly targeted and may contribute to worsening the clinical picture. Interestingly, a few cases have been reported with TTP episodes (173) and acquired ADAMTS13 deficiency in the context of IFN- β treatment for MS (174, 175). With the limitation of their low number, these reports highlighted acquired deficiency induced by auto-antibodies against ADAMTS13. Interestingly we have reported that ADAMTS13 levels were lower in MS than in control subjects. (176, 177). Additionally, several MS patients, who received alemtuzumab treatment, developed autoimmune TTP (178, 179).

Similarly, but with anticoagulant effects, FVIII inhibitors may arise in autoimmune diseases, during and after pregnancy, and during drug therapy including IFN- α (used to

treat leukemia and blood disorders such as TTP) with the outcome of acquired severe hemophilia. The first case report of an MS patient who developed hemorrhagic disorder was described as a rare case for developing antibodies against FIX and FVIII (180). The second case of acquired FVIII inhibitor was later described (181) and an additional case was reported in a MS patient after IFN- β treatment (182). Acquired hemophilia has also been described also as an extremely rare complication in patients treated with alemtuzumab. Another case report described two sisters with MS who had a quantitative deficit of factor VIII-vWF complex (183). These phenomena could be mediated by secondary B cell-mediated autoimmune complications which lead to inhibitory autoantibodies to coagulation FVIII (184). However, a reference study for thrombophilia reported that among the 4311 patients with a first episode of venous thrombosis, 30 had MS with increased FVIII activity levels (185).

Chapter 2

Aims of the present work

An increasing number of studies are providing insights on the tight relationship among vascular alterations, neuroinflammation, autoimmunity, and neurodegeneration, supporting the contribution of hemostasis components in MS.

To improve our knowledge on this issue, the present work is focused on hemostasis and supported by multi-center research collaboration. The main goal is to highlight candidate genes/proteins in MS pathophysiology, which could also be used as disease progression biomarkers.

Taken into account the biochemical complexity underlying the interplay among hemostasis components and the multi-factorial nature of MS, the study design was planned through different levels of investigation, which include genomics, transcriptomics, and proteomics. Each of the aforementioned areas of investigation required the use of distinct methodologies with collective characterization and quantification of pools of biological molecules:

I) Whole exome sequencing was applied for the analysis of the protein-coding portion of the patients' genome. Based on the hypothesis of the contribution of low-frequency variants to MS, part of the work was focused on rare codon changes through a combination of variant prioritization strategies.

II) Microarrays were used for quantitative transcripts levels evaluation of a large number of genes in the frame of patients' vasculature alteration. Based on findings that support the interactions between vascular and neurodegenerative mechanisms of MS, the contribution of the extracranial venous compartment was questioned. This part of the study was accomplished through the expression profile analysis of internal jugular vein (which drains blood from the CNS) and related plasma protein levels evaluation.

III) Simultaneous measurement of proteins in patients' plasma using multiplex assay was applied for a comprehensive proteomic survey. Whether components of hemostatic system correlate with clinical features and levels of other plasma metabolites is still largely unknown and deserves deep investigation.

After identification of candidate proteins in MS pathophysiology, their potential application as disease progression biomarkers was explored.

Taken advantage of quantitative measurements, brain atrophy was chosen to investigate clinical disease phenotypes in relation to expression/concentration of hemostasis components, offering a unique opportunity to assess their contribution into disease course. For this purpose, MRI provided the defined quantitative measures that characterize the progression of neurodegeneration in MS patients. To note, physical disability escalation of MS, which is a more qualitative measure, was also used for the association because it is directly related to demyelination and grey matter lesions.

Among the hemostasis factors, we addressed our attention toward those which have been modestly investigated, and with the main open questions.

Few works suggested the contribution of coagulation factors in MS, and in particular, the most recent data highlight a new role for FXII, with a poorly defined role of its circulating protein levels and activation. Therefore in the first part of the work, the aim was to investigate FXII in patients by several biochemical methodologies: FXII antigen and activity were explored by ELISA and coagulation assays (aPPT) in combination with the kinetic evaluation of intrinsic thrombin generation.

Afterward, because individual measurement of hemostasis components may not capture the global effect of all these elements in MS, the systematic measurement of a panel of pro-coagulant and anti-coagulant proteins in plasma was performed. In particular, the goal was to assess if anticoagulant/anti-inflammatory components are candidates to play a protective role in disease progression.

Hemostasis inhibitors were selected for representing the regulation of the coagulation system on different levels. In particular: I) TFPI is the first line of extrinsic coagulation inhibition, acting against TF:FVIIa:FXa; II) HCII has an inhibitory action against thrombin, supported by specific glycosaminoglycans (GAGs); III) TM as soluble form may reflect endothelial damage; IV) ADAMTS13 regulates platelet adhesion and aggregation, which represents a cell-based model mechanism of inhibition; V) PAI-1 is the inhibitor of fibrinolysis, whose impairment has been reported in MS lesions.

Therefore, investigation of inhibitors plasma levels in association with clinical and MRI measures was performed. Of note, given the important roles of hemostasis components in the regulation of bleeding and iron deposition, the association analysis was also accomplished with cerebral microbleeds frequency and quantitative susceptibility mapping (QSM) of deep gray matter structures respectively, both quantitatively measured by MRI.

Moreover, thanks to the expression data from the transcriptomics approach, further investigation of selected candidate proteins were accomplished in associations with MS features, both MRI and clinical phenotypes.

With the limitation of the time frame of a Ph.D. program, the embrace of multidisciplinary approaches was aimed to expand, through an integrated view, our understanding of the biological role of hemostasis components in MS.

Expectations/contribution to the field:

- Plasma protein levels in patients, grouped by phenotype, and in controls.
- Correlations between plasma level variation of components of the hemostatic system and clinical indices and MRI data.
- Plasma level variation of components of the hemostatic system as plasma biomarkers of the disease and its forms/progression.
- Results could highlight vascular mediators playing a role in the crosstalk between hemostasis- inflammation- immunity interactions in MS.
- Improved knowledge of the hemostasis components in MS could favor the design of strategies aimed at combatting the disease through specific inhibition of pro-coagulant factors or potentiation of the anticoagulant/anti-inflammatory pathway.
- Identification of low-frequency and functional variants associated with MS.

Chapter 3

Study populations

3.1 ITALIAN STUDY POPULATIONS

The Italian study population for FXII investigation

The Italian study population for FXII investigation included MS patients, the majority of which participated in the RAGTIME study (ClinicalTrials.gov ID:NCT02421731) (186). This clinical trial compares robot-assisted gait training versus conventional therapy on mobility in severely disabled progressive MS patients.

All MS patients underwent neurological visits, MRI examinations, and assessment of the Expanded Disability Status Scale (EDSS). Subjects with the following characteristics were included in the present study: age between 18 to 79 years, MS diagnosis according to the revised McDonald criteria (187), lack of MS worsening in the previous 3 months.

Table 3.1. Demographic and clinical characteristics of the Italian study population.

	All MS	RR-MS	SP-MS	PP-MS	HS
Sample size, n	74	12	34	28	49
Female, n (%)	48 (64.9)	8 (66.7)	19 (55.9)	21 (75)	25 (51)
Age, mean±SD	53.5±10.7	43.5±9	52.2±8.9	59.3±9.9	40.6±13.3
EDSS, median (IQR)	6 (0.5)	3 (2)	6.5 (0.5)	6 (0.5)	-
Disease duration, mean±SD	14.4±10.0	7.4±5.2	18.0±8.1	13.5±11.7	-
Treatment, n (%)					
Disease-modifying	5 (6.8)	-	1 (2.9)	4 (14.3)	
Symptomatic	17 (22.9)	-	7 (20.6)	10 (35.7)	-
Both	7 (9.5)	1 (8.3)	5 (14.7)	1 (3.6)	
None	45 (60.8)	11 (91.7)	21 (61.8)	13 (46.4)	

Age and disease duration in years are reported as mean ± standard deviation. For the ordinal EDSS, the median (interquartile range) is given.

DMTs were as follow: 1 (RR) Rituximab; 1 (SP) interferon-beta; 1 (SP) glatiramer acetate; 1 (SP) methotrexate; 1 (SP) teriflunomide; 2 (1 SP and 1 PP) fingolimod; 2 (1 SP and 1 PP) azathioprine; 2 (PP) natalizumab; 1 (PP) cyclophosphamide.

Symptomatic treatments were as follow: 16 (1 RR, 6 SP and 9 PP) oral baclofen; 2 (SP) Pregabalin; 1 (SP) oral baclofen plus gabapentin; 1 (SP) tetrahydrocannabinol plus cannabidiol; 1 (SP) combination of clonazepam, tetrahydrocannabinol and cannabidiol; 2 (1 SP and 1 PP) oral baclofen plus amitriptyline; 1 (PP) amantadine.

Legend: MS, Multiple Sclerosis; RR-MS, Relapsing Remitting Multiple Sclerosis; SP-MS, Secondary Progressive Multiple Sclerosis; PP-MS, Primary Progressive Multiple Sclerosis; HS, Healthy Subjects; n, number; SD, standard deviation; EDSS, Expanded Disability Status Scale; IQR, interquartile range.

The healthy subjects (HS) group was represented by healthy volunteers, who were never diagnosed with MS, neurological disorder, other chronic inflammatory disease and cardiovascular disease. Patients were not under treatment with anticoagulant drugs.

Written informed consent was obtained from all subjects, and the study was approved by the Ethical Committee of the S. Anna University-Hospital, Ferrara, Italy.

The demographic and clinical characteristics of this Italian study population, which included 74 MS patients and 49 HS, are summarized in Table 3.1.

The Fisher's exact test was used to compare differences in categorical variables and Student's *t*-test was used to compare age between total MS and HI groups.

Age was significantly different between MS and HS ($p < 0.001$, Student *t*-test, Table 1), while the gender difference was not significant ($p = 0.138$, Fisher's exact test).

The total number of patients under disease-modifying treatments (DMTs) at blood sampling was 12 (5 patients under DMTs and 7 patients under both DMTs and symptomatic treatments), as detailed in Table 3.1. Five patients (three RR-MS and two SP-MS) with discontinuation of DMTs before their enrollment in the present study were included in the group "None treatment" since at sampling they were not under treatment.

Italian study populations for the transcriptomic-based approach

The first (1st) study population was represented by a group of 19 Italian subjects with MS and positive screening CCSVI. Diagnosis of MS was in accordance to the McDonald criteria (188). Patients' screening through flow quantification by means of a combination of validated echo-color Doppler (ECD) model with magnetic resonance venography morphological and flow evaluation protocol, and cerebral perfusion evaluation by SPECT-CT, have been previously detailed (189-191). The patients presented truncular venous malformation in at least one IJV, in form of segmental hypoplasia, defective valves with incomplete or absent opening of their leaflets, other intraluminal obstacles, and muscular compression. The 19 patients belonged to a cohort of patients who were eligible for surgical reconstruction of internal jugular vein by angioplasty and entered the study approved by the Ethical Committee of the S. Anna University-Hospital of Ferrara. The details about enrolment and inclusion/exclusion criteria have been previously described (191). 1st MS population demographics are reported in Table 3.2.

The second (2nd) study population included 60 Italian MS patients, who participated in the RAGTIME study (ClinicalTrials.gov ID:NCT02421731) (186). This clinical trial compares robot-assisted gait training versus conventional therapy on mobility in severely disabled progressive MS patients. The demographics and clinical characteristics of the 2nd MS population are reported in Table 3.3.

Thirty-four Italian healthy subjects (mean age 41.3 ± 9.0 ; 21 women and 13 men), who have never diagnosed with MS, neurological disorder or other chronic inflammatory diseases, were recruited for protein level analysis in plasma. Eight healthy subjects were recruited and added to the healthy group (total subjects= 42; mean age 41.29 ± 11.4 ; 26 women and 16 men) as control for the 2nd study MS population.

Table 3.2. First study population demographics.

	MS-CCSVI Patients n= 19	Healthy subjects n= 34
Age, mean \pm SD	46.5 \pm 8.6	41.3 \pm 9
Gender, M/F	10/9	13/21
MS clinical class		
RR	11	-
SP	7	
PP	1	
Disease duration RR, mean \pm SD	10 \pm 4	-
Disease duration SP – PP, mean \pm SD	13 \pm 4	-
EDSS, mean \pm SD	4 \pm 2	-
MRI T1 gadolinium-enhancing lesions, n	5/19	-
M-mode IJV defective valves, n	29/38	-

Age and disease duration are reported in years.

Legend: RR, relapsing remitting; SP, secondary progressive; PP, primary progressive; EDSS, expanded disability status scale; M-mode, echo Doppler.

Table 3.3. Demographics and clinical characteristics of the 2nd study MS population.

	All cohort n= 60	PP-MS n= 28	SP-MS n= 32
Age, mean \pm SD	55.5 \pm 10.5	58.5 \pm 11.1	52.8 \pm 9.3
Gender, M/F	21/39	6/22	15/17
Disease duration, mean \pm SD	15.1 \pm 10.5	12.6 \pm 11.7	17.35 \pm 8.7
EDSS, mean \pm SD	6 \pm 0.5	6 \pm 0.5	6.5 \pm 0.5

Age and disease duration are reported in years.

Legend: RR, relapsing remitting; SP, secondary progressive; PP, primary progressive; EDSS, expanded disability status scale.

3.2. US STUDY POPULATION

The US study population included subjects who participated in a case-control study of cardiovascular, environmental and genetic risk factors for disease progression in patients with MS (CEG-MS study; IRB ID: MODCR00000352) (42).

The selection criteria for the study included: a) having MS according to the revised McDonald criteria (192), b) having relapsing-remitting (RR-MS) or progressive (P-MS) course or being a healthy individual (HI), c) having an MRI scan on the same 3T scanner using a standardized MRI protocol, d) age between 18–75 years and e) physical/neurologic examination within 30 days from the standardized MRI study protocol. The exclusion criteria consisted of: a) presence of relapse and steroid treatment within the 30 days preceding study entry, b) pre-existing medical conditions known to be associated with brain pathology (e.g., neurodegenerative disorders, cerebrovascular disease, positive history of alcohol abuse, etc.) and c) pregnancy.

All subjects underwent to neurological and MRI examinations and EDSS was assessed in MS patients. The study protocol was approved by the local Institutional Review Board and all participants gave their written informed consent.

Demographic and clinical information of the 138 MS patients (85 RR-MS, 53 P-MS) and the 42 HI subjects enrolled in the present study are reported in Table 3.4. The Fisher's exact test was used to compare differences in categorical variables and Student's t-test was used to compare age between total MS and HI groups. The demographic characteristics of the MS and HI groups were similar: the frequency of females to males was 72.5% in MS vs. 73.8% in HI ($p=1.0$) and the mean age in the MS group ($54.3 \pm SD 10.8$ years) was similar ($p=0.27$) to that in the HI group (51.0 ± 14.3 years). The majority of MS patients were on DMT; only 19.6% were not on DMT.

MRI Acquisition and Image analysis of US study population

The neurological and MRI examinations of the cohort have been performed by the clinicians at the Buffalo Neuroimaging Analysis Center (BNAC) in Buffalo, USA.

MRI acquisition and imaging analysis were conducted as follow. Subjects were examined on a General Electric (GE) 3T Signa Excite HD 12.0 scanner (Milwaukee, WI) using an eight-channel head and neck coil.

Acquisition of 2D T2/PD-weighted images (WI), fluid-attenuated inversion recovery (FLAIR), spin-echo T1-WI without gadolinium contrast, 3D high-resolution T1-WI and susceptibility-weighted imaging (SWI) was performed. In particular, 2D sequences were acquired using a 256×192 matrix and $256 \times 192 \text{mm}^2$ FOV, resulting in a nominal in-plane resolution of $1 \times 1 \text{mm}^2$. 48 gap-less 3mm thick slices were acquired for whole-brain

coverage. Sequence-specific parameters were: dual FSE proton density and T2-WI (TE1/TE2/TR=9ms/98ms/5300ms; echo-train length=14), 4:31 min long; FLAIR (TE/TI/TR=120ms/2100ms/8500ms; flip angle=90°; echo-train length=24), 4:16 min long; and spin-echo T1-WI (TE/TR=16ms/600ms), 4:07 min long. In addition, a 3D high-resolution T1WI fast spoiled gradient echo sequence with a magnetization-prepared inversion recovery pulse was acquired (TE/TI/TR=2.8ms/900ms/5.9ms, flip angle=10°), 4:39 min long, with 184 slices of 1mm thickness, resulting in isotropic resolution. SWI was acquired using an unaccelerated 3D single-echo spoiled GRE sequence with first-order flow compensation in read and slice directions, a matrix of 512x192x64 and a nominal resolution of 0.5 x 1 x 2 mm³ (FOV=256x192x128 mm³), flip angle = 12°, TE/TR=22ms/40ms, bandwidth=13.89 kHz, and 8:46 min acquisition time (42).

MRI analysts were blinded to the subject's physical and neurologic condition.

For the image analysis, T2- and T1 lesion volumes (LV) were assessed using a semi-automated edge detection contouring/thresholding technique (193). Prior to tissue segmentation, lesion filling was utilized to minimize the impact of T1 hypointensities (194). SIENAX software (version 2.6 (195)) was used for normalized brain volume (NBV) extraction and sub-segmentation of volumes which made gray matter (GMV), white matter (WMV), cortex (CV) and lateral ventricles (LVV). Deep gray matter (DGM) volume and thalamic volume were calculated using FIRST (196), and subsequently normalized using the SIENAX-derived scaling factor.

Magnitude and phase GRE images were reconstructed offline (197). To achieve isotropic in-plane resolution, the k-space was zero-padded in phase-encode direction prior to the processing. In-plane distortions due to imaging gradient non-linearity were compensated (198). Phase images were unwrapped with a best-path algorithm (199), background-field corrected with V-SHARP (radius 5mm; TSVD threshold 0.05) (200) and converted to magnetic susceptibility maps using the HEIDI algorithm (201). Magnetic susceptibility (QSM) was referenced (0 ppb) to the average susceptibility of the brain. All data processing was performed with in-house developed algorithms in MATLAB (2013b, The MathWorks, Natick, MA) (202).

Cerebral microbleeds (CMBs) analysis was performed on SWI minimum intensity projection images and susceptibility maps by two experienced neuroimagers who were also blinded to MR images obtained with other sequences. CMBs were classified as focal, small, round to ovoid punctuate areas of signal hypointensity on SWI minimum intensity projection images (42). Signal voids caused by sulcal vessels, calcifications, and signal averaging from bone were considered mimics of microbleeds. The presence and number of definite CMBs were determined on SWI minimum intensity projection images by using the

Microbleed Anatomic Rating Scale (203). The CMB volume was calculated on susceptibility maps by using a semi-automated edge detection contouring and thresholding technique (193).

Lesions, CMBs and brain volumes of the US study population used for the investigations, are reported in Table 3.5. Student's t-test was used to compare brain volume measurements between total MS and HI groups. As expected, all brain MRI measures were significantly different between total MS and HI (Table 3.5).

Table 3.4. Demographic and clinical characteristics of the cohort.

	All MS	RR-MS	P-MS	HI
Sample size, n	138	85	53	42
Female, n (%)	100 (72.5)	60 (70.6)	40 (75.5)	31 (73.8)
Age, years	54.3±10.8	50.1±10.7	60.9±7.2	51.0±14.3
BMI	27.6±6.0	27.9±6.4	27.2±5.5	26.1±5.5
Age onset in years	32.9±9.5	32.6±9.1	33.3±10.1	-
Disease duration, years	21.1±10.6	17.0±8.8	27.6±10.0	-
EDSS, median (IQR)	3.5 (2-6)	2 (1.5-3.5)	6 (4-6.5)	-
Annual relapse rate	0.2 (0.4)	0.2 (0.4)	0.1 (0.3)	-
DMT status, n (%)				
Interferon-beta	45 (32.6)	30 (35.3)	15 (28.3)	
Glatiramer acetate	42 (30.4)	23 (27.1)	19 (35.9)	
Natalizumab	5 (3.6)	4 (4.7)	1 (1.9)	-
Other DMT*	19 (13.8)	13 (15.3)	6 (11.3)	
No DMT	27 (19.6)	15 (17.6)	12 (22.6)	

All continuous variables (age and disease duration) are mean ± standard deviation. For the ordinal EDSS, the median (interquartile range) is given. Body mass index (BMI) was derived from the subject's height and weight.

46 secondary-progressive and 7 primary-progressive MS were categorized in P-MS group for the purpose of the analyses.

* Other DMTs included intravenous immunoglobulin, mitoxantrone and methotrexate.

Legend: MS: Multiple Sclerosis; RR-MS: Relapsing Remitting Multiple Sclerosis; P-MS: Progressive Multiple Sclerosis; HI: Healthy Individuals; BMI: body mass index; EDSS: Expanded Disability Status Scale; IQR: interquartile range; SD: standard deviation; n: number; DMT: disease-modifying treatment.

Table 3.5. MRI characteristics of the US study cohort.

	All MS n=138	RR-MS n=85	P-MS n=53	HI n=42	MS vs. HI <i>p</i> -value
T2-LV, ml	15.8 ± 19.0	11.8 ± 15.9	22.2 ± 21.9	0.2 ± 0.6	< 0.001
T1-LV, ml	2.9 ± 6.2	2.0 ± 4.6	4.4 ± 8.1	0.0 ± 0.0	< 0.001
NBV, ml	1438 ± 92.1	1469 ± 82.4	1387 ± 85.2	1528 ± 97.9	< 0.001
NCV, ml	591 ± 48.6	606 ± 44.8	567 ± 44.8	630 ± 53.3	< 0.001
LVV, ml	55.1 ± 27.0	50.7 ± 5.2	62.3 ± 28.5	32.2 ± 14.5	< 0.001
DGM volume, ml	53.6 ± 7.1	55.5 ± 6.5	50.4 ± 6.9	60.5 ± 46.4	< 0.001
Thalamic volume, ml	17.7 ± 2.5	18.4 ± 2.3	16.5 ± 2.4	20.3 ± 1.9	< 0.001
QSM DGM	26.1 ± 5.9	25.5 ± 5.6	27.0 ± 6.1	25.3 ± 6.4	0.470
Cerebral Microbleeds (CMB)					
Individuals with CMB, n (%)	12 (9.6)	5 (6.3)	7 (15.2)	3 (7.3)	
Number of CMB:					
NA	13	6	7	1	
0	113	74	39	38	
1	9	4	5	2	
2	2	-	2	-	
≥ 3	1	1	-	1	
CMB volume, mm³	22.9 ± 21.0	33.4 ± 29	15.4 ± 9.8	14.8 ± 13.7	

Lesion and brain volumes are expressed in milliliters and QSM values in part per billion. Data are reported as mean ± standard deviation.

P-values represent MS and HI group comparisons and were derived using Student's t-test.

10 CMBs patients were under the following DMTs: 6, glatiramer acetate; 2 interferon-beta; 1, natalizumab; 1, fingolimod.

Legend: MS: Multiple Sclerosis; RR-MS: Relapsing Remitting Multiple Sclerosis; P-MS: Progressive Multiple Sclerosis; HI: Healthy Individuals; LV: lesion volume; NBV: normalized brain volume; NCV: normalized cortical volume; LVV: lateral ventricular volume; DGM: deep grey matter; QSM: quantitative susceptibility mapping; n: number; NA: data not available.

Chapter 4 Coagulation FXII levels and intrinsic thrombin generation in multiple sclerosis

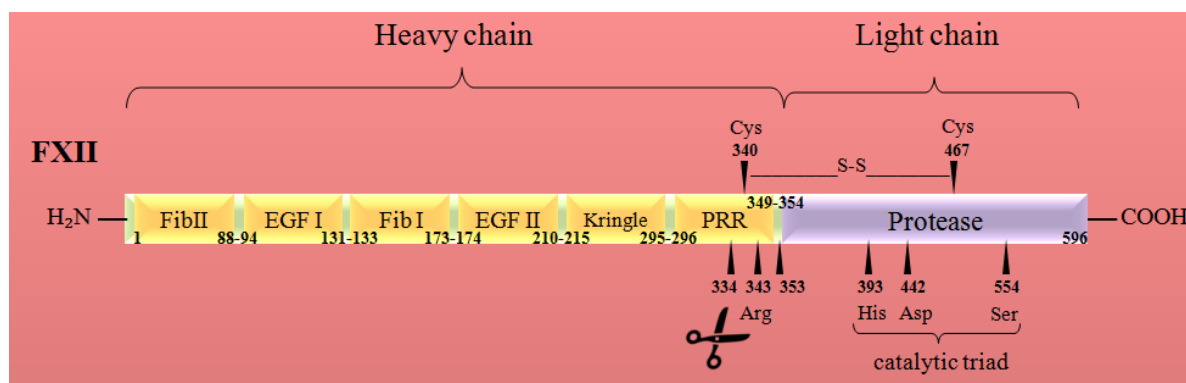
Ziliotto N, Baroni M, Straudi S, Manfredini F, Mari R, Menegatti E, Voltan R, Secchiero P, Zamboni P, Basaglia N, Marchetti G, Bernardi F.

Based on:
Front. Neurol. 2018; 9:245
doi:10.3389/fneur.2018.00245

4.1 BACKGROUND AND RATIONALE

As already introduced, FXII also called Hageman factor, is the initiator of the intrinsic pathway of the coagulation cascade (204-206). It is a glycoprotein produced by the liver as zymogen, with a molecular weight of 80 kDa. The FXII self-activation is triggered by interaction with negative charges that can be presented by surfaces containing non-soluble activators, or by anionic polymers which are soluble (207). In both cases, this interaction determinates a conformational change (208). Recent findings suggest that inactive FXII has a very low intrinsic proteolytic activity (103). After activation of the contact system, activated FXII (FXIIa) is exponentially accumulated (supported by the KAL activation loop) conferring the full pro-coagulating activity of the FXII (209). The basic FXII protein structure consists of a N-terminal heavy chain with six domains for substrates interaction, and a C-terminal light chain which includes the catalytic domain, with a molecular weight of 50 kDa and 30 kDa, respectively (Figure 4.1) (103, 207, 210, 211). The heavy and light chains are linked by a disulfide bridge between Cysteine 340 and Cysteine 467 as result of self-activation or activation mediated by KAL. The proteolytic domain in FXII light chain consists of the catalytic triad Histidine 393, Aspartic acid 442, and Serine 544 (Figure 4.1) (212-214). Two main isoforms of FXIIa are described in literature: i) α FXIIa is produced by self-activation or mediated by KAL with a cut after Arginine 353, which essential for the development of enzymatic activity; ii) β FXIIa derives from a subsequent cut at the Arginine 334 with releasing of the activated light chain fragment which promotes the contact system activation in a fluid phase (103, 214-216). Another cut at Arginine 343 is known to occurs instead of Arginine 353, but the functional consequences still remain to be elucidated (214, 217).

Figure 4.1. Schematic structure of FXII.



Amino acids 1-88 fibronectin type II domain, 89-130 EGF-like domain, 131-173 fibronectin type I domain, 174-210 EGF-like domain, 211-295 kringle domain, 296-349 proline-rich region, 354-596 catalytic domain or light chain. Amino acids 1-353 constitute the heavy chain.

In the figure are shown I) the disulfide bridge between Cysteine 340 and Cysteine 467; II) the catalytic triad Histidine 393, Aspartic acid 442, and Serine 544; III) the cleavage sites represented by Arginines.

However, it has been proposed that instead of being an auxiliary site of activation of FXII, it is a functional control site for its enzymatic activity towards specific substrates, since the sequence has 9 amino acids less.

Recently it has been shown that in EAE, FXII depletion had protective effects, reducing susceptibility to CNS inflammation, delaying disease onset, decreasing disease severity and production of T helper 17 (Th17) cells (52). In mice, FXII stimulates expression of the CD87 receptor (known also as uPAR) on dendritic cells (DCs), which is crucial for inducing Th17 cells differentiation. CD87/uPAR, a key receptor in the plasminogen-urokinase activation system, mediates plasminogen activation to plasmin at endothelial cell level as well as FXII-mediated cell signaling influencing angiogenesis (218). Because CD87/uPAR does not have an intracellular domain, the study also identified integrin CD11b as a membrane adapter and mediator of signaling for the excessive production of cytokines induced by FXII via CD87/uPAR (52). To note, both FXIIa and zymogen FXII forms were found to modulate conventional DCs function inducing excessive production of cytokines during neuroinflammation in CNS. The study also measured the amount of fibrin(ogen) in the CNS of the EAE depleted of FXII compared to wild-type EAE mice, demonstrating the absence of differences. In support of these findings, FXI deficiencies (directly activated by FXIIa) do not alter the clinical course, demyelination and cytokine levels or the infiltration of immune cells in the CNS of EAE model. The result supports the hypothesis that FXII does not participate through the system of the intrinsic coagulation pathway. Nevertheless, the FXII levels in plasma are usually assessed by a procoagulant assay (FXII:c). In fact, FXII:c has been found significantly increased in patients with relapsing-remitting MS (RR-MS) and secondary progressive MS (SP-MS) compared with healthy donors. Additionally, enhanced FXII:c was associated with relapses and shorter relapse-free period, independently from immune-modulatory therapy (52). Furthermore, histological analysis of CNS tissue from MS patients identified FXII light chain depositions nearby DCs expressing CD87/uPAR (52). It has been proposed that FXII inhibition could represent a new approach in MS therapy, as indicated by the reduced number and severity of relapses in the EAE mouse model by injection of a recognized FXII inhibitor (52, 106). This would probably not cause bleeding tendency in patients, because it is well known that FXII deficiency does not compromise effective hemostasis (219, 220). Interestingly, clinical and genetic reports point at a FXII role in thrombosis (105, 221, 222). Local and systemic thrombotic events have been described in MS potentially in relation to the over-stimulation of innate immunity for both its inflammatory and coagulant components (223). Recently, the hypercoagulability and potentially prothrombotic state in MS patients has been investigated by thrombin generation (TG),

triggered by extrinsic activation (145). The poorly defined role of FXII forms and features, and the paucity of studies in patients, strongly support the investigation of FXII in MS. The aim of the study was to investigate multiple FXII-related variables, as well as FXII activation in the intrinsic thrombin generation (TG), to explore their association with MS.

4.2 MATERIALS AND METHODS

Study population

The demographic and clinical characteristics of the study populations, which included 74 MS patients (12 RR-MS; 28 PP-MS; 34 SP-MS) and 49 HS, are summarized in Table 3.1 (page 33).

Plasma samples

Venous peripheral blood samples from both MS patients and HS were collected into sodium citrate tubes. Patients enrolled in the RAGTIME study, provided blood sampling at four time point: T0) baseline point, prior to the first rehabilitative session; T1) intermediate point, after six training sessions; T2) end of treatment, 12 completed rehabilitative sessions, 1 month after T0; T3) follow-up, after 3 months from the end of training program. Plasma samples were obtained after two consecutive centrifugations of blood samples, at room temperature (2500g for 15 min and 11000g for 5 min). Aliquots were stored at -80°C until use.

FXII activity and FXII antigen

Coagulant activity of FXII (FXII:c) in plasma samples was assessed by an activated partial thromboplastin time (aPTT)-based assay (HemosIL aPTT SynthASil kit, Instrumentation Laboratory, Lexington, MA, USA). Activity and coagulation times were recorded by the ACLTOP 700 instrument (HemosIL, Instrumentation Laboratory). The inter-assay coefficient of variation, assessed over multiple runs, was 2.1%.

Plasma FXII antigen (FXII:Ag) concentrations were determined using a sandwich enzyme-linked immunosorbent assay (ELISA) kit (LS-F10418, LifeSpan Biosciences, Seattle, WA, USA), following the manufacturer's instructions. The assay uses a polyclonal capture antibody for FXII and a mouse primary monoclonal antibody raised against the heavy chain of FXII as detection antibody. The plasma samples were tested with a dilution of 1:3000. The results were expressed as relative units in percentage generated from concentration values normalized to a pool normal plasma loaded in all plates. The inter-assay coefficient of variation for plasma measurements was 2.6 %.

Intrinsic thrombin generation

Thrombin generation (TG) in plasma samples was evaluated by the addition of a specific thrombin fluorogenic substrate (Calbiochem-Novobiochem, La Jolla, CA, USA) (224, 225). Plasma samples were diluted (1/5) in a HBS buffer (Hepes 20 mM, NaCl 150 mM, PEG-8000 0.1%, pH 7.4) and incubated for 5 minutes at 37°C. TG through intrinsic activation was conducted by addition of a volume mixture of ellagic acid (Dade Actin FS, Siemens) and phospholipid vesicles (4 μ M, MP-reagent, Stago), as previously reported (226, 227). TG was also evaluated by further addition of nucleic acid (NA) as trigger (1 μ M) for the activation. Final concentrations of CaCl₂ and thrombin fluorogenic substrate were 2.5 mM and 250 μ M, respectively. The fluorescence was measured over time in a fluorometer (Fluoroskan Ascent BioMed) and the amount of the generated thrombin was calculated using a normal pooled human plasma (Hyphen BioMed) as a standard. As negative control of contact activation the FXII inhibitor “corn trypsin inhibitor” was added to the normal pooled plasma in each assay condition (single/double trigger).

Specific parameters of TG -lag time, time to peak (TTP), peak height and endogenous thrombin potential (ETP, area under the curve)- were obtained by a nonlinear regression analysis of the first derivative of relative fluorescence units (RFU) using the software version 6.01 (GraphPad Software, Inc. La Jolla, CA, USA).

Statistical analysis

All statistical analyses were performed using IBM® SPSS® Statistics version 24 software (IBM Corp. Armonk, NY, USA) and figures were produced by GraphPad Prism version 6.01 (GraphPad Software, Inc. La Jolla, CA, USA).

The Shapiro-Wilk test was used to test for normality of continuous variables. Comparisons of MS vs. HS and of males vs. females of FXII:c, FXII:Ag and FXII:c/FXII:Ag ratio (FXII:ratio), were conducted with the ANCOVA test using age as covariate. Comparisons for FXII levels among clinical subgroups were performed with ANCOVA test using age as covariate and, in case of a significant p-value, pairwise comparisons were Bonferroni corrected for multiple testing (q-values).

To assess whether FXII levels were significantly different among patients receiving DMTs, symptomatic treatments, or none current treatment, one-way ANOVA was used and, in case of a significant p-value, pairwise comparisons were Bonferroni corrected for multiple testing (q-values).

Pearson's test was used to assess correlation over time for FXII:c and FXII:Ag. ANOVA for repeated measures was used to test FXII:c, FXII:Ag and FXII:ratio across the four-time points and, in case of a significant p-value, pairwise comparisons were Bonferroni corrected (q-values). Student's t-test was used to compare TG parameters of MS patients

with those of HS, while paired Student's t-test was used to assess differences in TG after NA addition in MS and HS.

4.3 RESULTS AND DISCUSSION

In this study, multiple FXII-related variables were investigated to better define the relation between FXII and disease. This approach was coupled with a global evaluation of the intrinsic pathway, with FXII activation obtained by artificial and natural molecules. The main aims were to reveal differences between MS patients and HS, among MS clinical phenotypes, and in addition to evaluate in MS patients the variation over time of FXII-related variables.

FXII coagulant activity (FXII:c), FXII protein concentration (FXII:Ag) and their ratio, providing quantitative information about the FXII activity in relation to the amount of circulating protein, were evaluated in plasma of MS patients and of HS and summarized in Table 4.1. Comparison between MS and HS groups revealed significant differences in FXII:Ag ($p=0.003$) and FXII:ratio ($p<0.001$) but not in FXII:c ($p=0.421$). No differences within clinical subgroups (RR-MS, SP-MS and PP-MS) were detected for FXII:c ($p=0.296$), FXII:Ag ($p=0.248$) and FXII:ratio ($p=0.765$). Comparison between male and female within MS and HS groups, after age adjustment, did not reveal difference in FXII:c (MS $p=0.74$, HS $p=0.374$), FXII:Ag (MS $p=0.256$, HS $p=0.622$), and showed a trend in difference in FXII:ratio in HS ($p=0.045$) but not in MS ($p=0.11$).

The investigation on FXII:Ag revealed significantly increased levels in MS patients. FXII:Ag provides information about the concentration of circulating FXII protein independently from its activation and activity, the presence of inhibitors, and other factors participating in the coagulation pathway. Here, it was not observed, even as a trend, higher levels of FXII:c in RR-MS and SP-MS patients compared to HS as reported by a previous study (52). However in the current investigation, the cohorts were smaller (with exception of the PP-MS group) than those of the German study and, in accordance with our study design, FXII:c was not investigated during relapse. Further comparison between data in German and Italian MS patients is hampered by the absence of information about FXII protein levels (FXII antigen) in German patients. Nevertheless, the increased FXII:Ag levels detected in Italian MS patients and the increased FXII:c detected in German MS patients are both candidates to increase FXII-related immunomodulatory function.

Table 4.1. FXII activity, antigen, and ratio in multiple sclerosis patients and healthy subjects.

	Multiple Sclerosis						Healthy Subjects			MS vs HS
	<i>N</i>	Female	Male	RR	PP	SP	Female	Male	P-value	
	74	48	26	12	28	34	49	25	24	
FXII:c %										0.421
Mean	115.0	113.9	116.9	111.3	115.0	116.2	123.7	127.5	119.8	
Lower 95% CI	110.3	108.7	107.1	97.3	108.5	108.3	116.5	115.3	111.7	
Upper 95% CI	119.7	119.1	126.7	125.2	121.5	124.1	130.9	139.8	127.8	
FXII:Ag %										0.003
Mean	106.7	102.7	114.2	106.2	108.1	105.8	99.3	99.0	99.6	
Lower 95% CI	99.3	93.6	101.0	85.3	95.2	94.8	91.4	85.5	90.5	
Upper 95% CI	114.1	111.7	127.4	127.1	121.0	116.8	107.2	112.5	108.8	
FXII:ratio										<0.001
Mean	1.14	1.18	1.06	1.09	1.15	1.15	1.30	1.36	1.24	
Lower 95% CI	1.07	1.09	0.98	0.96	1.02	1.06	1.22	1.23	1.14	
Upper 95% CI	1.21	1.28	1.13	1.21	1.27	1.25	1.38	1.48	1.33	

MS, Multiple Sclerosis; HS, Healthy Subjects; RR-MS, Relapsing Remitting Multiple Sclerosis; SP-MS, Secondary Progressive Multiple Sclerosis; PP-MS, Primary Progressive Multiple Sclerosis; FXII:c, Factor XII activity; FXII:Ag, Factor XII Antigen; FXII:ratio, FXII:c/FXII:Ag; CI, confidence interval; N, number. Analysis were conducted with the ANCOVA test, using age as covariate.

Of note, both FXII protein forms, the zymogen, and the active ones, would express the immunomodulatory role independently from FXII activation in the coagulation pathway.

Aimed at improving knowledge about the FXII role in the disease, we provided quantitative information about the FXII procoagulant activity in relation to the amount of circulating protein, by evaluating their ratio. This analysis indicated a significantly lower FXII:ratio in MS patients. This novel finding prompted us to investigate in selected groups of MS patients and HS the intrinsic pathway by TG, which provides kinetic information and potentially mechanistic interpretation of differences (see next paragraph).

The potential modulation of FXII levels by treatments was investigated. Patients under both DMTs and symptomatic treatments (Table 3.1, page 33) were categorized in DMTs group for the purpose of the analyses. No difference according to DMTs, symptomatic treatments, or none current treatments were detected for FXII:c ($p=0.98$), FXII:Ag ($p=0.81$) and FXII:ratio ($p=0.97$).

The low number of patients under DMTs and the extremely heterogeneous DMTs did not permit a productive analysis of FXII levels in relation to DMTs. Nevertheless, these study features enabled us to obtain FXII- related values reasonably independent from drugs, like interferon that is known to heavily influence gene expression in several tissues. These values could better reflect the "biological" relation between FXII and (untreated) disease. On the other hand, the investigation of DMTs effects on FXII-related variables in a properly designed study would provide a comprehensive picture of this poorly defined field. A large portion of patients under study were characterized by a small range of EDSS (6-6.5), which does not favor the investigation of the relation between EDSS and FXII levels.

Repeated evaluation over 4 months of FXII:c, FXII:Ag levels and FXII:ratio were instrumental to investigate their variation over time in patients. FXII:c, FXII:Ag and FXII:ratio levels were also investigated over 4-time points (Table 4.2) in 49 MS (23 PP-MS and 26 SP-MS). A significant difference over time was detected for FXII:c ($p=0.031$, Table 4.2). In particular pairwise analysis revealed differences between T0-T1 ($p=0.004$; $q=0.023$) and T0-T3 ($p=0.005$; $q=0.027$). The potential influence on FXII:c over time variations of MS phenotype or drug treatments was investigated. Differences were not detected within each clinical MS group (SP-MS, $p=0.079$; PP-MS, $p=0.093$), as well as within drug treatment groups (DMTs, $p=0.188$; symptomatic treatment, $p=0.345$; none, $p=0.142$). No differences over time were detected for FXII:Ag ($p=0.596$) and FXII:ratio ($p=0.151$) (Table 4.2).

Table 4.2. FXII activity, antigen, and ratio in multiple sclerosis patients over four-time points.

	Time points				P-value
	N 49	T0	T1	T2	
FXII:c %					0.031
Mean		114.5	110.4	114.1	110.0
Lower 95% CI		108.6	104.5	107.3	103.8
Upper 95% CI		120.4	116.3	120.8	116.2
FXII:Ag %					0.596
Mean		105.1	107.8	108.8	105.8
Lower 95% CI		95.87	98.06	99.54	96.87
Upper 95% CI		114.4	117.5	118.0	114.8
FXII:ratio					0.151
Mean		1.16	1.10	1.10	1.09
Lower 95% CI		1.07	1.01	1.03	1.02
Upper 95% CI		1.25	1.18	1.17	1.16

FXII:c, Factor XII activity; FXII:Ag, Factor XII antigen; FXII:ratio, FXII:c/FXII:Ag; CI, confidence interval; N, number.
ANOVA for repeated measures was used to test FXII:c, FXII:Ag and FXII:ratio across the four time points.

Table 4.3. Correlations of factor XII activity and antigen over four-time points in multiple sclerosis patients.

	T0	T1	T2
FXII:c			
T1	0.90		
T2	0.80	0.82	
T3	0.88	0.84	0.75
FXII:Ag			
T1	0.81		
T2	0.81	0.79	
T3	0.63	0.70	0.84

Pearson's test was used to assess correlation over time for factor FXII activity (FXII:c) and antigen (FXII:Ag).

T0) baseline point, prior to the first rehabilitative session; T1) intermediate point, after six training sessions; T2) end of training, 12 completed rehabilitative sessions, 1 month after T0; T3) follow-up, after 3 months from the end of training program.

Interestingly, FXII:c was the only one to display a trend for variation across the time points. This could highlight changes dependent on the rehabilitative treatment, as inferred by comparison of FXII:c at T0 and T1 time points, as well as independent from treatment, as inferred by measurements prior and after three months of the rehabilitative training program (T0 vs T3). Noteworthy, analysis of correlations among time points for each FXII parameter (Table 4.3) showed that FXII:c levels were highly correlated (T0-T1, $r^2=0.90$; T1-T2, $r^2=0.82$; T2-T3, $r^2=0.75$; $p<0.001$) as well as FXII:Ag levels (T0-T1, $r^2=0.81$; T1-T2, $r^2=0.79$; T2-T3, $r^2=0.84$; $p<0.001$). High correlation among time points for each FXII parameter was observed. This feature could support a meaningful investigation of FXII contribution to disease phenotype and progression in future prospective studies.

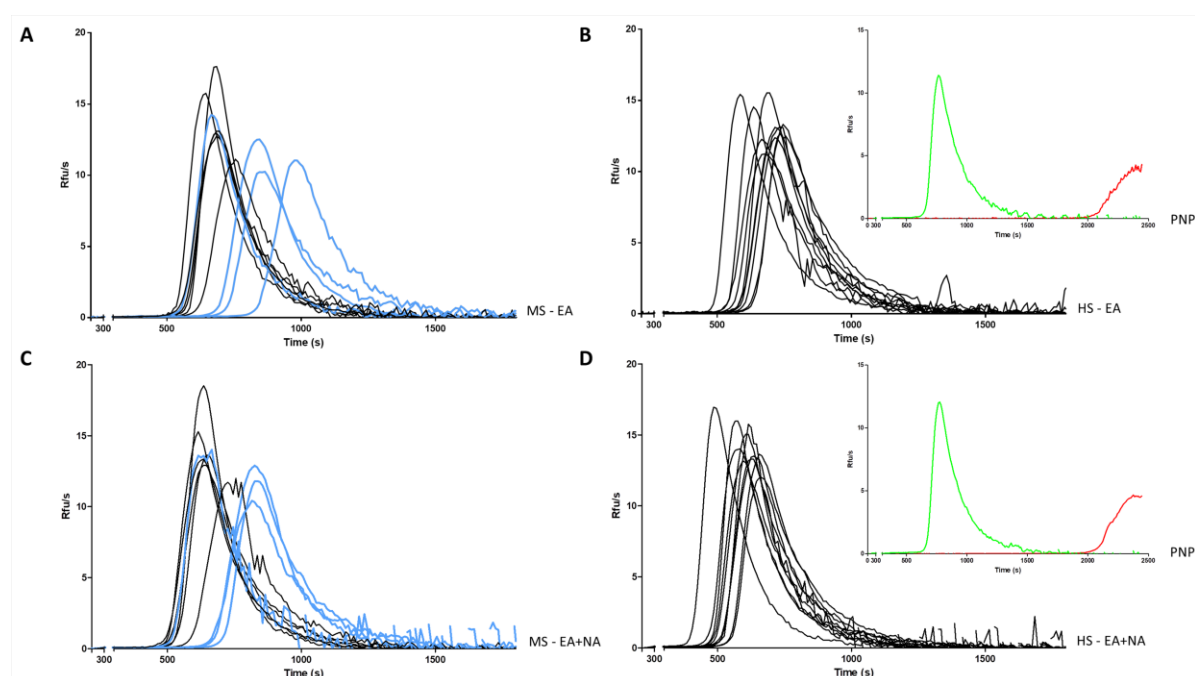
The decreased FXII:ratio values in MS patients prompted us to investigate the potential variation of FXII specific activity through a global plasma assay (TG), which describes all phases of coagulation process and the integrated amount of generated thrombin (228). In particular, to provide kinetic information about the coagulation pathway triggered by intrinsic activation, a single classic activation (ellagic acid) was conducted in parallel with a double activation (Figure 4.2), by adding as trigger molecules of nucleic acid. This natural substance, released after cell death, has been recognized among true physiological activators of the contact pathway (102, 229). Interestingly, nucleic acids released from dead and dying cells may induce an autoimmune response by activating specific sensing receptors (66), thus representing candidate molecules of the complex crosstalk between coagulation pathway, inflammation, and immune system.

To magnify FXII-related differences in TG, 10 patients' plasma, obtained at T0 (4 PP-MS, 6 SP-MS), were selected for the lowest FXII:ratio (≤ 0.93), virtually undetectable in HS, and compared with 10 HS plasma with the highest FXII:ratio (≥ 1.4), which on the other hand was rare in MS patients. TG curves and parameters are reported in Figure 4.2 and in Table 4.4, respectively. TG activated by ellagic acid showed only a trend in lower thrombin potential (ETP) in MS patients compared with HS (2631 ± 166 vs. 2780 ± 136 , $p=0.042$). The TG triggered, in the same experiment, with the addition of nucleic acid, produced a clear decrease in main time parameters both in MS patients and in HS. As compared with the single ellagic acid trigger, both lag time and TTP were shorter in MS patients (612 ± 97 vs. 561 ± 81 , $p=0.006$; 750 ± 109 vs. 706 ± 91 , $p=0.014$, respectively) and in HS (564 ± 44 vs. 487 ± 44 , $p<0.0001$; 690 ± 51 vs. 605 ± 51 , $p<0.0001$). After the double induction, the increase in thrombin peak height and ETP differed between patients and HS. Particularly the ETP value increased only in MS patients (2631 ± 166 vs. 2748 ± 133 , $p=0.004$), whereas the peak height was significantly increased only in HS (13.4 ± 1.4 vs. 14.3 ± 1.5 , $p=0.008$). Coherently with the decreased FXII:ratio, we report in MS patients a

trend of lower amounts of thrombin potential, ETP, a stable and highly affordable parameter. Additional trigger by nucleic acid prolonged time parameters in MS patients as compared with HS. Lag time was longer as a trend (561 ± 81 vs. 487 ± 44 in HS, $p=0.02$) and TTP was around 100-seconds longer (706 ± 91 vs. 605 ± 51 in HS, $p=0.007$). To note, three out of four PP-MS patients showed the most prolonged time parameters (Figure 4A and 4C). Worth noting that the significant differences in TG parameters between MS and HS (Table 4.4) were observed in the presence of high correlations between time parameters, both in MS patients and in HS (Figure 4.3).

Overall, the lower FXII:ratio and longer TG time parameters suggested that in part of MS patients i) FXII could be less active per antigen unit, and ii) FXII response to contact activation and its support to the intrinsic coagulation pathway could be reduced.

Figure 4.2. Intrinsic generation of thrombin in plasma of multiple sclerosis patients and healthy subjects.



Thrombin generation activity in plasma samples was triggered by ellagic acid in MS patients (A) and in HS (B), or ellagic acid plus nucleic acid in MS patients (C) and in HS (D). Curves from PP-MS are shown in light blue. Curves of PNP (insets) in the same conditions of MS patients and HS (green), and after addition of FXII inhibitor (red) are reported as control.

MS: Multiple Sclerosis; PP-MS: Primary Progressive Multiple Sclerosis; HS: Healthy Subjects; EA: ellagic acid; NA: nucleic acid; PNP: pooled normal plasma; Rfu: relative fluorescence units; s: seconds.

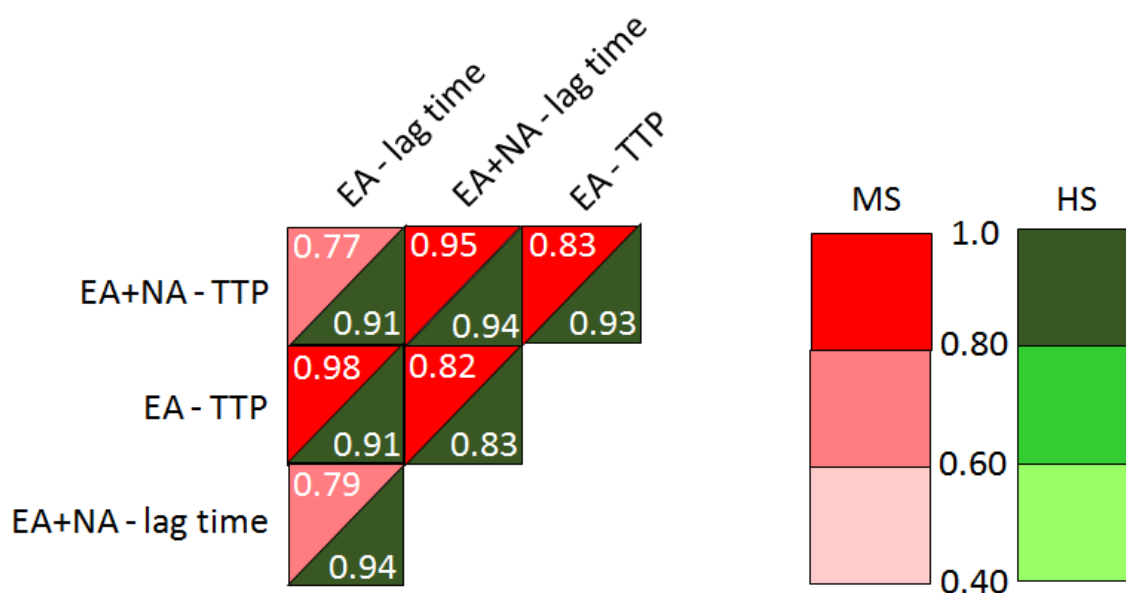
Table 4.4. Generation of thrombin in plasma of multiple sclerosis patients and healthy subjects.

	EA			EA+NA			EA vs EA+NA P-value	
	MS	HS	P-value	MS	HS	P-value	MS	HS
Lag Time (s)	612 ± 97	564 ± 44	0.175	561 ± 81	487 ± 44	0.02	0.006	<0.0001
TTP (s)	750 ± 109	690 ± 51	0.132	706 ± 91	605 ± 51	0.007	0.014	<0.0001
Peak (Rfu/s)	13.1 ± 2.3	13.4 ± 1.4	0.804	13.5 ± 2.2	14.3 ± 1.5	0.335	0.153	0.008
ETP (Rfu)	2631 ± 166	2780 ± 136	0.042	2748 ± 133	2746 ± 38	0.964	0.004	0.506

MS: Multiple Sclerosis; HS: Healthy Subjects; ETP: Endogenous Thrombin Potential; EA: Ellagic Acid; NA: Nucleic Acid; TTP: Time To Peak; Rfu: Relative fluorescence units; s: seconds.

Student's t-test was used to compare TG parameters of MS patients with those of HS, while paired Student's t-test was used to assess differences in TG after NA addition in MS and HS (P-value EA vs EA+NA).

Figure 4.3. Correlations between time parameters from the intrinsic thrombin generation triggered by ellagic acid or by ellagic plus nucleic acids.



MS: Multiple Sclerosis; HS: Healthy Subjects; EA: ellagic acid; NA: nucleic acid; TTP: time to peak. Linear models were generated to determine the relationship between thrombin generation parameters.

Interestingly, it has been recently reported that in TG, triggered by extrinsic activation, time parameters were shorter in MS patients (145), which does not conflict with our data because extrinsic TG does not explore FXII contribution. Noteworthy, both the intrinsic TG, firstly reported in our study, and the extrinsic TG (145) tightly depend on activation and activity of coagulation factors in the common pathway, essential to generate thrombin. Although indirectly, our study does not support the presence of a prothrombotic state in the MS patients under study. In light of the increased FXII protein levels and decreased activation that we report, pharmacological inhibition of FXII, proposed as a potential new approach to MS treatment, needs deep investigation.

In summary, the study evaluated the ratio of FXII:C and the amount of circulating protein, which showed the presence of increased FXII protein level and reduced function within the intrinsic coagulation pathway (146). Although indirectly, intrinsic thrombin generation did not support the presence of a prothrombotic state in the evaluated PMS patients (146).

In conclusion, the study points toward FXII-related differences between MS patients and HS, with the limitation of the small sample size. Multiple specific and global coagulation assays could help stratification of patients to better define FXII contribution to disease phenotype and progression.

Chapter 5 Hemostasis biomarkers in multiple sclerosis

Ziliotto N, Bernardi F, Jakimovski D, Baroni M,
Marchetti G, Bergsland N, Ramasamy DP,
Weinstock-Guttman B, Schweser F, Zamboni P,
Ramanathan M, Zivadinov R.

Based on:
Eur J Neurol. 2018;
25(9):1169-1176
doi:10.1111/ene.13681

5.1 BACKGROUND AND RATIONALE

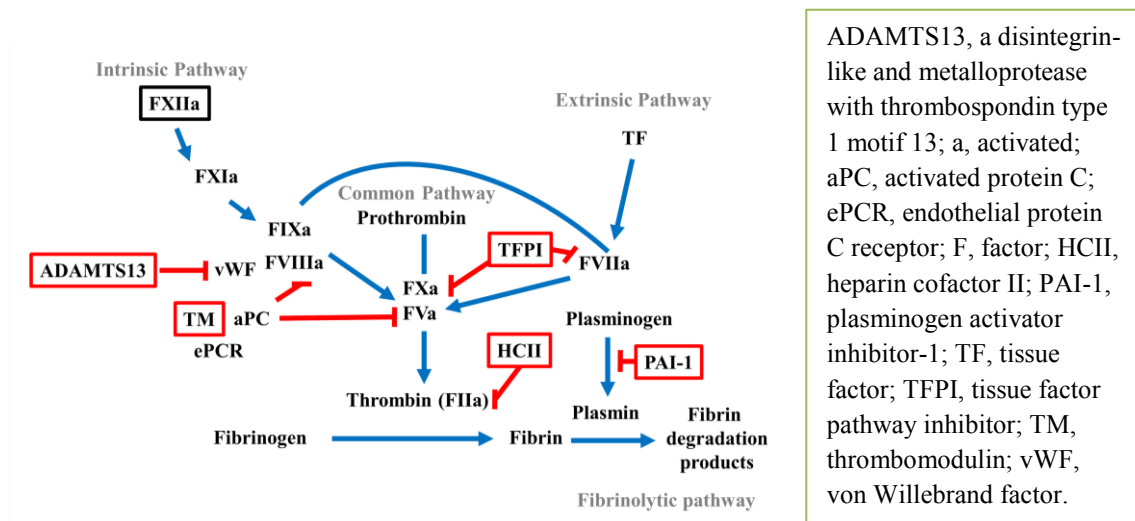
Growing evidence suggest the crosstalk between hemostasis components, inflammation and immune system which appear to be involved in MS pathophysiology as extensively described in this thesis introduction (see chapter 1). In vivo, coagulation factors are regulated by positive and negative feedback loops, the last provided by multiple coagulation inhibitors/anticoagulant proteins, which are also activated in a cascade-like fashion and influenced by feedback loops. The relationship of the coagulation pathway with disease processes could be further supported by recent findings, showing that anticoagulants ameliorated clinical course of experimental autoimmune encephalomyelitis (EAE), an animal model of MS (230, 231).

Previous studies of the coagulation pathway in MS patients have examined only a limited number of individual hemostasis components. However, the inter-connectedness of the coagulation pathway requires a systems approach that includes simultaneous measurements of both pro-coagulant and anti-coagulant biomarkers.

Taken into account the aforementioned findings, hemostasis inhibitors of the current investigation were selected for representing the regulation of the coagulation system on different levels. In particular: I) tissue factor pathway inhibitor (TFPI) was selected for being the first line of extrinsic coagulation inhibition acting against TF:FVIIa:FXa; II) heparin cofactor II (HCII) delineates the inhibitory action supported by specific glycosaminoglycans (GAGs) directly against thrombin; III) thrombomodulin (TM), the main receptor for activation of the anticoagulant protein C, was chosen because its soluble form may reflect endothelial damage; IV) disintegrin-like and metalloprotease with thrombospondin type 1 motif 13 (ADAMTS13) expresses its inhibitory action regulating platelet adhesion and aggregation, thus involving a cell-based model mechanism of inhibition; V) PAI-1 is the inhibitor of fibrinolysis, whose impairment has been reported in MS lesions (232-236). To note, TFPI, heparin cofactor-II (HCII) and ADAMTS13, have not been investigated systematically in MS patients.

Furthermore, previous studies have not included MRI measures of disease severity, which provide quantitative and more sensitive measures of MS pathophysiology. Therefore, the purpose of this study was to systematically measure a panel of pro-coagulant and anti-coagulant biomarkers in MS plasma (Figure 5.1) and to investigate their associations with clinical and MRI measures. In particular, given the important roles of hemostasis biomarkers in the regulation of bleeding and iron deposition, we hypothesized that altered hemostasis biomarkers will be associated with focal extravascular leakage of blood components that can be measured on MRI by evaluating the CMBs frequency and susceptibility values of DGM structures.

Figure 5.1. Schematic representation of the coagulation pathways. The components investigated in the study are highlighted.



5.2 MATERIALS AND METHODS

The study included 138 total MS patients (85 RR-MS, 53 P-MS) and 42 HI. The demographic and clinical characteristics of the study sample are summarized in Table 3.4 (page 38), while the MRI measurements are in Table 3.5 (page 39).

Hemostasis components were measured in EDTA plasma samples obtained at the follow-up visit by analysts who were blinded to sample status.

FXII and HCII protein levels were measured using ELISA kits (LS-F10418, LifeSpan Biosciences, Seattle, WA, USA for FXII and CSB-E09492h, Cusabio, Wuhan, Hubei, China for HCII) following the manufacturer's instructions. The inter-assay coefficient of variation (CV) was 4.3% for FXII and 9.6% for HCII. Total PAI-1 levels were assayed using Milliplex™ magnetic bead kits (human neurodegenerative disease panel 3, HNDG3MAG-36K, Merck Millipore, Germany) whereas ADAMTS13, TM and TFPI protein levels were similarly measured using custom-designed Luminex Screening Assays magnetic bead kits (Luminex R&D Systems Inc., Minneapolis, MN, USA). Data were acquired using the Luminex® 100 system and analyzed using Bioplex Manager Software version 6.0 (both from Biorad Laboratories, Hercules, CA). The calculated inter-assay CVs for ADAMTS13, TM, TFPI and PAI-1 were 2.1%, 3.0%, 4.5% and 5.7%, respectively.

All statistical analyses were performed using Statistical Package for Social Sciences software (version 24, IBM Corp. Armonk, NY, USA).

The Kolmogorov–Smirnov test was used to test for normality of continuous variables. The associations among the protein levels, and with demographic characteristics, EDSS and disease duration, were assessed with Spearman's rank correlation.

Comparisons of protein levels for MS vs. HI and RR-MS vs. P-MS were conducted with the Mann–Whitney test. The associations of the protein levels with clinical and MRI outcomes were assessed with the partial correlation using age and gender as covariates. The Kruskal-Wallis test, followed by Mann-Whitney test was used to investigate whether various disease-modifying treatments (DMTs) are associated with protein levels.

Logistic regression analysis was used to determinate associations of hemostasis components with the presence of CMBs.

The Benjamini-Hochberg method was used to adjust for the multiple comparisons with a target false discovery rate of $q \leq 0.05$. The tables and results present the unadjusted p-values and adjusted p-values (q-values) for those associations when unadjusted p-values were ≤ 0.05 using two-tailed tests.

5.3 RESULTS AND DISCUSSION

In this study, plasma levels of six key hemostasis components, FXII, PAI-1, TM, ADAMTS13, HCII and TFPI in a large cohort of MS patients and assessed their associations with clinical and MRI outcomes.

The levels of hemostasis components in the MS and HI groups are summarized in Figure 5.2. ADAMTS13 were lower in MS patients compared to HI (1548 ± 481 ng/mL vs. 1733 ± 562 ng/mL; $p=0.008$). PAI-1 levels were higher in the MS group compared to HI (121.1 ± 64.9 ng/mL vs. 103.6 ± 71.4 ng/mL; $p=0.02$).

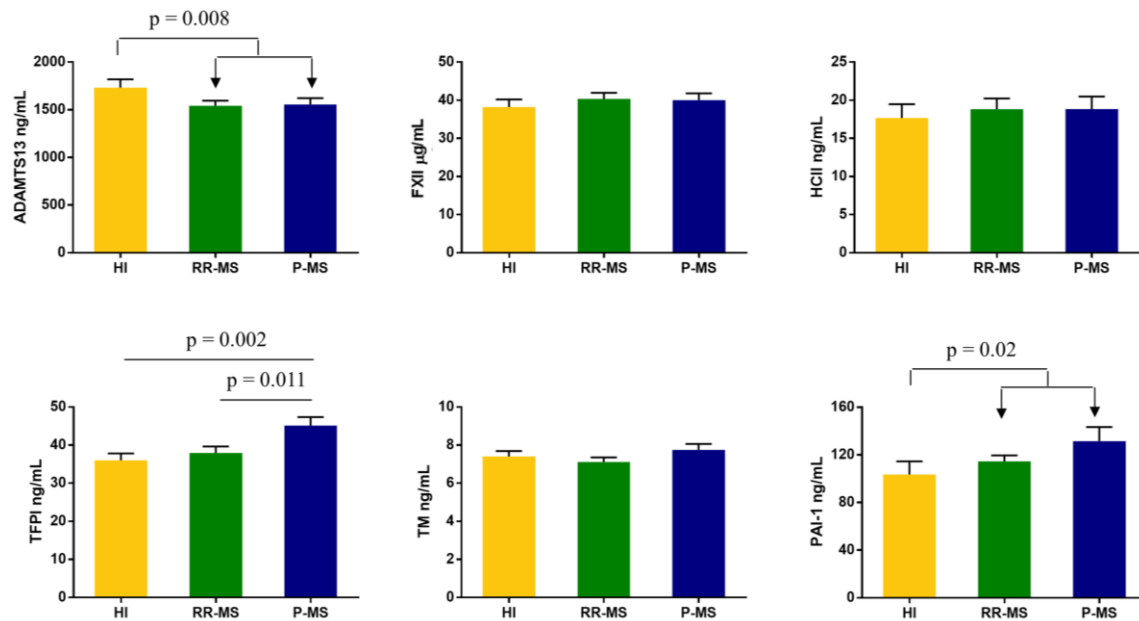
No significant differences in plasma levels of FXII, HCII, TFPI, and TM were observed between MS and HI groups (Figure 5.2). However, TFPI levels were higher ($p=0.011$) in the P-MS compared to RR-MS patients (45.1 ± 16.3 ng/mL vs. 37.9 ± 15.9 ng/mL, $p=0.011$) and compared to HI (36.0 ± 11.8 ng/mL, $p=0.002$).

The hemostasis components levels were not associated with EDSS nor disease duration.

No significant differences were detected according to the type of DMTs (Figure 5.3) in proteins levels (ADAMTS13, $p=0.83$; FXII, $p=0.20$; HCII, $p=0.77$; TFPI, $p=0.10$; TM, $p=0.69$; PAI-1, $p=0.17$). In addition, comparison between treated ($n=111$) vs. not treated ($n=27$) MS patients did not yield significant differences.

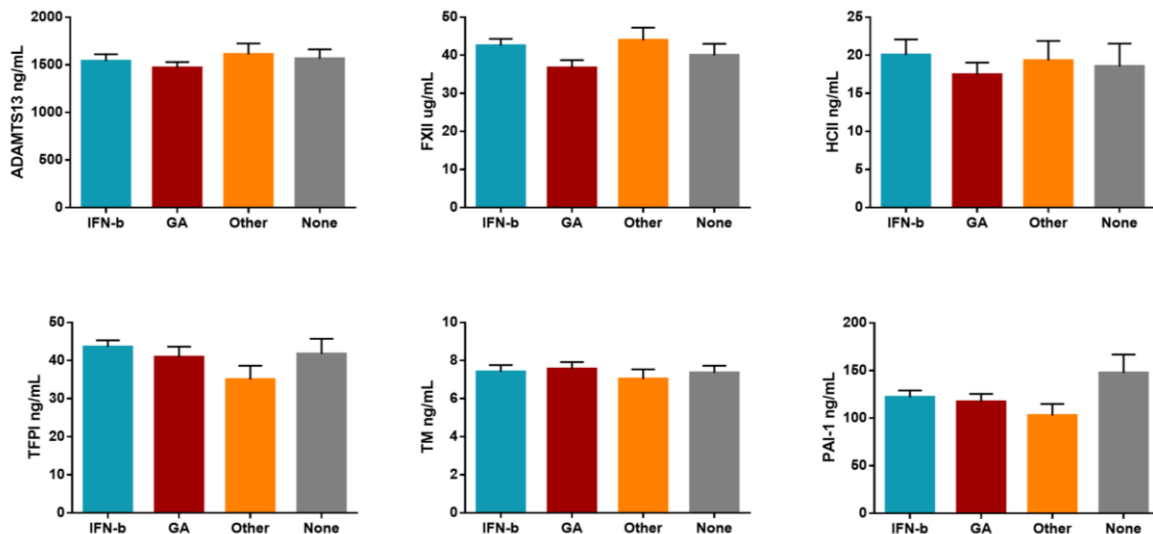
The association among the investigated hemostasis components was explored both in MS and HI groups. In MS, TFPI was associated with higher levels of TM ($r=0.24$, $p=0.004$). Moreover, PAI-1 was positively associated with higher levels of FXII ($r=0.28$, $p=0.001$) and inversely correlated with HCII ($r= -0.21$, $p=0.014$). These associations were not detected in HI (TFPI vs. TM $r=0.134$, $p=0.398$; PAI-1 vs. FXII $r= -0.057$, $p=0.718$; PAI-1 vs HCII $r= -0.081$, $p=0.608$).

Figure 5.2. Hemostasis components levels in healthy individuals, relapsing-remitting and progressive multiple sclerosis.



The p-values from a Mann–Whitney test are provided. The error bars indicate the standard error of the mean.

Figure 5.3. Hemostasis components levels in multiple sclerosis cohort according to the disease-modifying treatment.



The p-values from a Mann–Whitney test are provided. The error bars indicate the standard error of the mean.

Legend: IFN-b: Interferon beta; GA: glatiramer acetate; Other: other disease-modifying treatment; None: no disease-modifying treatment; ADAMTS13: A Disintegrin-like And Metalloprotease with ThromboSpondin type 1 motif 13; FXII: Factor XII; HCII: Heparin Cofactor II; TFPI: Tissue Factor Pathway Inhibitor; TM: Thrombomodulin; PAI-1: Plasminogen activator inhibitor-1.

In HI, trends for positive association were found between TFPI and PAI-1 ($r=0.33$, $p=0.032$) and between TM and ADAMTS13 ($r=0.34$, $p=0.027$).

Limited evidence for dysregulation of associations among hemostasis protein levels in plasma were found. In MS patients, levels of TFPI and TM, both anticoagulant and anti-inflammatory proteins, were positively associated. Differently, PAI-1 was associated with higher levels of FXII and lower levels of HCII, which altogether are expected to enhance both the deposition and stability of fibrin. These associations were not detected in HI.

FXII is a pro-coagulant component in the intrinsic coagulation pathway at the interface with innate inflammation (52). FXII activity has been reported higher in RR-MS and SP-MS compared to HI, and it was associated with relapses and shorter relapse-free period, independently from immunomodulatory therapy (52). However, we did not find differences, nor any association with DMTs, in FXII protein concentration, which is a potentially improved measure of the autoimmune function as compared to coagulation activity assays, which depends on several plasma factors.

We detected higher PAI-1 levels in MS patients compared to controls, as previously reported (164, 165). Further, PAI-1 levels were not associated with clinical or MRI outcomes. In addition, we did not find any associations of clinical or MRI outcomes with TM, which has been suggested to confer protection from demyelination in a mouse model of MS (237). The literature data on TM levels in MS are discordant (158-160). As previously reported, we did not find differences in TM levels between MS vs. HI, but we failed to confirm an association between TM levels and more severe disability (160). Despite the greater sample size in our study, we failed to confirm an association between GA and TM levels (158).

We observed significantly higher TFPI levels in P-MS subgroup when compared to RR-MS and to HI, and an association between TM and TFPI in MS. These are novel data because TFPI has not been systematically investigated in MS. It is known that age influences the levels of hemostasis components (238). Indeed, correlations of hemostasis components levels with MRI outcomes were assessed using age as a covariate in our statistical analysis. Taking into account this aspect, our data should be interpreted with caution, as increased TFPI levels in P-MS may be in part due to the older age of this group. The associations between the hemostasis biomarker levels and MRI outcomes were evaluated (Tables 5.1 and 5.2). None of these associations were significant when adjusted for multiple comparisons. In MS, higher FXII levels showed a trend for correlation with lower ventricular ($r=-0.19$, $p=0.027$, $q=0.42$) and higher DGM ($r=0.18$, $p=0.047$, $q=0.42$) volumes, while higher HCII levels showed a trend for correlation with lower brain ($r=-0.21$, $p=0.017$, $q=0.42$) and cortical ($r=-0.18$, $p=0.046$, $q=0.49$) volumes and higher DGM

volume ($r=0.19$, $p=0.034$, $q=0.42$). In addition, higher TFPI levels showed a trend for correlation with lower DGM volume ($r=-0.18$, $p=0.041$, $q=0.42$). No associations were found between QSM measurements and hemostasis components levels in MS patients (Table 5.1).

In HI, a trend for association between higher HCII levels and lower cortical volume ($r= -0.36$, $p=0.024$, $q=0.43$) was detected. Additionally, higher PAI-1 levels showed a trend for correlation with higher QSM of DGM ($r= 0.41$, $p=0.013$, $q=0.43$) (Table 5.2).

Association between hemostasis components and the presence of CMBs are reported in Table 5.3. Of all the hemostasis components analyzed, ADAMTS13, which displayed lower levels in patients than HI (Figure 5.2), also showed significantly lower levels in MS patients with cerebral microbleeds compared to those without (1257 ± 459 ng/mL vs. 1566 ± 479 ng/mL; $p=0.034$).

Table 5.1. Association analysis of hemostasis inhibitors with MRI outcomes within multiple sclerosis group.

		ADAMTS13	FXII	HCII	TFPI	TM	PAI-1
T2-LV	Rho	-0.059	-0.126	0.118	0.078	-0.016	-0.030
	P value	0.499	0.147	0.177	0.371	0.858	0.735
T1-LV	Rho	-0.012	-0.057	0.129	0.066	-0.083	0.009
	P value	0.892	0.521	0.143	0.457	0.348	0.920
NBV	Rho	-0.032	0.119	-0.209	-0.133	-0.043	0.094
	P value	0.718	0.179	0.017	0.130	0.625	0.288
NCV	Rho	-0.013	0.079	-0.176	-0.140	-0.012	0.023
	P value	0.888	0.370	0.046	0.112	0.890	0.798
LVV	Rho	0.003	-0.194	0.186	0.129	0.075	-0.145
	P value	0.976	0.027	0.034	0.145	0.396	0.100
DGM	Rho	0.020	0.175	-0.077	-0.180	-0.147	0.070
	P value	0.825	0.047	0.381	0.041	0.095	0.427
QSM DGM	Rho	-0.046	-0.044	-0.071	0.019	0.039	-0.103
	P value	0.623	0.639	0.451	0.842	0.678	0.272

The Benjamini-Hochberg method was used to adjust for the multiple comparisons with a target false discovery rate of $q \leq 0.05$. The table shows the unadjusted p-values. Values provided represent the Spearman correlation coefficient and p-values. Age and gender were used as covariates.

Legend: ADAMTS13: A Disintegrin-like And Metalloprotease with Thrombospondin type 1 motif 13; FXII: Factor XII; HCII: Heparin Cofactor II; TFPI: Tissue Factor Pathway Inhibitor; TM: Thrombomodulin; PAI-1: Plasminogen activator inhibitor-1; LV: lesion volume; NBV: normalized brain volume; NCV: normalized cortical volume; LVV: lateral ventricular volume; DGM: deep grey matter; QSM: quantitative susceptibility mapping.

Table 5.2. Association analysis of hemostasis inhibitors with MRI outcomes within healthy individuals group.

		ADAMTS13	FXII	HCII	TFPI	TM	PAI-1
T2-LV	Rho	0.209	-0.036	0.172	0.207	0.181	0.199
	P value	0.201	0.829	0.295	0.206	0.271	0.226
NBV	Rho	-0.232	-0.271	-0.252	0.044	-0.067	-0.042
	P value	0.156	0.095	0.121	0.792	0.683	0.798
NCV	Rho	-0.183	-0.197	-0.360	0.056	-0.063	-0.048
	P value	0.265	0.229	0.024	0.735	0.704	0.770
LVV	Rho	-0.025	-0.075	0.103	0.072	-0.139	-0.108
	P value	0.882	0.650	0.532	0.662	0.399	0.514
DGM	Rho	0.020	-0.246	-0.087	0.074	-0.224	-0.151
	P value	0.903	0.131	0.600	0.655	0.171	0.360
QSM DGM	Rho	-0.125	0.218	-0.045	0.113	0.095	0.412
	P value	0.468	0.202	0.796	0.512	0.582	0.013

The Benjamini-Hochberg method was used to adjust for the multiple comparisons with a target false discovery rate of $q \leq 0.05$. The table shows the unadjusted p-values. Values provided represent the Spearman correlation coefficient and p-values. Age and gender were used as covariates.

Legend: ADAMTS13: A Disintegrin-like And Metalloprotease with Thrombospondin type 1 motif 13; FXII: Factor XII; HCII: Heparin Cofactor II; TFPI: Tissue Factor Pathway Inhibitor; TM: Thrombomodulin; PAI-1: Plasminogen activator inhibitor-1; LV: lesion volume; NBV: normalized brain volume; NCV: normalized cortical volume; LVV: lateral ventricular volume; DGM: deep grey matter; QSM: quantitative susceptibility mapping.

ADAMTS13 levels in HI with CMBs were not significantly different than those without (1630 ± 623 ng/mL vs. 1758 ± 562 ng/mL; $p=0.7$). No significant associations were observed between coagulation inhibitors and number of CMBs.

In MS, we found lower levels of ADAMTS13, whose deficiency is associated with microangiopathic hemolytic anemia (173). Acquired ADAMTS13 deficiency and thrombotic microangiopathy were described in two MS patients treated with interferon-beta (174, 175). We did not find lower ADAMTS13 levels in MS patients treated with interferon-beta, or other DMTs. On the other hand, decreased ADAMTS13 levels were detected in MS patients with CMBs, which have been reported to be more frequent in MS patients of older age (42). In animal models, ADAMTS13 was found to attenuate brain injury after intracerebral hemorrhage, and it was suggested as a new therapeutic strategy for intracerebral hemorrhage, able to regulate pathological inflammation and BBB function (239). In light of these observations, the finding of decreased ADAMTS13 levels, particularly in MS patients with CMBs, is intriguing. Our study is the first to investigate HCII in MS patients.

Table 5.3. Associations of hemostasis biomarkers with cerebral microbleeds in MS patients.

Biomarker	Cerebral Microbleeds		<i>p</i> -value
	Present	Not Present	
Sample size, <i>n</i>	12	113	
ADAMTS13 (ng/mL)	1257 ± 459	1566 ± 479	0.034
FXII (µg/mL)	43.5 ± 10.5	40.6 ± 13.4	0.31
HCII (ng/mL)	19.7 ± 16.8	18.5 ± 12.0	0.97
TFPI (ng/mL)	43.0 ± 21.7	39.7 ± 15.2	0.76
TM (ng/mL)	7.8 ± 3.0	7.3 ± 2.1	0.40
PAI-1 (ng/mL)	135 ± 104	121 ± 61.9	0.93

The mean values ± SD of hemostasis biomarkers and the *p*-values from logistic regression to determinate associations of hemostasis biomarkers with the presence of cerebral microbleeds, are shown.

Legend: ADAMTS13: A Disintegrin-like And Metalloprotease with ThromboSpondin type 1 motif 13; FXII: Factor XII; HCII: Heparin Cofactor II; TFPI: Tissue Factor Pathway Inhibitor; TM: Thrombomodulin; PAI-1; Plasminogen activator inhibitor-1.

HCII exclusively inactivates thrombin by a complex with glycosaminoglycans, such as heparin, thus regulating both hemostasis and cellular effects of thrombin (240). The cellular effects which are mediated by protease-activated receptors, include tube formation, migration, and proliferation of endothelial cells. Hence, HCII is required for maintenance of angiogenesis (241). We did not detect significant differences between MS and HI or in relation to DMTs and MRI outcomes.

Our results should be confirmed by future investigations. Because inhibition of FXII has been proposed as an important mechanism in the pathogenesis of MS, the potential influence on its levels, as well as the impact on the disease activity, deserve additional studies. The main limitation of the present study is that patients were not evaluated at the time of relapse or occurrence of contrast-enhancing lesions. Thus, our cohort is not representative of the underlying acute inflammatory activity. Future investigations of hemostasis components levels should address this issue by including MS patients in an active phase of the disease along with the use of inflammatory/non-inflammatory CNS conditions as comparator groups.

In conclusion, one of the first extensive surveys of hemostasis inhibitor levels in plasma of MS patients detected decreased ADAMTS13 levels, and particularly in those who presented CMBs, increased PAI-1 levels, and increased TFPI in P-MS group. We did not

find a relationship between hemostasis components and clinical and MRI outcomes. Clinical usefulness of plasma levels of these hemostasis proteins as biomarkers of disease progression and treatment effects in MS is likely limited.

Chapter 6

Changes in expression profiles of internal jugular vein wall and plasma protein levels in multiple sclerosis

Marchetti G, **Ziliotto N**, Meneghetti S, Baroni M, Lunghi B, Menegatti E, Pedriali M, Salvi F, Bartolomei I, Straudi S, Manfredini F, Voltan R, Basaglia N, Mascoli F, Zamboni P, Bernardi F.

Based on:

Mol Med. 2018; 24(1):42

doi: 10.1186/s10020-018-0043-4

6.1 BACKGROUND AND RATIONALE

Several observations suggest that vascular components are involved in the multifactorial pathogenetic interplay and/ or in disease progression, severity and comorbidities development (33, 242, 243).

The vascular cerebral system, and particularly the venous compartment, early received attention because of venous thrombosis in the brain of MS patients, and plaques of demyelination development around venules and perivascular infiltrations of inflammatory cells just next to small and medium-size venous of CNS (244).

The condition named chronic cerebrospinal venous insufficiency (CCSVI) provided the possible association of MS with extra-cranial venous abnormalities which impaired venous outflow (245, 246). Although highly debated whether associated with MS, and not leading to a viable treatment option in patients (247), this condition favors a better understanding of the function and role of the extracranial venous system in MS (248). On the other hand, a perspective of reduced blood supply to the brain (249), further argue for the relevance of the vascular component in the disease.

Findings on these conditions associated with MS foster more investigations of both intracranial and extracranial vascular compartments changes in MS (248, 250).

Vascular features associated with MS have been deeply investigated (34, 189), with the central vein sign recently proposed as a MRI biomarker of MS (36). Studies focusing on circulating and endothelial components, which participate in the complex network of immune-vascular interactions have been reported (251). De-regulated patterns of gene expression have been detected in peripheral whole blood or peripheral blood mononuclear cells (PBMC) of MS patients (252-257).

To shed light on vascular gene expression changes in MS with associated CCSVI, we focused on the internal jugular vein (IJV), which drains blood from the brain. In particular, we explored gene expression changes by using two informative approaches and their combination, transcriptomic analysis on IJV specimens and specific protein assays on plasma from both jugular and peripheral veins.

6.2 MATERIALS AND METHODS

Study populations

The first (1st) study population was represented by a group of 19 Italian subjects with MS and positive screening CCSVI, while the second (2nd) study population included 60 Italian MS patients. The demographics and clinical characteristics of the 1st and 2nd MS populations are reported in Tables 3.2 and 3.3 (page 35), respectively.

Jugular wall specimens

IJV specimens were obtained at surgery from patients. In MS patients, the surgical procedure included an unilateral or bilateral supra-clavicular transverse incision of about 5cm. The IJV was isolated at the junction with the subclavian vein. The latter was tangentially clamped following systemic injection of heparin. An endo-phlebectomy was subsequently performed with complete removal of the jugular valve/septum and of a tiny specimen of the jugular wall, followed by a patch angioplasty using the autologous great saphenous vein. Omohyoid muscle section was performed, if the pre-operative finding of extrinsic compression was confirmed in the surgical theatre.

Control IJV specimens were obtained from patients without MS or other neurological diseases, undergoing carotid endarterectomy (CEA) for high-grade carotid stenosis. In these five patients ECD analysis of carotid, vertebral and subclavian arteries, and jugular veins, documented the presence of atherosclerotic plaque, mostly localized at carotid bifurcation, and did not detect jugular vein alterations.

During the CEA procedure, the access to common carotid artery needs to separate the small facial vein, crossing the carotid artery just at the level of bifurcation, from the jugular vein. A very small full thickness specimen of the jugular wall was taken during this maneuver. Written informed consent was obtained from all subjects. Specimens retrieved at surgery were immediately placed into RNAlater (Ambion Inc., Austin, TX) and then stored at -80°C.

Microarray-based transcriptome analysis of jugular vein walls

From homogenized wall specimens (TRIZOL Reagent, Invitrogen Carlsbad, CA), total RNA was extracted using the miRNeasy Mini Kit (Qiagen, Hilden, Germany) and its quality was assessed with Agilent 2100 Bioanalyzer (Agilent Technologies, Palo Alto, CA). Labeled cRNA was synthesized from 100 ng of total RNA using the Low RNA Input Linear Amplification Kit (Agilent Technologies) in the presence of cyanine 3-CTP (Perkin-Elmer Life Sciences, Boston, MA). Hybridization on Agilent whole human genome oligo microarray (Cat.No. G4851A, Agilent Technologies), which represents

60,000 unique human transcripts, was performed in accordance to manufacturer's indications.

Microarray raw-data were obtained with Feature Extraction software v.10.7 (Agilent Technologies) and analyzed by using the GeneSpring GX v.14 software (Agilent Technologies) as previously described (258, 259).

cDNA preparation and quantitative real-time polymerase chain reaction (qRT-PCR)

cDNA was obtained from 0.150 µg of total RNA by reverse transcription using M-MLV Reverse Transcriptase (Invitrogen Carlsab, CA) and a mixture of oligo(dT) and random primers. Aliquots of diluted cDNA were amplified using SsoFast EvaGreen Supermix (BioRad, Hercules, CA). As general approach for qRT-PCR the specific primers were chosen to amplify the regions recognized by oligonucleotide probes in the microarray analysis. Forward and reverse primers are reported in the Table 6.1.

Table 6.1. qRT-PCR Forward and Reverse Primers.

* endogenous controls.

GENE	SEQUENCE
<i>ANGPT1</i>	5'- GAGGATGGTGGTTTGATGCT-3' 5'- CAATATTGTTTGCTTCTGAAGTTTTC-3'
<i>AOC3</i>	5'- TACCAGCTGGCTGTGACC-3' 5'- TGGGATATGCAGAAAACCAG-3'
<i>CD86</i>	5'- GGAAGAGAGTGAACAGACCAAGA-3' 5'- AATGTCTTTTTGCCTTCTGGA- 3'
<i>L1CAM</i>	5'- AGGACACCCAGGTGGACTC-3' 5'- TCCTCGTTGAACTGAACATCC-3'
<i>SELL</i>	5'- CTCTGGGTTGGCATTATCA-3' 5'- CTTCCCAGATGCACTGAAGG-3'
<i>ACTB*</i>	5'- CATCGAGCACGGCATCGTCA-3' 5'- TAGCACAGCCTGGATAGCAAC-3'
<i>B2M*</i>	5'- TTTCATCCATCCGACATTGA-3' 5'- CCTCCATGATGCTGCTTACA-3'

PCR protocol was: 95°C for 30 seconds, then 40 cycles of 10 seconds at 95°C and 15 seconds at 58°C. Each reaction was performed in triplicate. All qRT-PCRs were performed on an CFX96 Real-Time PCR Detection System instrument (BioRad, Hercules, CA) according to the manufacturer's instructions. The relative levels of mRNAs were calculated by $2^{-\Delta\Delta Ct}$ method using ACTB and B2M as endogenous controls. Values were expressed as mean fold change \pm standard error of the mean.

Plasma samples

For the 1st study MS population (N=17 patients) blood samples were drawn during the surgical procedure, before systemic injection of heparin, from both IJV (right or left) and a peripheral vein. At time of blood sampling patients were free of therapy for at least one month. All blood samples were drawn at fasting in citrate tubes.

MS patients from the 2nd population, enrolled in the RAGTIME study, provided blood sampling at four time point: T0) baseline point, prior to the first rehabilitative session; T1) intermediate point, after six training sessions; T2) end of treatment, 12 completed rehabilitative sessions, 1 month after T0; T3) follow-up, after 3 months from the end of training program (146).

Peripheral venous blood samples were also collected from the healthy volunteers (n=34, or plus eight subjects n=42, as control group for the 2nd MS population).

All plasma samples were separated by two centrifugations (15 min at 2500g and 5 min at 11000g at room temperature), aliquoted and frozen at -80°C until use.

Protein antigen levels were quantified by a custom-designed Luminex Screening Assays magnetic bead kits (Luminex R&D Systems Inc., Minneapolis, MN, USA) according to the manufacturer's instructions. Data were acquired using the Luminex[®] 100 system and analyzed using Bioplex Manager Software version 6.0 (both from Biorad Laboratories, Hercules, CA). Soluble CD86 was measured by an enzyme-linked immunosorbent (ELISA)-based assay according to the manufacturer's protocol (Abcam, Cambridge, UK). The inter assay variability assessed by using coefficients of variation (CV%) were as follows: 1.1 (NCAM1), 1.2 (ANGPT1), 2.1 (CCL13), 2.3 (VAP1), 2.6 (CCL18), 3 (SELL), and 3.2 (CD86).

Statistical Analysis

In tissue microarray a filter on low gene expression was used to keep only the probes expressed in at least one sample (flagged as Marginal or Present). Then, samples were grouped in accordance to their disease status (MS and Controls) and compared. To evaluate similarities or differences among each group (MS and Controls) principal component analysis was performed on the normalized data using the GeneSpring GX v.14 software (Agilent Technologies). Differentially expressed genes were selected as having a 2-fold expression difference between their geometrical mean in the two groups and a statistically significant p-value (<0.05) by a moderate t-test, followed by the application of Benjamini- Hochberg multiple testing correction.

Differentially expressed genes were employed for Cluster Analysis of samples, using the Manhattan correlation as a measure of similarity. Functional categorization was assigned using Gene Ontology (GO) by free access DAVID Bioinformatics database 6.7.

Gene expression levels between MS and control jugular walls in qRT-PCR analysis were compared by means of unpaired t-test.

Protein plasma levels were expressed as mean \pm SD. Differences between plasma sample groups were assessed by paired or unpaired Student's t test and by ANCOVA test using age as covariate. A p-value <0.05 was considered statistically significant. Pearson's test was used to assess correlation between jugular and peripheral plasma levels in MS patients and to assess correlation over time for ANGPT1, CCL13, CCL18, NCAM1, SELL and VAP1 plasma levels. ANOVA for repeated measures was used to test differences across the four time points and, in case of a significant p-value, pairwise comparisons were Bonferroni corrected (q-values). All statistical analyses were performed using IBM® SPSS® Statistics version 24 software (IBM Corp. Armonk, NY, USA).

6.3 RESULTS AND DISCUSSION

Analysis of gene expression profiles in jugular vein specimens

To explore the expression pattern of IJV wall of patients with MS as compared to unaffected jugular walls, total RNAs extracted from MS specimens (n=4) and from control specimens (n=5) were subjected to microarray analysis. Using the criteria of at least a 2-fold difference in the expression level (corrected P value <0.05) between the two groups of RNA samples (see Methods), a total of 924 transcripts were found to be differentially expressed (data not shown).

Clustering analysis (Figure 6.1a) indicated that 409 transcripts were up- and 515 down-regulated in MS J wall. Testing for RNA function in NCBI database showed that up regulation was observed for 300 coding and 109 non-coding or uncharacterized RNAs, whereas down regulation was detected for 429 coding and 86 non-coding RNAs.

To assign a functional annotation to the 924 transcripts/genes, GO analysis by the Functional Annotation Chart Instrument of DAVID Bioinformatics 6.7 was conducted. The most enriched biological processes ($P < 0.05$, Benjamini test) are reported in Figure 6.1b. In this selection the highest significance was related to the terms “muscle”/“smooth muscle contraction” ($P = 1.2 \times 10^{-4}$ and $P = 0.008$ respectively) and “biological adhesion” ($P = 0.003$), with the term “smooth muscle contraction” showing the highest fold enrichment (7.35).

When sub-analysing up- and down- regulated transcripts ($P \leq 0.05$, Benjamini test), the terms “pattern specification process” and “nucleosome organization” were overrepresented among up-regulated genes. The biological process “pattern specification” included several homeobox (HOX) genes (*HOXA5*, *HOXA6*, *HOXA7*, *HOXB5*, *HOXB6*, *HOXC4* e *HOXC5*), which encode for transcription factors. The GO term “nucleosome organization”

comprised several histone subunit genes, and in particular, three H3 variant genes (*HIST1H3D*, *HIST1H3F* e *HIST1H3H*) were included in the list of the most significantly ($P = 0.002$) up-regulated coding RNAs. Among the down regulated genes, the terms related to smooth muscle contraction showed the highest fold enrichment (12.0). Concerning the enriched adhesion terms, 51 genes were found downregulated, of which *LICAM*, encoding for the neural cell adhesion molecule L1, was included among the top 10 most significantly downregulated genes ($P = 5 \times 10^{-4}$).

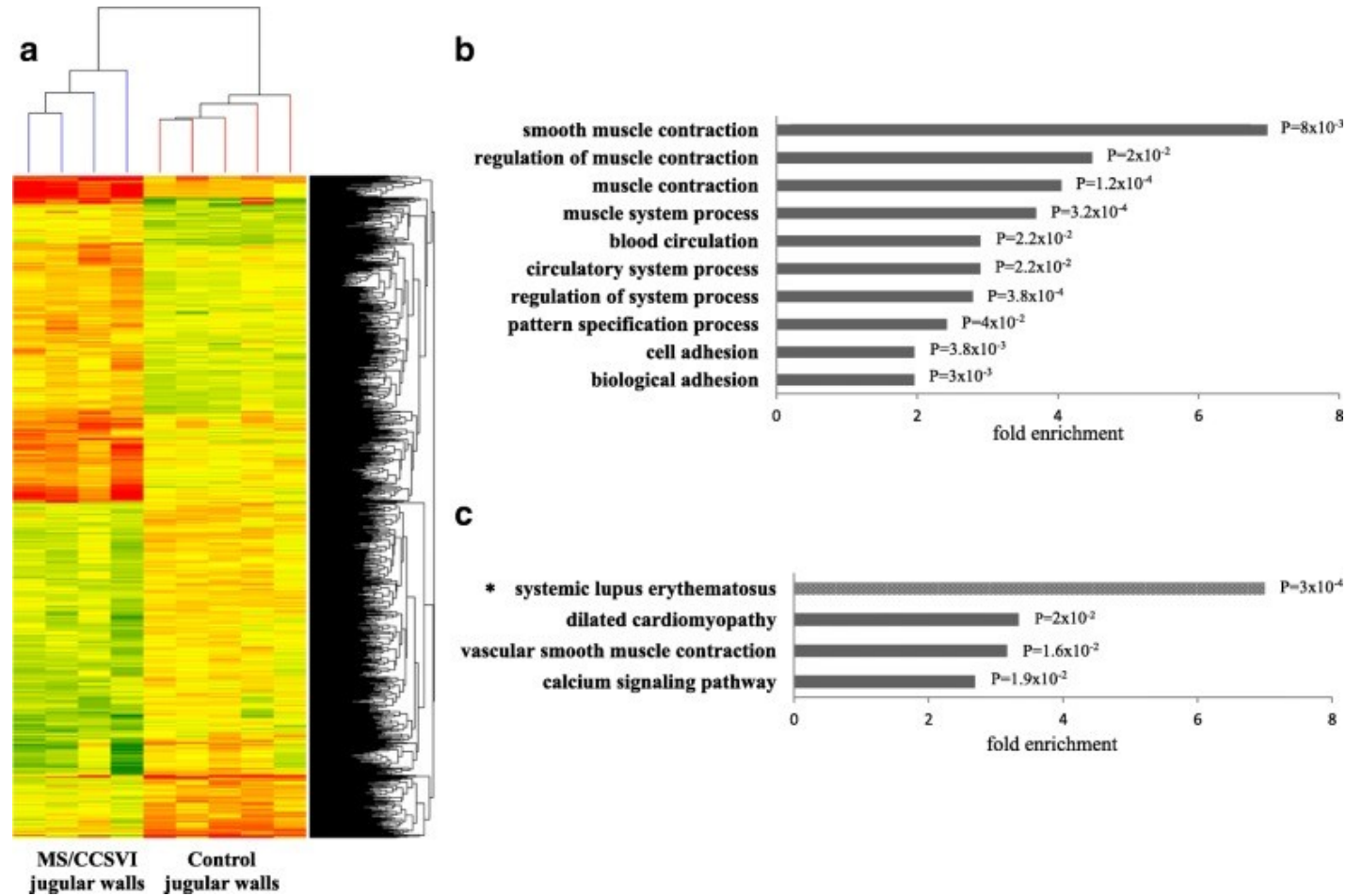
To gain further insight into functional associations, analysis of KEGG and BIOCARTA pathways by DAVID Bioinformatics resource for the 924 transcripts/genes was performed. The selection for enrichment ($P < 0.05$, Benjamini test) provided the terms “vascular smooth muscle contraction”, “dilated cardiomyopathy” and “calcium signaling pathway” (Figure 6.1c). Among the up-regulated genes, the only enriched term (fold enrichment 7.0, $P = 3 \times 10^{-4}$) was the “systemic lupus erythematosus” pathway (Figure 6.1c).

Expression analysis by quantitative real time PCR (qRT-PCR)

Aimed at supporting microarray profiling results by a different assay, qRT-PCR analyses were performed on additional jugular wall samples of MS patients ($N=7$) and of controls ($N=4$). Five genes were selected (*ANGPT1*, *AOC3*, *CD86*, *LICAM* and *SELL*), three of which included in the biological process “adhesion”. Three genes were also included in the list of the top ten most significantly up regulated (*CD86*) or down regulated (*LICAM*, *ANGPT1*) genes (data not shown).

Significant differences (Table 6.2) were observed for *LICAM* (*ACTB*, $P=0.0004$; *B2M*, $P=0.005$) and for *ANGPT1* with *B2M* ($P=0.013$). For *SELL*, a trend for down regulation was observed with *B2M* ($P=0.08$) and *ACTB* ($P= 0.11$). For *AOC3*, a trend for down regulation was observed only with *B2M* ($P=0.08$). For *CD86*, the significant differences in expression levels revealed by microarray analysis were not detected by qRT-PCR with both *ACTB* and *B2M*.

Figure 6.1. Transcriptomic analysis in internal jugular vein walls.



a. Heat map representation of the 924 differentially expressed genes (1408 probes). Each column represents one RNA sample (MS/CCSVI and control jugular walls) and each row represents one gene (probe). Colors represent the expression level fold change: higher-red, lower- green and no difference-yellow. **b.** Enriched biological processes and **c.** pathways associated to the 924 genes differentially expressed between MS and control jugular walls. Significantly overrepresented terms (Benjamini test $P < 0.05$) were selected from DAVID bioinformatics 6.7 by the Functional Annotation Chart resource. *Pathway significantly overrepresented only among up-regulated genes.

Table 6.2. qRT-PCR expression levels of selected genes in MS vs control jugular vein walls.

Gene symbol	Description	Fold-change	Fold-change	Regulation in microarray
		mean \pm SEM B2M	mean \pm SEM ACTB	
<i>ANGPT1</i> [§]	Angiopoietin1	0.63 \pm 0.18	0.74 \pm 0.25	down
<i>AOC3</i> ^{&} (<i>VAP-1</i>)	Amine oxidase copper containing 3	0.59 \pm 0.22	0.98 \pm 0.19	down
<i>CD86</i> [#]	Cluster of differentiation 86	1.1 \pm 0.30	1.49 \pm 0.43	up
<i>LICAM</i> ^{&}	L1 cell adhesion molecule	0.32 \pm 0.06	0.27 \pm 0.12	down
<i>SELL</i> ^{&}	Selectin L	1.34 \pm 0.51	1.43 \pm 0.50	up

Expression values obtained by qRT-PCR are reported as mean fold change \pm standard error of the mean (SEM). *AOC3* is also known as *VAP-1*, vascular adhesion protein 1. Main processes from Gene Ontology database: [#] immune/inflammatory response, [§]angiogenesis, [&]adhesion.

This inconsistency between microarray and qRT-PCR data could derive from the several protein coding transcripts of *CD86* gene (http://www.ensembl.org/Homo_sapiens/Gene/Summary?db=core;g=ENSG00000114013;r=3:122055366-122121139), two of which are recognized by the microarray probe in the 3' UTR and six (four additional transcripts) are potentially amplified by the q-PCR primers, bridging the last exons. With the exception of *CD86*, the expression regulation (up or down) in MS- vs control jugular walls indicated by microarray analysis was supported by qRT-PCR analysis (Table 6.2).

Analysis of protein levels in jugular and peripheral plasma

In order to investigate whether differences in the transcriptome profiles between MS- and control jugular walls would correlate with differences in protein expression levels, we selected genes whose protein products could be measured in plasma, and particularly by using a multiplex detection approach. Ten candidate proteins were eligible (Table 6.3). In addition, *CD86*, in the list of the top ten most significantly up regulated coding genes and showing the highest fold-change, was measured as soluble antigen in plasma by a single ELISA. The selected proteins mainly participate in adhesion (*NCAM1*, *VAP1*, *SELL*), which was among the most significantly enriched process revealed by jugular wall transcriptome analysis, immune/inflammatory responses (*CD86*, *TNF*, *TNFRSF6B*, *CCL3*, *CCL13*, *CCL18*), angiogenesis (*ANGPT1*) and cytoskeleton/organelle organization (*MAPT*).

Protein levels were evaluated in jugular and peripheral plasma from 17 patients (MS 1st population) and in peripheral plasma from 34 healthy subjects (Table 6.4).

Table 6.3. List of genes, differentially expressed in MS jugular vein walls (MS-IJW) compared to control vein walls (C-IJW), selected for protein level analysis in plasma.

Gene symbol	Description	Regulation	Expression MS-IJW mean \pm SD	Expression C-IJW mean \pm SD	Fold change	P value*
<i>CD86</i> [#]	Cluster of differentiation 86	Up	14.38 \pm 0.89	11.30 \pm 0.38	8.47	0.002
<i>ANGPT1</i> [§]	Angiopoietin1	Down	9.20 \pm 0.14	10.48 \pm 0.29	2.02	0.002
<i>CCL18</i> [#]	C-C motif chemokine ligand 18	Down	8.50 \pm 0.41	10.99 \pm 0.88	5.60	0.005
<i>TNF</i> [#]	Tumor necrosis factor	Up	9.21 \pm 1.24	6.34 \pm 0.76	7.31	0.009
<i>NCAM1</i> ^{&}	Neural cell adhesion molecule 1	Up	4.00 \pm 0.35	2.57 \pm 0.70	2.69	0.016
<i>TNFRSF6B</i> [#]	TNF receptor superfamily member 6b	Down	6.33 \pm 0.62	7.48 \pm 0.33	2.22	0.017
<i>AOC3</i> [£] (<i>VAP-1</i>)	Amine oxidase copper containing 3	Down	11.54 \pm 1.29	13.85 \pm 0.78	4.94	0.020
<i>CCL13</i> [#]	C-C motif chemokine ligand 13	Down	6.78 \pm 1.28	9.28 \pm 1.12	5.66	0.024
<i>CCL3</i> [#]	C-C motif chemokine ligand 3	Up	14.04 \pm 1.54	9.83 \pm 2.64	18.43	0.032
<i>SELL</i> ^{&}	Selectin L	Up	9.34 \pm 0.73	7.86 \pm 0.98	2.78	0.045
<i>MAPT</i> [£]	Microtubule associated protein tau	Down	7.22 \pm 0.35	8.35 \pm 0.86	2.19	0.048

Genes are ordered according to differential expression P values. * by moderate t-test, followed by the application of Benjamini- Hochberg multiple testing correction. The mean \pm SD of the log-transformed (log₂) expression values is reported. The fold change is presented as an absolute value. Main processes from Gene Ontology database: [#] immune/inflammatory response, [§]angiogenesis, [&]adhesion, [£] cytoskeleton organization. *AOC3* is also known as *VAP-1*, vascular adhesion protein 1.

Table 6.4. Protein plasma levels in the jugular vein (1st MS population) and in peripheral vein (1st MS population and healthy subjects).

PROTEINS	MS/CCSVI JUGULAR PLASMA (n=17)	P*	MS/CCSVI PERIPHERAL PLASMA (n=17)	P [#]	HEALTHY PERIPHERAL PLASMA (n=34)	mRNA PROFILING
ANGPT1	2.6 \pm 0.90	0.016	3.6 \pm 1.7	0.02	6.2 \pm 2.8	↓
CCL13	87.3 \pm 32.8	0.22	79.6 \pm 23.2	0.33	89.7 \pm 39.6	↓
CCL18	27.2 \pm 9.3	0.048	30.4 \pm 11.1	0.30	34.7 \pm 15.5	↓
CD86	183.9 \pm 50.7	0.004	221.3 \pm 66.4	0.7	214.2 \pm 62.4 [§]	↑
NCAM1	138.2 \pm 57	0.005	149.9 \pm 58.3	0.08	123.5 \pm 44.2	↑
SELL	451.4 \pm 97.5	0.002	522.7 \pm 117.2	0.16	584.4 \pm 158.8	↑
VAP1	223.8 \pm 45.6	0.06	241.7 \pm 43.5	0.09	272.0 \pm 65.8	↓

Proteins: ANGPT1, angiopoietin 1; CCL13, chemokine ligand 13; 1CCL18, chemokine ligand 18; CD86, cluster of differentiation 86; NCAM1, neural cell adhesion molecule 1; SELL, selectin L; VAP1(AOC3), vascular adhesion protein 1(amine oxidase copper containing 3). Protein concentrations are reported in ng/ml, except for CD86 (U/ml). All values are expressed as mean \pm standard deviation. Arrows indicate up (↑) or down (↓) mRNA regulation in MS vs non-MS jugular wall. *P values from paired t-test (MS jugular plasma vs MS peripheral plasma). [#]P value from t-test on peripheral plasma (MS patients vs healthy subjects). [§] evaluated in 28 plasma controls.

The comparison of peripheral plasma levels between MS patients and healthy subjects showed significant differences for ANGPT1(3.6 \pm 1.7 vs 6.2 \pm 2.8 ng/ml, P=0.02). For

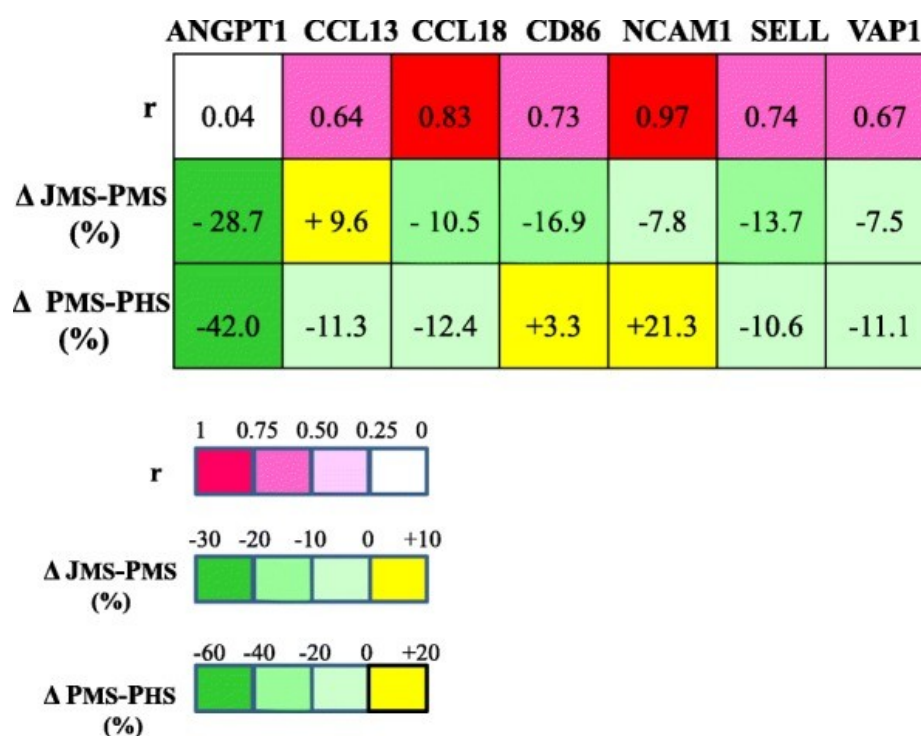
NCAM1 and VAP1, the P values (0.08 and 0.09 respectively) suggested a trend for differences between patients and healthy subjects.

The lower levels of ANGPT1 and VAP1, and the trend for higher levels of NCAM1 in patients might mimic the RNA expression regulation in the MS jugular wall estimated by transcriptomic analysis (Table 6.4).

In MS patients, the correlation between jugular vein and peripheral plasma concentrations ranged from very high ($r=0.97$, NCAM1) to virtually absent ($r=0.04$, ANGPT1) (Figure 6.2). Concentrations of ANGPT1, CD86, NCAM1 and SELL were significantly lower (paired t-test) in jugular than in peripheral plasma, with ANGPT1 showing the highest percentage difference ($\Delta = -28.7\%$, Figure 6.2).

Four proteins (CCL3, MAPT, TNF, and TNFRSF6B) resulted undetectable in the majority of plasma samples in the multiplex assay condition (data not shown).

Figure 6.2. Correlations and variations in protein plasma levels in the 1th MS population.



r , Pearson coefficient of the correlation between jugular and peripheral plasma levels in MS patients. Δ JMS-PMS %, percentage difference between jugular and peripheral (100%) plasma levels in MS patients. Δ PMS-PHS %, percentage difference between MS and healthy (100%) peripheral plasma levels.

Analysis of protein levels in peripheral plasma- 2nd MS Population

Peripheral plasma levels of ANGPT1, CCL13, CCL18, NCAM1, SELL and VAP1 were further analysed in an independent MS population (2nd study population). The levels were investigated in 60 patients, grouped by PP-MS and SP-MS clinical phenotypes (Table 6.5), and over 4-time points in 56 of them (Table 6.6). Peripheral plasma protein levels of the

2nd MS population were compared with those of the 1st MS population and of healthy subjects (Table 6.7). No differences in plasma protein levels between clinical subgroups, PP-MS and SP-MS were detected either at time 0 (Table 6.5) or overtime (data not reported). As significant age differences were present among clinical groups (PP-MS vs SP-MS, $P < 0.001$), ANCOVA adjusted for age was used to evaluate plasma levels, which did not reveal differences (Table 6.5).

Table 6.5. Plasma protein levels in the 2nd MS population according to clinical phenotypes.

	MS			PP-MS vs SP-MS	
	All MS n=60	PP-MS n=28	SP-MS n=32	t-test P-value	ANCOVA P-value
ANGPT1	6.4 ± 4	6.5 ± 3.6	6.4 ± 4.4	0.941	0.974
CCL13	116.3 ± 54.7	126.2 ± 64.6	107.6 ± 43.6	0.191	0.417
CCL18	44.6 ± 20.2	48.6 ± 24.2	41.1 ± 15.6	0.152	0.495
NCAM1	137.3 ± 54.5	145.3 ± 64.6	130.3 ± 43.9	0.292	0.189
SELL	558.6 ± 118.2	568.9 ± 118.6	549.6 ± 119	0.531	0.340
VAP1	313.8 ± 83.5	312.4 ± 77	315.1 ± 90	0.902	0.417

PP-MS: primary progressive multiple sclerosis; SP-MS: secondary progressive multiple sclerosis. The P values of t-test and ANCOVA (using age as covariate) are reported.

Proteins: ANGPT1, angiopoietin 1; CCL13, chemokine ligand 13; CCL18, chemokine ligand 18; NCAM1, neural cell adhesion molecule 1; SELL, selectin L; VAP1(AOC3), vascular adhesion protein 1(amine oxidase copper containing 3).

Table 6.6. Protein plasma levels over four-time points in the 2nd MS population.

	Time points				P-value	R
	T0	T1	T2	T3		
ANGPT1	6.3 ± 4	5.6 ± 3	6.3 ± 3.5	6.6 ± 4.1	0.186	0.675
CCL13	113.9 ± 53.6	108.2 ± 44.7	111.8 ± 44.4	116.5 ± 50.5	0.266	0.832
CCL18	44.6 ± 20.8	43.6 ± 20.5	44.9 ± 20.5	43.9 ± 21.9	0.568	0.945
NCAM1	137.5 ± 56.3	135.3 ± 54.2	133.4 ± 53.8	135.2 ± 58	0.137	0.980
SELL	553.2 ± 115.4	553 ± 113	527.6 ± 105.2	512.3 ± 103.9	<0.0001	0.897
VAP1	315.6 ± 84.8	306 ± 81.8	310.5 ± 82.5	310.1 ± 81.4	0.383	0.905

Protein levels were evaluated in 56/60 patients. Protein abbreviations are reported as in Table 2.

The P value of ANOVA for repeated measures across time is reported.

r= Pearson coefficient of correlations across 4 time points.

The comparison between the 2nd MS population and healthy subjects (Table 6.7) showed, after t-test, significant differences for CCL13, CCL18 and VAP1. However, after correction for age, only NCAM1 showed higher levels in MS patients than healthy subjects (137.3±54.5 ng/mL vs. 124±44 ng/mL; $P=0.050$).

The comparison between the 1st and 2nd MS populations (Table 6.7) showed significant differences (t-test) for AGPT1, CCL13, CCL18, and VAP1. After correction for age significant differences were observed for ANGPT1 and VAP1, and as a trend for CCL18 and SELL.

Table 6.7. Comparison of protein plasma levels in MS patients (1st and 2nd populations) and healthy subjects.

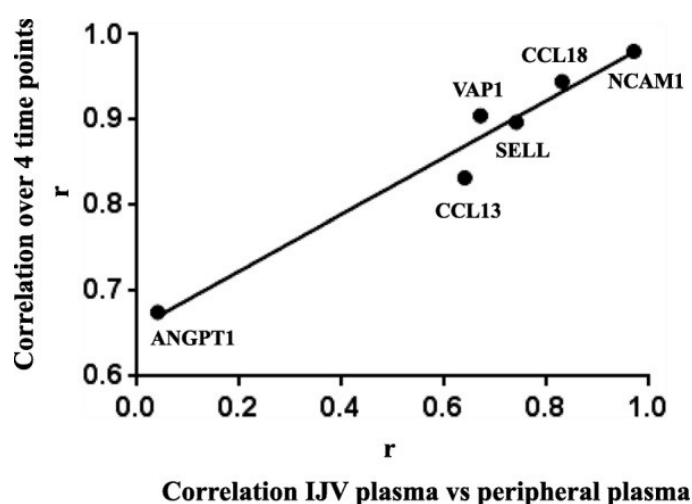
	2 nd Population vs 1 st Population		2 nd Population vs Healthy subjects	
	t-test	ANCOVA	t-test	ANCOVA
ANGPT1	0.021	0.033	0.261	0.330
CCL13	0.021	0.167	0.013	0.690
CCL18	0.004	0.082	0.002	0.302
NCAM1	0.231	0.332	0.204	0.050
SELL	0.241	0.079	0.914	0.161
VAP1	0.001	0.025	0.007	0.389

Protein levels were evaluated in 42 healthy subjects. The P values of t-test and ANCOVA (using age as covariate) are reported.

The analysis overtime of plasma protein levels in the 2nd population, aimed at evaluating the stability of protein levels in plasma, detected a significant difference over time only for SELL ($P < 0.0001$). In particular, the pairwise analysis revealed differences between several time points (T0-T1, $q = 0.023$; T0-T2, $q = 0.011$); T0-T3, $q < 0.0001$; T1-T3, $q = 0.048$). High correlation among time points for each protein was observed, ranging from $r = 0.67$ (ANGPT1) to $r = 0.98$, the noteworthy value for NCAM1.

Repeated protein assays in the 1st MS population (jugular and peripheral plasma) and in the 2nd MS population (four-time points in peripheral plasma) offered the opportunity to compare, in independent experiments, concentration variation between vascular bed compartments and overtime. The relation between correlation coefficients is shown in Figure 6.3. Interestingly, the r values between jugular and peripheral plasma protein concentrations in the 1st MS population, which ranged from virtually absent ($r = 0.04$, ANGPT1) to very high ($r = 0.97$, NCAM1, Figure 6.2), and that observed over time in the 2nd MS population (Table 6.6) were highly correlated ($R^2 = 0.96$, $P < 0.001$, r Pearson = 0.981, Figure 6.3).

Figure 6.3. Correlations of protein plasma levels: the relation between 1st and 2nd MS population values.



X axis: Pearson coefficients (r) of the correlation between jugular and peripheral plasma in 1st MS population. Y axis: Pearson coefficients (r) of the correlation over 4 time points in the peripheral plasma of the 2nd MS population.

Early and recent observations (242) suggest interactions between vascular abnormalities and neurodegenerative component in the manifestations of MS, which supports the investigation of both circulating and wall-associated factors. We aimed at contributing to these issues, in particular to the involvement of venous compartment, both by transcriptome and plasma protein investigation in MS patients. Surgical reconstruction of malformed IJV in patients was instrumental for the analysis of the transcriptome of the jugular vein wall, which in our knowledge has never been performed.

In transcriptomic profiling, confirmed by qRT-PCR, *LICAM* emerged as the most significantly downregulated gene, among several coding for proteins participating in adhesion processes. This neural cell adhesion molecule has been shown to function in a variety of dynamic neurological processes and to support adhesion by multiple vascular and platelet integrins (260) with implication in vascular processes.

Noticeably, transcriptomic data indicated dysregulation of the “pattern specification” and “nucleosome organization” processes, that could be related to the altered features of jugular flow observed in MS patients with associated chronic cerebrospinal venous insufficiency. Several members of the HOX transcription factors family, overexpressed in patients’ jugular wall transcriptome and belonging to the “pattern specification” process, are known to regulate embryogenesis, development and also processes in adult tissues, among which vasculature pathways (261). In particular, *HOXA5*, and *HOXB5* have been found to be blood flow-sensitive in endothelial cells (262). Disturbed flow conditions have been found to affect also expression of histone genes (“nucleosome organization”) in cultured endothelial cells from human carotid artery (263). Our findings link altered

transcriptional profiles of the jugular wall in patients to a number of important experimental observations obtained at the gene expression level in cellular and animal models unrelated to MS. Further, the down-regulation of several genes, related to muscle contraction, muscular/cytoskeleton system and members of the large collagen family, might be related to altered features and properties of the internal jugular vein, and particularly anatomy, histology and flow abnormalities (245, 264). However, only the availability of jugular wall expression profiling from MS patients not meeting the criteria for CCSVI, an unattainable goal, would permit to specifically attribute expression changes to MS or to vascular changes in MS-related CCSVI.

The strong up-regulation in patients' jugular wall transcriptome of CD86, a costimulatory protein involved in several mechanisms of immune response (265), could be related to immune activation at the level of jugular wall, potentially including immune cells adhering to the vessel surface, coherently with the well-known autoimmune features of MS. Remarkably, overexpression of CD86 transcripts in PBMC at all the stages of MS compared with healthy controls was recently reported (266).

Altogether the transcriptome analysis in jugular wall and the transcriptome analysis in PBMC from MS patients (256, 266, 267) suggest dysregulation of histone, cytoskeleton and CD86 genes as a general signature of altered gene expression in different cells and tissues of MS patients.

Investigation of changes observed at RNA level was combined with that in plasma at the protein level, through analysis of molecules acting in immune-inflammatory, in cell adhesion/neuronal cell adhesion and angiogenesis processes, all known to play a role in MS pathogenesis.

In addition to the 1st population of MS/CCSVI patients, a 2nd population with progressive MS phenotypes was analyzed for deeper investigation at the plasma protein level and to increase the robustness of our study. The repeated measurements help to define particularly conserved plasma patterns, well exemplified by the statistical analysis of CCL18 and VAP-1 values (Table 6.6).

VAP1, an amine oxidase with also adhesive activities (268), involved in a rat model of MS in CNS inflammatory lesion development (269), was previously found to be significantly lower in RR and in SP patients with absence of MRI active lesions than in controls (270). The Finnish cohort mirrors the 1st MS population of our study, in which the majority of patients were free from gadolinium-enhancing lesions at preoperative MRI (Table 3.2, page 35), and thus with absence of ongoing inflammatory activity within the brain. Further, the analysis conducted in the 2nd MS population clearly indicated both age and disease phenotypes as important determinants of VAP1 plasma levels.

To further characterize features of the IJV compartment in patients, the concentration of several proteins was analyzed in paired jugular and peripheral vein plasma samples. For most molecules, the good to excellent jugular-peripheral correlations, which were highly related to those observed over time in the 2nd MS population, support the quality of our analysis, conducted by a multiplex assay that prevents most of the bias in experimental condition among protein antigens. This approach also permitted to compare variation between vascular compartments with variation over time of specific protein levels. Protein biosynthesis, bio-distribution, and stability could participate in producing the different extent of correlation observed for each protein.

Noticeably, significantly lower levels in jugular were assessed for most proteins, with CCL13 being the only exception. The paucity of studies in literature, comparing jugular and peripheral plasma profiles in MS patients, and the unavailability of jugular plasma from healthy individuals limit the interpretation of the observed differences.

Although NCAM1 is thought to be involved in several processes, like neuronal development, organization of synapses and myelination/remyelination process, that take place in MS (271), data concerning plasma levels of NCAM1 in MS patients are not available in the literature. In our study, both MS populations showed as a trend higher levels than healthy subjects. Taking into account the tight correlations ($r = 0.97$) between jugular and peripheral plasma levels of NCAM1 and among repeated evaluations over time ($r=0.98$) performed in the 2nd MS population, which indicate the presence of particularly conserved individual plasma patterns in two MS disease cohorts, our findings suggest that NCAM1 plasma levels could be related to MS disease, independently from the CCSVI status.

Finding significant SELL level variation over time, in presence of high correlation, could highlight persisting changes dependent on the rehabilitative treatment in patients, as inferred by decreasing SELL concentrations from T0 to T3 time points.

ANGPT1, investigated for the first time in plasma of MS patients, showed remarkably lower levels in the jugular vein than in peripheral plasma. ANGPT1 levels in the 2nd MS population was similar to those in healthy subjects and higher than in the 1st MS population, even after correction for age, which suggests a CCSVI-related association. Further, the absence of correlation between values in jugular/peripheral compartments ($r=0.04$), compared with the good correlation estimated in repeated overtime measurements ($r=0.67$), would support the presence of specific mechanisms regulating ANGPT1 levels and, as jugular vein drains blood from the brain, cerebral expression/uptake might be candidate. The lower levels of ANGPT1 in plasma from the first MS population might

mimic the lower RNA expression in the MS jugular wall estimated by transcriptomic analysis.

Intriguingly, ANGPT1 is thought to play an essential role in microvascular endothelial and blood-brain barrier integrity. Indeed, ANGPT1, produced by endothelial cells, through the Tie-2 receptor is implicated on blood vessel stability and integrity by inhibiting blood vessel leakage, and reducing the infiltration of inflammatory cells (272, 273). This protective role of ANGPT1 has been suggested in experimental allergic encephalomyelitis studies (274), and interestingly mutations in the Tie-2 receptor were found to be associated with venous malformations (275).

The “long way” from jugular wall RNA to plasma protein is a remarkable limitation to study the parallel between mRNA and plasma protein concentrations. As a matter of fact, for CD86 several transcripts have been reported and the plasma assay (276) is able to detect only the soluble protein form of this membrane receptor, produced either by shedding or by alternative mRNA splicing. These CD86 mRNA and protein features have prevented detection of the relation between mRNA and protein expression. Our study presents other limitations. First, the small number of vascular wall specimens undergoing transcriptomic analysis, tiny specimens of the internal jugular wall, which represent by necessity very rare samples. Another limitation concerns the “control” CEA samples, being virtually unavailable jugular samples (wall) from MS patients, not meeting criteria for CCSVI, and from healthy individuals. Nevertheless, the analysis of protein levels in peripheral plasma in two independent MS populations, and in addition through repeated assays, favored investigation of MS-related variations.

In conclusion, the study provides for the first time expression profiles of the IJV wall and suggests signatures of altered vascular mRNA profiles in MS disease. Repeated measurements in plasma indicate conserved plasma patterns for immune-inflammatory and adhesion proteins. The combined transcriptome-protein analysis provides intriguing links between IJV wall transcript alteration and plasma protein expression, thus highlighting proteins of interest for MS pathophysiology.

Chapter 7**Increased CCL18
plasma levels are
associated with
neurodegenerative
MRI outcomes in
multiple sclerosis
patients**

**Ziliotto N, Bernardi F, Jakimovski D, Baroni M,
Bergsland N, Ramasamy DP, Weinstock-Guttman
B, Zamboni P, Marchetti G, Zivadinov R,
Ramanathan M.**

Based on:

Mult Scler Relat Disord. 2018;
25:37-42

doi:10.1016/j.msard.2018.07.009

7.1 BACKGROUND AND RATIONALE

The formation of MS plaques begins with activation of myelin-reactive T lymphocytes by antigen presenting cells, leading to multifocal immune cell infiltration into the CNS. The immunoreactive processes are sustained by activated T lymphocytes that secrete cytokines and chemokines. These molecules regulate recruitment and migration of lymphocytes and monocytes/macrophages to the damaged CNS regions and promote their differentiation (12, 277). Macrophage infiltration is associated with more severe tissue destruction and the balance between macrophage subpopulations is important for the formation, progression, and regression of MS plaques (278-281). The pro-inflammatory classically activated or type I macrophages (CAM or M1) have been observed predominantly in initial stages of active MS lesions, while the anti-inflammatory alternatively activated or type II macrophages (AAM or M2) might be induced through re-polarization after myelin ingestion (281, 282).

The C-C motif ligand 18 (CCL18 - also called Pulmonary and Activation-Regulated Chemokine, PARC, or Alternative Macrophage Activation-Associated CC-chemokine, AMAC-1) is the most highly expressed chemokine in several human chronic inflammatory diseases, as Gaucher disease and rheumatoid arthritis (283). It is synthesized by monocytes and dendritic cells upon infection or inflammation to attract T cells and is known for being a specific marker of M2 macrophages (284-286).

The chemokine C-C motif ligand 5 (CCL5 or regulated upon activation normal T-cell expressed and secreted, RANTES) is a marker of M1 (286). CCL5 has been detected in actively demyelinating MS lesions (287). Moreover, a genetic polymorphism of CCL5, able to influence the chemokine levels, was associated with a worse progression of MS disability (high-producer allele) or reduced risk of severe axonal loss (low-producer allele) (288). However, several studies investigated CCL5 serum and cerebrospinal fluid (CSF) levels in MS patients with discordant results (289-292).

The monomeric/oligomer states of chemokines, both CCL5 and CCL18, influence their half-life in blood thus enabling their detection and modulate their functions through the activation of their cognate receptors (293).

CD86 is a membrane protein member of the immunoglobulin superfamily expressed by antigen-presenting cells, which positively or negatively regulates T-cell activation, depending on differential receptor binding (294). CD86 is involved in initial co-stimulatory signaling in the immune response and the soluble form (sCD86), produced either by shedding or by alternative mRNA splicing, is detectable in plasma could be a marker of non-activated monocytes (M0) (295).

Given their important roles in macrophage function, CCL18, CCL5, and sCD86 could potentially modulate MS disease progression. However, the association of their levels in plasma with inflammatory and neurodegenerative magnetic resonance imaging (MRI) outcomes has not been systematically investigated. In this study, we used lesion volumes (LV) as MRI indicators of brain inflammation, and global and regional brain atrophy as neurodegenerative MRI biomarkers. We investigated the association between CCL18, CCL5 and sCD86 plasma levels with clinical and MRI outcomes in MS patients.

7.2 MATERIALS AND METHODS

Study Population

The study included 138 total MS patients (85 RR-MS, 53 P-MS) and 42 HI. The demographic and clinical characteristics of the study sample are summarized in Table 3.4 (page 38), while the MRI measurements are in Table 3.5 (page 39).

Assays for CCL18, CCL5, and sCD86

EDTA plasma samples for CCL18, CCL5, and sCD86 investigation were obtained at the visit. Analysts were blinded to the clinical status of samples.

CCL18 levels were assayed using Luminex Screening Assays magnetic bead kits (Luminex R&D Systems Inc., Minneapolis, MN, USA) whereas CCL5 levels were measured using Milliplex™ magnetic bead kits (human neurodegenerative disease panel 3, HNDG3MAG-36K, Merck Millipore, Germany). Data were acquired using the Luminex® 100 system and analyzed using Bioplex Manager Software version 6.0 (both from Biorad Laboratories, Hercules, CA). Concentrations were calculated according to each standard curve generated for the specific target and expressed as ng/mL.

sCD86 levels were measured using ELISA kits (ab45921, Abcam, United Kingdom) following the manufacturer's instructions. CD86 levels were expressed in U/mL. The inter-assay coefficient of variations for CCL18, CCL5 and sCD86 were 3.2%, 4.7% and 3.2%, respectively. CCL18 levels were not assessed for 1 MS patient and 2 HI, because the values were outside the range of the standard curve.

Statistical Analysis

All statistical analyses were performed using IBM® SPSS® Statistics version 24 software (IBM Corp. Armonk, NY, USA) and figures were produced by Graphpad Prism version 6.01 (GraphPad Software, Inc. La Jolla, CA, USA).

The Kolmogorov–Smirnov test was used to test the normal distribution of the data. Spearman's rank correlation was used to assess associations among the protein levels, and with demographic characteristics, disability status and disease duration.

Comparisons of CCL18, CCL5 and sCD86 levels between HI, RR-MS and P-MS were conducted with Kruskal-Wallis test followed by the Mann-Whitney U test. The same tests were used to assess whether CCL18, CCL5, and sCD86 levels were significantly different between patients receiving IFN-b, GA, other or no current DMTs. Multiple regression analysis was used for the following dependent variables: T2-LV, T1 LV, NBV, NCV, LVV, DGM, and thalamic volume. Age, gender, having P-MS, and protein of interest were used as predictor variables. BMI was included as predictor variable in the regression analysis of MRI measures with CCL18, because of its established influence on CCL18. A conservative p-value ≤ 0.01 was used for significance assessment given the multiple testing involved. A p-value ≤ 0.05 was considered a trend.

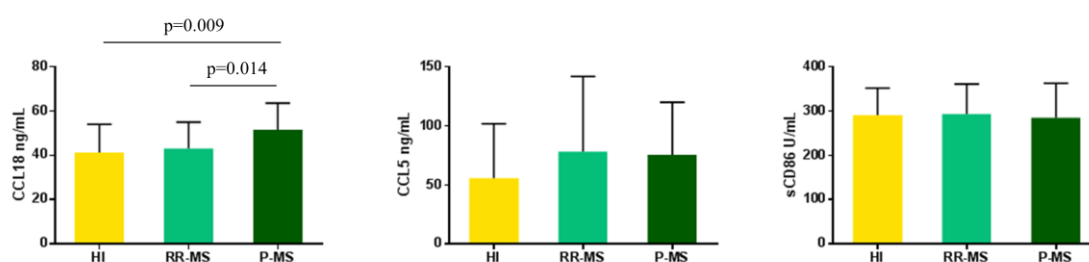
7.3 RESULTS AND DISCUSSION

Taking into account the role of macrophage infiltration in tissue destruction, and the role of CCL18, CCL5, and sCD86 in macrophage activation, we hypothesized that the expression of these proteins could be associated disease stage or progression.

The levels of CCL18, CCL5, and sCD86 in the MS and HI groups are summarized in Figure 7.1.

Differences between groups were present only for CCL18 levels ($p=0.015$, Kruskal-Wallis test). CCL18 levels were higher in P-MS (median=51.5, IQR=41.0-63.6 ng/mL) compared to RR-MS (median=43.0, IQR=29.1-55.0 ng/mL, $p=0.014$, Mann-Whitney U test) and to HI (median=41.3, IQR=30.9-54.1 ng/mL, $p=0.009$). No significant differences in CCL5 and sCD86 levels were observed between RR-MS, P-MS and HI groups.

Figure 7.1. CCL18, CCL5 and sCD86 levels in healthy individuals (HI), relapsing-remitting multiple sclerosis (RR-MS) and progressive MS (P-MS).

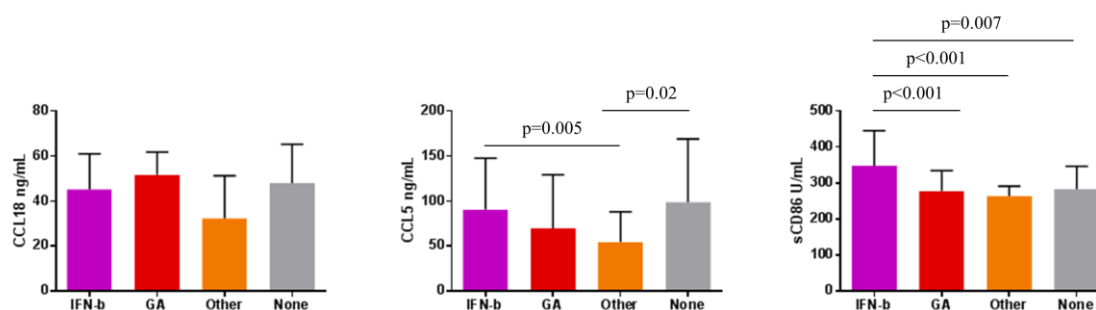


The p-values from a Mann-Whitney U test are provided for comparisons between groups where Kruskal-Wallis test resulted significant. The error bars indicate the interquartile range.
 CCL18: C-C motif ligand 18; CCL5: C-C motif ligand 5; sCD86: soluble cluster of differentiation 86.

Then, differences among DMT subgroups (interferon-beta, IFN-b; glatiramer acetate, GA; other or no DMTs; Figure 7.2) were explored, which were displayed only for CCL5 ($p=0.036$, Kruskal-Wallis test) and sCD86 ($p<0.001$). CCL5 levels were lower in MS

treated with other DMT (median=54.7, IQR=34.4-88.0 ng/mL) compared to IFN-b (median=90.6, IQR=54.0-147.5 ng/mL, $p=0.005$, Mann-Whitney U test) and to no DMTs (median=98.6, IQR=40.1-168.9 ng/mL, $p=0.02$). sCD86 levels were higher in MS treated with IFN-b (median=348.2, IQR=288.0-444.9 U/mL) compared to GA (median=278.0, IQR=240.0-334.3 U/mL, $p<0.001$, Mann-Whitney U test), to other (median=263.5, IQR=241.4-291.3 U/mL, $p<0.001$) and none DMTs (median=282.9, IQR=248.3-346.3 U/mL, $p=0.007$).

Figure 7.2. CCL18, CCL5 and sCD86 levels in multiple sclerosis cohort according to the disease-modifying treatment.



The p-values from a Mann-Whitney U test are provided for comparisons between groups where Kruskal-Wallis test resulted significant. The error bars indicate interquartile range.
 CCL18: C-C motif ligand 18; CCL5: C-C motif ligand 5; sCD86: soluble cluster of differentiation 86;
 GA: Glatiramer acetate; IFN-b: Interferon-beta; None: no disease-modifying therapy; Other: other disease-modifying therapy.

Quantitative measurements of brain atrophy have been shown to be the most robust correlates and long-term predictors of both cognitive and clinical disability (296). The associations of CCL18, CCL5, and sCD86 with MRI measures were investigated within MS and HI groups, and they are reported in Tables 7.1 and 7.2.

CCL18 levels were associated with increased LVV and T2-LV, and with decreased DGM and thalamic volumes. The regression analysis results suggested that a 1 ng/mL increase in CCL18 corresponded to an increase of 0.24 mL in LVV ($p=0.006$) and of 0.13 mL in T2-LV ($p=0.034$). For each 1 ng/mL increase in CCL18, the DGM volume decreased by 0.062 mL ($p=0.006$) and the thalamic volume decreased by 0.02 mL ($p=0.007$). CCL5 and sCD86 were not associated with any of the assessed MRI measures. Moreover, plasma levels of CCL18, CCL5 and sCD86 were not associated with EDSS or disease duration.

Overall in this study, CCL18 levels were found to be associated with inflammatory and neurodegenerative brain MRI outcomes, thus supporting a role for CCL18 in the progression of MS. In fact, higher CCL18 levels were found in P-MS compared to RR-MS and to HI, and multiple and coherent correlations with MRI measurements were observed.

In particular, higher CCL18 levels were associated with increased T2-LV and LVV, and with decreased NCV, DGM, and thalamic volumes.

Table 7.1. Association of CCL18, CCL5, and sCD86 with MRI characteristics of the MS cohort.

	CCL18		CCL5		sCD86	
	r_p	P	r_p	P	r_p	P
T2-LV	0.188	0.034	0.028	0.75	-0.031	0.72
T1-LV	0.100	0.27	0.002	0.98	0.010	0.91
NBV	-0.151	0.093	0.098	0.27	-0.017	0.85
NCV	-0.230	0.010	0.096	0.28	0.022	0.80
LVV	0.246	0.006	-0.035	0.70	-0.027	0.76
DGM volume	-0.247	0.006	0.104	0.24	0.073	0.41
Thalamic volume	-0.239	0.007	0.111	0.21	0.059	0.50

Partial correlation (r_p) and P value from regression analysis are shown. Multiple regression model: each MRI characteristic was used as the dependent variable while gender, age, being P-MS and the protein of interest as predictor variables. Additionally, BMI was included as predictor variables in the multiple regression model with CCL18.

CCL18: C-C motif ligand 18; CCL5: C-C motif ligand 5; sCD86: soluble cluster of differentiation 86; LV: lesion volume; NBV: normalized brain volume; NCV: normalized cortical volume; LVV: lateral ventricular volume; DGM: deep grey matter.

Table 7.2. Association of CCL18, CCL5, and sCD86 with MRI characteristics of the HI cohort.

	CCL18		CCL5		sCD86	
	r_p	P	r_p	P	r_p	P
T2-LV	-0.13	0.46	-0.037	0.82	-0.10	0.54
NBV	-0.015	0.93	-0.067	0.68	0.13	0.42
NCV	-0.084	0.64	-0.14	0.40	0.020	0.90
LVV	0.22	0.21	-0.25	0.13	-0.22	0.18
DGM volume	-0.17	0.33	-0.21	0.16	-0.029	0.86
Thalamic volume	-0.14	0.44	-0.056	0.74	0.15	0.35

Partial correlation (r_p) and P value from regression analysis are shown. Multiple regression model: each MRI characteristic was used as dependent variable while gender, age and the protein of interest were predictor variables. Additionally, BMI was included as predictor variables in the multiple regression model with CCL18.

CCL18: C-C motif ligand 18; CCL5: C-C motif ligand 5; sCD86: soluble cluster of differentiation 86; LV: lesion volume; NBV: normalized brain volume; NCV: normalized cortical volume; LVV: lateral ventricular volume; DGM: deep grey matter.

We report for the first time evidence that plasma CCL18 concentration might reflect the underlying disease progression within CNS. Despite the positive association between CCL18 levels and MRI measurements, no association was found between CCL18 levels with EDSS and disease duration.

We investigated for the first time the effects of DMTs on CCL18 levels, in particular IFN- β and GA which are commonly used first-line therapies in MS, and we did not detect any significant modification. Hence, the observed CCL18 correlation with MRI measurements could depend on disease progression mechanisms rather than relating to DMTs.

In light of the distribution of CCL18 plasma levels within the RR-MS, P-MS and HI groups, the range of variability limits the utility of CCL18 levels as diagnostic or prognostic biomarker. However, changes in plasma CCL18 have not been previously investigated in MS and our study provides insight into the pathways altered by dysimmune pathological mechanisms in MS. Indeed, CCL18 is known to be involved in chemotaxis of immune cells and exerts regulatory effects on them (297). Higher CCL18 levels in P-MS compared to RR-MS seem to corroborate the idea that more severe brain injury, defined as increase in lesions volumes and more advanced GM and central atrophy (30), is associated with increased levels of this chemokine.

Intriguingly, CCL18 is evolutionary present only in primates (285), which could have implication for human brain disease. Furthermore, a recent study identified CCL18 as a top-3 upregulated gene in the rim of chronic active MS lesions, where foamy, myelin-accumulating macrophages are abundant. These findings would also indicate that demyelinating sites around chronic active lesions are indeed expanding in time (298). In agreement, chronic active plaques are typically associated with P-MS and, as neurodegeneration in P-MS continues, preexisting chronic plaques may increase in size, resulting in slowly expanding, “smoldering” plaques (14, 299). Our *in vivo* results, using lesion volumes as MRI indicators of brain inflammation, and global and regional brain atrophy as neurodegenerative MRI outcomes, would support this model. Nevertheless, it is difficult to reconcile the potential anti-inflammatory role of CCL18 in relation to its expression by M2, with the worsening of clinical and MRI outcomes associated to increased CCL18 levels in patients.

Interestingly, CCL18 is involved in the lipid uptake and its levels were extremely elevated, between one and two orders of magnitude, in plasma of Gaucher disease patients, in whom a genetic deficiency in lysosomal glucocerebrosidase activity leads all macrophages to accumulate specific lipids (300). In cancer, infiltration of tumor-associated macrophages, and their CCL18 expression correlate with serum infection titers of Epstein-Barr virus (EBV) (301), an environmental risk factor in MS patients. In previous studies, we

suggested that higher levels of EBV antibodies are associated with increased MRI lesion activity and greater brain atrophy, particularly of the GM (302). Further studies are needed to investigate the hypothesis of mechanistic association of EBV with CCL18 in MS progression.

Similarly to previous studies (289, 291), we observed that CCL5 levels in plasma did not differ significantly in stable RR-MS group compared to controls. Additionally, stable RR compared to P-MS did not show differences in CCL5 levels (290). The increased levels detectable during relapse in MS patients as compared to stable RR-patients or controls (289-291), which could depict the ongoing inflammatory state, cannot be investigated in our cohort of MS patients, which did not include those in relapse. It is worth noting that our data, obtained in a larger cohort of patients, display ample variability in levels of each clinical and treatment groups, despite low inter-assay and intra-assay variations. Nevertheless, we detected significant DMTs related variations albeit not associated with GA treatment in accordance with previous data (303). We did not detect a trend for lower CCL5 levels after IFN- β treatment compared to none DMT (304).

Taking into account the DMT-related variations that we observed, these treatments could substantially contribute to produce heterogeneity in CCL5 levels.

A recent study, which investigated CCL5 levels in CSF of a patients' cohort comparable to ours, reported an association with the presence of gadolinium-enhanced brain MRI lesions (292). Our attempt to correlate peripheral CCL5 levels with MRI measures of lesion volumes and brain atrophy in a large cohort of MS patients failed to find an association.

Higher sCD86 levels were reported in autoimmune disorders such as systemic lupus erythematosus and rheumatoid arthritis (276, 305). The current study, which for the first time evaluated sCD86 plasma levels in MS, did not detect differences between MS clinical subgroups and with HI. Noteworthy significantly increased sCD86 levels were detected in relation to disease treatment with IFN- β . Accordingly, it is known that INF- β upregulates CD86 on monocytes of MS patients, who positively responded to the treatment (306). We infer that INF- β treatment could also induce CD86 mRNA alternative splicing/protein shedding, leading to the release of the evaluated soluble form (295). We did not detect any significant correlation of sCD86 with MRI measures. However, we have not investigated sCD86 plasma levels in the early stage of MS, as a potential marker of predisposition to the disease onset (295).

Our study presents some limitations. First, we studied peripheral plasma chemokines levels as indirect measure of macrophages-mediated expression, even if we did not investigate the number of circulating antigen-presenting cell populations. Second, the assay that we used for quantifying the chemokine concentration does not distinguish the different forms

(e.g., homodimers, heterodimers and oligomers) that are known to induce different pathways according to the activated receptor (293).

In conclusion, our results provide evidence that higher CCL18 plasma levels are associated with more severe inflammatory and neurodegenerative brain MRI outcomes in MS. Data support further investigation of plasma CCL18 levels in MS patients in association to disease progression, as well as functional and inhibition studies of CCL18, aimed at providing new insights into pathogenic mechanisms of MS.

Chapter 8

Plasma levels of soluble NCAM in multiple sclerosis

Ziliotto N, Zivadinov R, Jakimovski D, Baroni M, Tisato V, Secchiero P, Bergsland N, Ramasamy DP, Weinstock-Guttman B, Bernardi F, Ramanathan M, Marchetti G.

Based on:

J Neurol Sci. 2018; 396:36-41
doi: 10.1016/j.jns.2018.10.023

8.1 BACKGROUND AND RATIONALE

The members of the immunoglobulin superfamily, intercellular adhesion molecule-1 (ICAM-1) and vascular adhesion molecule-1 (VCAM-1), through binding to integrins LFA-1 and VLA-4 respectively, are critical in leucocyte-endothelia interaction, promoting the immuno-inflammatory response in MS (21, 22). The soluble forms sICAM-1 and sVCAM-1 are considered to be markers of BBB disruption (307) and might regulate functions of the corresponding cell-bound forms (308-310). A large number of studies investigated plasma or serum levels of sICAM-1 and sVCAM-1 in MS providing often conflicting data and highlighting heterogeneity in “immunological/adhesion pattern” among MS clinical phenotypes (311-315).

The neural cell adhesion molecule (NCAM, also known as CD56), another member of the immunoglobulin superfamily, is involved in cell migration, axonal growth, and fasciculation, organization, and modulation of synapses (reviewed in (316)). Its possible involvement in the reparative mechanisms and in the remyelination processes, key issues in MS (317), has been suggested (271). Shedding of sNCAM molecules from the cell membrane of neural and glial cells might have a role in brain plasticity, as it differentially alters neurite branching in a cell-type dependent manner (318, 319).

The large majority of the studies have investigated sNCAM levels in the cerebrospinal fluid (CSF), which appeared to be lower in MS patients CSF compared to controls and to decrease in a step-wise manner through the progression of MS disease (reviewed in (316)). Differently, only one study investigated sNCAM in the serum of MS patients (320).

Neuroimaging investigation of MS–adhesion molecule associations received considerable attention over the years, mainly evaluating the presence/absence of brain lesions, or T2 lesion volumes (315, 321-323) by magnetic resonance imaging (MRI). Brain atrophy assessment has become important for the evaluation of neurodegeneration and MS disease progression. The whole brain volume (BV), the cortical volume (CV) or lateral ventricular volume (LVV), reflect regional axonal loss as well as demyelination in white and gray matter tissue structures (30, 324). Moreover, atrophy of the deep gray matter (DGM) and particularly of the thalamus, which has a prominent role in integrating signals of complex cognitive and motor functions, is associated to physical and cognitive disability in MS (31). Up to now, the relationship between brain atrophy parameters and levels in plasma of soluble forms of adhesion molecules has not been explored in MS.

In this study, we aimed at investigating associations of soluble plasma levels of key adhesion molecules, the seldom studied sNCAM and as comparison sICAM-1 and sVCAM-1, with clinical and MRI measures of disease severity, in a cohort of MS patients and in healthy individuals (HI).

8.2 MATERIALS AND METHODS

Study Population

The study included 138 total MS patients (85 RR-MS, 53 P-MS) and 42 HI. The demographic and clinical characteristics of the study sample are summarized in Table 3.4 (page 38), while the MRI measurements are in Table 3.5 (page 39).

Assays for adhesion molecules

Adhesion molecules were measured in EDTA plasma samples obtained only once at the time of the neurological and MRI examinations. sNCAM, sICAM-1, and sVCAM-1 levels were assayed using Milliplex™ magnetic bead kits (human neurodegenerative disease bead panel 3, HNDG3MAG-36K, Merck Millipore, Germany). Based on the producer's information, this assay recognizes total sNCAM and not a specific isoform. Samples were processed following the manufacturer recommended protocols and read on a MAGPIX instrument equipped with the MILLIPIX-Analyst Software 5.1 (Merk Millipore) using a five-parameter nonlinear regression formula to compute sample concentrations from the standard curves. Concentrations were expressed as ng/mL. The calculated inter-assay coefficient of variations for sNCAM, sICAM-1 and sVCAM-1 were 4.9%, 5.7% and 7.3% respectively, while intra-assay coefficient of variations were 3.3%, 4.0% and 6.8%. The lower limits of detection for sNCAM, sICAM-1 and sVCAM-1 were 4.81 pg/mL, 6.29 pg/mL and 6.44 pg/mL, respectively. Assays were performed blinded to clinical status.

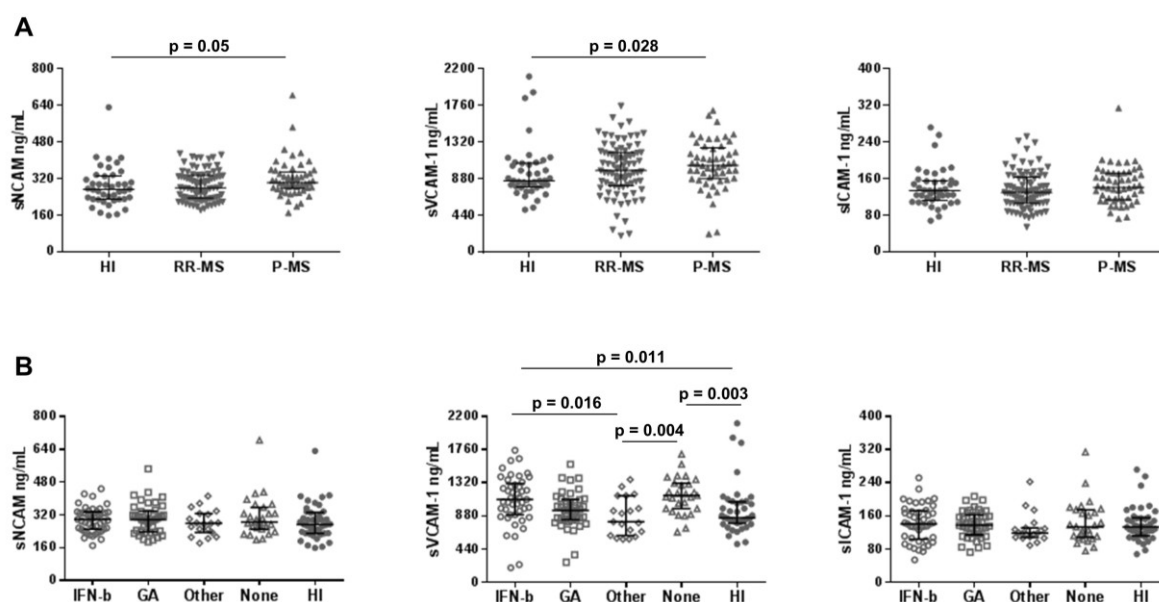
Statistical analysis

SPSS (IBM Corp. Armonk, NY, USA, version 24.0) statistical software was used for all statistical analyses and GraphPad (GraphPad Software, Inc. La Jolla, CA, USA, prism version 6.01) for the figures. Data were assessed for normality using the Kolmogorov–Smirnov test. Spearman's rank correlation was used to assess associations among the adhesion molecules levels and with demographic characteristics, EDSS and disease duration. Differences in adhesion molecules levels between clinical MS subgroups and HI were determined by the Kruskal-Wallis test, followed by Dunn's multiple comparison test. The same statistical tests were used to analyze variations of adhesion molecules levels in the presence of different disease-modifying treatments (DMTs). P -values ≤ 0.05 were considered as statistically significant. The associations of MRI measures with adhesion molecules were assessed using multiple regression analysis, with the MRI measure of interest as the dependent variable, and age, gender, drug-treatment and the adhesion molecule of interest as the predictor variables. Given the multiple testing involved, a conservative p -value ≤ 0.01 was used for significance assessment and a p -value ≤ 0.05 was considered a trend.

8.3 RESULTS AND DISCUSSION

Adhesion molecules are suggested to take part in the different processes that lead to the development of lesions and neurodegeneration in MS. Based on the functional importance in MS pathogenesis, we investigated the levels of sNCAM, and in comparison, those of sICAM-1 and sVCAM-1, in a large cohort of subjects, in which multiple clinical and MRI measures of disease severity were assessed. Levels were evaluated in plasma by a multiplex assay, which favors the detection of associations by decreasing experimental variations. The adhesion molecules levels in plasma of MS and HI groups are summarized in Figure 8.1A.

Figure 8.1. Adhesion molecules levels in MS patients and in healthy individuals (A) and in relation to MS disease-modifying treatment (B).



The adjusted p-values from Dunn's multiple comparison test are provided. The error bars indicate median and the interquartile range.

HI: healthy individuals; RR-MS: relapsing-remitting multiple sclerosis; P-MS: progressive multiple sclerosis; sNCAM: soluble neural cell adhesion molecule; sICAM-1: soluble intercellular adhesion molecule 1; sVCAM-1: soluble vascular cell adhesion molecule 1; GA: Glatiramer acetate; IFN- β : interferon-beta; None: no disease-modifying therapy; Other: other disease-modifying therapy.

The levels of sNCAM and sVCAM-1 differed among MS and HI ($p=0.033$ for both proteins, Kruskal-Wallis test). Higher levels in P-MS compared to HI were detected for sNCAM (median=302.6, IQR=276.8-349.3 ng/mL vs. 272.8, IQR=230.2-331.8 ng/mL; $p=0.050$) and for sVCAM-1 (median=1039, IQR=881.5-1249 ng/mL vs. median=855.3, IQR=782.6-1066 ng/mL; $p=0.028$) by Dunn's multiple comparison test. No significant differences in sICAM-1 plasma levels were observed between the study groups (Figure 8.1A).

Therefore, higher plasma levels of sNCAM in P-MS patients compared to HI were detected, a novel observation in the MS literature, in which data for the soluble form of NCAM in plasma are scanty.

Interestingly, increased levels of sNCAM were recently detected in sera of patients with various types of peripheral neuropathies (325) and peripheral neuropathy has been reported in MS without being associated with EDSS (326-328). The hypothesis that increased levels of sNCAM in progressive MS could be associated with the presence of peripheral neuropathy deserves further investigation. On the other hand in CSF, sNCAM levels were found either reduced in MS (329) as well as in SPMS as compared to RRMS (330) or increased in MS patients in the acute phase of the disease and undergoing steroid treatment (271). However, one of the limitations of our study is that we did not investigate sNCAM levels in CSF, which makes it difficult to speculate further.

Although sICAM-1 and sVCAM-1 have been extensively investigated in plasma (309, 312, 313, 331, 332), comparison with the previous and often conflicting observations is difficult because of different recruitment criteria of patients, and differently grouped clinical MS phenotypes. Our cross-sectional study did not include patients with signs of relapse provided by Gd-contrast, and thus the relapse-associated disease activity was not explored, a potential limitation of the present investigation.

The association among the adhesion molecules levels was explored in the MS and HI groups (Table 8.1). Highly significant correlations between plasma levels of sNCAM and sVCAM-1 were detected both in patients and HI ($r = 0.26$, $p = 0.002$ in MS and $r = 0.49$, $p = 0.001$ in HI). The noticeable values of the correlation coefficients for these molecules, which are produced by different genes and might be expressed by different cells, add further interest to this observation.

This relation, that we report here for the first time, could reflect a coordinated regulation of NCAM and VCAM-1 expression and/or shedding, present in healthy and disease conditions. The correlation coefficient, lower in MS patients than in HI, suggests that the biological pathways linking these adhesion molecules are altered in MS by still undefined molecular components, which deserves further investigation. Differently, the correlation between sICAM-1 and sVCAM-1 was observed only in MS patients ($r = 0.20$, $p = 0.021$), which might be explained by the role of their membrane forms, involved in the coordinated multi-step leukocytes adhesion process in disease (310).

As the plasma levels of adhesion molecules can be influenced by DMTs for level analysis (Figure 8.1B), those were categorized into four groups: IFN-beta, GA, Other and None. Since very few patients (Table 3.4, page 38) had been treated with natalizumab, they were not included in the analysis.

The levels of sVCAM-1 differed ($p < 0.001$, Kruskal-Wallis test) among the DMT groups and HI sVCAM-1 levels were higher in MS patients treated with IFN-b (median=1098, IQR=895.2-1311 ng/mL) compared to Other DMTs (median=802.4, IQR=619.6-1148 ng/mL; $p=0.016$) and to HI (median=855.3, IQR=782.6-1066 ng/mL, $p=0.011$).

Table 8.1. Correlations among adhesion molecules levels in multiple sclerosis patients and healthy individuals.

		sNCAM	sICAM-1
<i>Multiple sclerosis patients</i>			
sICAM-1	<i>Rho:</i>	-0.08	
	<i>P value:</i>	0.382	
sVCAM-1	<i>Rho:</i>	0.26	0.20
	<i>P value:</i>	0.002	0.021
<i>Healthy individuals</i>			
sICAM-1	<i>Rho:</i>	0.21	
	<i>P value:</i>	0.182	
sVCAM-1	<i>Rho:</i>	0.49	0.25
	<i>P value:</i>	0.001	0.107

Spearman correlation coefficient and p-values are reported.

sNCAM: soluble neural cell adhesion molecule; sICAM-1: soluble intercellular adhesion molecule; sVCAM-1: soluble vascular cell adhesion molecule 1.

Additionally, sVCAM-1 levels were higher in MS with None treatment (median=1149 ng/mL, IQR=975.2-1314) compared to HI (median 855.3, IQR=782.6-1066 ng/mL; $p=0.003$) and to Other treatment (median=802.4, IQR=619.6-1148 ng/mL; $p=0.004$). Neither sNCAM or sICAM1 levels showed significant differences among patients receiving different DMTs.

We provide the first evaluation for sNCAM in relation to several DMTs, which did not appear to influence plasma levels of this adhesion molecule. This would support the relation of the higher sNCAM concentration with MS progressive phenotype.

Although we found a noticeable correlation between sNCAM and sVCAM-1 plasma levels, only for sVCAM-1 we observed level differences in patients grouped by DMTs and higher levels in patients without treatment than in HI. Moreover, patients treated by drugs other than IFN-b and GA displayed the lowest levels. The study design and the heterogeneity of DMTs in this group do not enable to relate this observation to a specific treatment, which requires further investigation.

Finally, we investigated whether adhesion molecule levels could be associated with MRI measures in MS patients by regression analyses adjusting for age, gender and type of DMTs.

Brain atrophy is emerging as a meaningful indicator of neurodegeneration and clinical disease progression in MS patients and is at least partially independent of the effects of conventional MRI lesions (30, 333). None of the adhesion molecules investigated was associated with the MRI measures either in the whole MS and HI populations (Table 8.2 and 8.3, respectively) or in the P-MS group (data not shown). In addition, an association of levels with disability and disease duration did not emerge. As a matter of fact, a longitudinal study failed to find a correlation between mean levels of sICAM-1 and sVCAM-1 with MRI data of disease progression (322). On the other hand, patients with diagnosis of progressive MS in the present study presented higher levels of sVCAM and sNCAM and significant differences in MRI measures of disease severity as compared to HI.

Table 8.2. Association of adhesion molecules levels with MRI characteristics of the MS cohort.

	sNCAM		sICAM-1		sVCAM-1	
	r_p	P	r_p	P	r_p	P
T2-LV	0.006	0.95	0.044	0.61	-0.12	0.17
T1-LV	0.13	0.14	-0.033	0.71	-0.012	0.89
NBV	-0.14	0.12	-0.006	0.95	0.052	0.56
NCV	-0.051	0.56	-0.064	0.47	0.126	0.15
LVV	0.072	0.42	-0.025	0.78	0.023	0.80
DGM	-0.016	0.85	-0.061	0.49	0.13	0.14
Thalamus	-0.057	0.520	-0.047	0.60	0.046	0.60

Partial correlation (r_p) and P value from regression are shown. Multiple regression model: each MRI characteristic was used as dependent variable while gender, age, drug-treatment and the adhesion molecule of interest as predictor variables.

sNCAM: soluble neural cell adhesion molecule; sICAM-1: soluble intercellular adhesion molecule 1; sVCAM-1: soluble vascular cell adhesion molecule 1; LV: lesion volume; NBV: normalized brain volume; NCV: normalized cortical volume; LVV: lateral ventricular volume; DGM: deep grey matter.

Table 8.3. Association of adhesion molecules levels with MRI characteristics of the HI cohort.

	sNCAM		sICAM-1		sVCAM-1	
	r_p	P	r_p	P	r_p	P
T2-LV	0.018	0.91	-0.066	0.69	-0.063	0.70
NBV	-0.080	0.63	0.012	0.94	-0.115	0.49
NCV	0.001	0.99	0.021	0.90	-0.034	0.84
LVV	0.005	0.98	0.099	0.55	0.028	0.86
DGM	-0.108	0.51	-0.096	0.56	-0.222	0.18
Thalamus	-0.210	0.20	-0.096	0.56	-0.175	0.29

Partial correlation (r_p) and P value from regression are shown. Multiple regression model: each MRI characteristic was used as dependent variable while gender, age and the adhesion molecule of interest as predictor variables.

sNCAM: soluble neural cell adhesion molecule; sICAM-1: soluble intercellular adhesion molecule 1; sVCAM-1: soluble vascular cell adhesion molecule 1; LV: lesion volume; NBV: normalized brain

Overall, in a large cohort of patients characterized for multiple MRI measures of disease severity, sNCAM levels in plasma were evaluated for the first time, and compared with those of sICAM-1 and sVCAM-1. Plasma levels of sNCAM, sICAM-1 and sVCAM-1 did not correlate with clinical and MRI measures of disease severity.

Whereas the correlation between plasma levels of sNCAM and sVCAM-1 were detectable both in patients and HI, that between sICAM-1 and sVCAM-1 was observed only in MS patients. In progressive MS, as compared with HI, increased levels of sNCAM and sVCAM-1 were detected. This association was confirmed even after the evaluation of adhesion molecules levels in patients grouped by DMTs, which appear to modulate only sVCAM-1 plasma levels.

Chapter 9

Are plasma levels of VAP-1 associated both with cerebral microbleeds in multiple sclerosis and intracerebral hemorrhages in stroke?

Ziliotto N, Zivadinov R, Jakimovski D, Bergsland N, Ramasamy DP, Weinstock-Guttman B, Ramanathan M, Marchetti G, Bernardi F.

Based on:
Thromb Haemost. 2019;
119(1):175-178
doi: 10.1055/s-0038-1676346

9.1 BACKGROUND AND RATIONALE

Cerebral microbleeds (CMBs) are defined as small and hypointense areas which could correspond to clusters of haemosiderin-laden macrophages resulting from small self-limiting hemorrhages (42, 334). CMBs have been associated with aging, traumatic brain injury, stroke, and neurodegenerative disorders, among them the cerebral amyloid angiopathy. CMBs are potentially a radiological biomarker of the cerebral small vessel disease prone to bleeding and developing spontaneous intracerebral hemorrhages (ICH) (335, 336). Recently, in patients with atrial fibrillation anticoagulated after ischaemic stroke or transient ischaemic attack, the presence of CMBs was independently associated with symptomatic ICH risk, and could be used to inform anticoagulation decisions (337, 338).

Failure of blood-brain barrier integrity leading to focal extravascular leakage of blood components is a decisive event in the pathogenesis of MS, a disease characterized by multifocal demyelinated lesions within the central nervous system (339). Extravascular leakage of blood may have the features of radiologically measurable CMBs (40). Adhesion molecules participating in blood-brain barrier disruption and in inflammatory responses, supported by fibrinogen extravasation and promoting tissue factor expression (128, 340-342), in turn could be involved in the formation of CMBs.

Vascular adhesion protein-1 (VAP-1) facilitates leukocyte infiltration into inflamed tissue (343) through an enzymatic activity that mediates cell binding to the vessel wall. VAP-1 catalyzes the formation of free-radicals from its substrates on leukocytes, providing an inflammatory microenvironment and causing expression of additional adhesion molecules (268). VAP-1 is both a cell-surface and a circulating protein, released through cleavage mechanisms that are only partially defined (268, 344).

Higher plasma activity level of VAP-1 has been found both in consecutive patients with spontaneous ICH (345) and in patients with stroke treated with tissue plasminogen activator, who subsequently experienced ICH (346). In animal models, VAP-1 inhibition decreased both immune cell infiltration after ICH and microvascular dysfunction (347, 348).

Taking advantage of MS as disease model (42, 146, 177), we aimed at extending our knowledge about the association between plasma levels of VAP-1 and occurrence of CMBs in MS patients, assessed by magnetic resonance imaging (MRI) measures in a cross-sectional study (see Tables 3.4 and 3.5, pages 38-39). In turn, this could underline potential biological relations between CMBs and ICH.

9.2 MATERIALS AND METHODS

The demographic and clinical characteristics of the study sample are summarized in Table 3.4 (page 38), while the MRI measurements are in Table 3.5 (page 39).

The concentration of soluble VAP-1 molecule was measured in EDTA plasma samples using a multiplex assay (Luminex Screening Assays magnetic bead kits, R&D Systems Inc., Minneapolis, MN, USA), which permitted the parallel investigation of several adhesion molecules.

Samples were processed following the manufacturer recommended protocols and read on a MAGPIX instrument equipped with the MILLIPLEX-Analyst Software 5.1 (Merk Millipore) using a five-parameter nonlinear regression formula to compute sample concentrations from the standard curves. Concentrations were expressed as ng/mL. The calculated inter-assay coefficient of variations for sVAP-1 was 3.7%.

SPSS (IBM Corp. Armonk, NY, USA, version 24.0) statistical software was used for all statistical analyses and GraphPad (GraphPad Software, Inc. La Jolla, CA, USA, prism version 6.01) for the figures. Spearman's rank correlation was used to assess associations of sVAP-1 levels with demographic characteristics, EDSS and disease duration. The difference in sVAP-1 levels between MS patients with or without CMBs was assessed using the Mann Whitney U test. Linear regression was used to detect association between VAP-1 and CMBs volume.

The associations of MRI measures with sVAP-1 were assessed using multiple regression analysis. All regression analyses included the MRI measure of interest as the dependent variable; the predictor variables were age, sex, drug-treatment, and sVAP-1.

The Kruskal-Wallis test followed by Dunn's multiple comparison test was used to analyze variations of sVAP-1 levels according to disease-modifying treatments (DMTs). P-values ≤ 0.05 were considered as statistically significant.

9.3 RESULTS AND DISCUSSION

Analysis of VAP-1 concentration by non-parametric Mann Whitney U test revealed a trend for higher VAP-1 in MS(+)CMB vs. MS(-)CMB (median=300.9, IQR=192.2-401.5 ng/mL vs. median=237.2, IQR=195.8-276.1 ng/mL, $p=0.076$, Figure 9.1A).

VAP-1 levels were not associated with CMBs volume ($p=0.86$, linear regression). Interestingly, mean levels of this soluble adhesion molecule were numerically 32% higher in MS patients with CMBs than in healthy individuals (HI) (300 ± 105 ng/mL vs 227.3 ± 50 ng/mL), and 35% higher in ICH patients than in controls (345), a very similar proportion.

None of the other MRI measures (T2-LV, T1-LV, normalized brain, normalized cortical, lateral ventricular, deep gray matter, and thalamus volumes) in MS patients were associated with VAP-1 concentration by regression analyses (data not shown).

Taking into account that DMTs could potentially influence VAP-1 levels, the proportional distribution of DMTs use between MS(+)CMB vs. MS(-)CMB was also assessed ($P=0.761$, χ^2). Analysis among MS patients on DMTs, patients without treatment, and HI groups provided a significant variation in VAP-1 levels ($p=0.001$, Kruskal-Wallis test, Figure 9.1B). In particular, MS patients on DMTs had lower VAP-1 levels than those without treatment (median=231.1, IQR=190.3-276.3 ng/mL vs. median=272.7, IQR=251.6-324 ng/mL; $p=0.002$ Dunn's multiple comparison test). Further, VAP-1 levels in MS patients without treatment were higher than in HI (median=272.7, IQR=251.6-324 ng/mL vs. median=233.2, IQR=181.1-263.5 ng/mL; $p=0.002$ Dunn's multiple comparison test, Figure 9.1B).

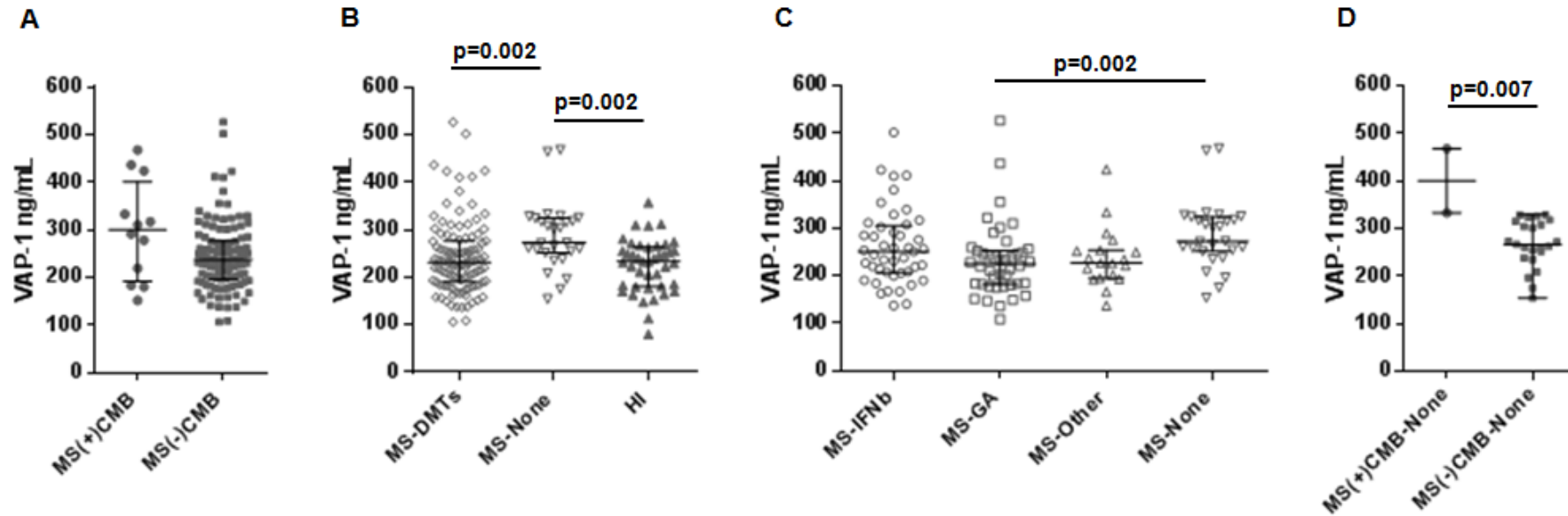
Modulation of VAP-1 levels by these drugs (see table 3.4 page 38, and legend of Table 3.5 page 39) was further investigated in MS patients ($p=0.002$, Kruskal-Wallis test, Figure 9.1C). This comparison showed that the decrease in VAP-1 levels was mostly influenced by glatiramer acetate (GA) treatment compared to MS without treatment (median=225.3, IQR=181.9-253.3 ng/mL vs. median=272.7, IQR=251.6-324 ng/mL; $p=0.002$, Dunn's multiple comparison test, Figure 9.1C). Finding higher VAP-1 concentration in plasma of MS patients without any DMT and lower in those on DMTs, clearly indicated that DMTs were not responsible for the higher VAP-1 levels in patients with CMBs. Instead, DMTs could mask even higher VAP-1 levels in patients with CMBs as indicated by comparison of patients not on DMTs (MS(+)CMB no DMT median=400.8, IQR=333.2-468.4 ng/mL vs. MS(-)CMB no DMT median=266.5, IQR=238-315, $p=0.007$ Mann Whitney U test, Figure 9.1D).

Of note, in patients with CMBs, plasma concentration differences were observed for VAP-1 and not for other soluble adhesion molecules (NCAM, ICAM-1 and VCAM-1), investigated in multiplex assays (data not shown).

Our observations have some limitations, I) CMBs are heterogeneous as suggested by their radiographic appearance (41), and in MS they are likely smaller in size as compared to CMBs investigated in ICH (338); II) we have evaluated in peripheral blood the soluble VAP-1, the level and role of which in brain vessel endothelium are only inferred; III) the VAP-1 activity values have the potential to reveal the presence of a functional enzyme in plasma (345, 346), whereas we measured the VAP-1 protein concentration, which however corresponds well to the level of enzymatic activity found in serum or plasma (268); IV) the number of patients with CMBs in our study was low; V) we are unaware of the effects and/or the biological implications of VAP-1 levels on CMBs over time. To confirm and detail this association further investigation in prospective studies of VAP-1 levels in larger cohorts of patients with CMBs is needed, including cerebral amyloid angiopathy, CADASIL and small vessel diseases patients.

In light of the previously detected association between CMBs and ICH occurrence (338), finding increased plasma levels of VAP-1 both in patients with ICH (345) and, at least as a trend for increased levels in MS with CMBs, is hypothesis generating. VAP-1, present in endothelium and smooth muscle cells of brain vessel (349), may promote inflammatory cell recruitment (350), which in turn might be associated with the conveyance of procoagulant mediators to sites of vascular injury (351). It is tempting to speculate that VAP-1 contributes both to cerebral microvascular endothelial cells dysfunction and to small and self-limiting hemorrhages, revealed by MRI. Our data foster the investigation in prospective studies of VAP-1 and other molecules potentially bridging ICH and CMBs.

Figure 9.1. VAP-1 levels in the cohort.



A. Soluble vascular adhesion protein 1 (VAP-1) concentration in multiple sclerosis patients with cerebral microbleeds (MS(+)/CMB, n=12), MS without CMB (MS(-)/CMB, n=113). Mann Whitney U test showed a trend for difference p=0.076.

B. VAP-1 levels among patients on disease-modifying treatments (MS-DMTs, n=111), patients without treatment (MS-none, n=27) and healthy individuals (HI, n=42) groups. The adjusted p-values from Dunn's multiple comparison test are provided for comparisons between groups where Kruskal-Wallis test was significant.

C. VAP-1 levels in MS cohort according to the disease-modifying treatment (DMT) (IFNb: Interferon-beta n=45; GA: Glatiramer acetate n=42; Other: other DMTs n=19; None: no DMT n=27). Since very few patients (Table 1) had been treated with natalizumab, we did not include them in this panel of analysis. The adjusted p-values from Dunn's multiple comparison test are provided for comparisons between groups where Kruskal-Wallis test resulted significant.

D. VAP-1 concentration in MS patients without treatment (none DMTs, n=25) grouped for presence of CMBs (MS(+)/CMB-none, (n=2) and MS(-)/CMB-none, (n=23)). The significant p-value from Mann Whitney U test is shown.

In all panels, median values and interquartile ranges are shown.

Chapter 10 C6orf10 low-frequency and rare variants in Italian multiple sclerosis patients

Ziliotto N, Marchetti G, Scapoli C, Bovolenta M, Meneghetti S, Benazzo A, Lunghi B, Laino LA, Bozzini N, Guidi I, Salvi F, Straudi S, Gemmati D, Menegatti E, Zamboni P, Bernardi F.

10.1 BACKGROUND AND RATIONALE

The heterogeneous manifestation and clinical course of MS are explained by its complex multi-factorial nature, where the interaction of genetic, lifestyle and environmental factors confer the susceptibility (10, 352). The heritable non-mendelian contribution to MS risk is supported by investigations on families (7).

To date, the majority of genetic studies on MS have been focused on susceptibility variants. In particular, several genome-wide association studies (GWAS), and subsequent replication studies, have identified hundreds of variants within susceptibility gene loci (353). The SNPs identified through GWAS are mainly located within non-coding regions of the genome, which could pinpoint the presence of disease-associated variants in linkage disequilibrium.

The very recent study, made by the International Multiple Sclerosis Genetics Consortium, provides for the first time the evidence that low-frequency variants (MAF<5%) explain 11.34% of the observed difference between cases and controls (354). The majority of low-frequency variants which contributed to MS risk were not individually detectable at genome-wide thresholds and among those associated with MS, only 1/3 were in linkage disequilibrium with the common variants from the GWAS (354).

Genetic studies in MS have used whole exome sequencing (WES) to investigate somatic mutations (355), to define the genetic contribution to MS clinical outcomes (356) and to suggest new potential causative variants in families (357-360) or unrelated patients (361). Some detection attempts of monogenic forms of the disease caused by rare variants with strong functional impact, using WES on families (362, 363), failed to overcome the subsequent replication studies (364-366). Based on the aforementioned findings, decoding the genetic risk components of MS still represents a challenge, and novel strategies are required to prioritize variants (367).

We set up a targeted WES-based pilot study in MS families, followed by low-frequency variants investigation in a cohort of unrelated patients in Italy, where a high prevalence and incidence of MS have been reported (5, 368). Being the HLA genes extensively studied in MS (reviewed in (19, 353)), we did not include them in our analysis.

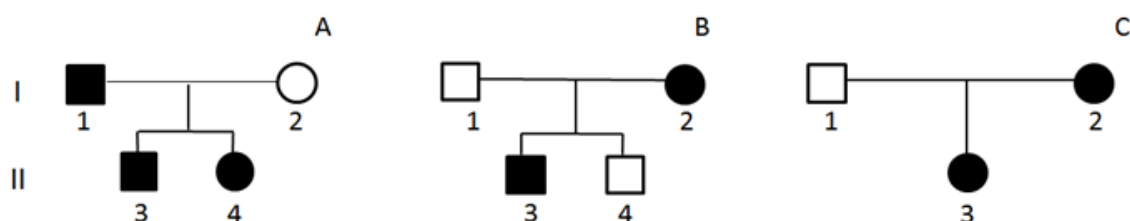
The main aim of this study was to identify new exonic and potentially functional low-frequency variants for MS risk within genes marked by intragenic common variants from the GWAS.

10.2 MATERIALS AND METHODS

Study population

The study population included three Italian families with MS-affected members (clinical characteristics and pedigree shown in Figure 10.1) and 120 Italian unrelated MS patients, selected from previous studies (186, 369). The selection criteria for the present study included age of MS onset under 52 years and MS diagnosis according to the 2010 revised McDonald criteria (187). All MS patients underwent neurological visits, MRI examinations and assessment of the Expanded Disability Status Scale (EDSS). Written informed consent was obtained from all subjects, and the study was approved by the Ethical Committee of the S. Anna University-Hospital, Ferrara, Italy. Demographic and clinical characteristics of the unrelated MS patients are summarized in Table 10.1.

Figure 10.1. Pedigree of families with multiple sclerosis and clinical characteristics of the affected family members.



	A-I-1	A-II-3	A-II-4	B-I-2	B-II-3	C-I-2	C-II-3
Age at onset	39	36	31	26	24	48	35
Age at examination	65	39	32	55	36	63	43
Phenotype at examination	SP-MS	RR-MS	RR-MS	RR-MS	RR-MS	RR-MS	RR-MS
EDSS at examination	6	1	1.5	1.5	1	3	4

Legend: RR-MS, relapsing-remitting multiple sclerosis; SP-MS, secondary-progressive multiple sclerosis; PP-MS, primary progressive multiple sclerosis; EDSS, expanded disability status scale.

Table 10.1. Demographic and clinical characteristics of the unrelated MS patients cohort.

	Clinical phenotype at examination			
	All MS	RR-MS	SP-MS	PP-MS
Sample size, n	120	44	53	23
Female, n (%)	74 (61.7)	27 (61.4)	31 (58.5)	16 (69.6)
Onset, mean y\pmSD	34.5 \pm 9.7	33.9 \pm 9.3	32.9 \pm 9.5	39.1 \pm 9.8
EDSS at examination, median (IQR)	6 (2-6.5)	2 (1-2.5)	6.5 (6-6.5)	6 (6-6.5)

Legend: RR-MS, relapsing-remitting multiple sclerosis; SP-MS, secondary-progressive multiple sclerosis; PP-MS, primary progressive multiple sclerosis; n, number; SD, standard deviation; y, years; EDSS, expanded disability status scale; IQR, inter quartile range.

Search strategy and selection criteria of candidate genes

A systematic review of the literature was performed for all years available through 31 December 2017. The primary source was the PubMed database (<http://www.ncbi.nlm.nih.gov/pubmed/>), for which search terms “GWAS” and “multiple sclerosis” were used. Further search included NHGRI-EBI GWAS catalog (<http://www.ebi.ac.uk/gwas>). Variants identified by GWAS in MS were selected for being intragenic, non-HLA, and having p-value $\leq 5 \times 10^{-6}$. On the basis of these selected common variants, we generated the final gene reference list for the present study (Table 10.2). The study design is schematically described in Figure 10.2.

Table 10.2. List of 141 intragenic SNPs in 107 genes from MS GWAS.

Gene	rs ID	Locus	Localization	Position (GRCh38/hg38)	References
<i>ADAMTS3</i>	rs78862524	4q13.3	INTRONIC	72305473	(370)
<i>AGAP2</i>	rs12368653	12q14.1	INTRONIC	57739473	(371)
<i>AGBL2</i>	rs7120737	11p11.2	INTRONIC	47680843	(372)
<i>AH11</i>	rs11154801	6q23.3	INTRONIC	135418217	(371, 372)
<i>ANKRD55</i>	rs6859219	5q11.2	INTRONIC	56142753	(373)
<i>ANKRD55</i>	rs71624119	5q11.2	INTRONIC	56144903	(372)
<i>BACH2</i>	rs12212193	6q15	INTRONIC	90287050	(371)
<i>BACH3</i>	rs72928038	6q15	INTRONIC	90267049	(372)
<i>BATF</i>	rs2300603	14q24.3	INTRONIC	75539214	(371)
<i>BTNL2</i>	rs4248166	6p21.32	NTRONIC	32398644	(374)
<i>C1orf106</i>	rs7522462	1q32.1	INTRONIC	200912467	(371)
<i>C1orf106</i>	rs55838263	1q32.1	INTRONIC	200905600	(372)
<i>C6orf10</i>	rs3129934	6p21.32	INTRONIC	32368410	(375)
<i>CBLB</i>	rs2028597	3q13.11	INTRONIC	105839993	(371)
<i>CBLB</i>	rs9657904	3q13.11	INTRONIC	105867870	(376)

<i>CD40</i>	rs4810485	20q13.12	INTRONIC	46119308	(372)
<i>CD58</i>	rs2300747	1p13.1	INTRONIC	116561593	(377)
<i>CD58</i>	rs1335532	1p13.1	INTRONIC	116558335	(371)
<i>CD6</i>	rs17824933	11q12.2	INTRONIC	60993140	(377)
<i>CD60</i>	rs6677309	1p13.1	INTRONIC	116537544	(372)
<i>CD69</i>	rs11052877	12p13.31	3'UTR	9753094	(372)
<i>CD86</i>	rs9282641	3q13.33	EXONIC	122077921	(371)
<i>CDH3</i>	rs1886700	16q22.1	INTRONIC	68652002	(372)
<i>CENPO</i>	rs4665719	2p23.3	INTRONIC	24794991	(372)
<i>CLEC16A</i>	rs6498168	16p13.13	INTRONIC	11141273	(373)
<i>CLEC16A</i>	rs6498169	16p13.13	INTRONIC	11155472	(378)
<i>CLEC16A</i>	rs11865121	16p13.13	INTRONIC	11072831	(377)
<i>CLEC16A</i>	rs7200786	16p13.13	INTRONIC	11083944	(371)
<i>CLEC16A</i>	rs6498160	16p13.13	INTRONIC	11105590	(376)
<i>CLEC16A</i>	rs12927355	16p13.13	INTRONIC	11100914	(372)
<i>CLECL1</i>	rs10466829	12p13.31	INTRONIC	9723495	(371)
<i>COPB1</i>	rs55665837	11p15.2	INTRONIC	14473503	(370)
<i>CXCR5</i>	rs523604	11q23.3	INTRONIC	118885029	(372)
<i>CXCR5</i>	rs630923	11q23.3	INTRONIC	118883644	(371, 379)
<i>CYP24A1</i>	rs2248359	20q13.2	5'UTR	54174979	(371)
<i>DDAH1</i>	rs11587876	1p22.3	INTRONIC	85449500	(372)
<i>DKKL1</i>	rs2303759	19q13.33	EXONIC	49365794	(371)
<i>DKKL1</i>	rs8107548	19q13.33	INTRONIC	49367386	(372)
<i>DLEU1</i>	rs806349	13q14.2	INTRONIC	50285854	(380)
<i>DLEU1</i>	rs9591325	13q14.2	INTRONIC	50237084	(373)
<i>DLEU1</i>	rs2812197	13q14.2	INTRONIC	50243690	(373)
<i>DLEU1</i>	rs806321	13q14.2	INTRONIC	50267187	(373)
<i>DLEU1</i>	rs9596270	13q14.2	INTRONIC	50268304	(373)
<i>ELMO1</i>	rs60600003	7p14.1	INTRONIC	37342861	(372)
<i>EPS15L1</i>	rs1870071	19p13.11	INTRONIC	16394295	(372)
<i>ERG</i>	rs2836425	21q22.3	INTRONIC	38466902	(373)
<i>ETS1</i>	rs3809006	11q24.3	INTRONIC	128540941	(380)
<i>EVI5</i>	rs11810217	1p22.1	INTRONIC	92682820	(371)
<i>EVI5</i>	rs11808092	1p22.1	EXONIC	92607671	(374)
<i>EVI5</i>	rs41286801	1p22.1	3'UTR	92509907	(372)
<i>FAM69A; RPL5</i>	rs6604026	1p22.1	INTRONIC	92838046	(381)
<i>FCRL1</i>	rs2050568	1q23.1	INTRONIC	157800451	(372)
<i>FLJ42102</i>	rs185378533	11q13.4	INTRONIC	71422087	(370)
<i>FOXP1</i>	rs9828629	3p13	INTRONIC	71481195	(372)
<i>GALC</i>	rs74796499	14q31.3	INTRONIC	87965984	(372)
<i>GC</i>	rs4588	4q13.3	EXONIC	71752606	(370)
<i>GEMIN2</i>	rs2277458	14q21.1	5'UTR	39114277	(370)
<i>GFII</i>	rs6689470	1p22.1	INTRONIC	92485653	(373)
<i>HAL</i>	rs3819817	12q23.1	INTRONIC	95984993	(370)
<i>IFI30</i>	rs11554159	19p13.11	EXONIC	18175134	(372)
<i>IFNGR2</i>	rs9808753	21q22.11	EXONIC	33415005	(380)

<i>IL12A</i>	rs4680534	3q25.33	INTRONIC	159981157	(377)
<i>IL12A</i>	rs2243123	3q25.33	INTRONIC	159991864	(371)
<i>IL12A-AS1</i>	rs1014486	3q25.33	INTRONIC	159973324	(372)
<i>IL2RA</i>	rs12722489	10p15.1	INTRONIC	6060049	(378)
<i>IL2RA</i>	rs2104286	10p15.1	INTRONIC	6057082	(372)
<i>IL2RA</i>	rs12253981	10p15.1	INTRONIC	6050383	(376)
<i>IL2RA</i>	rs3118470	10p15.1	INTRONIC	6059750	(371)
<i>IL2RA</i>	rs12722561	10p15.1	INTRONIC	6027930	(374)
<i>IL7R</i>	rs6897932	5p13.2	EXONIC	35874473	(371)
<i>IL7R</i>	rs6881706	5p13.2	3'UTR	35879054	(372)
<i>ILDRI</i>	rs2681424	3q13.33	INTRONIC	122050675	(373)
<i>ILDRI</i>	rs2255214	3q.13.33	INTRONIC	122051692	(372)
<i>IQCB1</i>	rs1920296	3q13.33	INTRONIC	121824730	(372)
<i>IQGAP1</i>	rs8042861	15q26.1	INTRONIC	90434101	(372)
<i>JAZF1</i>	rs9117116	7p14.1	INTRONIC	28133120	(372)
<i>L3MBTL3</i>	rs4364506	6q23.1	INTRONIC	130068795	(373)
<i>loc100506047</i>	rs2163226	2p21	INTRONIC	43134117	(372)
<i>loc105376481</i>	rs1891621	10p11.23	INTRONIC	31101198	(373)
<i>LPIN3</i>	rs6072343	20q12	3'UTR	41339548	(380)
<i>LPP</i>	rs4686953	3q26	INTRONIC	188365131	(380)
<i>LRP2</i>	rs12988804	2q31.1	INTRONIC	169261301	(382)
<i>MALTI</i>	rs7238078	18q21.32	INTRONIC	58716960	(371)
<i>MANBA</i>	rs228614	4q24	INTRONIC	102657480	(371, 379)
<i>MAPK1</i>	rs2283792	22q11.21	INTRONIC	21776836	(371, 372)
<i>MAZ</i>	rs34286592	16p11.2	INTRONIC	29809159	(373)
<i>MERTK</i>	rs17174870	2q13	INTRONIC	111907624	(371)
<i>METTL1</i>	rs703842	12q14.1	3'UTR	57768956	(381)
<i>MMEL1</i>	rs3748817	1p36.32	INTRONIC	2594226	(372)
<i>MPV17L2</i>	rs874628	19p13.11	EXONIC	18193890	(371)
<i>NADSYN1</i>	rs4423214	11q13.4	INTRONIC	71462208	(370)
<i>NCOA5</i>	rs2425752	20q13.12	INTRONIC	46073481	(371)
<i>NDFIP1</i>	rs1062158	5q31.3	INTRONIC	142143435	(371)
<i>NDFIP2</i>	rs1036207	5q31.3	INTRONIC	142119476	(372)
<i>ODF3B</i>	rs140522	22q13.33	3'UTR	50532837	(371, 380)
<i>PDE3B</i>	rs116970203	11p15.2	INTRONIC	14855172	(370)
<i>PHGDH</i>	rs666930	1p12	INTRONIC	119716347	(372)
<i>PITPNM2</i>	rs7132277	12q24.31	INTRONIC	123108835	(372)
<i>PITPNM2</i>	rs949143	12q24.31	INTRONIC	123110616	(371)
<i>PLEKHG5</i>	rs3007421	1p36.31	INTRONIC	6470129	(372)
<i>PVT1</i>	rs4410871	8q24.21	INTRONIC	127802783	(371)
<i>PXT1</i>	rs941816	6p21.31	INTRONIC	36407527	(372)
<i>RGS1</i>	rs7535818	1q31	INTRONIC	192575969	(373)
<i>RGS14</i>	rs4976646	5q35.3	INTRONIC	177361569	(372)
<i>RPS6KB1</i>	rs180515	17q23.1	3'UTR	59946914	(371, 380)
<i>RRAS2</i>	rs182244780	11p15.2	INTRONIC	14363985	(370)
<i>SLAMF7</i>	rs35967351	1q23.3	INTRONIC	160742014	(372)

<i>SLC2A4RG</i>	rs2256814	20q13.33	INTRONIC	63742630	(372)
<i>SLC30A7</i>	rs11581062	1p21.2	INTRONIC	100941963	(371)
<i>SLC44A2</i>	rs2288904	19p13.2	EXONIC	10631494	(372)
<i>SLC9A8</i>	rs17785991	20q13.13	INTRONIC	49822224	(372)
<i>SP140</i>	rs10201872	2q37.1	INTRONIC	230242009	(371)
<i>SP140</i>	rs9989735	2q37.1	INTRONIC	230250739	(372)
<i>SPON1</i>	rs117865811	11p15.2	INTRONIC	14180763	(370)
<i>STAT3</i>	rs744166	17q21.2	INTRONIC	42362183	(383)
<i>STAT3</i>	rs9891119	17q21.2	INTRONIC	42355962	(371)
<i>STAT3</i>	rs2293152	17q21.2	INTRONIC	42329511	(384)
<i>STAT3</i>	rs4796791	17q21.2	INTRONIC	42378745	(372)
<i>STAT4</i>	rs996792	2p14.1	INTRONIC	191109709	(372)
<i>TAGAP</i>	rs1738074	6q25.3	5'UTR	159044945	(371)
<i>TET2</i>	rs2726518	4q24	INTRONIC	105252042	(372)
<i>TIMMDC1</i>	rs2293370	3q13.33	INTRONIC	19501087	(371)
<i>TIMMDC2</i>	rs1131265	3q13.33	EXONIC	119503609	(372)
<i>TNFRSF1A</i>	rs4149584	12p13.31	EXONIC	6333477	(377)
<i>TNFRSF1A</i>	rs1800693	12p13.31	INTRONIC	6330843	(371, 372)
<i>TNFSF14</i>	rs1077667	19p13.3	INTRONIC	6668961	(371, 372)
<i>TOP3A</i>	rs4925166	17p11.2	INTRONIC	18307496	(373)
<i>TRAF3</i>	rs12148050	14q32.32	INTRONIC	102797451	(372)
<i>TSM</i>	rs201202118	12q14.1	INTRONIC	57788279	(372)
<i>TYK2</i>	rs34536443	19p13.2	EXONIC	10352442	(372)
<i>VMP1</i>	rs8070345	17q23.1	INTRONIC	59739396	(372)
<i>WWOX</i>	rs12149527	16q23.1	INTRONIC	79076699	(372)
<i>ZBTB38</i>	rs9846396	3q23	INTRONIC	141422126	(380)
<i>ZBTB46</i>	rs6062314	20q13.33	INTRONIC	63778360	(371, 380)
<i>ZFP36L1</i>	rs2236262	14q24.1	INTRONIC	68794755	(372)
<i>ZFP36L1</i>	rs4902647	14q24.1	5'UTR	68787474	(371)
<i>ZMIZ1</i>	rs1250540	10q22.3	INTRONIC	79276250	(377)
<i>ZMIZ1</i>	rs1250550	10q22.3	INTRONIC	79300560	(371)
<i>ZMIZ1</i>	rs1250542	10q22.3	INTRONIC	79274913	(384)
<i>ZMIZ1</i>	rs1782645	10q22.3	INTRONIC	79288854	(372)
<i>ZNF767P</i>	rs354033	7q36.1	INTRONIC	149592373	(371)

DNA samples/ Genomic DNA extraction

The genomic DNA (gDNA) was extracted from blood using the Wizard® Genomic DNA Purification Kit (Promega, Madison, WI, USA), according to the manufacturer's instructions. The gDNA integrity was checked on 0.8% agarose gel stained with GelRed® (Biotium, Fremont, CA, USA) by analyzing gel on UVITEC Cambridge Gel Documentation System fire-reader XS (Cleaver Scientific Ltd, Warwickshire, UK). The gDNA concentrations were measured at 260 nm with BioSpec-nano Spectrophotometer (Shimadzu Corporation, Kyoto, Japan), then samples were stored at -20 °C until use.

Whole-exome sequencing and analysis

Whole-exome sequencing (WES) was performed on eleven individuals, seven diagnosed with MS and four unaffected, from three independent families (Figure 10.1).

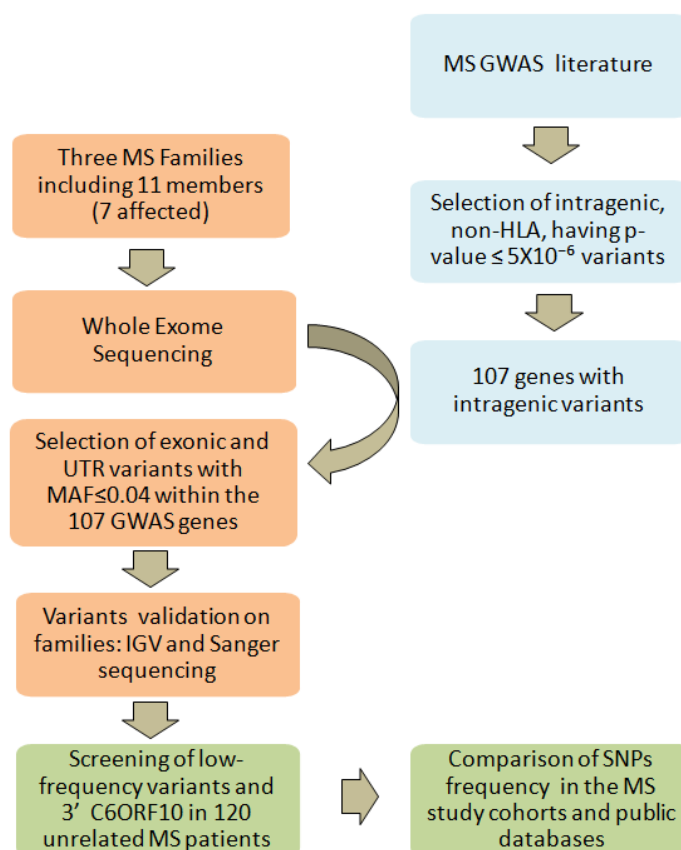
Sequencing was performed by BGI (Shenzhen, China) using nanoarray-based short-read sequencing-by-ligation technology (cPAL™). Reads were mapped against the hg19 human reference sequence (<http://genome.ucsc.edu/>) using SOAPaligner (<http://soap.genomics.org.cn/>).

Variants calling was performed with the Complete Genomics Small Variant Caller (http://www.completegenomics.com/documents/Small_Variant_Assembler_Methods.pdf).

Genetic variations were verified in the database of Single-Nucleotide Polymorphisms (dbSNP, Build 150, <http://www.ncbi.nlm.nih.gov/projects/SNP/>) and the 1000 Genomes Project databases (<http://www.1000genomes.org/data>).

The filtering performed on WES-data is schematically described in Figure 10.2. In order to remove systematic artifacts, we visually verified the filtered low-frequency variants with IGV (<http://software.broadinstitute.org/software/igv/>).

Figure 10.2. Study design.



Multiple sclerosis (MS) GWAS and WES SNP filtering is schematically described.

In light blue, the search strategy and selection criteria of candidate genes; in orange the Whole-exome sequencing and the analysis on MS families; in green the screening strategy in the unrelated MS patients.

The effects of new coding variations on protein structure and function were predicted using Provean/SIFT (http://sift.jcvi.org/www/SIFT_enst_submit.html), while the effects of low-frequency coding variations, already reported on databases as prediction by SIFT/PolyPhen, were extrapolated from Ensembl (<http://www.ensembl.org/index.html>).

Mutation screening

A selection of low-frequency variants, identified through the filtering in MS families, were confirmed by Sanger sequencing or restriction analysis. Primers to amplify the coding sequences containing the identified low-frequency variants were designed with Primer3 software v0.04.0 (<http://bioinfo.ut.ee/primer3-0.4.0/>). A total of 50 ng of gDNA was amplified by polymerase chain reaction (PCR) using a standard protocol with AmpliTaq Gold 360 DNA polymerase (Applied Biosystems, Foster City, CA, USA).

PCR conditions were set up as follows: an initial denaturation at 94°C for 5 minutes and then at 65°C for 3 minutes, followed by 35 cycles at 94°C for 30 seconds, specific temperatures for each couple of primers for 30 seconds, 72°C for 30 second or 1 minute, and a final elongation at 72°C for 7 minutes.

The PCR products were purified with CleanSweep™ PCR Purification (Applied Biosystems) prior to direct sequencing (Macrogen, Madrid, Spain). Sequences were analyzed using the software NovoSNP (385). Size of PCR amplicons and following digestion products were examined through agarose gel electrophoresis. All primer sequences, PCR conditions and restriction enzymes used in this study are listed in Tables 10.3 and 10.4.

The presence of the selected low-frequency variants was investigated in a sample set of 120 Italian unrelated MS patients through Sanger sequencing or restriction analysis.

Statistical Analysis

For populations comparison, we used MAFs obtained from: i) the “dbSNP Build 150” (Homo sapiens Annotation Release 108) which combines all available frequencies from submitted SNPs clustered together into a reference SNP, and ii) 1000 Genome Project which contains allelic frequencies for a sample of 107 subjects from Tuscany, Italy, an optimal reference population for our MS samples. Moreover, the prevalence of MS in Tuscany (188 per 100'000 individuals (386) supports the healthy condition of the Tuscany control sample.

To test the difference in MAFs between reference populations and the allelic frequencies observed in the study population, a two-proportion z-test, with a 0.05 two-sided significance level, was applied. A threshold of $p < 0.0042$, assuming the Bonferroni correction for multiple testing, was used for significance.

The potential enrichment of exonic low-frequency variants in MS patients was evaluated using a permutation approach based on the observed exonic polymorphisms. We first generated the null distribution of the number of low-frequency variants in a random sample of 107 genes, considering the exons composing the longest isoform of each gene, as defined by the human genome annotation (GRCh37/hg19). We took into account both the number and the length of exons, dividing the number of low-frequency variants by the total exon length, for each gene set. Then, we repeated the permutation process 1,000 times and the empirical p-value was defined as the proportion of replicates showing a number of variants higher than the observed value.

Table 10.3. Mutation screening by sequencing.

Gene	SNP position GRCh37/hg19	SNP ID	Forward primer sequence (5'-3') Reverse primer sequence (5'-3')	T _m (°C)	Length (bp)
<i>ANKRD55</i>	5:55407449	rs77017041	TTGTCACTCCAGTTCCTAGCTT CCTGATGAAGCATGTGGAAT	60	850
<i>C6orf10</i>	6:32261153	rs16870005	TTTAGGCAATGGCTGGGATA TGTGCCAAGAAGACAGGAATC	60	658
<i>CD86</i>	3:121774281	rs11575853	TCTTCCTCAAGTGTGGTCAAAA GCACCATCTTCAACCTCAGC	60	297
<i>EVI5</i>	1:92979432	rs41286809	TGGCAATGGTAAATCAGTGG CATGGAATGTTTGCTTTTTGG	60	595
<i>IL2RA</i>	10:6054765	rs12722600	ATAGAGACAAGGTTGCCACTGC CCACAGCTATTGTCTGCCATATAAA	66	468
<i>MALT1</i>	18:56367823	rs74847855	CACTTTCAAAGCTTCATACTGAAATC AAGACAAAACACATGGATCAAATCT	60	427
<i>MMEL1</i>	1:2530169	rs147248515	TAACCCCTCATGTCCCACAC GGGGCTGGGTTTCTTAGATT	63	353
<i>STAT4</i>	2:191899319	-	GAAATTCTCAAACCCCATGT AAATTGAGCACAAAATTGAAGC	60	209
<i>TET2</i>	4:106156163	rs61744960	TATTATCCAGATTGTGTTTCCATTG CTTAGTGAACACTGAGCTTTGCTT	63	471
<i>TOP3A</i>	17:18217958	rs2230153	TCGCCTTCATCTCGATTCTT TGAGCCTCATCTCTGGCTTC	55	342
<i>TRAF3</i>	14:103371923	rs138943371	ATGTGTGCCAGGGTCTACCT TCTTGAAGCTGCTGCTGTTG	63	220
<i>WWOX</i>	16:78458807	rs7201683	AAAGAATTTCTCATTCCCGAAG CACCCACATGTCTCAAGCAG	60	444

Table 10.4. Mutation screening by restriction.

Gene	SNP position GRCh37/hg19	SNP ID	Forward primer sequence (5'-3')	Reverse primer sequence (5'-3')	T _m (°C)	Ref allele SNP allele	Restriction enzyme
<i>ADAMTS3</i>	4:73414590	---	TCACCCACAGATTTACCA <u>T</u> TA	GGGCTTTAGTCGCAGATGAA	60	A:139+46+20 G:159+46	<i>MseI</i>
<i>ANKRD55</i>	5:55407449	rs77017041	GGTGATGATGTCATTGACT <u>G</u> CTG	TACTCACATATCATCCCTGCTCTTT	60	A:201+21 G:222	<i>Bpu10I</i>
<i>CD86</i>	3:121774281	rs11575853	CTGCTGTAACAGGGACTAGC <u>T</u> CA	AGGAACTAAGTGAAGGACACACATC	60	A:176+23 G:199	<i>Hpy188I</i>
<i>EVI5</i>	1:92979432	rs41286809	ACACATAGAAGGCACTCAAAAATTAG	CTATAAAATCTTCATCGGAGGA <u>C</u> TG	60	C:250+25 T: 275	<i>Bsr I</i>
<i>GC</i>	4:72669661	rs76781122	CCACTAATGCCAGCCAATCT	TGCTTTGCACAGAAATCCTC	60	G:361+48 T:266+95+48	<i>ApoI</i>
<i>IL2RA</i>	10:6054765	rs12722600	AACAGAAGTCATGAAGCCCA <u>C</u> GT	AGTGGTTTTGCCCTTCCTC	60	G:219+21 A:240	<i>PmlI</i>
<i>MALT1</i>	18:56367823	rs74847855	CACTTTCAAAGCTTCATACTGAAATC	AAGACAAAACACATGGATCAAATCT	60	A:248+179 G:427	<i>Hpy188III</i>
<i>MMEL1</i>	1:2530169	rs147248515	CACTAAAGCTTAACCCCTCATGTC	TATCCTCTGTCAAAATCAAGCTG <u>G</u> T	60	G:221+27 T:248	<i>BanI</i>
<i>TET2</i>	4:106156163	rs61744960	CTGATGATGCTGATAATGCCAGT	GTAAGCACCATTTCATTTTATTGT	60	G:134+75+39 A:134+114	<i>NlaIV</i>
<i>TOP3A</i>	17:18217958	rs2230153	TCGCCTTCATCTCGATTCTT	TGAGCCTCATCTCTGGCTTC	55	G:190+134+18 A:190+152	<i>EaeI</i>
<i>TRAF3</i>	14:103371923	rs138943371	ATGTGTGCCAGGGTCTACCT	TCTTGAAGCTGCTGCTGTTG	63	C:146+62 T:208	<i>AvaII</i>
<i>TYK2</i>	19:10472452	rs12720355	GGACCCTAGTCACCATGA <u>G</u> AT	GTCTCGTAGAAGGCCTGTGG	60	C:197+18 T:215	<i>MboI</i>
<i>WWOX</i>	16:78458807	rs7201683	AAAGAATTTCTCATTCCCGAAG	CACCCACATGTCTCAAGCAG	60	C:444 G:259+185	<i>RsaI</i>

To verify the presence of the selected mutations, PCR products were digested with restriction enzymes. Nucleotides in bold and underlined are those modified to create specific restriction sites.

10.3 RESULTS AND DISCUSSION

Taken into account the complex multi-factorial nature of MS, and the recently estimated contribution of low-frequency variants into disease risk, the aim of the study was to investigate genetic risk components through a combination of variant prioritization strategies.

Since GWAS and classical linkage studies have extensively investigated the HLA locus, harboring the greatest genetic risk for MS (reviewed in (19)), HLA genes were not included in this study.

The review of GWAS in MS literature, reporting polymorphisms associated with MS in case-control studies, identified 141 variants which were selected for being intragenic and for having a p -value $\leq 5 \times 10^{-6}$, an arbitrary threshold potentially highlighting genes with remarkable disease association. These common variants established the list of 107 genes used for the purpose of this study. Variants and corresponding genes are listed in Table 10.2.

A targeted analysis within the 107 MS susceptibility genes for exonic low-frequency variants was conducted on WES data of three independent Italian MS families with at least two affected members in each pedigree (Figure 10.1).

SNPs with $MAF \leq 0.04$ were taken into account when present in at least one affected family member. The selection of SNPs with $MAF \leq 0.04$ was aimed at filtering low-frequency variants which did not emerge in GWAS.

These filtering criteria revealed 17 exonic mutations (10 missense, seven synonymous) and three in the UnTranslated Regions (UTRs), all in the heterozygous condition (Table 10.5).

Among the 20 exonic and UTRs variants, nine were present only in the affected members of the families (rs77017041, *ANKRD55*; rs16870005, *C6orf10*; rs41286809, *EVI5*; rs76781122, *GC*; rs147248515, *MMEL1*; the new synonymous variant on *STAT4*; rs61744960, *TET2*; rs138943371, *TRAF3*; rs12720355, *TYK2*) and 14 variants were detected in at least two affected family members with parent-child transmission.

The number of low-frequency exonic variants in these families was investigated by a permutation test. No significant difference was observed between our result and that expected by chance ($p = 0.231$).

Then, the investigation was focused on the 14 low-frequency variants with parent-child transmission and on the new variant of *ADAMTS3* (Table 10.6). The 15 candidate SNPs were explored in a sample set of 120 Italian unrelated MS patients (Table 10.1), selected for having a mean age of MS onset (34.5 ± 9.7) similar to that of the affected family members (34.1 ± 8.2 ; student's t -test p -value=0.371).

Table 10.5. List of low-frequency variants identified in the MS families.

Gene	SNP position GRCh37/hg19	SNP ID	MAF % dbSNP150	Mutation type	SNPs carriers
ADAMTS3	4:73178175	rs150270324	0.926	Missense	A-I-2+ A-II-3
ADAMTS3	4:73414590	---		Missense	B-I-1+ B-II-3 + B-II-4
ANKRD55	5:55407449	rs77017041	0.427	Missense	C-I-2+C-II-3
BTNL2	6:32363893	rs28362679	1.825	Missense	B-I-1+ C-I-1+ C-I-2
C6orf10	6:32261153	rs16870005	1.250	Missense	B-I-2+ B-II-3
GC	4:72669661	rs76781122	1.611	Missense	B-I-2+ B-II-3
MALTI	18:56367823	rs74847855	3.734	Missense	B-I-2+ B-II-3 + B-II-4
MMEL1	1:2530169	rs147248515	0.022	Missense	B-I-2+ B-II-3
TET2	4:106156163	rs61744960	2.641	Missense	B-I-2+ B-II-3+ C-I-2+C-II-3+ A-I-1+ A-II-4
WWOX	16:78458807	rs7201683	1.989	Missense	B-I-2+ B-II-3 + B-II-4+ C-I-2
EVI5	1:92979432	rs41286809	1.116	Synonymous	C-I-2+C-II-3+ A-I-1+ A-II-3+ A-II-4
GC	4:72620788	rs76803094	1.799	Synonymous	B-I-1+ B-II-3 + B-II-4
GEMIN2	14:39587220	rs150986614	0.251	Synonymous	A-I-2+ A-II-3 + A-II-4
STAT4	2:191899319	---		Synonymous	C-I-2+C-II-3
TRAF3	14:103371923	rs138943371	0.245	Synonymous	C-I-2+C-II-3
TOP3A	17:18217958	rs2230153	1.692	Synonymous	C-I-2+C-II-3 + A-I-2
TYK2	19:10472452	rs12720355	0.962	Synonymous	C-I-2+C-II-3
CD86	3:121774281	rs11575853	1.078	UTR 5'	B-I-2+ B-II-3 + C-I-1
IL2RA	10:6054765	rs12722600	1.777	UTR 3'	B-I-2+ B-II-3 + C-I-1+ C-II-3
RRAS2	11:14300827	---		UTR 3'	B-I-2 + B-II-4

In bold the genes including the exonic variants present only in affected family members (red) defined as in Figure 1.

The predicted effects of the 15 analyzed low-frequency variants, each on the main encoded transcript, are reported in Table 3. In addition to the mutation of the start codon (*GC*, Met1Ile), expected to reduce the amount of the translated protein, missense variants were predicted as damaging (*ANKRD55* Ser376Pro; *TET2* Gly355Asp) or potentially damaging (*MMEL1* Pro368Thr). For the rs147248515 (*MMEL1*) the proline to threonine change produced discrepant predictions. Among the four SNPs predicted as benign, two cause noticeable changes in amino acid polarity and size (Arg to Gly in *MALTI*; Ala to Thr in *C6orf10*).

Aiming at prioritizing low-frequency variants that may contribute to the disease risk, the MAFs observed in the unrelated MS cohort were compared with those reported in public databases (Table 10.6). The new variants on *STAT4* and *ADAMTS3* genes were not found in the cohort of unrelated MS. Therefore, these two variants were private of the families under study, which might support the notion that a proportion of the unexplained MS heritability is accounted by additive effects of individual variants (354).

Noticeably, the screening identified a number of significant differences in the observed allelic frequencies as compared with the dbSNP150 and Tuscany databases.

The *C6orf10* rs16870005 and *IL2RA* rs12722600 are the main signals identified in this study, as confirmed by the allelic frequencies comparison with both dbSNP150 and Tuscany populations (even after Bonferroni's correction).

The rs61744960 (*TET2*) showed significant MAF differences between MS patients and dbSNP150 and a nominal borderline p-values with the Italian Tuscany population.

Although we detected the low-frequency *TET2* rs61744960 variant in MS patients of all the three families, and the comparison of this SNP frequency between our unrelated MS patients cohort and those of dbSNP150 showed a significant difference, the uncertain difference with the Tuscany cohort prevents further discussion of this finding in relation to MS. However, it is of note that the SNP rs61744960 has been previously reported in an Italian study focused on leukemia, and two of the six patients, who carried this variant, had MS as a primary disease (387).

For three SNPs (rs11575853, *CD86*; rs76781122, *TRAF3*, and rs76781122, *GC*) significant differences were observed only in the comparison between MS patients and the dbSNP150 population. Of note, for the rs2230153 (*TOP3A*), rs74847855 (*MALTI*), and rs7201683 (*WWOX*) highly significant MAFs differences between MS and Tuscany subjects were observed, that may reflect increased frequency of low-frequency alleles in MS Italian patients.

Although in the GWAS MS candidate genes we did not detect an increased number of low-frequency variants in our MS families, those variants firstly found with parent-child transmission in MS families were detected in several combinations in unrelated patients. Within the unrelated MS cohort, 17 patients were carriers of two low-frequency variants and five patients were carrier of three variants. The combinations repeatedly included the *C6orf10*, *TET2* and *IL2RA* variants (Table 10.7). The variants detected in combination were always located on different chromosomes. The *IL2RA* rs12722600 and the *TRAF3* rs138943371 were detected in the homozygous condition.

These observations may highlight the complexity of the MS genetic risk components.

Finding of the *IL2RA* 3'UTR low-frequency variant (rs12722600) i) in two MS families, ii) with a significantly higher frequency in the unrelated MS cohort than in the public databases, and iii) in several combinations with the other low-frequency SNPs, is particularly intriguing. As for the other *IL2RA* polymorphisms previously associated with the risk of developing the disease (388, 389), the functional consequence of the rs12722600 can be only proposed (390) as affecting the post-transcriptional regulation of the *IL2RA* mRNA, of which little is known (391). Interestingly, therapies for MS have been already developed to avoid the formation of the interleukin-2 receptor complex, and particularly targeting CD25 (392), the α -subunit encoded by the *IL2RA*.

Table 10.6. Selected rare variants in the cohort of 120 unrelated multiple sclerosis patients.

Gene	SNP position GRCh37/hg19	SNP ID	Transcript (Exon)	Amino acid change	SIFT/PolyPhen prediction	Nucleotide change	MAF % dbSNP150	MAF % 1000 GP (Tuscany) alleles n=214	MAF % in MS patients alleles n=240 (n alleles)	P-value ^o (dbSNP150)	P-value ^o (Tuscany)
<i>ADAMTS3</i>	4:73414590	---	ENST00000286657 (3/22)	Lys37Glu	0.17 / -0.01 ^s	T>C	---	---	0 (0)	---	---
<i>ANKRD55</i>	5:55407449	rs77017041	ENST00000341048 (10/12)	Ser376Pro	0.01 / 0.767	A>G	0.427	0.47	0 (0)	0.3103	0.2871
<i>C6orf10</i>	6:32261153	rs16870005	ENST00000533191 (26/26)	Ala431Thr	0.46 / 0.028	C>T	1.250	1.4	3.75 (9)	0.00049	0.0019
<i>CD86</i>	3:121774281	rs11575853	ENST00000330540 (5'UTR)	-56bp from +1 Met	n.a.	A>G	1.078	2.8	3.75 (9)	6.1 E-05	0.3723
<i>EVIS</i>	1:92979432	rs41286809	ENST00000540033 (18/18)	Phe749Phe	-	G>A	1.116	0.47	0.83 (2)	0.6768	0.4105
<i>GC</i>	4:72669661	rs76781122	ENST00000504199 (1/14)	Met1Ile	0.2 / 0 Start codon	G>T	1.611	5.61	4.58 (11)	0.00025	0.4895
<i>IL2RA</i>	10:6054765	rs12722600	ENST00000379959 (3'UTR)	+70 from 273 stop	n.a.	G>A	1.777	4.21	7.92 (19)	6.0 E-13	0.0042
<i>MALTI</i>	18:56367823	rs74847855	ENST00000348428 (4/17)	Arg217Gly	0.69 / 0	A>G	3.734	1.9	4.58 (11)	0.4877	0.0019
<i>MMEL1</i>	1:2530169	rs147248515	ENST00000378412 (12/24)	Pro368Thr	0.14 / 0.326	G>T	0.022	0	0 (0)	---	---
<i>STAT4</i>	2:191899319	---	ENST00000392320 (18/24)	Gln525Gln	-	A>G	---	---	0* (0)	---	---
<i>TET2</i>	4:106156163	rs61744960	ENST00000540549 (3/11)	Gly355Asp	0.01 / 0.282	G>A	2.614	5.6	8.33 (20)	2.8 E-08	0.0667
<i>TOP3A</i>	17:18217958	rs2230153	ENST00000542570 (1/19)	Ala45Ala	-	G>A	1.692	0.47	1.66 (4)	0.9757	0.0067
<i>TRAF3</i>	14:103371923	rs138943371	ENST00000347662 (11/11)	Ser478Ser	-	C>T	0.245	0.47	1.25 (3)	0.00164	0.0773
<i>TYK2</i>	19:10472452	rs12720355	ENST00000525621 (13/25)	Ile651Ile	-	C>T	0.962	1.4	1.66 (4)	0.2634	0.7251
<i>WWOX</i>	16:78458807	rs7201683	ENST00000566780 (7/9)	Leu216Val	0.19 / 0.04	C>G	1.989	0.47	2.08 (5)	0.9166	0.00026

The SIFT and PolyPhen scores (0.0 to 1.0) have opposite meanings. Prediction of the SIFT score ranges 0.0 to 0.05 deleterious; 0.05 to 1.0 tolerated. Prediction of the PolyPhen score ranges: 0.0 to 0.15, benign; 0.15 to 1.0 possibly damaging; 0.85 to 1.0 damaging. Prediction for damaging is highlighted in red. n.a., not applicable.

^sSIFT / Provean prediction for *ADAMTS3* = (0.17) tolerated / (-0.01) neutral. *investigated in 218 alleles. ^o Bonferroni's correction p-value set to 0.0042.

Table 10.7. Unrelated multiple sclerosis patients carriers of at least 2 low-frequency variants.

ID	Gender	Age of MS onset	Phenotype at examination	<i>C6orf10</i> rs16870005	<i>CD86</i> rs11575853	<i>EV15</i> rs41286809	<i>GC</i> rs76781122	<i>IL2RA</i> rs12722600	<i>MALT1</i> rs74847855	<i>TET2</i> rs61744960	<i>TOP3A</i> rs2230153	<i>TRAF3</i> rs138943371	<i>TYK2</i> rs12720355	<i>WWOX</i> rs7201683
132 ZM	F	20	RR							Het	Het			
159 ZM	M	26	RR							Het	Het			
173 ZM	F	31	RR							Het	Het			
194 ZM	F	31	RR				Het	Hom*						Het
27-WP3	M	31	SP	Het			Het							
43-WP3	F	31	PP		Het			Het						
155 ZM	F	33	SP							Het		Het		
51-WP3	M	33	SP	Het						Het				
109 ZM	F	37	SP		Het	Het								
63-WP3	F	37	SP	Het	Het					Het				
115 ZM	F	38	SP						Het	Het				Het
69-WP3	M	40	SP				Het		Het					
111 ZM	F	41	RR	Het				Het		Het				
49-WP3	F	42	PP				Het	Het						
57-WP3	M	42	SP	Het				Het					Het	
208 ZM	F	44	RR					Het						Het
MS18	F	45	SP		Het							Hom*		
184 ZM	M	47	SP					Het						Het
192 ZM	F	48	RR	Het				Het						
72-WP3	F	48	PP						Het	Het				
204 ZM	M	50	RR					Het	Het					
MS07	M	n.d. [§]	SP		Het						Het			

The heterozygous (Het) or homozygous (Hom*) condition of the variants is specified. In bold, patients with combination of 3 low-frequency variants.

[§] Age of onset below 50 year old.

Our findings support further studies aimed at characterizing the *IL2RA* 3'UTR in patients undergoing this therapeutic approach.

Overall, the rs16870005 within *C6orf10*, a scarcely investigated locus, resulted the only missense variant with a significantly increased frequency in our cohort compared to both dbSNP-Build150 and Tuscany of 1000 Genome Project (Table 10.6) and, in addition, it was frequently present in combination with other low-frequency variants (Table 10.7). Further, the nucleotide change C>T (rs16870005) in the 3' region of the *C6orf10* transcripts would substitute threonine for alanine in the carboxyl-terminal region of all the predicted proteins (reference transcript used for the study shown in Figure 10.3).

Based on these observations we sequenced the region chr6:32261295-32260757 in the 120 MS patients, which revealed the presence of 14 low-frequency mutations ($MAF \leq 0.04$), 10 not previously reported (Table 10.8).

Table 10.8. Low-frequency variants in 3' exon of *C6orf10* detected by Sanger sequencing within the cohort of 120 unrelated multiple sclerosis patients.

SNP position GRCh37/hg19	SNP ID	Amino acid change	Provean / SIFT prediction	Nucleotide change	MAF % dbSNP150	MAF % in 120 MS patients (n alleles)
6:32260761	---	Glu561Asp	(-1.16) neutral / (0) damaging	C>G	-	0.42 (1)
6:32260769	---	Val559Leu	(-0.86) neutral / (0.31) damaging	C>G	-	0.42 (1)
6:32260774	---	Lys557Ile	(-1.6) neutral / (0.004) damaging	T>A	-	0.42 (1)
6:32260878	---	Asp522Asp	neutral/tolerated	G>A	-	1.25 (3)
6:32260898	---	Asp516Tyr	(-2.38) neutral / (0.011) damaging	C>A	-	0.42 (1)
6:32260927	---	Glu506Val	(-1.42) neutral / (0.028) damaging	T>A	-	0.42 (1)
6:32260933	rs766126891	Asp504Val	(-2.42) neutral / (0) damaging	T>A	0.001	0.42 (1)
6:32261014	rs7751028	Gly477Val	(-3.43) deleterious / (0.008) damaging	C>A	2.480	0.42 (1)
6:32261075	---	Lys457stop	Damaging	T>A	-	0.42 (1)
6:32261084	---	Ser454Xfr	Damaging	A>insG	-	0.42 (1)
6:32261093	---	Gly451stop	Damaging	C>A	-	0.42 (1)
6:32261158	rs114543649	Thr429Ser	(1.30) neutral / (1) tolerated	G>C	2.479	0.42 (1)
6:32261277	---	Ser389Xfr	Damaging	T>delT	-	0.83 (2)
6:32261291	---	Gln385Glu	(1.38) neutral / (1) tolerated	G>C	2.482	0.42 (1)

The sequenced 3' exonic region spans chr6:32261295-32260757 (GRCh37/hg19). The reference transcript is ENST00000533191.5, and the reference protein is ENSP00000431199 (exon position 26/26).

The Provean cut off: equal or below -2.5, deleterious; above -2.5, neutral. The SIFT score range prediction: 0.0 to 0.05 deleterious; 0.05 to 1.0 tolerated.

All variants were detected in heterozygous condition with the exception of Ser389Xfr (homozygous condition, bold and black). In bold and gray, the variants in repetitive regions.

Of note, two mutations predicted premature termination of translation and two translational frameshifts. Inspection of *C6orf10* variants (Figure 10.3) pointed out that the four null mutations affected all *C6orf10* transcripts. Among these, the ENST0000442822.6, after splicing, is shorter and encodes a different 3' sequence. In the transcripts other than ENST0000442822.6, null mutations would remove a larger C-terminus portion (Figure 10.3) in which we detected several missense SNPs.

For missense changes, the algorithms predicted discordant effects (Table 10.8), with the exception of the damaging Gly477Val (rs7751028).

By inspection of the Ensembl database for low-frequency ($MAF \leq 0.04$) exonic variants within the full *C6orf10* transcript ENST00000533191.5 (total length 80 Kb), 53 variants were found, of which one nonsense and one frameshift. The comparison of the number of variants identified in our study with those in the Ensembl database indicated, in addition to the remarkable increase in the number of low frequency mutations in the sequenced exonic region (14 mutations in 538 bp vs 53 in 80 Kb), a significantly higher number (four out of 14) of null variants ($p = 0.0296$, Fisher's exact test).

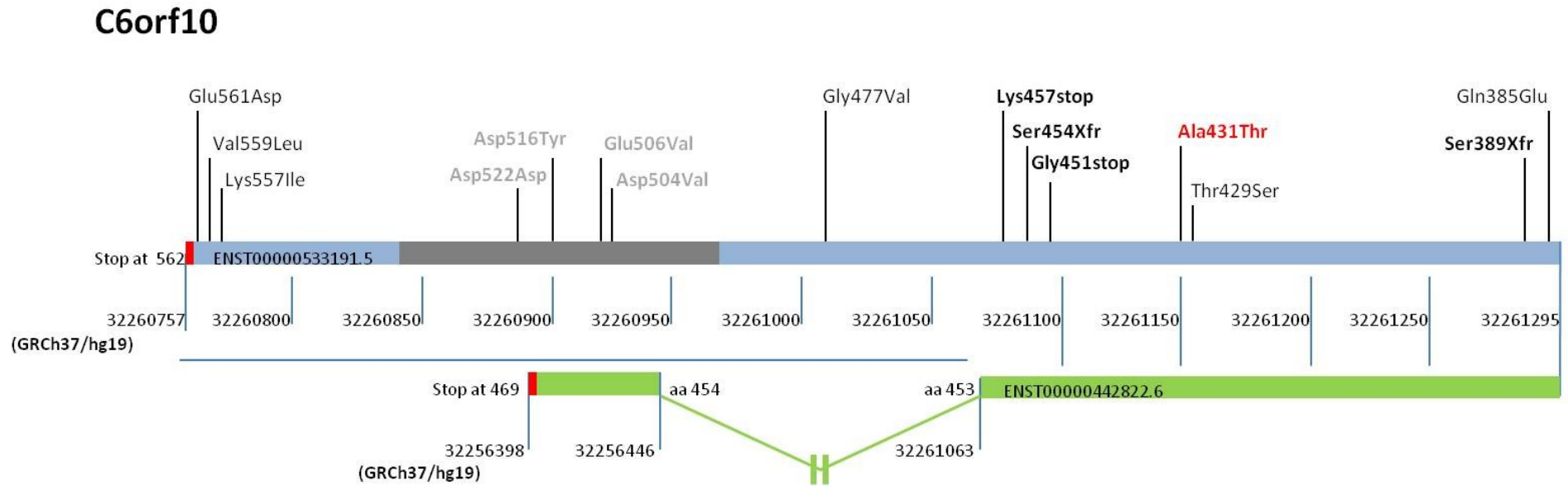
The distribution of the 14 low-frequency *C6orf10* variants detected by Sanger sequencing in the unrelated MS patients is shown in Table 10.9.

Table 10.9. Low-frequency variant genotypes in 3' exon of *C6orf10* within the unrelated multiple sclerosis patients.

ID	Gender	Age of MS onset	Phenotype at examination	<i>C6orf10</i>
138 ZM	F	21	RR	Ser454Xfr (Het)
221 ZM	M	22	RR	Val559Leu (Het) Glu561Asp (Het)
150 ZM	F	25	RR	Ser389Xfr (Hom)
194 ZM	F	31	RR	Gln385Glu (Het) Thr429Ser (Het) Gly477Val (Het)
106 ZM	M	32	SP	Asp504Val (Het) Asp522Asp (Het)
128 ZM	F	32	RR	Glu506Val (Het)
109 ZM	F	37	SP	Asp522Asp (Het)
115 ZM	F	38	SP	Lys457stop (Het)
MS23	F	38	RR	Gly451stop (Het)
112 ZM	F	41	RR	Lys557Ile (Het)
25-WP3	F	51	PP	Asp516Tyr (Het)
65-WP3	F	51	SP	Asp522Asp (Het)

MS patients carrying low-frequency *C6orf10* variants (within the region chr6:32261295-32260757) are reported. The heterozygous (Het) or homozygous (Hom) condition of the variants is specified. In bold and black, the *C6orf10* stop and frame shift variants. In bold and gray, the *C6orf10* variants in repetitive regions.

Figure 10.3. Schematic representation of the sequenced region and mutations in the 3' exon of *C6orf10*.



The low-frequency variants discovered by 3' exon sequencing in the unrelated MS are reported upper the bar (light blue/gray) of the ENST00000533191.5 transcript, used as reference. The grey bar indicates the repetitive regions, and the red bars the translational stop codons of transcripts. The reference nucleotide position in GRCh37/hg19 is also shown below the transcript bars.

The first variant identified by our WES is reported bold and red. The stop and frame shift variants are highlighted in bold and black. The transcript ENST0000442822.6, the only one undergoing splicing and ending at position 32256398 of Chr 6, is represented as a green bar. A blue horizontal line highlights the 3' region with the different reference nucleotide position for each transcript. The out of scale intron is indicated with an interruption symbol. The different numbering of this transcript in the 3' region is reported. The change in the reference nucleotide position in the ENST0000442822.6 starts after the aminoacid (aa) 453 at position 32261063.

Table 10.10. Combination of the low-frequency variants in *C6orf10* with WES variants within the unrelated multiple sclerosis patients.

ID	Gender	Age of MS onset	Phenotype at examination	<i>C6orf10</i>	<i>CD86</i> rs11575853	<i>EVI5</i> rs41286809	<i>GC</i> rs76781122	<i>IL2RA</i> rs12722600	<i>MALT1</i> rs74847855	<i>TET2</i> rs61744960	<i>WWOX</i> rs7201683
138 ZM	F	21	RR	Ser454Xfr (Het)							
221 ZM	M	22	RR	Val559Leu (Het) Glu561Asp (Het)			Het				
150 ZM	F	25	RR	Ser389Xfr (Hom)							
194 ZM	F	31	RR	Gln385Glu (Het) Thr429Ser (Het) Gly477Val (Het)			Het	Hom			Het
106 ZM	M	32	SP	Asp504Val (Het) Asp522Asp (Het)							
128 ZM	F	32	RR	Glu506Val (Het)							
109 ZM	F	37	SP	Asp522Asp (Het)	Het	Het					
115 ZM	F	38	SP	Lys457stop (Het)					Het	Het	Het
MS23	F	38	RR	Gly451stop (Het)	Het						
112 ZM	F	41	RR	Lys557Ile (Het)				Het			
25-WP3	F	51	PP	Asp516Tyr (Het)							
65-WP3	F	51	SP	Asp522Asp (Het)				Het			

The heterozygous (Het) or homozygous (Hom) condition of the variants is specified.

In bold and black, the *C6orf10* stop gained and frame shift variants are highlighted. In bold and gray, the *C6orf10* variants that were in repetitive regions.

Three patients were carriers of two/three missense *C6orf10* mutations. None of the 14 low-frequency variants was associated with the presence of the *C6orf10* rs16870005.

Seven patients over the 11 carriers of the *C6orf10* variants were also carriers of SNPs detected in the family WES study (Table 10.10). To note, the frameshift mutations, of which the Ser389Xfr in the homozygous condition, were detected in two patients with young age of disease onset (21 and 25 years).

Although anecdotal, finding the homozygous Ser389Xfr in a patient with early onset of the MS disease fosters further investigation in relation to the recent study suggesting that *C6orf10* could be implicated in the age of onset of other neurodegenerative disease (393).

The interpretation of potential functional consequences was hampered by the *C6orf10* chromosomal location and structure. As a matter of fact, this ORF is located on chromosome 6p21.32, in the MHC region which contains the major MS-associated risk gene HLA-DRB1 (353). The *C6orf10* structure comprises several transcripts, including three isoforms of a validated, but not characterized, long non-coding RNA (NR_136244.1, NR_136245.1, NR_136246.1) and a pseudogene hnRNP (HNRNPA1P2). Thus, the null mutations that we have found in the MS cohort would affect the C-terminal portion of several uncharacterized proteins expressed in brain and B cells

(http://www.genenetwork.org/webqtl/WebQTL.py?cmd=sch&refseq=NM_006781&species=human), both tissues of interest for MS.

The small sample size and the statistical power derived from our population do not permit an informative evaluation of the possible impact of the numerous newly detected *C6orf10* variants on the disease onset or clinical course within an integrated multiple variants model.

In conclusion, this study supports further investigation aimed at evaluating multiple low-frequency risk variants in coding regions of MS candidate genes. Expression of protein variants, and their combinations, could provide functional insights into the heterogeneous pathogenetic mechanisms contributing to MS.

Chapter 11 General discussion and conclusions

The experimental approaches of this work have permitted a productive investigation of the contribution of a few hemostasis components in MS patients, to identify new candidate genes/proteins, and to estimate new and specific correlations between levels of numerous plasma proteins in MS pathophysiology (Table 11.1 and Table 11.2). To note, the study design aimed at identifying signals firstly in vivo on patients, and then to prioritize these signals for subsequent mechanistic studies in vitro and animal models, at present underrepresented in this thesis.

The Genetic overlap between multiple sclerosis and several cardiovascular disease risk factors, as observed in GWAS studies (38), and the synergic action of genetic and environmental factors could participate in the vasculature changes and the BBB disruption. By reviewing MS GWAS, we prioritized candidate loci marked by intragenic SNPs with remarkable association.

In light of the complex nature of multiple MS and the recently estimated contribution of low-frequency variants into disease (see chapter 10 (354)), we aimed at magnifying rare and functional nucleotide changes through the WES performed on 3 selected MS families, taking into account that: I) GWAS use common DNA variations; II) often the strong associated variations lack of apparent functional disease consequence and III) because of linkage disequilibrium, the GWAS variants predict other nearby unknown mutations which are potentially the true risk variants.

The GWAS genomics approach, which provided the list of genes analyzed by WES, did not contain MS risk loci closely related to hemostasis, that we plan to investigate in the second part of the WES analysis, prompted by the promising results of the first part of this genetic approach. In particular, the *C6orf10* rs16870005 and *IL2RA* rs12722600 were the main identified signals, with significantly higher allelic frequencies in MS patients as compared with those reported by public databases. Further, sequencing in the MS cohort of the *C6orf10* 3' region, including the potentially damaging variant rs16870005, revealed 14 rare mutations, of which 10 were not previously reported and four were null, a quite unexpected finding. The number of *C6orf10* null variants detected in our study was significantly higher than in the Ensembl database. Moreover, the *C6orf10* rare variants were observed in combinations both intra-locus and with other low-frequency SNPs. Taking into account the potential functional impact of the identified exonic variants, their identification provides the bases for expression studies at the protein level, and potentially in the observed combination. Although the cellular and molecular phenotypes to be associated with the *C6orf10* mutations are at present not defined, and substantially complicated by the number of potential transcripts and poorly defined tissue localization, our original results could foster functional insights in the heterogeneous pathogenetic

mechanisms contributing to MS. Whereas the first part of the study has essentially been conducted by cooperations within the Ferrara University, the ample perspective of expression and characterization of several mutants in multiple genes will require international cooperation, providing tissue repository and a high number of patients' samples.

On the side of hemostasis factors, we addressed our attention toward those modestly investigated in MS, and with main open questions in relation to the disease.

Based on the recent findings of the contribution of FXII in MS (52), in the current study the contribution of FXII in the disease was explored through evaluation of the ratio of FXII:C and the amount of circulating protein (see chapter 4). The results showed the presence of increased FXII protein levels in relation to activity, leading to a decreased FXII activity/antigen ratio in MS patients compared to controls (146). Although these results are preliminary and require to be confirmed in a higher number of MS patients, they might support that FXII contribution in MS is not directly correlated with its "intrinsic" procoagulant activity. Further, immune-modulatory function in relation to/independent from coagulation activity, particularly for FXII, still remains to be elucidated in MS.

Since individual measurements of hemostasis components may not favor detection in MS of the relationship among pathway elements, the systematic measurement of a panel of hemostasis components in plasma (chapter 5), and of inflammatory/immunomodulatory- (chapter 7) and adhesion (chapter 8 and 9) molecules was performed. With the limitation of assays in fluids outside of the CNS, the goal was to assess if anticoagulant/anti-inflammatory components were candidates to play a protective role in the disease progression and to establish useful correlations among a number of proteins, potentially related in biological and disease processes.

Hence, we investigated correlations (Table 11.1 and Table 11.2), between peripheral EDTA plasma levels of coagulation inhibitors (TFPI, ADAMTS13, HCII and TM), and in addition of FXII, with MRI measures, providing a number of quantitative and "intermediate" phenotypes tightly related to MS neurodegeneration and evaluating disease progression (177).

In the current study, patients under disease-modifying treatments (DMTs) were mostly treated with INF-beta, and with GA, which are known to modify gene transcription (394-396). The evaluation according to the DMTs status of patients provided us with potential modifiers of coagulation factor gene expression, that have not previously been investigated. This part of the study is potentially relevant for patients' treatment as well as

to extend our knowledge of the modulation in vivo of a group of genes, extensively investigated in relation to acquired and genetic conditions. We did not detect significant alterations in the circulating levels of these hemostasis proteins in relation to INF-beta and GA (177). However, the ample variability of levels in patients, and particularly those of PAI-1, could have prevented difference detection.

Concerning the correlation among coagulation factors/inhibitors levels (Table 11.1 and Table 11.2), we detected positive associations of TFPI with TM only in MS patients, pointing out alteration of endothelium, which hosts both proteins and could “coordinate” their release from membranes. Worth noting that release mechanisms of TFPI and TM do not overlap: TFPI α / β alternative splicing, TFPI β C-terminus truncation, TFPI α release induced by thrombin or heparin vs truncation of the native TM in membrane potentiated by endothelial “injury” (397, 398). This would imply that the endothelium alteration in MS acts on multiple mechanisms of release.

In MS, but not in healthy subjects, we also detected a positive association between PAI-1 and FXII concentrations, and a negative association between PAI-1 and HCII concentrations (Table 11.1 and Table 11.2). These proteins are mainly secreted by hepatocytes (96, 97, 399), which would imply that in patients disease mechanisms influence different tissues, a hypothesis supported by the systemic manifestations observed in MS patients. Nevertheless, the effects of these association would fit with a fluctuating fibrin formation-fibrinolysis balance: thrombin inhibition (HCII) decreases fibrin formation, in turn reducing the need for fibrinolysis. On the other hand, FXII can stimulate fibrinolysis through uPAR, whereas PAI-1 inhibits it.

Moreover, higher PAI-1 levels were detected in MS patients when compared to controls (177), in accordance with previous observations. Although the histological studies point to fibrin(ogen), as the principal contributor to neuroinflammation and neurodegeneration in MS, these processes are certainly supported, and may be potentiated, by perturbed (decreased) fibrinolysis (54). In particular, increased PAI-1 synthesis and decreased tPA activity in MS lesions reflect an impaired clearance of fibrin due to the formation of tPA/PAI-1 complex (140), thus further contributing to the inflammatory stage of the demyelination (53, 54).

In MS patients, several correlations between hemostasis components plasma levels and MRI measures were detected: 1) higher FXII levels with lower ventricular and higher deep gray matter (DGM) volumes, 2) higher HCII levels with lower brain and cortical volumes and higher ventricular volume, 3) higher TFPI levels with lower DGM volume. However, after correction for multiple comparisons, no significant relationship between hemostasis

component levels and MRI measures remained. Whereas the multiple correction approach is useful to prevent false positive findings, it also discards several plausible biological associations. Taking into account that HCII inhibits thrombin only, and that inhibition is supported by specific glycosaminoglycans (GAGs) as cofactors, these association data are intriguing (400). In fact, GAGs differ substantially in their structural composition, forming four main families, and their subsequent sulfation, deacetylation, and epimerization modifications, influence their activity, providing a role in inflammatory process (400), as well as in normal function of CNS or pathological conditions (MS included, reviewed in (401)). Hence, the contribution of HCII in MS deserves further investigation. Indeed the inclusion of the “neglected” HCII in our study has been supported by its differences when compared to the main inhibitor, antithrombin, and by the lower concentration in plasma (HCII <1 mM as compared to AT 2.4 mM (96)).

We also hypothesized that altered plasma levels, and in particular coagulation (TFPI, HCII) and hemostasis (ADAMTS13) inhibitors, would be more prevalent in MS patients with focal extravascular leakage of blood components, measured as CMBs and as increased iron deposition within the DGM structures. In this respect, an ample and ongoing survey of APC pathway components, which will substantially expand our investigation on this field, has not been included in the present Ph.D. thesis. Interestingly, lower ADAMTS13 levels were detected in MS patients and in particular in MS patients with cerebral microbleeds (176, 177). Whereas reduced ADAMTS13 concentration could favor a prothrombotic condition, particularly in microvessels, which would fit with vascular comorbidity in MS patients, the association of even lower levels of ADAMTS13 in patients with microbleeds is counterintuitive. This finding stimulates further investigation, which will involve the ADASMTS13 substrate, vWF, poorly investigated in MS. Enhanced vWF activity (ristocetin cofactor activity?) in plasma of MS patients has been suggested by Japanese investigators (writing in Japanese (157)), as a marker for evaluating the endothelial damage, leading to BBB breakdown.

Overall, this part of the study did not detect striking difference between patients and healthy subjects, which could suggest that the investigated anticoagulant/anti-inflammatory peripheral components might not reflect their role in the CNS of patients, and/or play a secondary role in the disease progression. On the other hand, ADAMTS13 findings are certainly of interest, and when confirmed and detailed by investigation of the functional correlate of the antigen increase in plasma, might reveal novel effects of endothelial dysregulation in relation to the disease physiopathology.

Regardless of the cause, BBB disruption and vascular changes, including cerebral hypoperfusion and tissue hypoxia, are important factors in MS pathogenesis, which interact in a vicious cycle favoring the altered immune trafficking and the inflammatory events (32-34). Taken into account the literature data, that support the interactions between vascular and neurodegenerative mechanisms of MS, the contribution of the extracranial venous compartment was explored by investigating the expression profiles of internal jugular vein wall in patients and controls (chapter 6). This original study produced a wealth of information on several biological pathways that, at present, have been partially investigated by us. The ongoing specific analysis of the hemostasis and coagulation factors/inhibitors mRNA profile is not included in this Ph.D. thesis. Among the several differentially expressed genes, the immune-related *CD86* emerged in the up-regulated genes (N=409) (402). Moreover, genes encoding HOX transcription factors and histones, potentially regulated by blood flow, were overexpressed. Smooth muscle contraction and cell adhesion processes emerged among down-regulated genes (N=515) (402). Measurements of selected protein products in jugular/peripheral plasma and the overtime evaluation in peripheral plasma showed conserved individual plasma patterns for immune-inflammatory (CCL13, CCL18) and adhesion (NCAM1, VAP1, SELL) proteins, despite significant variations over time. Both age and MS disease phenotypes were determinants of VAP1 plasma levels (402).

The combined transcriptome-protein analysis provides intriguing links between IJV wall transcript alteration and plasma protein expression, thus highlighting proteins of interest for MS pathophysiology. Indeed, thanks to the expression data from the transcriptomics approach, further investigation of selected candidate proteins was performed in associations with MS features both at clinical and MRI phenotypes.

In particular, higher CCL18 plasma levels were found in P-MS compared to RR-MS and to HI. Strikingly, higher CCL18 levels were associated with increased lateral ventricular volume and T2 lesion volume (LV), and decreased grey matter, thalamic and cortical volumes (403). These results provide the first evidence that CCL18 plasma levels are associated with more severe inflammatory and neurodegenerative brain MRI outcomes in MS. CCL18 has a number of features that have been discussed in chapter 7. It is worth noting that altered expression of CCL18 is not limited to MS, but it has been observed in other clinical manifestations as cancer, and particularly in Gaucher disease, where its very high levels mirror the impairment of lipid metabolism (297, 300, 404). It remains to be established if homodimers, heterodimers or oligomer forms of CCL18 are involved in the MS (293), and if the contribution involves CCL18 interaction with GAGs (405).

In this study, we also observed that IFN- β was associated with higher sCD86 and, collectively, several DMTs (a heterogeneous list including intravenous immunoglobulin, mitoxantrone, and methotrexate) could modulate levels of both CCL5 and sCD86 (403). Whereas these findings are in accordance with the possible regulation of immunomodulatory action by drugs, their heterogeneity hides at present a meaningful relation between specific molecules and expression of CCL5 and sCD86. This limitation provides the bases for biologically and clinically relevant investigations.

Finally, the contribution of adhesion molecules in MS, suggested by the transcriptomic analysis, was explored (chapters 8 and 9 (406)). sNCAM levels in plasma were evaluated for the first time in associations with clinical and MRI measures, and compared with those of sICAM-1 and sVCAM-1. Interestingly, the correlation between plasma levels of sNCAM and sVCAM-1 were detectable both in patients and HI (Table 11.1). The notion that NCAM and VCAM-1 might be expressed by different cells adds further interest/complexity to this observation. As a matter of fact, expression of these molecules includes several processes, transcription, mRNA translation, post-translation modifications and shedding from membranes. We can only speculate about direct or, more likely, indirect relationships in the physiological co-regulation of these proteins, which however differ in structure and isoforms (407, 408). Unfortunately, one of the study limitation is that the use of the multiplex assay prevented the identification of the isoforms of the measured adhesion molecules. The correlation coefficient, lower in MS patients than in HI, suggests that the biological pathways linking these adhesion molecules are altered in MS by still undefined molecular components, which deserves further investigation.

Differently, the positive correlation between sICAM-1 and sVCAM-1 was observed, as for several molecules, only in MS patients (Table 11.1, purple). Co-regulation of sICAM-1 and sVCAM-1 in disease might be explained by their common expression in endothelial and white blood cells, both cell types affected in MS.

In progressive MS, as compared with HI, increased levels of sNCAM and sVCAM-1 were detected. Overall, plasma levels of several adhesion molecules were increased in patients, and part of them modulated by specific disease-modifying therapies. Although increased levels were associated with the P-MS phenotype, they did not correlate with MRI measures of disease severity (406). Our results support the hypothesis that adhesion molecules, considered as inflammatory markers, will not necessarily correlate with the progression of brain atrophy.

Indeed this pattern, i.e. the association with the disease condition but not with the decreased brain volumes, characterized most of our findings with the exception of CCL18.

The progressive failure of BBB integrity, which may have the pathological features of CMBs (40), leads to focal extravascular leakage of blood components (see both chapters 5 and 9), which are known to induce several inflammatory responses (39). VAP-1 is a non-classical adhesion molecule with an enzymatic activity that catalyzes oxidative deamination of primary amines. As adhesion molecule, VAP-1 mediates leukocyte binding to the vessel wall, which facilitates their infiltration through inflamed tissue. On the other hand, its catalytic activity induces the formation of free-radicals from its substrates on leukocytes, providing an inflammatory microenvironment and causing expression of additional adhesion molecules (reviewed in (268)). Interestingly high plasma VAP-1 activity has been found in patients according to the grade of intracranial hemorrhage (346), and VAP-1 inhibition decreased adhesion molecule expression and immune cell infiltration after intracerebral hemorrhage and microvascular dysfunction in animal models (347, 348). The current study showed that DMTs for MS were associated with VAP-1 levels and, in particular, GA was the most influential molecule. This finding indicated that DMTs were not responsible for the higher VAP-1 levels in patients with CMBs. Instead, DMTs could mask even higher VAP-1 levels in patients with CMBs, as indicated by comparison of patients not on DMTs. These results, which bring the attention to the potential biological relevance of VAP-1 in CMBs, still need to be analysed in light of findings reported in chapter 5. This will bring us the opportunity to investigate the expression at the plasma level of two noticeable enzymes, the specific plasma protease ADAMTS13 and the amino oxidase VAP-1, endowed with adhesion molecule properties. The investigation of both molecules, at the activity and protein concentration levels, will offer us the opportunity to distinguish between increased/decreased expression and increased/decreased function.

More work is needed to investigate how hemostasis components contribute to inflammatory and immune responses in MS patients, by use of high throughput transcriptomic and proteomic techniques. We realize that our survey, aimed at extracting among a huge amount of candidates those displaying meaningful association with the disease, needs specific functional studies aimed at substantiating and implementing with activity correlates the observed association. This is certainly true for the rare mutations detected in the WES, as well as in relation to the proteins showing level differences in patients versus controls or level correlations in patients. The modulation by current DMTs in MS of the selected genes/proteins offers an ideal “experiment” in vivo, directly at the patients’ level, to study induced variations at the protein concentration and activity levels.

Newly acquired molecular details of how hemostasis components trigger neuroinflammation and neurodegeneration could in turn favor development of novel therapeutic approaches to ameliorate the disease evolution, favored by the wealth of powerful inhibitors or potentiators of hemostasis, designed for prothrombotic and hemorrhagic disorders.

Table 11.1. Protein levels correlations in multiple sclerosis patients.

Proteins		FXII µg/mL	ADAMTS13 ng/mL	HCII ng/mL	TFPI ng/mL	TM ng/mL	PAI-1 ng/mL	CCL18 ng/mL	CCL5 ng/mL	CD86 U/mL	sNCAM ng/mL	sICAM-1 ng/mL	sVCAM-1 ng/mL
ADAMTS13 ng/mL	Rho: P value:	0.029 0.732											
HCII ng/mL	Rho: P value:	0.044 0.604	-0.100 0.241										
TFPI ng/mL	Rho: P value:	0.010 0.909	0.062 0.472	-0.080 0.351									
TM ng/mL	Rho: P value:	-0.005 0.954	0.072 0.400	-0.012 0.890	0.240 0.004								
PAI-1 ng/mL	Rho: P value:	0.284 0.001	-0.060 0.484	-0.209 0.014	0.153 0.073	-0.050 0.562							
CCL18 ng/mL	Rho: P value:	0.037 0.669	-0.098 0.252	-0.345 <0.001	0.207 0.015	0.082 0.342	0.340 <0.001						
CCL5 ng/mL	Rho: P value:	0.089 0.302	-0.239 0.005	0.117 0.173	-0.027 0.750	-0.155 0.069	0.542 <0.001	0.047 0.583					
CD86 U/mL	Rho: P value:	0.149 0.082	-0.084 0.326	0.110 0.199	0.092 0.281	0.098 0.254	0.051 0.553	0.082 0.339	0.105 0.222				
sNCAM ng/mL	Rho: P value:	0.102 0.236	0.068 0.430	0.089 0.301	0.145 0.089	0.287 0.001	-0.017 0.841	-0.090 0.293	-0.052 0.542	0.209 0.014			
sICAM-1 ng/mL	Rho: P value:	-0.184 0.031	-0.032 0.711	-0.152 0.075	0.096 0.236	0.303 <0.001	-0.132 0.122	0.207 0.015	-0.232 0.006	0.232 0.006	-0.075 0.382		
sVCAM-1 ng/mL	Rho: P value:	0.049 0.565	-0.067 0.438	0.109 0.201	0.119 0.164	0.173 0.042	0.202 0.017	0.149 0.082	0.137 0.109	0.406 <0.001	0.264 0.002	0.197 0.021	
VAP-1 ng/mL	Rho: P value:	0.113 0.187	-0.004 0.965	0.038 0.660	0.214 0.012	0.198 0.020	0.060 0.485	0.087 0.313	-0.059 0.492	0.305 <0.001	0.385 <0.001	0.190 0.026	0.398 <0.001

Spearman correlation coefficient and p-values are reported. The list of proteins are presented according to the following groups: yellow, hemostasis components; green, immune-modulatory function; orange, adhesion molecules. The purple cells indicate differences in the presence of correlations (white font, loss of correlation in patients; black font, correlation acquired in patients) between patients and healthy subjects. Light purple cells indicate slight differences as provided by a trend for significant p-value.

ADAMTS13: A Disintegrin-like And Metalloprotease with ThromboSpondin type 1 motif 13; FXII: Factor XII; HCII: Heparin Cofactor II; TFPI: Tissue Factor Pathway Inhibitor; TM: Thrombomodulin; PAI-1: Plasminogen activator inhibitor-1; CCL18: C-C motif ligand 18; CCL5: C-C motif ligand 5; sCD86: soluble cluster of differentiation 86; sNCAM: soluble neural cell adhesion molecule; sICAM-1: soluble intercellular adhesion molecule; sVCAM-1: soluble vascular cell adhesion molecule 1; VAP-1: vascular adhesion protein-

Table 11.2. Protein levels correlations in healthy individuals.

HI		FXII μg/mL	ADAMTS13 ng/mL	HCII ng/mL	TFPI ng/mL	TM ng/mL	PAI-1 ng/mL	CCL18 ng/mL	CCL5 ng/mL	CD86 U/mL	sNCAM ng/mL	sICAM-1 ng/mL	sVCAM-1 ng/mL
ADAMTS13 ng/mL	Rho: P value:	-0.047 0.765											
HCII ng/mL	Rho: P value:	0.139 0.381	-0.023 0.886										
TFPI ng/mL	Rho: P value:	-0.163 0.302	0.029 0.853	0.066 0.680									
TM ng/mL	Rho: P value:	0.048 0.761	0.342 0.027	0.114 0.474	0.134 0.398								
PAI-1 ng/mL	Rho: P value:	-0.057 0.718	-0.042 0.793	-0.081 0.608	0.331 0.032	0.222 0.158							
CCL18 ng/mL	Rho: P value:	-0.141 0.386	0.026 0.875	0.004 0.979	0.356 0.024	0.118 0.470	0.392 0.012						
CCL5 ng/mL	Rho: P value:	0.121 0.443	-0.159 0.313	0.081 0.612	-0.111 0.483	-0.006 0.971	0.553 <0.001	0.033 0.837					
CD86 U/mL	Rho: P value:	-0.012 0.942	0.318 0.040	0.023 0.884	0.243 0.121	0.340 0.028	0.248 0.113	0.009 0.954	0.179 0.257				
sNCAM ng/mL	Rho: P value:	-0.136 0.389	0.204 0.195	0.139 0.380	0.267 0.088	0.247 0.115	0.002 0.989	0.084 0.605	0.032 0.843	0.328 0.034			
sICAM-1 ng/mL	Rho: P value:	0 1.0	0.084 0.597	-0.127 0.424	0.108 0.497	0.042 0.790	0.302 0.052	0.197 0.224	0.150 0.344	0.364 0.018	0.210 0.182		
sVCAM-1 ng/mL	Rho: P value:	-0.045 0.778	0.119 0.452	0.313 0.044	0.409 0.007	0.225 0.151	0.333 0.031	0.318 0.046	-0.034 0.829	0.275 0.078	0.491 0.001	0.253 0.107	
VAP-1 ng/mL	Rho: P value:	0.046 0.771	0.039 0.806	0.408 0.007	0.265 0.090	0.053 0.738	0.283 0.069	0.318 0.046	0.213 0.176	0.328 0.034	0.528 <0.001	0.204 0.194	0.489 0.001

Spearman correlation coefficient and p-values are reported. The list of proteins are presented according to the following groups: light yellow, hemostasis components; green, immune-modulatory function; orange, adhesion molecules. The dark yellow cells indicate the presence of correlations in both patients and healthy subjects.

ADAMTS13: A Disintegrin-like And Metalloprotease with Thrombospondin type 1 motif 13; FXII: Factor XII; HCII: Heparin Cofactor II; TFPI: Tissue Factor Pathway Inhibitor; TM: Thrombomodulin; PAI-1: Plasminogen activator inhibitor-1; CCL18: C-C motif ligand 18; CCL5: C-C motif ligand 5; sCD86: soluble cluster of differentiation 86; sNCAM: soluble neural cell adhesion molecule; sICAM-1: soluble intercellular adhesion molecule; sVCAM-1: soluble vascular cell adhesion molecule 1; VAP-1: vascular adhesion protein-1.

BIBLIOGRAPHY

1. Reich DS, Lucchinetti CF, Calabresi PA. Multiple Sclerosis. *N Engl J Med*. 2018;378(2):169-80.
2. Benedict RH, Zivadinov R. Risk factors for and management of cognitive dysfunction in multiple sclerosis. *Nat Rev Neurol*. 2011;7(6):332-42.
3. Browne P, Chandraratna D, Angood C, Tremlett H, Baker C, Taylor BV, et al. Atlas of Multiple Sclerosis 2013: A growing global problem with widespread inequity. *Neurology*. 2014;83(11):1022-4.
4. Gitto L. Living with Multiple Sclerosis in Europe: Pharmacological Treatments, Cost of Illness, and Health-Related Quality of Life Across Countries. In: Zagon IS, McLaughlin PJ, editors. *Multiple Sclerosis: Perspectives in Treatment and Pathogenesis*. Brisbane (AU)2017.
5. Battaglia MA, Bezzini D. Estimated prevalence of multiple sclerosis in Italy in 2015. *Neurol Sci*. 2017;38(3):473-9.
6. Barizzone N, Zara I, Sorosina M, Lupoli S, Porcu E, Pitzalis M, et al. The burden of multiple sclerosis variants in continental Italians and Sardinians. *Mult Scler*. 2015;21(11):1385-95.
7. Patsopoulos NA. Genetics of Multiple Sclerosis: An Overview and New Directions. *Cold Spring Harb Perspect Med*. 2018;8(7).
8. Dendrou CA, Fugger L, Friese MA. Immunopathology of multiple sclerosis. *Nat Rev Immunol*. 2015;15(9):545-58.
9. Voskuhl RR, Gold SM. Sex-related factors in multiple sclerosis susceptibility and progression. *Nat Rev Neurol*. 2012;8(5):255-63.
10. Olsson T, Barcellos LF, Alfredsson L. Interactions between genetic, lifestyle and environmental risk factors for multiple sclerosis. *Nat Rev Neurol*. 2017;13(1):25-36.
11. Belbasis L, Bellou V, Evangelou E, Ioannidis JP, Tzoulaki I. Environmental risk factors and multiple sclerosis: an umbrella review of systematic reviews and meta-analyses. *Lancet Neurol*. 2015;14(3):263-73.
12. Minagar A, Alexander JS. Blood-brain barrier disruption in multiple sclerosis. *Mult Scler*. 2003;9(6):540-9.
13. Thompson AJ, Baranzini SE, Geurts J, Hemmer B, Ciccarelli O. Multiple sclerosis. *Lancet*. 2018;391(10130):1622-36.
14. Zeydan B, Kantarci OH. Progressive Forms of Multiple Sclerosis: Distinct Entity or Age-Dependent Phenomena. *Neurol Clin*. 2018;36(1):163-71.
15. Vidal-Jordana A, Montalban X. Multiple Sclerosis: Epidemiologic, Clinical, and Therapeutic Aspects. *Neuroimaging Clin N Am*. 2017;27(2):195-204.
16. Mao Z, Alvarez-Gonzalez C, De Trane S, Yildiz O, Albor C, Doctor G, et al. Cladribine: Off-label disease modification for people with multiple sclerosis in resource-poor settings? *Mult Scler J Exp Transl Clin*. 2018;4(2):2055217318783767.
17. Li R, Patterson KR, Bar-Or A. Reassessing B cell contributions in multiple sclerosis. *Nat Immunol*. 2018;19(7):696-707.
18. Grigoriadis N, van Pesch V, Paradig MSG. A basic overview of multiple sclerosis immunopathology. *Eur J Neurol*. 2015;22 Suppl 2:3-13.
19. Hollenbach JA, Oksenberg JR. The immunogenetics of multiple sclerosis: A comprehensive review. *J Autoimmun*. 2015;64:13-25.
20. Laroche C, Alvarez JI, Prat A. How do immune cells overcome the blood-brain barrier in multiple sclerosis? *FEBS Lett*. 2011;585(23):3770-80.
21. Takeshita Y, Ransohoff RM. Inflammatory cell trafficking across the blood-brain barrier: chemokine regulation and in vitro models. *Immunol Rev*. 2012;248(1):228-39.
22. Marcos-Ramiro B, Garcia-Weber D, Millan J. TNF-induced endothelial barrier disruption: beyond actin and Rho. *Thromb Haemost*. 2014;112(6):1088-102.
23. Auricchio F, Scavone C, Cimmaruta D, Di Mauro G, Capuano A, Sportiello L, et al. Drugs approved for the treatment of multiple sclerosis: review of their safety profile. *Expert Opin Drug Saf*. 2017;16(12):1359-71.
24. Michel L, Touil H, Pikor NB, Gommerman JL, Prat A, Bar-Or A. B Cells in the Multiple Sclerosis Central Nervous System: Trafficking and Contribution to CNS-Compartmentalized Inflammation. *Front Immunol*. 2015;6:636.
25. Rivera A, Chen CC, Ron N, Dougherty JP, Ron Y. Role of B cells as antigen-presenting cells in vivo revisited: antigen-specific B cells are essential for T cell expansion in lymph nodes and for systemic T cell responses to low antigen concentrations. *Int Immunol*. 2001;13(12):1583-93.
26. Louveau A, Da Mesquita S, Kipnis J. Lymphatics in Neurological Disorders: A Neuro-Lympho-Vascular Component of Multiple Sclerosis and Alzheimer's Disease? *Neuron*. 2016;91(5):957-73.
27. Louveau A, Smirnov I, Keyes TJ, Eccles JD, Rouhani SJ, Peske JD, et al. Structural and functional features of central nervous system lymphatic vessels. *Nature*. 2015;523(7560):337-41.
28. Lassmann H, van Horssen J, Mahad D. Progressive multiple sclerosis: pathology and pathogenesis. *Nat Rev Neurol*. 2012;8(11):647-56.
29. Calabrese M, Magliozzi R, Ciccarelli O, Geurts JJ, Reynolds R, Martin R. Exploring the origins of grey matter damage in multiple sclerosis. *Nat Rev Neurosci*. 2015;16(3):147-58.

30. Zivadinov R, Jakimovski D, Gandhi S, Ahmed R, Dwyer MG, Horakova D, et al. Clinical relevance of brain atrophy assessment in multiple sclerosis. Implications for its use in a clinical routine. *Expert Rev Neurother*. 2016;16(7):777-93.
31. Bergsland N, Zivadinov R, Dwyer MG, Weinstock-Guttman B, Benedict RH. Localized atrophy of the thalamus and slowed cognitive processing speed in MS patients. *Mult Scler*. 2016;22(10):1327-36.
32. Marrie RA, Rudick R, Horwitz R, Cutter G, Tyry T, Campagnolo D, et al. Vascular comorbidity is associated with more rapid disability progression in multiple sclerosis. *Neurology*. 2010;74(13):1041-7.
33. Spencer JJ, Bell JS, DeLuca GC. Vascular pathology in multiple sclerosis: reframing pathogenesis around the blood-brain barrier. *J Neurol Neurosurg Psychiatry*. 2018;89(1):42-52.
34. D'Haeseleer M, Cambron M, Vanopdenbosch L, De Keyser J. Vascular aspects of multiple sclerosis. *Lancet Neurol*. 2011;10(7):657-66.
35. Rae-Grant AD, Wong C, Bernatowicz R, Fox RJ. Observations on the brain vasculature in multiple sclerosis: A historical perspective. *Mult Scler Relat Disord*. 2014;3(2):156-62.
36. Sati P, Oh J, Constable RT, Evangelou N, Guttmann CR, Henry RG, et al. The central vein sign and its clinical evaluation for the diagnosis of multiple sclerosis: a consensus statement from the North American Imaging in Multiple Sclerosis Cooperative. *Nat Rev Neurol*. 2016;12(12):714-22.
37. Sparacia G, Agnello F, Gambino A, Sciortino M, Midiri M. Multiple sclerosis: High prevalence of the 'central vein' sign in white matter lesions on susceptibility-weighted images. *Neuroradiol J*. 2018;31(4):356-61.
38. Wang Y, Bos SD, Harbo HF, Thompson WK, Schork AJ, Bettella F, et al. Genetic overlap between multiple sclerosis and several cardiovascular disease risk factors. *Mult Scler*. 2016;22(14):1783-93.
39. Chu AJ. Tissue factor, blood coagulation, and beyond: an overview. *Int J Inflamm*. 2011;2011:367284.
40. Fisher MJ. Brain regulation of thrombosis and hemostasis: from theory to practice. *Stroke*. 2013;44(11):3275-85.
41. Renard D. Cerebral microbleeds: a magnetic resonance imaging review of common and less common causes. *Eur J Neurol*. 2018;25(3):441-50.
42. Zivadinov R, Ramasamy DP, Benedict RR, Polak P, Hagemeyer J, Magnano C, et al. Cerebral Microbleeds in Multiple Sclerosis Evaluated on Susceptibility-weighted Images and Quantitative Susceptibility Maps: A Case-Control Study. *Radiology*. 2016;281(3):884-95.
43. Versteeg HH, Heemskerk JW, Levi M, Reitsma PH. New fundamentals in hemostasis. *Physiol Rev*. 2013;93(1):327-58.
44. Vos CM, Geurts JJ, Montagne L, van Haastert ES, Bo L, van der Valk P, et al. Blood-brain barrier alterations in both focal and diffuse abnormalities on postmortem MRI in multiple sclerosis. *Neurobiol Dis*. 2005;20(3):953-60.
45. Leech S, Kirk J, Plumb J, McQuaid S. Persistent endothelial abnormalities and blood-brain barrier leak in primary and secondary progressive multiple sclerosis. *Neuropathol Appl Neurobiol*. 2007;33(1):86-98.
46. Sweeney MD, Sagare AP, Zlokovic BV. Blood-brain barrier breakdown in Alzheimer disease and other neurodegenerative disorders. *Nat Rev Neurol*. 2018;14(3):133-50.
47. Alvarez JJ, Saint-Laurent O, Godschalk A, Terouz S, Briels C, Larouche S, et al. Focal disturbances in the blood-brain barrier are associated with formation of neuroinflammatory lesions. *Neurobiol Dis*. 2015;74:14-24.
48. Davalos D, Ryu JK, Merlini M, Baeten KM, Le Moan N, Petersen MA, et al. Fibrinogen-induced perivascular microglial clustering is required for the development of axonal damage in neuroinflammation. *Nat Commun*. 2012;3:1227.
49. Adams RA, Bauer J, Flick MJ, Sikorski SL, Nuriel T, Lassmann H, et al. The fibrin-derived gamma377-395 peptide inhibits microglia activation and suppresses relapsing paralysis in central nervous system autoimmune disease. *J Exp Med*. 2007;204(3):571-82.
50. Ryu JK, Petersen MA, Murray SG, Baeten KM, Meyer-Franke A, Chan JP, et al. Blood coagulation protein fibrinogen promotes autoimmunity and demyelination via chemokine release and antigen presentation. *Nat Commun*. 2015;6:8164.
51. Petersen MA, Ryu JK, Chang KJ, Etxeberria A, Bardehle S, Mendiola AS, et al. Fibrinogen Activates BMP Signaling in Oligodendrocyte Progenitor Cells and Inhibits Remyelination after Vascular Damage. *Neuron*. 2017;96(5):1003-12 e7.
52. Gobel K, Pankratz S, Asaridou CM, Herrmann AM, Bittner S, Merker M, et al. Blood coagulation factor XII drives adaptive immunity during neuroinflammation via CD87-mediated modulation of dendritic cells. *Nat Commun*. 2016;7:11626.
53. Marik C, Felts PA, Bauer J, Lassmann H, Smith KJ. Lesion genesis in a subset of patients with multiple sclerosis: a role for innate immunity? *Brain*. 2007;130(Pt 11):2800-15.
54. Yates RL, Esiri MM, Palace J, Jacobs B, Perera R, DeLuca GC. Fibrin(ogen) and neurodegeneration in the progressive multiple sclerosis cortex. *Ann Neurol*. 2017;82(2):259-70.
55. Szaba FM, Smiley ST. Roles for thrombin and fibrin(ogen) in cytokine/chemokine production and macrophage adhesion in vivo. *Blood*. 2002;99(3):1053-9.

56. Gobel K, Eichler S, Wiendl H, Chavakis T, Kleinschnitz C, Meuth SG. The Coagulation Factors Fibrinogen, Thrombin, and Factor XII in Inflammatory Disorders-A Systematic Review. *Front Immunol.* 2018;9:1731.
57. Bach RR. Tissue factor encryption. *Arterioscler Thromb Vasc Biol.* 2006;26(3):456-61.
58. De Palma R, Cirillo P, Ciccarelli G, Barra G, Conte S, Pellegrino G, et al. Expression of functional tissue factor in activated T-lymphocytes in vitro and in vivo: A possible contribution of immunity to thrombosis? *Int J Cardiol.* 2016;218:188-95.
59. Zelaya H, Rothmeier AS, Ruf W. Tissue factor at the crossroad of coagulation and cell signaling. *J Thromb Haemost.* 2018;16(10):1941-52.
60. Bogdanov VY, Balasubramanian V, Hathcock J, Vele O, Lieb M, Nemerson Y. Alternatively spliced human tissue factor: a circulating, soluble, thrombogenic protein. *Nat Med.* 2003;9(4):458-62.
61. Roy S, Paborsky LR, Vehar GA. Self-association of tissue factor as revealed by chemical crosslinking. *J Biol Chem.* 1991;266(8):4665-8.
62. Reinhardt C, von Bruhl ML, Manukyan D, Grahl L, Lorenz M, Altmann B, et al. Protein disulfide isomerase acts as an injury response signal that enhances fibrin generation via tissue factor activation. *J Clin Invest.* 2008;118(3):1110-22.
63. Del Conde I, Shrimpton CN, Thiagarajan P, Lopez JA. Tissue-factor-bearing microvesicles arise from lipid rafts and fuse with activated platelets to initiate coagulation. *Blood.* 2005;106(5):1604-11.
64. Chiva-Blanch G, Laake K, Myhre P, Bratseth V, Arnesen H, Solheim S, et al. Platelet-, monocyte-derived and tissue factor-carrying circulating microparticles are related to acute myocardial infarction severity. *PLoS One.* 2017;12(2):e0172558.
65. Engelmann B, Massberg S. Thrombosis as an intravascular effector of innate immunity. *Nat Rev Immunol.* 2013;13(1):34-45.
66. Eppensteiner J, Davis RP, Barbas AS, Kwun J, Lee J. Immunothrombotic Activity of Damage-Associated Molecular Patterns and Extracellular Vesicles in Secondary Organ Failure Induced by Trauma and Sterile Insults. *Front Immunol.* 2018;9:190.
67. Drake TA, Morrissey JH, Edgington TS. Selective cellular expression of tissue factor in human tissues. Implications for disorders of hemostasis and thrombosis. *Am J Pathol.* 1989;134(5):1087-97.
68. Fleck RA, Rao LV, Rapaport SI, Varki N. Localization of human tissue factor antigen by immunostaining with monospecific, polyclonal anti-human tissue factor antibody. *Thromb Res.* 1990;59(2):421-37.
69. Eddleston M, de la Torre JC, Oldstone MB, Loskutoff DJ, Edgington TS, Mackman N. Astrocytes are the primary source of tissue factor in the murine central nervous system. A role for astrocytes in cerebral hemostasis. *J Clin Invest.* 1993;92(1):349-58.
70. Monroe DM, Hoffman M, Roberts HR. Transmission of a procoagulant signal from tissue factor-bearing cell to platelets. *Blood Coagul Fibrinolysis.* 1996;7(4):459-64.
71. Lancellotti S, Basso M, De Cristofaro R. Proteolytic processing of von Willebrand factor by adamts13 and leukocyte proteases. *Mediterr J Hematol Infect Dis.* 2013;5(1):e2013058.
72. Lenting PJ, Casari C, Christophe OD, Denis CV. von Willebrand factor: the old, the new and the unknown. *J Thromb Haemost.* 2012;10(12):2428-37.
73. Rezaie AR. Protease-activated receptor signalling by coagulation proteases in endothelial cells. *Thromb Haemost.* 2014;112(5):876-82.
74. Griffin JH, Zlokovic BV, Mosnier LO. Activated protein C: biased for translation. *Blood.* 2015;125(19):2898-907.
75. Krenzlin H, Lorenz V, Danckwardt S, Kempfski O, Alessandri B. The Importance of Thrombin in Cerebral Injury and Disease. *Int J Mol Sci.* 2016;17(1).
76. Daubie V, Cauwenberghs S, Senden NH, Pochet R, Lindhout T, Buurman WA, et al. Factor Xa and thrombin evoke additive calcium and proinflammatory responses in endothelial cells subjected to coagulation. *Biochim Biophys Acta.* 2006;1763(8):860-9.
77. Senden NH, Jeunhomme TM, Heemskerk JW, Wagenvoort R, van't Veer C, Hemker HC, et al. Factor Xa induces cytokine production and expression of adhesion molecules by human umbilical vein endothelial cells. *J Immunol.* 1998;161(8):4318-24.
78. Dolmetsch RE, Xu K, Lewis RS. Calcium oscillations increase the efficiency and specificity of gene expression. *Nature.* 1998;392(6679):933-6.
79. Languino LR, Plescia J, Duperray A, Brian AA, Plow EF, Geltosky JE, et al. Fibrinogen mediates leukocyte adhesion to vascular endothelium through an ICAM-1-dependent pathway. *Cell.* 1993;73(7):1423-34.
80. Alabanza LM, Bynoe MS. Thrombin induces an inflammatory phenotype in a human brain endothelial cell line. *J Neuroimmunol.* 2012;245(1-2):48-55.
81. Yamada T, Nagai Y. Immunohistochemical studies of human tissues with antibody to factor Xa. *Histochem J.* 1996;28(1):73-7.
82. Dihanich M, Kaser M, Reinhard E, Cunningham D, Monard D. Prothrombin mRNA is expressed by cells of the nervous system. *Neuron.* 1991;6(4):575-81.
83. Deschepper CF, Bigornia V, Berens ME, Lapointe MC. Production of thrombin and antithrombin III by brain and astroglial cell cultures. *Brain Res Mol Brain Res.* 1991;11(3-4):355-8.

84. Arai T, Miklossy J, Klegeris A, Guo JP, McGeer PL. Thrombin and prothrombin are expressed by neurons and glial cells and accumulate in neurofibrillary tangles in Alzheimer disease brain. *J Neuropathol Exp Neurol.* 2006;65(1):19-25.
85. Anderson M, Matthews KB, Stuart J. Coagulation and fibrinolytic activity of cerebrospinal fluid. *J Clin Pathol.* 1978;31(5):488-92.
86. Verbout NG, Yu X, Healy LD, Phillips KG, Tucker EI, Gruber A, et al. Thrombin mutant W215A/E217A treatment improves neurological outcome and attenuates central nervous system damage in experimental autoimmune encephalomyelitis. *Metab Brain Dis.* 2015;30(1):57-65.
87. Moller T, Weinstein JR, Hanisch UK. Activation of microglial cells by thrombin: past, present, and future. *Semin Thromb Hemost.* 2006;32 Suppl 1:69-76.
88. Lee NJ, Ha SK, Sati P, Absinta M, Luciano NJ, Lefevre JA, et al. Spatiotemporal distribution of fibrinogen in marmoset and human inflammatory demyelination. *Brain.* 2018;141(6):1637-49.
89. Ryu JK, Rafalski VA, Meyer-Franke A, Adams RA, Poda SB, Rios Coronado PE, et al. Fibrin-targeting immunotherapy protects against neuroinflammation and neurodegeneration. *Nat Immunol.* 2018;19(11):1212-23.
90. Gveric D, Hanemaaijer R, Newcombe J, van Lent NA, Sier CF, Cuzner ML. Plasminogen activators in multiple sclerosis lesions: implications for the inflammatory response and axonal damage. *Brain.* 2001;124(Pt 10):1978-88.
91. Fredriksson L, Lawrence DA, Medcalf RL. tPA Modulation of the Blood-Brain Barrier: A Unifying Explanation for the Pleiotropic Effects of tPA in the CNS. *Semin Thromb Hemost.* 2017;43(2):154-68.
92. Marcos-Contreras OA, Martinez de Lizarrondo S, Bardou I, Orset C, Pruvost M, Anfray A, et al. Hyperfibrinolysis increases blood-brain barrier permeability by a plasmin- and bradykinin-dependent mechanism. *Blood.* 2016;128(20):2423-34.
93. Cunningham O, Campion S, Perry VH, Murray C, Sidenius N, Docagne F, et al. Microglia and the urokinase plasminogen activator receptor/uPA system in innate brain inflammation. *Glia.* 2009;57(16):1802-14.
94. Merino P, Diaz A, Jeanneret V, Wu F, Torre E, Cheng L, et al. Urokinase-type Plasminogen Activator (uPA) Binding to the uPA Receptor (uPAR) Promotes Axonal Regeneration in the Central Nervous System. *J Biol Chem.* 2017;292(7):2741-53.
95. Beschorner R, Schluesener HJ, Nguyen TD, Magdolen V, Luther T, Pedal I, et al. Lesion-associated accumulation of uPAR/CD87- expressing infiltrating granulocytes, activated microglial cells/macrophages and upregulation by endothelial cells following TBI and FCI in humans. *Neuropathol Appl Neurobiol.* 2000;26(6):522-7.
96. Bhakuni T, Ali MF, Ahmad I, Bano S, Ansari S, Jairajpuri MA. Role of heparin and non heparin binding serpins in coagulation and angiogenesis: A complex interplay. *Arch Biochem Biophys.* 2016;604:128-42.
97. Dellas C, Loskutoff DJ. Historical analysis of PAI-1 from its discovery to its potential role in cell motility and disease. *Thromb Haemost.* 2005;93(4):631-40.
98. Jeon H, Kim JH, Kim JH, Lee WH, Lee MS, Suk K. Plasminogen activator inhibitor type 1 regulates microglial motility and phagocytic activity. *J Neuroinflammation.* 2012;9:149.
99. Pelisch N, Dan T, Ichimura A, Sekiguchi H, Vaughan DE, van Ypersele de Strihou C, et al. Plasminogen Activator Inhibitor-1 Antagonist TM5484 Attenuates Demyelination and Axonal Degeneration in a Mice Model of Multiple Sclerosis. *PLoS One.* 2015;10(4):e0124510.
100. East E, Baker D, Pryce G, Lijnen HR, Cuzner ML, Gveric D. A role for the plasminogen activator system in inflammation and neurodegeneration in the central nervous system during experimental allergic encephalomyelitis. *Am J Pathol.* 2005;167(2):545-54.
101. Ratnoff OD, Margolius A, Jr. Hageman trait: an asymptomatic disorder of blood coagulation. *Trans Assoc Am Physicians.* 1955;68:149-54.
102. Schmaier AH. The contact activation and kallikrein/kinin systems: pathophysiologic and physiologic activities. *J Thromb Haemost.* 2016;14(1):28-39.
103. Ivanov I, Matafonov A, Sun MF, Cheng Q, Dickeson SK, Verhamme IM, et al. Proteolytic properties of single-chain factor XII: a mechanism for triggering contact activation. *Blood.* 2017;129(11):1527-37.
104. Bernardi F, Marchetti G, Patracchini P, del Senno L, Tripodi M, Fantoni A, et al. Factor XII gene alteration in Hageman trait detected by TaqI restriction enzyme. *Blood.* 1987;69(5):1421-4.
105. Matafonov A, Leung PY, Gailani AE, Grach SL, Puy C, Cheng Q, et al. Factor XII inhibition reduces thrombus formation in a primate thrombosis model. *Blood.* 2014;123(11):1739-46.
106. Xu Y, Cai TQ, Castriota G, Zhou Y, Hoos L, Jochnowitz N, et al. Factor XIIa inhibition by Infestin-4: in vitro mode of action and in vivo antithrombotic benefit. *Thromb Haemost.* 2014;111(4):694-704.
107. Colman RW. Activation of plasminogen by human plasma kallikrein. *Biochem Biophys Res Commun.* 1969;35(2):273-9.
108. Gobel K, Pankratz S, Schneider-Hohendorf T, Bittner S, Schuhmann MK, Langer HF, et al. Blockade of the kinin receptor B1 protects from autoimmune CNS disease by reducing leukocyte trafficking. *J Autoimmun.* 2011;36(2):106-14.

109. Conway EM. Reincarnation of ancient links between coagulation and complement. *J Thromb Haemost.* 2015;13 Suppl 1:S121-32.
110. Keragala CB, Draxler DF, McQuilten ZK, Medcalf RL. Haemostasis and innate immunity - a complementary relationship: A review of the intricate relationship between coagulation and complement pathways. *Br J Haematol.* 2018;180(6):782-98.
111. Oschatz C, Maas C, Lecher B, Jansen T, Bjorkqvist J, Tradler T, et al. Mast cells increase vascular permeability by heparin-initiated bradykinin formation in vivo. *Immunity.* 2011;34(2):258-68.
112. Fuchs TA, Brill A, Duerschmied D, Schatzberg D, Monestier M, Myers DD, Jr., et al. Extracellular DNA traps promote thrombosis. *Proc Natl Acad Sci U S A.* 2010;107(36):15880-5.
113. Putnam TJ. Evidences of Vascular Occlusion in Multiple Sclerosis and "Encephalomyelitis". *Archives of Neurology And Psychiatry.* 1937;37(6):1298-321.
114. Putnam TJ, Chiavacci LV, et al. Results of treatment of multiple sclerosis with dicoumarin. *Arch Neurol Psychiatry.* 1947;57(1):1-13.
115. Shulman MH, Alexander L, Ehrentheil OF, Gross R. Capillary resistance studies in multiple sclerosis. *J Neuropathol Exp Neurol.* 1950;9(4):420-9.
116. Swank RL. Subcutaneous hemorrhages in multiple sclerosis. *Neurology.* 1958;8(6):497-8.
117. Persson I. Variations in the plasma fibrinogen during the course of multiple sclerosis. *AMA Arch Neurol Psychiatry.* 1955;74(1):17-30.
118. Davalos D, Akassoglou K. Fibrinogen as a key regulator of inflammation in disease. *Semin Immunopathol.* 2012;34(1):43-62.
119. Feldman S, Izak G, Nelken D. Blood coagulation studies and serotonin determinations in serum and cerebrospinal fluid in multiple sclerosis. *Acta Psychiatr Neurol Scand.* 1957;32(1):37-49.
120. Albright SD, 3rd, Kupfer HG, Kinne DR. A study of coagulation factors in blood and spinal fluid in multiple sclerosis. *Arch Neurol.* 1959;1:315-26.
121. Gaertner HA, Lisiewicz J, Caen J. Antithrombin activity of normal and pathological cerebrospinal fluid. *Nature.* 1961;192:1164-6.
122. Niewiarowski S, Hausmanowa-Petrusewicz I, Wegrzynowicz Z. Blood clotting factors in cerebrospinal fluid. *J Clin Pathol.* 1962;15:497-500.
123. Menon IS, Dewar HA, Newell DJ. Fibrinolytic activity of venous blood of patients with multiple sclerosis. *Neurology.* 1969;19(1):101-4.
124. Millac P. Platelet stickiness in multiple sclerosis. *Dtsch Z Nervenheilkd.* 1967;191(1):74-9.
125. Dohnal K, Vagner B, Lupinek Z, Hule V. Notes on the influence of adrenocorticotrophic hormone on platelet stickiness in multiple sclerosis. *J Neurol Sci.* 1971;13(4):443-6.
126. Wright HP, Thompson RH, Zilkha KJ. Platelet adhesiveness in multiple sclerosis. *Lancet.* 1965;2(7422):1109-10.
127. Friese MA, Schattling B, Fugger L. Mechanisms of neurodegeneration and axonal dysfunction in multiple sclerosis. *Nat Rev Neurol.* 2014;10(4):225-38.
128. Petersen MA, Ryu JK, Akassoglou K. Fibrinogen in neurological diseases: mechanisms, imaging and therapeutics. *Nat Rev Neurosci.* 2018;19(5):283-301.
129. Weisel JW, Litvinov RI. Fibrin Formation, Structure and Properties. *Subcell Biochem.* 2017;82:405-56.
130. Jankovic J, Derman H, Armstrong D. Haemorrhagic complications of multiple sclerosis. *J Neurol Neurosurg Psychiatry.* 1980;43(1):76-81.
131. Kirk J, Plumb J, Mirakhor M, McQuaid S. Tight junctional abnormality in multiple sclerosis white matter affects all calibres of vessel and is associated with blood-brain barrier leakage and active demyelination. *J Pathol.* 2003;201(2):319-27.
132. Gay D, Esiri M. Blood-brain barrier damage in acute multiple sclerosis plaques. An immunocytological study. *Brain.* 1991;114 (Pt 1B):557-72.
133. Kwon EE, Prineas JW. Blood-brain barrier abnormalities in longstanding multiple sclerosis lesions. An immunohistochemical study. *J Neuropathol Exp Neurol.* 1994;53(6):625-36.
134. Gay FW, Drye TJ, Dick GW, Esiri MM. The application of multifactorial cluster analysis in the staging of plaques in early multiple sclerosis. Identification and characterization of the primary demyelinating lesion. *Brain.* 1997;120 (Pt 8):1461-83.
135. Plumb J, McQuaid S, Mirakhor M, Kirk J. Abnormal endothelial tight junctions in active lesions and normal-appearing white matter in multiple sclerosis. *Brain Pathol.* 2002;12(2):154-69.
136. Han MH, Hwang SI, Roy DB, Lundgren DH, Price JV, Ousman SS, et al. Proteomic analysis of active multiple sclerosis lesions reveals therapeutic targets. *Nature.* 2008;451(7182):1076-81.
137. Ingram G, Loveless S, Howell OW, Hakobyan S, Dancey B, Harris CL, et al. Complement activation in multiple sclerosis plaques: an immunohistochemical analysis. *Acta Neuropathol Commun.* 2014;2:53.
138. Hirsch HE, Blanco CE, Parks ME. Fibrinolytic activity of plaques and white matter in multiple sclerosis. *J Neuropathol Exp Neurol.* 1981;40(3):271-80.
139. Cuzner ML, Gveric D, Strand C, Loughlin AJ, Paemen L, Opdenakker G, et al. The expression of tissue-type plasminogen activator, matrix metalloproteases and endogenous inhibitors in the central nervous

- system in multiple sclerosis: comparison of stages in lesion evolution. *J Neuropathol Exp Neurol.* 1996;55(12):1194-204.
140. Gveric D, Herrera B, Petzold A, Lawrence DA, Cuzner ML. Impaired fibrinolysis in multiple sclerosis: a role for tissue plasminogen activator inhibitors. *Brain.* 2003;126(Pt 7):1590-8.
141. Gveric D, Herrera BM, Cuzner ML. tPA receptors and the fibrinolytic response in multiple sclerosis lesions. *Am J Pathol.* 2005;166(4):1143-51.
142. Pardridge WM, Yang J, Eisenberg J, Tourtellotte WW. Isolation of intact capillaries and capillary plasma membranes from frozen human brain. *J Neurosci Res.* 1987;18(2):352-7.
143. Aksungar FB, Topkaya AE, Yildiz Z, Sahin S, Turk U. Coagulation status and biochemical and inflammatory markers in multiple sclerosis. *J Clin Neurosci.* 2008;15(4):393-7.
144. Gobel K, Kraft P, Pankratz S, Gross CC, Korsukewitz C, Kwiecien R, et al. Prothrombin and factor X are elevated in multiple sclerosis patients. *Ann Neurol.* 2016;80(6):946-51.
145. Parsons ME, O'Connell K, Allen S, Egan K, Szklanna PB, McGuigan C, et al. Thrombin generation correlates with disease duration in multiple sclerosis (MS): Novel insights into the MS-associated prothrombotic state. *Mult Scler J Exp Transl Clin.* 2017;3(4):2055217317747624.
146. Ziliotto N, Baroni M, Straudi S, Manfredini F, Mari R, Menegatti E, et al. Coagulation Factor XII Levels and Intrinsic Thrombin Generation in Multiple Sclerosis. *Frontiers in Neurology.* 2018;9(245).
147. Duchemin J, Pan-Petes B, Arnaud B, Blouch MT, Abgrall JF. Influence of coagulation factors and tissue factor concentration on the thrombin generation test in plasma. *Thromb Haemost.* 2008;99(4):767-73.
148. Castoldi E, Rosing J. Thrombin generation tests. *Thromb Res.* 2011;127 Suppl 3:S21-5.
149. Campos-de-Magalhaes M, de Almeida AJ, Papaiz-Alvarenga RM, Gadelha T, Morais-de-Sa CA, Alves-Leon SV. Normal plasma antithrombin activity in patients with relapsing-remitting and secondary progressive multiple sclerosis. *Clin Neurol Neurosurg.* 2009;111(5):407-11.
150. Maimone D, Reder AT, Gregory S. T cell lymphokine-induced secretion of cytokines by monocytes from patients with multiple sclerosis. *Cell Immunol.* 1993;146(1):96-106.
151. Ehling R, Pauli FD, Lackner P, Kuenz B, Santner W, Lutterotti A, et al. Fibrinogen is not elevated in the cerebrospinal fluid of patients with multiple sclerosis. *Fluids Barriers CNS.* 2011;8(1):25.
152. Fuvesi J, Hanrieder J, Bencsik K, Rajda C, Kovacs SK, Kaizer L, et al. Proteomic analysis of cerebrospinal fluid in a fulminant case of multiple sclerosis. *Int J Mol Sci.* 2012;13(6):7676-93.
153. Liguori M, Quattieri A, Tortorella C, Dorenzo V, Bagala A, Mastrapasqua M, et al. Proteomic profiling in multiple sclerosis clinical courses reveals potential biomarkers of neurodegeneration. *PLoS One.* 2014;9(8):e103984.
154. Miranda Acuna J, Hidalgo de la Cruz M, Ros AL, Tapia SP, Martinez Gines ML, de Andres Frutos CD. Elevated plasma fibrinogen levels in multiple sclerosis patients during relapse. *Mult Scler Relat Disord.* 2017;18:157-60.
155. Wallin MT, Oh U, Nyalwidhe J, Semmes J, Kislinger T, Coffman P, et al. Serum proteomic analysis of a pre-symptomatic multiple sclerosis cohort. *Eur J Neurol.* 2015;22(3):591-9.
156. Frigerio S, Ariano C, Bernardi G, Ciusani E, Massa G, La Mantia L, et al. Cerebrospinal fluid thrombomodulin and sVCAM-1 in different clinical stages of multiple sclerosis patients. *J Neuroimmunol.* 1998;87(1-2):88-93.
157. Kohriyama T, Maruyama H, Kurokawa K, Harada T, Nakamura S. [Endothelial cell activation and/or injury in multiple sclerosis: analysis with von Willebrand factor and thrombomodulin]. *Rinsho Shinkeigaku.* 1997;37(4):287-91.
158. Festoff BW, Li C, Woodhams B, Lynch S. Soluble thrombomodulin levels in plasma of multiple sclerosis patients and their implication. *J Neurol Sci.* 2012;323(1-2):61-5.
159. Tsukada N, Matsuda M, Miyagi K, Yanagisawa N. Thrombomodulin in the sera of patients with multiple sclerosis and human lymphotropic virus type-1-associated myelopathy. *J Neuroimmunol.* 1995;56(1):113-6.
160. Balkuv E, Varoglu AO, Isik N, Isbilen B, Duruyen S, Basaran R, et al. The effects of thrombomodulin and activated protein C on the pathogenesis of multiple sclerosis. *Mult Scler Relat Disord.* 2016;8:131-5.
161. Giovannoni G, Thorpe JW, Kidd D, Kendall BE, Moseley IF, Thompson AJ, et al. Soluble E-selectin in multiple sclerosis: raised concentrations in patients with primary progressive disease. *J Neurol Neurosurg Psychiatry.* 1996;60(1):20-6.
162. Wildenauer DB, Korschhausen D, Hoechtlen W, Ackenheil M, Kehl M, Lottspeich F. Analysis of cerebrospinal fluid from patients with psychiatric and neurological disorders by two-dimensional electrophoresis: identification of disease-associated polypeptides as fibrin fragments. *Electrophoresis.* 1991;12(7-8):487-92.
163. Akenami FO, Siren V, Koskiniemi M, Siimes MA, Teravainen H, Vaheri A. Cerebrospinal fluid activity of tissue plasminogen activator in patients with neurological diseases. *J Clin Pathol.* 1996;49(7):577-80.
164. Akenami FO, Koskiniemi M, Farkkila M, Vaheri A. Cerebrospinal fluid plasminogen activator inhibitor-1 in patients with neurological disease. *J Clin Pathol.* 1997;50(2):157-60.

165. Onodera H, Nakashima I, Fujihara K, Nagata T, Itoyama Y. Elevated plasma level of plasminogen activator inhibitor-1 (PAI-1) in patients with relapsing-remitting multiple sclerosis. *Tohoku J Exp Med.* 1999;189(4):259-65.
166. Sciacca FL, Ciusani E, Silvani A, Corsini E, Frigerio S, Pogliani S, et al. Genetic and plasma markers of venous thromboembolism in patients with high grade glioma. *Clin Cancer Res.* 2004;10(4):1312-7.
167. Brunetti A, Ricchieri GL, Patrassi GM, Girolami A, Tavalato B. Rheological and fibrinolytic findings in multiple sclerosis. *J Neurol Neurosurg Psychiatry.* 1981;44(4):340-3.
168. Fissolo N, Pignolet B, Matute-Blanch C, Trivino JC, Miro B, Mota M, et al. Matrix metalloproteinase 9 is decreased in natalizumab-treated multiple sclerosis patients at risk for progressive multifocal leukoencephalopathy. *Ann Neurol.* 2017;82(2):186-95.
169. Frank RD, Altenwerth B, Brandenburg VM, Nolden-Koch M, Block F. Effect of intravenous high-dose methylprednisolone on coagulation and fibrinolysis markers. *Thromb Haemost.* 2005;94(2):467-8.
170. Kalande H, Harandi AA, Alidaei S, Heidari D, Shahbeigi S, Ghorbani M. Venous thrombosis in multiple sclerosis patients after high-dose intravenous methylprednisolone: the preventive effect of enoxaparin. *Thrombosis.* 2011;2011:785459.
171. Festoff BW, Li C, Woodhams B, Lynch S. Soluble thrombomodulin levels in plasma of multiple sclerosis patients and their implication. *J Neurol Sci.* 2012;323(1-2):61-5.
172. Bidot CJ, Horstman LL, Jy W, Jimenez JJ, Bidot C, Jr., Ahn YS, et al. Clinical and neuroimaging correlates of antiphospholipid antibodies in multiple sclerosis: a preliminary study. *BMC Neurol.* 2007;7:36.
173. Dimopoulou D, Dimosiari A, Mandala E, Dimitroulas T, Garyfallos A. Autoimmune Thrombotic Thrombocytopenic Purpura: Two Rare Cases Associated with Juvenile Idiopathic Arthritis and Multiple Sclerosis. *Front Med (Lausanne).* 2017;4:89.
174. Orvain C, Augusto JF, Besson V, Marc G, Coppo P, Subra JF, et al. Thrombotic microangiopathy due to acquired ADAMTS13 deficiency in a patient receiving interferon-beta treatment for multiple sclerosis. *Int Urol Nephrol.* 2014;46(1):239-42.
175. Nishio H, Tsukamoto T, Matsubara T, Okada Y, Takahashi R, Yanagita M. Thrombotic microangiopathy caused by interferon beta-1b for multiple sclerosis: a case report. *CEN Case Rep.* 2016;5(2):179-83.
176. Ziliotto N, Bernardi F, Jakimovski D, Baroni M, Marchetti G, Bergsland N, et al. Plasma levels of hemostasis inhibitors and MRI outcomes in multiple sclerosis (P3.368). *Neurology.* 2018;90(15 Supplement).
177. Ziliotto N, Bernardi F, Jakimovski D, Baroni M, Marchetti G, Bergsland N, et al. Hemostasis biomarkers in multiple sclerosis. *Eur J Neurol.* 2018;25(9):1169-76.
178. Loh Y, Oyama Y, Statkute L, Quigley K, Young K, Gonda E, et al. Development of a secondary autoimmune disorder after hematopoietic stem cell transplantation for autoimmune diseases: role of conditioning regimen used. *Blood.* 2007;109(6):2643-548.
179. Cuker A, Coles AJ, Sullivan H, Fox E, Goldberg M, Oyuela P, et al. A distinctive form of immune thrombocytopenia in a phase 2 study of alemtuzumab for the treatment of relapsing-remitting multiple sclerosis. *Blood.* 2011;118(24):6299-305.
180. Moake JL, Kent CJ, Meta LD, Wright LC. Circulating IgG antibodies against factors IX and VIII in multiple sclerosis. *Acta Haematol.* 1976;55(1):53-9.
181. Hoyle C, Ludlam CA. Acquired factor VIII inhibitor associated with multiple sclerosis, successfully treated with porcine factor VIII. *Thromb Haemost.* 1987;57(2):233.
182. Kaloyannidis P, Sakellari I, Fassas A, Fragia T, Vakalopoulou S, Kartsios C, et al. Acquired hemophilia-A in a patient with multiple sclerosis treated with autologous hematopoietic stem cell transplantation and interferon beta-1a. *Bone Marrow Transplant.* 2004;34(2):187-8.
183. Capra R, Mattioli F, Kalman B, Marciano N, Berenzi A, Benetti A. Two sisters with multiple sclerosis, lamellar ichthyosis, beta thalassaemia minor and a deficiency of factor VIII. *J Neurol.* 1993;240(6):336-8.
184. McCaughan G, Massey J, Sutton I, Curnow J. Acquired haemophilia A complicating alemtuzumab therapy for multiple sclerosis. *BMJ Case Rep.* 2017;2017.
185. Ocak G, Vossen CY, Verduijn M, Dekker FW, Rosendaal FR, Cannegieter SC, et al. Risk of venous thrombosis in patients with major illnesses: results from the MEGA study. *J Thromb Haemost.* 2013;11(1):116-23.
186. Straudi S, Manfredini F, Lamberti N, Zamboni P, Bernardi F, Marchetti G, et al. The effectiveness of Robot-Assisted Gait Training versus conventional therapy on mobility in severely disabled progressive Multiple sclerosis patients (RAGTIME): study protocol for a randomized controlled trial. *Trials.* 2017;18(1):88.
187. Polman CH, Reingold SC, Banwell B, Clanet M, Cohen JA, Filippi M, et al. Diagnostic criteria for multiple sclerosis: 2010 revisions to the McDonald criteria. *Ann Neurol.* 2011;69(2):292-302.
188. Polman CH, Reingold SC, Edan G, Filippi M, Hartung HP, Kappos L, et al. Diagnostic criteria for multiple sclerosis: 2005 revisions to the "McDonald Criteria". *Ann Neurol.* 2005;58(6):840-6.
189. Dolic K, Marr K, Valnarov V, Dwyer MG, Carl E, Karmon Y, et al. Intra- and extraluminal structural and functional venous anomalies in multiple sclerosis, as evidenced by 2 noninvasive imaging techniques. *AJNR Am J Neuroradiol.* 2012;33(1):16-23.

190. Zamboni P, Sisini F, Menegatti E, Taibi A, Malagoni AM, Morovic S, et al. An ultrasound model to calculate the brain blood outflow through collateral vessels: a pilot study. *BMC Neurol.* 2013;13:81.
191. Zamboni P, Menegatti E, Cittanti C, Sisini F, Gianesini S, Salvi F, et al. Fixing the jugular flow reduces ventricle volume and improves brain perfusion. *J Vasc Surg Venous Lymphat Disord.* 2016;4(4):434-45.
192. McDonald WI, Compston A, Edan G, Goodkin D, Hartung HP, Lublin FD, et al. Recommended diagnostic criteria for multiple sclerosis: guidelines from the International Panel on the diagnosis of multiple sclerosis. *Ann Neurol.* 2001;50(1):121-7.
193. Zivadinov R, Heininen-Brown M, Schirda CV, Poloni GU, Bergsland N, Magnano CR, et al. Abnormal subcortical deep-gray matter susceptibility-weighted imaging filtered phase measurements in patients with multiple sclerosis: a case-control study. *Neuroimage.* 2012;59(1):331-9.
194. Gelineau-Morel R, Tomassini V, Jenkinson M, Johansen-Berg H, Matthews PM, Palace J. The effect of hypointense white matter lesions on automated gray matter segmentation in multiple sclerosis. *Hum Brain Mapp.* 2012;33(12):2802-14.
195. Smith SM, Zhang Y, Jenkinson M, Chen J, Matthews PM, Federico A, et al. Accurate, robust, and automated longitudinal and cross-sectional brain change analysis. *Neuroimage.* 2002;17(1):479-89.
196. Patenaude B, Smith SM, Kennedy DN, Jenkinson M. A Bayesian model of shape and appearance for subcortical brain segmentation. *Neuroimage.* 2011;56(3):907-22.
197. Hammond KE, Lupo JM, Xu D, Metcalf M, Kelley DA, Pelletier D, et al. Development of a robust method for generating 7.0 T multichannel phase images of the brain with application to normal volunteers and patients with neurological diseases. *Neuroimage.* 2008;39(4):1682-92.
198. Polak P ZR, Schweser F. Gradient unwarping for phase imaging reconstruction. In *Proc Intl Soc Mag Reson Med* 2015:p3736.
199. Abdul-Rahman HS, Gdeisat MA, Burton DR, Lalor MJ, Lilley F, Moore CJ. Fast and robust three-dimensional best path phase unwrapping algorithm. *Appl Opt.* 2007;46(26):6623-35.
200. Schweser F, Deistung A, Lehr BW, Reichenbach JR. Quantitative imaging of intrinsic magnetic tissue properties using MRI signal phase: an approach to in vivo brain iron metabolism? *Neuroimage.* 2011;54(4):2789-807.
201. Schweser F, Sommer K, Deistung A, Reichenbach JR. Quantitative susceptibility mapping for investigating subtle susceptibility variations in the human brain. *Neuroimage.* 2012;62(3):2083-100.
202. Hagemeyer J, Zivadinov R, Dwyer MG, Polak P, Bergsland N, Weinstock-Guttman B, et al. Changes of deep gray matter magnetic susceptibility over 2 years in multiple sclerosis and healthy control brain. *NeuroImage: Clinical.* 2017.
203. Gregoire SM, Chaudhary UJ, Brown MM, Yousry TA, Kallis C, Jager HR, et al. The Microbleed Anatomical Rating Scale (MARS): reliability of a tool to map brain microbleeds. *Neurology.* 2009;73(21):1759-66.
204. Ghebrehiwet B, Silverberg M, Kaplan AP. Activation of the classical pathway of complement by Hageman factor fragment. *J Exp Med.* 1981;153(3):665-76.
205. Ratnoff OD, Colopy JE. A familial hemorrhagic trait associated with a deficiency of a clot-promoting fraction of plasma. *J Clin Invest.* 1955;34(4):602-13.
206. Davie EW, Ratnoff OD. Waterfall Sequence for Intrinsic Blood Clotting. *Science.* 1964;145(3638):1310-2.
207. Citarella F, Ravon DM, Pascucci B, Felici A, Fantoni A, Hack CE. Structure/function analysis of human factor XII using recombinant deletion mutants. Evidence for an additional region involved in the binding to negatively charged surfaces. *Eur J Biochem.* 1996;238(1):240-9.
208. Samuel M, Samuel E, Villanueva GB. Histidine residues are essential for the surface binding and autoactivation of human coagulation factor XII. *Biochem Biophys Res Commun.* 1993;191(1):110-7.
209. Citarella F, Wuillemin WA, Lubbers YT, Hack CE. Initiation of contact system activation in plasma is dependent on factor XII autoactivation and not on enhanced susceptibility of factor XII for kallikrein cleavage. *Br J Haematol.* 1997;99(1):197-205.
210. Cool DE, Edgell CJ, Louie GV, Zoller MJ, Brayer GD, MacGillivray RT. Characterization of human blood coagulation factor XII cDNA. Prediction of the primary structure of factor XII and the tertiary structure of beta-factor XIIa. *J Biol Chem.* 1985;260(25):13666-76.
211. Citarella F, te Velthuis H, Helmer-Citterich M, Hack CE. Identification of a putative binding site for negatively charged surfaces in the fibronectin type II domain of human factor XII--an immunochemical and homology modeling approach. *Thromb Haemost.* 2000;84(6):1057-65.
212. de Maat S, Maas C. Factor XII: form determines function. *J Thromb Haemost.* 2016;14(8):1498-506.
213. Fujikawa K, McMullen BA. Amino acid sequence of human beta-factor XIIa. *J Biol Chem.* 1983;258(18):10924-33.
214. De Maat S, Clark CC, Boertien M, Parr N, Sanrattana W, Hofman ZLM, et al. Factor XII truncation accelerates activation in solution. *J Thromb Haemost.* 2018.
215. Hovinga JK, Schaller J, Stricker H, Wuillemin WA, Furlan M, Lammler B. Coagulation factor XII Locarno: the functional defect is caused by the amino acid substitution Arg 353-->Pro leading to loss of a kallikrein cleavage site. *Blood.* 1994;84(4):1173-81.

216. Revak SD, Cochrane CG, Bouma BN, Griffin JH. Surface and fluid phase activities of two forms of activated Hageman factor produced during contact activation of plasma. *J Exp Med.* 1978;147(3):719-29.
217. Jukema BN, de Maat S, Maas C. Processing of Factor XII during Inflammatory Reactions. *Front Med (Lausanne).* 2016;3:52.
218. LaRusch GA, Mahdi F, Shariat-Madar Z, Adams G, Sitrin RG, Zhang WM, et al. Factor XII stimulates ERK1/2 and Akt through uPAR, integrins, and the EGFR to initiate angiogenesis. *Blood.* 2010;115(24):5111-20.
219. Stavrou E, Schmaier AH. Factor XII: what does it contribute to our understanding of the physiology and pathophysiology of hemostasis & thrombosis. *Thromb Res.* 2010;125(3):210-5.
220. Revenko AS, Gao D, Crosby JR, Bhattacharjee G, Zhao C, May C, et al. Selective depletion of plasma prekallikrein or coagulation factor XII inhibits thrombosis in mice without increased risk of bleeding. *Blood.* 2011;118(19):5302-11.
221. Helft G, Le Feuvre C, Metzger JP, Vacheron A, Monsuez JJ, Lachurie ML, et al. Factor XII deficiency associated with coronary stent thrombosis. *Am J Hematol.* 2000;64(4):322-3.
222. Soria JM, Almasy L, Souto JC, Bacq D, Buil A, Faure A, et al. A quantitative-trait locus in the human factor XII gene influences both plasma factor XII levels and susceptibility to thrombotic disease. *Am J Hum Genet.* 2002;70(3):567-74.
223. Koudriavtseva T. Thrombotic processes in multiple sclerosis as manifestation of innate immune activation. *Front Neurol.* 2014;5:119.
224. Olivieri O, Martinelli N, Baroni M, Branchini A, Girelli D, Friso S, et al. Factor II activity is similarly increased in patients with elevated apolipoprotein CIII and in carriers of the factor II 20210A allele. *J Am Heart Assoc.* 2013;2(6):e000440.
225. Martinelli N, Girelli D, Baroni M, Guarini P, Sandri M, Lunghi B, et al. Activated factor VII-antithrombin complex predicts mortality in patients with stable coronary artery disease: a cohort study. *J Thromb Haemost.* 2016;14(4):655-66.
226. Woodruff RS, Xu Y, Layzer J, Wu W, Ogletree ML, Sullenger BA. Inhibiting the intrinsic pathway of coagulation with a factor XII-targeting RNA aptamer. *J Thromb Haemost.* 2013;11(7):1364-73.
227. Vu TT, Leslie BA, Stafford AR, Zhou J, Fredenburgh JC, Weitz JI. Histidine-rich glycoprotein binds DNA and RNA and attenuates their capacity to activate the intrinsic coagulation pathway. *Thromb Haemost.* 2016;115(1):89-98.
228. Hemker HC, Giesen P, Al Dieri R, Regnault V, de Smedt E, Wagenvoort R, et al. Calibrated automated thrombin generation measurement in clotting plasma. *Pathophysiol Haemost Thromb.* 2003;33(1):4-15.
229. Morrissey JH, Smith SA. Polyphosphate as modulator of hemostasis, thrombosis, and inflammation. *J Thromb Haemost.* 2015;13 Suppl 1:S92-7.
230. Merker M, Eichler S, Herrmann AM, Wiendl H, Kleinschnitz C, Gobel K, et al. Rivaroxaban ameliorates disease course in an animal model of multiple sclerosis. *J Neuroimmunol.* 2017;313:125-8.
231. Stolz L, Derouiche A, Devraj K, Weber F, Brunkhorst R, Foerch C. Anticoagulation with warfarin and rivaroxaban ameliorates experimental autoimmune encephalomyelitis. *J Neuroinflammation.* 2017;14(1):152.
232. Esmon CT. Inflammation and the activated protein C anticoagulant pathway. *Semin Thromb Hemost.* 2006;32 Suppl 1:49-60.
233. Chapin JC, Hajjar KA. Fibrinolysis and the control of blood coagulation. *Blood Rev.* 2015;29(1):17-24.
234. Zheng XL. Structure-function and regulation of ADAMTS-13 protease. *J Thromb Haemost.* 2013;11 Suppl 1:11-23.
235. Hackeng TM, Maurissen LF, Castoldi E, Rosing J. Regulation of TFPI function by protein S. *J Thromb Haemost.* 2009;7 Suppl 1:165-8.
236. Huntington JA. Thrombin inhibition by the serpins. *J Thromb Haemost.* 2013;11 Suppl 1:254-64.
237. Wolter J, Schild L, Bock F, Hellwig A, Gadi I, Al-Dabet MM, et al. Thrombomodulin-dependent protein C activation is required for mitochondrial function and myelination in the central nervous system. *J Thromb Haemost.* 2016;14(11):2212-26.
238. Favaloro EJ, Franchini M, Lippi G. Aging hemostasis: changes to laboratory markers of hemostasis as we age - a narrative review. *Semin Thromb Hemost.* 2014;40(6):621-33.
239. Cai P, Luo H, Xu H, Zhu X, Xu W, Dai Y, et al. Recombinant ADAMTS 13 Attenuates Brain Injury After Intracerebral Hemorrhage. *Stroke.* 2015;46(9):2647-53.
240. Coughlin SR. How the protease thrombin talks to cells. *Proc Natl Acad Sci U S A.* 1999;96(20):11023-7.
241. Ikeda Y, Aihara K, Yoshida S, Iwase T, Tajima S, Izawa-Ishizawa Y, et al. Heparin cofactor II, a serine protease inhibitor, promotes angiogenesis via activation of the AMP-activated protein kinase-endothelial nitric-oxide synthase signaling pathway. *J Biol Chem.* 2012;287(41):34256-63.
242. Karmon Y, Ramanathan M, Minagar A, Zivadinov R, Weinstock-Guttman B. Arterial, venous and other vascular risk factors in multiple sclerosis. *Neurol Res.* 2012;34(8):754-60.

243. Kappus N, Weinstock-Guttman B, Hagemeyer J, Kennedy C, Melia R, Carl E, et al. Cardiovascular risk factors are associated with increased lesion burden and brain atrophy in multiple sclerosis. *J Neurol Neurosurg Psychiatry*. 2016;87(2):181-7.
244. Adams CW. Perivascular iron deposition and other vascular damage in multiple sclerosis. *J Neurol Neurosurg Psychiatry*. 1988;51(2):260-5.
245. Zamboni P, Galeotti R, Menegatti E, Malagoni AM, Tacconi G, Dall'Ara S, et al. Chronic cerebrospinal venous insufficiency in patients with multiple sclerosis. *J Neurol Neurosurg Psychiatry*. 2009;80(4):392-9.
246. Zivadinov R, Alexander SJ, Minagar A. Vascular pathology of multiple sclerosis. *Neurol Res*. 2012;34(8):735-7.
247. Zamboni P, Tesio L, Galimberti S, Massacesi L, Salvi F, D'Alessandro R, et al. Efficacy and Safety of Extracranial Vein Angioplasty in Multiple Sclerosis: A Randomized Clinical Trial. *JAMA Neurol*. 2018;75(1):35-43.
248. Zivadinov R, Weinstock-Guttman B. Multiple sclerosis: Extracranial venous angioplasty is ineffective to treat MS. *Nat Rev Neurol*. 2018;14(3):129-30.
249. D'Haeseleer M, Hostenbach S, Peeters I, Sankari SE, Nagels G, De Keyser J, et al. Cerebral hypoperfusion: a new pathophysiologic concept in multiple sclerosis? *J Cereb Blood Flow Metab*. 2015;35(9):1406-10.
250. Belov P, Jakimovski D, Krawiecki J, Magnano C, Hagemeyer J, Pelizzari L, et al. Lower Arterial Cross-Sectional Area of Carotid and Vertebral Arteries and Higher Frequency of Secondary Neck Vessels Are Associated with Multiple Sclerosis. *AJNR Am J Neuroradiol*. 2018;39(1):123-30.
251. Alexander JS, Prouty L, Tsunoda I, Ganta CV, Minagar A. Venous endothelial injury in central nervous system diseases. *BMC Med*. 2013;11:219.
252. Ramanathan M, Weinstock-Guttman B, Nguyen LT, Badgett D, Miller C, Patrick K, et al. In vivo gene expression revealed by cDNA arrays: the pattern in relapsing-remitting multiple sclerosis patients compared with normal subjects. *J Neuroimmunol*. 2001;116(2):213-9.
253. Ratzler R, Sondergaard HB, Christensen JR, Bornsen L, Borup R, Sorensen PS, et al. Gene expression analysis of relapsing-remitting, primary progressive and secondary progressive multiple sclerosis. *Mult Scler*. 2013;19(14):1841-8.
254. Nickles D, Chen HP, Li MM, Khankhanian P, Madireddy L, Caillier SJ, et al. Blood RNA profiling in a large cohort of multiple sclerosis patients and healthy controls. *Hum Mol Genet*. 2013;22(20):4194-205.
255. Paraboschi EM, Cardamone G, Rimoldi V, Gemmati D, Spreafico M, Duga S, et al. Meta-Analysis of Multiple Sclerosis Microarray Data Reveals Dysregulation in RNA Splicing Regulatory Genes. *Int J Mol Sci*. 2015;16(10):23463-81.
256. Comabella M, Canto E, Nurdinov R, Rio J, Villar LM, Picon C, et al. MRI phenotypes with high neurodegeneration are associated with peripheral blood B-cell changes. *Hum Mol Genet*. 2016;25(2):308-16.
257. Lindsey JW, Agarwal SK, Tan FK. Gene expression changes in multiple sclerosis relapse suggest activation of T and non-T cells. *Mol Med*. 2011;17(1-2):95-102.
258. Coen M, Marchetti G, Palagi PM, Zerbinati C, Guastella G, Gagliano T, et al. Calmodulin expression distinguishes the smooth muscle cell population of human carotid plaque. *Am J Pathol*. 2013;183(3):996-1009.
259. Marchetti G, Girelli D, Zerbinati C, Lunghi B, Friso S, Meneghetti S, et al. An integrated genomic-transcriptomic approach supports a role for the proto-oncogene BCL3 in atherosclerosis. *Thromb Haemost*. 2015;113(3):655-63.
260. Felding-Habermann B, Silletti S, Mei F, Siu CH, Yip PM, Brooks PC, et al. A single immunoglobulin-like domain of the human neural cell adhesion molecule L1 supports adhesion by multiple vascular and platelet integrins. *J Cell Biol*. 1997;139(6):1567-81.
261. Gorski DH, Walsh K. Control of vascular cell differentiation by homeobox transcription factors. *Trends Cardiovasc Med*. 2003;13(6):213-20.
262. Passerini AG, Polacek DC, Shi C, Francesco NM, Manduchi E, Grant GR, et al. Coexisting proinflammatory and antioxidative endothelial transcription profiles in a disturbed flow region of the adult porcine aorta. *Proc Natl Acad Sci U S A*. 2004;101(8):2482-7.
263. Aoki T, Yamamoto K, Fukuda M, Shimogonya Y, Fukuda S, Narumiya S. Sustained expression of MCP-1 by low wall shear stress loading concomitant with turbulent flow on endothelial cells of intracranial aneurysm. *Acta Neuropathol Commun*. 2016;4(1):48.
264. Coen M, Menegatti E, Salvi F, Mascoli F, Zamboni P, Gabbiani G, et al. Altered collagen expression in jugular veins in multiple sclerosis. *Cardiovasc Pathol*. 2013;22(1):33-8.
265. Jeannin P, Herbault N, Delneste Y, Magistrelli G, Lecoanet-Henchoz S, Caron G, et al. Human effector memory T cells express CD86: a functional role in naive T cell priming. *J Immunol*. 1999;162(4):2044-8.
266. Srinivasan S, Di Dario M, Russo A, Menon R, Brini E, Romeo M, et al. Dysregulation of MS risk genes and pathways at distinct stages of disease. *Neurol Neuroimmunol Neuroinflamm*. 2017;4(3):e337.
267. Iglesias AH, Camelo S, Hwang D, Villanueva R, Stephanopoulos G, Dangond F. Microarray detection of E2F pathway activation and other targets in multiple sclerosis peripheral blood mononuclear cells. *J Neuroimmunol*. 2004;150(1-2):163-77.

268. Salmi M, Jalkanen S. Vascular Adhesion Protein-1: A Cell Surface Amine Oxidase in Translation. *Antioxid Redox Signal*. 2017.
269. Elo P, Tadayon S, Liljenback H, Teuvo J, Kakela M, Koskensalo K, et al. Vascular adhesion protein-1 is actively involved in the development of inflammatory lesions in rat models of multiple sclerosis. *J Neuroinflammation*. 2018;15(1):128.
270. Airas L, Mikkola J, Vainio JM, Elovaara I, Smith DJ. Elevated serum soluble vascular adhesion protein-1 (VAP-1) in patients with active relapsing remitting multiple sclerosis. *J Neuroimmunol*. 2006;177(1-2):132-5.
271. Massaro AR. The role of NCAM in remyelination. *Neurol Sci*. 2002;22(6):429-35.
272. Thurston G, Rudge JS, Ioffe E, Zhou H, Ross L, Croll SD, et al. Angiopoietin-1 protects the adult vasculature against plasma leakage. *Nat Med*. 2000;6(4):460-3.
273. Lee SW, Won JY, Lee HY, Lee HJ, Youn SW, Lee JY, et al. Angiopoietin-1 protects heart against ischemia/reperfusion injury through VE-cadherin dephosphorylation and myocardial integrin-beta1/ERK/caspase-9 phosphorylation cascade. *Mol Med*. 2011;17(9-10):1095-106.
274. Wang B, Tian KW, Zhang F, Jiang H, Han S. Angiopoietin-1 and C16 Peptide Attenuate Vascular and Inflammatory Responses in Experimental Allergic Encephalomyelitis. *CNS Neurol Disord Drug Targets*. 2016;15(4):496-513.
275. Natynki M, Kangas J, Miinalainen I, Sormunen R, Pietila R, Soblet J, et al. Common and specific effects of TIE2 mutations causing venous malformations. *Hum Mol Genet*. 2015;24(22):6374-89.
276. Wong CK, Lit LC, Tam LS, Li EK, Lam CW. Aberrant production of soluble costimulatory molecules CTLA-4, CD28, CD80 and CD86 in patients with systemic lupus erythematosus. *Rheumatology (Oxford)*. 2005;44(8):989-94.
277. Vogel DY, Heijnen PD, Breur M, de Vries HE, Tool AT, Amor S, et al. Macrophages migrate in an activation-dependent manner to chemokines involved in neuroinflammation. *J Neuroinflammation*. 2014;11:23.
278. Boven LA, Van Meurs M, Van Zwam M, Wierenga-Wolf A, Hintzen RQ, Boot RG, et al. Myelin-laden macrophages are anti-inflammatory, consistent with foam cells in multiple sclerosis. *Brain*. 2006;129(Pt 2):517-26.
279. Vogel DY, Vereyken EJ, Glim JE, Heijnen PD, Moeton M, van der Valk P, et al. Macrophages in inflammatory multiple sclerosis lesions have an intermediate activation status. *J Neuroinflammation*. 2013;10:35.
280. Kuhlmann T, Ludwin S, Prat A, Antel J, Bruck W, Lassmann H. An updated histological classification system for multiple sclerosis lesions. *Acta Neuropathol*. 2017;133(1):13-24.
281. Zrzavy T, Hametner S, Wimmer I, Butovsky O, Weiner HL, Lassmann H. Loss of 'homeostatic' microglia and patterns of their activation in active multiple sclerosis. *Brain*. 2017;140(7):1900-13.
282. Porcheray F, Viaud S, Rimaniol AC, Leone C, Samah B, Dereuddre-Bosquet N, et al. Macrophage activation switching: an asset for the resolution of inflammation. *Clin Exp Immunol*. 2005;142(3):481-9.
283. Schutyser E, Richmond A, Van Damme J. Involvement of CC chemokine ligand 18 (CCL18) in normal and pathological processes. *J Leukoc Biol*. 2005;78(1):14-26.
284. Kodolja V, Muller C, Politz O, Hakij N, Orfanos CE, Goerdts S. Alternative macrophage activation-associated CC-chemokine-1, a novel structural homologue of macrophage inflammatory protein-1 alpha with a Th2-associated expression pattern. *J Immunol*. 1998;160(3):1411-8.
285. Schraufstatter IU, Zhao M, Khaldoyanidi SK, Discipio RG. The chemokine CCL18 causes maturation of cultured monocytes to macrophages in the M2 spectrum. *Immunology*. 2012;135(4):287-98.
286. Tarique AA, Logan J, Thomas E, Holt PG, Sly PD, Fantino E. Phenotypic, functional, and plasticity features of classical and alternatively activated human macrophages. *Am J Respir Cell Mol Biol*. 2015;53(5):676-88.
287. Simpson JE, Newcombe J, Cuzner ML, Woodroffe MN. Expression of monocyte chemoattractant protein-1 and other beta-chemokines by resident glia and inflammatory cells in multiple sclerosis lesions. *J Neuroimmunol*. 1998;84(2):238-49.
288. van Veen T, Nielsen J, Berkhof J, Barkhof F, Kamphorst W, Bo L, et al. CCL5 and CCR5 genotypes modify clinical, radiological and pathological features of multiple sclerosis. *J Neuroimmunol*. 2007;190(1-2):157-64.
289. Bartosik-Psujek H, Stelmasiak Z. The levels of chemokines CXCL8, CCL2 and CCL5 in multiple sclerosis patients are linked to the activity of the disease. *Eur J Neurol*. 2005;12(1):49-54.
290. Rentzos M, Nikolaou C, Rombos A, Evangelopoulos ME, Dimitrakopoulos A, Kararizou E, et al. Circulating interleukin-15 and RANTES chemokine in MS patients: effect of treatment with methylprednisolone in patients with relapse. *Neurol Res*. 2010;32(7):684-9.
291. Szczuczinski A, Losy J. CCL5, CXCL10 and CXCL11 chemokines in patients with active and stable relapsing-remitting multiple sclerosis. *Neuroimmunomodulation*. 2011;18(1):67-72.
292. Mori F, Nistico R, Nicoletti CG, Zagaglia S, Mandolesi G, Piccinin S, et al. RANTES correlates with inflammatory activity and synaptic excitability in multiple sclerosis. *Mult Scler*. 2016;22(11):1405-12.
293. von Hundelshausen P, Agten SM, Eckardt V, Blanchet X, Schmitt MM, Ippel H, et al. Chemokine interactome mapping enables tailored intervention in acute and chronic inflammation. *Sci Transl Med*. 2017;9(384).

294. Alegre ML, Frauwirth KA, Thompson CB. T-cell regulation by CD28 and CTLA-4. *Nat Rev Immunol.* 2001;1(3):220-8.
295. Jeannin P, Magistrelli G, Aubry JP, Caron G, Gauchat JF, Renno T, et al. Soluble CD86 is a costimulatory molecule for human T lymphocytes. *Immunity.* 2000;13(3):303-12.
296. Zivadinov R, Uher T, Hagemeyer J, Vaneckova M, Ramasamy DP, Tyblova M, et al. A serial 10-year follow-up study of brain atrophy and disability progression in RRMS patients. *Mult Scler.* 2016;22(13):1709-18.
297. Chenivresse C, Tscopoulos A. CCL18 - Beyond chemotaxis. *Cytokine.* 2018;109:52-6.
298. Hendrickx DAE, van Scheppingen J, van der Poel M, Bossers K, Schuurman KG, van Eden CG, et al. Gene Expression Profiling of Multiple Sclerosis Pathology Identifies Early Patterns of Demyelination Surrounding Chronic Active Lesions. *Front Immunol.* 2017;8:1810.
299. Frischer JM, Weigand SD, Guo Y, Kale N, Parisi JE, Pirko I, et al. Clinical and pathological insights into the dynamic nature of the white matter multiple sclerosis plaque. *Ann Neurol.* 2015;78(5):710-21.
300. Boot RG, Verhoek M, de Fost M, Hollak CE, Maas M, Bleijlevens B, et al. Marked elevation of the chemokine CCL18/PARC in Gaucher disease: a novel surrogate marker for assessing therapeutic intervention. *Blood.* 2004;103(1):33-9.
301. Huang D, Song SJ, Wu ZZ, Wu W, Cui XY, Chen JN, et al. Epstein-Barr Virus-Induced VEGF and GM-CSF Drive Nasopharyngeal Carcinoma Metastasis via Recruitment and Activation of Macrophages. *Cancer Res.* 2017;77(13):3591-604.
302. Zivadinov R, Cerza N, Hagemeyer J, Carl E, Badgett D, Ramasamy DP, et al. Humoral response to EBV is associated with cortical atrophy and lesion burden in patients with MS. *Neurol Neuroimmunol Neuroinflamm.* 2016;3(1):e190.
303. Losy J, Michalowska-Wender G, Kurdynska A, Wender M. CCL2 (MCP-1) and CCL5 (RANTES) levels in the peripheral blood of multiple sclerosis patients treated with Glatiramer Acetate (Copaxone). *Folia Neuropathol.* 2005;43(3):153-5.
304. Iarlori C, Reale M, Lugaresi A, De Luca G, Bonanni L, Di Iorio A, et al. RANTES production and expression is reduced in relapsing-remitting multiple sclerosis patients treated with interferon-beta-1b. *J Neuroimmunol.* 2000;107(1):100-7.
305. Hock BD, O'Donnell JL, Taylor K, Steinkasserer A, McKenzie JL, Rothwell AG, et al. Levels of the soluble forms of CD80, CD86, and CD83 are elevated in the synovial fluid of rheumatoid arthritis patients. *Tissue Antigens.* 2006;67(1):57-60.
306. Wiesemann E, Deb M, Trebst C, Hemmer B, Stangel M, Windhagen A. Effects of interferon-beta on co-signaling molecules: upregulation of CD40, CD86 and PD-L2 on monocytes in relation to clinical response to interferon-beta treatment in patients with multiple sclerosis. *Mult Scler.* 2008;14(2):166-76.
307. Ortiz GG, Pacheco-Moises FP, Macias-Islas MA, Flores-Alvarado LJ, Mireles-Ramirez MA, Gonzalez-Renovato ED, et al. Role of the blood-brain barrier in multiple sclerosis. *Arch Med Res.* 2014;45(8):687-97.
308. Rentzos M, Michalopoulou M, Nikolaou C, Cambouri C, Rombos A, Dimitrakopoulos A, et al. The role of soluble intercellular adhesion molecules in neurodegenerative disorders. *J Neurol Sci.* 2005;228(2):129-35.
309. Graber JJ, Dhib-Jalbut S. Biomarkers of disease activity in multiple sclerosis. *J Neurol Sci.* 2011;305(1-2):1-10.
310. Ma Q, Chen S, Klebe D, Zhang JH, Tang J. Adhesion molecules in CNS disorders: biomarker and therapeutic targets. *CNS Neurol Disord Drug Targets.* 2013;12(3):392-404.
311. Iwanowski P, Losy J. Immunological differences between classical phenotypes of multiple sclerosis. *J Neurol Sci.* 2015;349(1-2):10-4.
312. Duran I, Martinez-Caceres EM, Rio J, Barbera N, Marzo ME, Montalban X. Immunological profile of patients with primary progressive multiple sclerosis. Expression of adhesion molecules. *Brain.* 1999;122 (Pt 12):2297-307.
313. McDonnell GV, McMillan SA, Douglas JP, Droogan AG, Hawkins SA. Serum soluble adhesion molecules in multiple sclerosis: raised sVCAM-1, sICAM-1 and sE-selectin in primary progressive disease. *J Neurol.* 1999;246(2):87-92.
314. Baraczka K, Nekom K, Pozsonyi T, Jakab L, Szongoth M, Sesztak M. Concentration of soluble adhesion molecules (sVCAM-1, sICAM-1 and sL-selectin) in the cerebrospinal fluid and serum of patients with multiple sclerosis and systemic lupus erythematosus with central nervous involvement. *Neuroimmunomodulation.* 2001;9(1):49-54.
315. Kraus J, Engelhardt B, Chatzimanolis N, Bauer R, Tofighi J, Kuehne BS, et al. Cell surface bound and soluble adhesion molecules in CSF and blood in multiple sclerosis: correlation with MRI-measures of subclinical disease severity and activity. *J Neuroimmunol.* 2002;122(1-2):175-85.
316. Gnanapavan S, Giovannoni G. Neural cell adhesion molecules in brain plasticity and disease. *Mult Scler Relat Disord.* 2013;2(1):13-20.
317. Ksiazek-Winiarek DJ, Szpakowski P, Glabinski A. Neural Plasticity in Multiple Sclerosis: The Functional and Molecular Background. *Neural Plast.* 2015;2015:307175.
318. Hinkle CL, Diestel S, Lieberman J, Maness PF. Metalloprotease-induced ectodomain shedding of neural cell adhesion molecule (NCAM). *J Neurobiol.* 2006;66(12):1378-95.

319. Hubschmann MV, Skladchikova G, Bock E, Berezin V. Neural cell adhesion molecule function is regulated by metalloproteinase-mediated ectodomain release. *J Neurosci Res.* 2005;80(6):826-37.
320. Massaro AR, De Pascalis D, Carnevale A, Carbone G. The neural cell adhesion molecule (NCAM) present in the cerebrospinal fluid of multiple sclerosis patients is unsialylated. *Eur Rev Med Pharmacol Sci.* 2009;13(5):397-9.
321. Calabresi PA, Tranquill LR, Dambrosia JM, Stone LA, Maloni H, Bash CN, et al. Increases in soluble VCAM-1 correlate with a decrease in MRI lesions in multiple sclerosis treated with interferon beta-1b. *Ann Neurol.* 1997;41(5):669-74.
322. Giovannoni G, Miller DH, Losseff NA, Sailer M, Lewellyn-Smith N, Thompson AJ, et al. Serum inflammatory markers and clinical/MRI markers of disease progression in multiple sclerosis. *J Neurol.* 2001;248(6):487-95.
323. Rieckmann P, Kruse N, Nagelkerken L, Beckmann K, Miller D, Polman C, et al. Soluble vascular cell adhesion molecule (VCAM) is associated with treatment effects of interferon beta-1b in patients with secondary progressive multiple sclerosis. *J Neurol.* 2005;252(5):526-33.
324. Vollmer T, Signorovitch J, Huynh L, Galebach P, Kelley C, DiBernardo A, et al. The natural history of brain volume loss among patients with multiple sclerosis: a systematic literature review and meta-analysis. *J Neurol Sci.* 2015;357(1-2):8-18.
325. Niezgodna A, Michalak S, Losy J, Kalinowska-Lyszczarz A, Kozubski W. sNCAM as a specific marker of peripheral demyelination. *Immunol Lett.* 2017;185:93-7.
326. Sarova-Pinhas I, Achiron A, Gilad R, Lampl Y. Peripheral neuropathy in multiple sclerosis: a clinical and electrophysiologic study. *Acta Neurol Scand.* 1995;91(4):234-8.
327. Beiske AG, Pedersen ED, Czujko B, Myhr KM. Pain and sensory complaints in multiple sclerosis. *Eur J Neurol.* 2004;11(7):479-82.
328. Khan A, Kamran S, Ponirakis G, Akhtar N, Khan R, George P, et al. Peripheral neuropathy in patients with multiple sclerosis. *PLoS One.* 2018;13(3):e0193270.
329. Gnanapavan S, Grant D, Illes-Toth E, Lakdawala N, Keir G, Giovannoni G. Neural cell adhesion molecule--description of a CSF ELISA method and evidence of reduced levels in selected neurological disorders. *J Neuroimmunol.* 2010;225(1-2):118-22.
330. Gnanapavan S, Ho P, Heywood W, Jackson S, Grant D, Rantell K, et al. Progression in multiple sclerosis is associated with low endogenous NCAM. *J Neurochem.* 2013;125(5):766-73.
331. Dore-Duffy P, Newman W, Balabanov R, Lisak RP, Mainolfi E, Rothlein R, et al. Circulating, soluble adhesion proteins in cerebrospinal fluid and serum of patients with multiple sclerosis: correlation with clinical activity. *Ann Neurol.* 1995;37(1):55-62.
332. Rieckmann P, Altenhofen B, Riegel A, Baudewig J, Felgenhauer K. Soluble adhesion molecules (sVCAM-1 and sICAM-1) in cerebrospinal fluid and serum correlate with MRI activity in multiple sclerosis. *Ann Neurol.* 1997;41(3):326-33.
333. Zivadinov R. Can imaging techniques measure neuroprotection and remyelination in multiple sclerosis? *Neurology.* 2007;68(22 Suppl 3):S72-82; discussion S91-6.
334. Tanaka A, Ueno Y, Nakayama Y, Takano K, Takebayashi S. Small chronic hemorrhages and ischemic lesions in association with spontaneous intracerebral hematomas. *Stroke.* 1999;30(8):1637-42.
335. Wardlaw JM, Smith EE, Biessels GJ, Cordonnier C, Fazekas F, Frayne R, et al. Neuroimaging standards for research into small vessel disease and its contribution to ageing and neurodegeneration. *Lancet Neurol.* 2013;12(8):822-38.
336. Miwa K, Tanaka M, Okazaki S, Yagita Y, Sakaguchi M, Mochizuki H, et al. Multiple or mixed cerebral microbleeds and dementia in patients with vascular risk factors. *Neurology.* 2014;83(7):646-53.
337. Paciaroni M, Agnelli G, Ageno W, Caso V. Timing of anticoagulation therapy in patients with acute ischaemic stroke and atrial fibrillation. *Thromb Haemost.* 2016;116(3):410-6.
338. Wilson D, Ambler G, Shakeshaft C, Brown MM, Charidimou A, Al-Shahi Salman R, et al. Cerebral microbleeds and intracranial haemorrhage risk in patients anticoagulated for atrial fibrillation after acute ischaemic stroke or transient ischaemic attack (CROMIS-2): a multicentre observational cohort study. *Lancet Neurol.* 2018;17(6):539-47.
339. Frohman EM, Racke MK, Raine CS. Multiple sclerosis--the plaque and its pathogenesis. *N Engl J Med.* 2006;354(9):942-55.
340. Hoppe B. Fibrinogen and factor XIII at the intersection of coagulation, fibrinolysis and inflammation. *Thromb Haemost.* 2014;112(4):649-58.
341. Lopez ML, Bruges G, Crespo G, Salazar V, Deglesne PA, Schneider H, et al. Thrombin selectively induces transcription of genes in human monocytes involved in inflammation and wound healing. *Thromb Haemost.* 2014;112(5):992-1001.
342. Wang S, Reeves B, Pawlinski R. Astrocyte tissue factor controls CNS hemostasis and autoimmune inflammation. *Thromb Res.* 2016;141 Suppl 2:S65-7.
343. Salmi M, Jalkanen S. A 90-kilodalton endothelial cell molecule mediating lymphocyte binding in humans. *Science.* 1992;257(5075):1407-9.
344. Stolen CM, Yegutkin GG, Kurkijarvi R, Bono P, Alitalo K, Jalkanen S. Origins of serum semicarbazide-sensitive amine oxidase. *Circ Res.* 2004;95(1):50-7.

345. Hernandez-Guillamon M, Sole M, Delgado P, Garcia-Bonilla L, Giralt D, Boada C, et al. VAP-1/SSAO plasma activity and brain expression in human hemorrhagic stroke. *Cerebrovasc Dis*. 2012;33(1):55-63.
346. Hernandez-Guillamon M, Garcia-Bonilla L, Sole M, Sosti V, Pares M, Campos M, et al. Plasma VAP-1/SSAO activity predicts intracranial hemorrhages and adverse neurological outcome after tissue plasminogen activator treatment in stroke. *Stroke*. 2010;41(7):1528-35.
347. Ma Q, Manaenko A, Khatibi NH, Chen W, Zhang JH, Tang J. Vascular adhesion protein-1 inhibition provides antiinflammatory protection after an intracerebral hemorrhagic stroke in mice. *J Cereb Blood Flow Metab*. 2011;31(3):881-93.
348. Xu H, Testai FD, Valyi-Nagy T, M NP, Zhai F, Nanegrungsunk D, et al. VAP-1 blockade prevents subarachnoid hemorrhage-associated cerebrovascular dilating dysfunction via repression of a neutrophil recruitment-related mechanism. *Brain Res*. 2015;1603:141-9.
349. Airas L, Lindsberg PJ, Karjalainen-Lindsberg ML, Mononen I, Kotisaari K, Smith DJ, et al. Vascular adhesion protein-1 in human ischaemic stroke. *Neuropathol Appl Neurobiol*. 2008;34(4):394-402.
350. Jalkanen S, Karikoski M, Mercier N, Koskinen K, Henttinen T, Elima K, et al. The oxidase activity of vascular adhesion protein-1 (VAP-1) induces endothelial E- and P-selectins and leukocyte binding. *Blood*. 2007;110(6):1864-70.
351. Ghasemzadeh M, Hosseini E. Intravascular leukocyte migration through platelet thrombi: directing leukocytes to sites of vascular injury. *Thromb Haemost*. 2015;113(6):1224-35.
352. Morandi E, Tarlinton RE, Gran B. Multiple Sclerosis between Genetics and Infections: Human Endogenous Retroviruses in Monocytes and Macrophages. *Front Immunol*. 2015;6:647.
353. Bashinskaya VV, Kulakova OG, Boyko AN, Favorov AV, Favorova OO. A review of genome-wide association studies for multiple sclerosis: classical and hypothesis-driven approaches. *Hum Genet*. 2015;134(11-12):1143-62.
354. Mitrovic M, Patsopoulos N, Beecham A, Dankowski T, Goris A, Dubois B, et al. Low frequency and rare coding variation contributes to multiple sclerosis risk. *bioRxiv*. 2018.
355. Kempainen AK, Baker A, Liao W, Fiddes B, Jones J, Compston A, et al. Exome sequencing in single cells from the cerebrospinal fluid in multiple sclerosis. *Mult Scler*. 2014;20(12):1564-8.
356. Sadovnick AD, Traboulsee AL, Zhao Y, Bernales CQ, Encarnacion M, Ross JP, et al. Genetic modifiers of multiple sclerosis progression, severity and onset. *Clin Immunol*. 2017;180:100-5.
357. Maver A, Lavtar P, Ristic S, Stopinsek S, Simcic S, Hocesvar K, et al. Identification of rare genetic variation of NLRP1 gene in familial multiple sclerosis. *Sci Rep*. 2017;7(1):3715.
358. Garcia-Rosa S, de Amorim MG, Valieris R, Marques VD, Lorenzi JCC, Toller VB, et al. Exome sequencing of multiple-sclerosis patients and their unaffected first-degree relatives. *BMC Res Notes*. 2017;10(1):735.
359. Dymant DA, Cader MZ, Chao MJ, Lincoln MR, Morrison KM, Disanto G, et al. Exome sequencing identifies a novel multiple sclerosis susceptibility variant in the TYK2 gene. *Neurology*. 2012;79(5):406-11.
360. Mescheriakova JY, Verkerk AJ, Amin N, Uitterlinden AG, van Duijn CM, Hintzen RQ. Linkage analysis and whole exome sequencing identify a novel candidate gene in a Dutch multiple sclerosis family. *Mult Scler*. 2018;1352458518777202.
361. Bernales CQ, Encarnacion M, Criscuoli MG, Yee IM, Traboulsee AL, Sadovnick AD, et al. Analysis of NOD-like receptor NLRP1 in multiple sclerosis families. *Immunogenetics*. 2018;70(3):205-7.
362. Ramagopalan SV, Dymant DA, Cader MZ, Morrison KM, Disanto G, Morahan JM, et al. Rare variants in the CYP27B1 gene are associated with multiple sclerosis. *Ann Neurol*. 2011;70(6):881-6.
363. Wang Z, Sadovnick AD, Traboulsee AL, Ross JP, Bernales CQ, Encarnacion M, et al. Nuclear Receptor NR1H3 in Familial Multiple Sclerosis. *Neuron*. 2016;90(5):948-54.
364. Ban M, Caillier S, Mero IL, Myhr KM, Celius EG, Aarseth J, et al. No evidence of association between mutant alleles of the CYP27B1 gene and multiple sclerosis. *Ann Neurol*. 2013;73(3):430-2.
365. International Multiple Sclerosis Genetics Consortium. Electronic address cbo, International Multiple Sclerosis Genetics C. NR1H3 p.Arg415Gln Is Not Associated to Multiple Sclerosis Risk. *Neuron*. 2016;92(2):333-5.
366. Minikel EV, MacArthur DG. Publicly Available Data Provide Evidence against NR1H3 R415Q Causing Multiple Sclerosis. *Neuron*. 2016;92(2):336-8.
367. Wang X, Biernacka JM. Assessing the effects of multiple markers in genetic association studies. *Front Genet*. 2015;6:66.
368. Granieri E, De Mattia G, Laudisi M, Govoni V, Castellazzi M, Caniatti L, et al. Multiple Sclerosis in Italy: A 40-Year Follow-Up of the Prevalence in Ferrara. *Neuroepidemiology*. 2018;51(3-4):182-9.
369. Gemmati D, Zeri G, Orioli E, De Gaetano FE, Salvi F, Bartolomei I, et al. Polymorphisms in the genes coding for iron binding and transporting proteins are associated with disability, severity, and early progression in multiple sclerosis. *BMC Med Genet*. 2012;13:70.
370. Manousaki D, Dudding T, Haworth S, Hsu YH, Liu CT, Medina-Gomez C, et al. Low-Frequency Synonymous Coding Variation in CYP2R1 Has Large Effects on Vitamin D Levels and Risk of Multiple Sclerosis. *Am J Hum Genet*. 2017;101(2):227-38.

371. International Multiple Sclerosis Genetics C, Wellcome Trust Case Control C, Sawcer S, Hellenthal G, Pirinen M, Spencer CC, et al. Genetic risk and a primary role for cell-mediated immune mechanisms in multiple sclerosis. *Nature*. 2011;476(7359):214-9.
372. International Multiple Sclerosis Genetics C, Beecham AH, Patsopoulos NA, Xifara DK, Davis MF, Kempainen A, et al. Analysis of immune-related loci identifies 48 new susceptibility variants for multiple sclerosis. *Nat Genet*. 2013;45(11):1353-60.
373. Andlauer TF, Buck D, Antony G, Bayas A, Bechmann L, Berthele A, et al. Novel multiple sclerosis susceptibility loci implicated in epigenetic regulation. *Sci Adv*. 2016;2(6):e1501678.
374. Zhou Y, Zhu G, Charlesworth JC, Simpson S, Jr., Rubicz R, Goring HH, et al. Genetic loci for Epstein-Barr virus nuclear antigen-1 are associated with risk of multiple sclerosis. *Mult Scler*. 2016;22(13):1655-64.
375. Comabella M, Craig DW, Camina-Tato M, Morcillo C, Lopez C, Navarro A, et al. Identification of a novel risk locus for multiple sclerosis at 13q31.3 by a pooled genome-wide scan of 500,000 single nucleotide polymorphisms. *PLoS One*. 2008;3(10):e3490.
376. Steri M, Orru V, Idda ML, Pitzalis M, Pala M, Zara I, et al. Overexpression of the Cytokine BAFF and Autoimmunity Risk. *N Engl J Med*. 2017;376(17):1615-26.
377. De Jager PL, Jia X, Wang J, de Bakker PI, Ottoboni L, Aggarwal NT, et al. Meta-analysis of genome scans and replication identify CD6, IRF8 and TNFRSF1A as new multiple sclerosis susceptibility loci. *Nat Genet*. 2009;41(7):776-82.
378. International Multiple Sclerosis Genetics C, Hafler DA, Compston A, Sawcer S, Lander ES, Daly MJ, et al. Risk alleles for multiple sclerosis identified by a genomewide study. *N Engl J Med*. 2007;357(9):851-62.
379. International Multiple Sclerosis Genetics C, Lill CM, Schjeide BM, Graetz C, Ban M, Alcina A, et al. MANBA, CXCR5, SOX8, RPS6KB1 and ZBTB46 are genetic risk loci for multiple sclerosis. *Brain*. 2013;136(Pt 6):1778-82.
380. Lill CM, Luessi F, Alcina A, Sokolova EA, Ugidos N, de la Hera B, et al. Genome-wide significant association with seven novel multiple sclerosis risk loci. *J Med Genet*. 2015;52(12):848-55.
381. Australia, New Zealand Multiple Sclerosis Genetics C. Genome-wide association study identifies new multiple sclerosis susceptibility loci on chromosomes 12 and 20. *Nat Genet*. 2009;41(7):824-8.
382. Zhou Y, Graves JS, Simpson S, Jr., Charlesworth JC, Mei IV, Waubant E, et al. Genetic variation in the gene LRP2 increases relapse risk in multiple sclerosis. *J Neurol Neurosurg Psychiatry*. 2017;88(10):864-8.
383. Jakkula E, Leppä V, Sulonen AM, Varilo T, Kallio S, Kempainen A, et al. Genome-wide association study in a high-risk isolate for multiple sclerosis reveals associated variants in STAT3 gene. *Am J Hum Genet*. 2010;86(2):285-91.
384. Patsopoulos NA, Bayer Pharma MSGWG, Steering Committees of Studies Evaluating I-b, a CCRA, Consortium AN, GeneMsa, et al. Genome-wide meta-analysis identifies novel multiple sclerosis susceptibility loci. *Ann Neurol*. 2011;70(6):897-912.
385. Weckx S, Del-Favero J, Rademakers R, Claes L, Cruts M, De Jonghe P, et al. novoSNP, a novel computational tool for sequence variation discovery. *Genome Res*. 2005;15(3):436-42.
386. Bezzini D, Policardo L, Meucci G, Ulivelli M, Bartalini S, Profili F, et al. Prevalence of Multiple Sclerosis in Tuscany (Central Italy): A Study Based on Validated Administrative Data. *Neuroepidemiology*. 2016;46(1):37-42.
387. Ottone T, Cicconi L, Hasan SK, Lavorgna S, Divona M, Voso MT, et al. Comparative molecular analysis of therapy-related and de novo acute promyelocytic leukemia. *Leuk Res*. 2012;36(4):474-8.
388. Wang XX, Chen T. Meta-analysis of the association of IL2RA polymorphisms rs2104286 and rs12722489 with multiple sclerosis risk. *Immunol Invest*. 2018;47(5):431-42.
389. Matiello M, Weinshenker BG, Atkinson EJ, Schaefer-Klein J, Kantarci OH. Association of IL2RA polymorphisms with susceptibility to multiple sclerosis is not explained by missense mutations in IL2RA. *Mult Scler*. 2011;17(5):634-6.
390. Maier LM, Anderson DE, Severson CA, Baecher-Allan C, Healy B, Liu DV, et al. Soluble IL-2RA levels in multiple sclerosis subjects and the effect of soluble IL-2RA on immune responses. *J Immunol*. 2009;182(3):1541-7.
391. Techasintana P, Ellis JS, Glascock J, Gubin MM, Ridenhour SE, Magee JD, et al. The RNA-Binding Protein HuR Posttranscriptionally Regulates IL-2 Homeostasis and CD4(+) Th2 Differentiation. *Immunohorizons*. 2017;1(6):109-23.
392. Bielekova B. Daclizumab Therapy for Multiple Sclerosis. *Cold Spring Harb Perspect Med*. 2018.
393. Zhang M, Ferrari R, Tartaglia MC, Keith J, Surace EI, Wolf U, et al. A C6orf10/LOC101929163 locus is associated with age of onset in C9orf72 carriers. *Brain*. 2018;141(10):2895-907.
394. Paap BK, Hundeshagen A, Hecker M, Zettl UK. An inventory of short term and long term changes in gene expression under interferon beta treatment of relapsing remitting MS patients. *Curr Pharm Des*. 2012;18(29):4475-84.
395. Ma X, Zhou J, Zhong Y, Jiang L, Mu P, Li Y, et al. Expression, regulation and function of microRNAs in multiple sclerosis. *Int J Med Sci*. 2014;11(8):810-8.

396. Cordiglieri C, Baggi F, Bernasconi P, Kapetis D, Faggiani E, Consonni A, et al. Identification of a gene expression signature in peripheral blood of multiple sclerosis patients treated with disease-modifying therapies. *Clin Immunol*. 2016;173:133-46.
397. Maroney SA, Ellery PE, Wood JP, Ferrel JP, Martinez ND, Mast AE. Comparison of the inhibitory activities of human tissue factor pathway inhibitor (TFPI)alpha and TFPIbeta. *J Thromb Haemost*. 2013;11(5):911-8.
398. Rochfort KD, Cummins PM. Thrombomodulin regulation in human brain microvascular endothelial cells in vitro: role of cytokines and shear stress. *Microvasc Res*. 2015;97:1-5.
399. Bjorkqvist J, Nickel KF, Stavrou E, Renne T. In vivo activation and functions of the protease factor XII. *Thromb Haemost*. 2014;112(5):868-75.
400. Taylor KR, Gallo RL. Glycosaminoglycans and their proteoglycans: host-associated molecular patterns for initiation and modulation of inflammation. *FASEB J*. 2006;20(1):9-22.
401. Smith PD, Coulson-Thomas VJ, Foscarin S, Kwok JC, Fawcett JW. "GAG-ing with the neuron": The role of glycosaminoglycan patterning in the central nervous system. *Exp Neurol*. 2015;274(Pt B):100-14.
402. Marchetti G, Ziliotto N, Meneghetti S, Baroni M, Lunghi B, Menegatti E, et al. Changes in expression profiles of internal jugular vein wall and plasma protein levels in multiple sclerosis. *Mol Med*. 2018;24(1):42.
403. Ziliotto N, Bernardi F, Jakimovski D, Baroni M, Bergsland N, Ramasamy DP, et al. Increased CCL18 plasma levels are associated with neurodegenerative MRI outcomes in multiple sclerosis patients. *Mult Scler Relat Disord*. 2018;25:37-42.
404. Lin L, Chen YS, Yao YD, Chen JQ, Chen JN, Huang SY, et al. CCL18 from tumor-associated macrophages promotes angiogenesis in breast cancer. *Oncotarget*. 2015;6(33):34758-73.
405. Liang WG, Ren M, Zhao F, Tang WJ. Structures of human CCL18, CCL3, and CCL4 reveal molecular determinants for quaternary structures and sensitivity to insulin-degrading enzyme. *J Mol Biol*. 2015;427(6 Pt B):1345-58.
406. Ziliotto N, Zivadinov R, Jakimovski D, Baroni M, Tisato V, Secchiero P, et al. Plasma levels of soluble NCAM in multiple sclerosis. *J Neurol Sci*. 2018;396:36-41.
407. Homrich M, Gotthard I, Wobst H, Diestel S. Cell Adhesion Molecules and Ubiquitination-Functions and Significance. *Biology (Basel)*. 2015;5(1).
408. Dietrich JB. The adhesion molecule ICAM-1 and its regulation in relation with the blood-brain barrier. *J Neuroimmunol*. 2002;128(1-2):58-68.

RINGRAZIAMENTI

Questa tesi di dottorato coincide per me con il raggiungimento di uno dei più importanti traguardi e contemporaneamente punti di partenza della mia vita. E' l'espressione di un'esperienza umana e scientifica supportata dall'incontro con tante persone e permanenza in luoghi speciali.

A conclusione, sento di ringraziare tutte le persone che in modi diversi, mi sono state vicine o sono entrate a contatto con me durante questo periodo di dottorato, che mi hanno sostenuto e aiutato a crescere sia dal punto di vista professionale che umano.

Innanzitutto vorrei esprimere la mia immensa gratitudine al Relatore e Correlatrice di questa tesi, il Prof. Bernardi e la Prof.ssa Marchetti, che mi hanno dato la possibilità di intraprendere questo dottorato e hanno avuto un peso determinante nel conseguimento di questo risultato. Un ringraziamento sentito al Prof. Bernardi, che oltre ad esser stato una guida paterna, competente e solerte per la mia crescita formativa, è stato di esempio di inesauribile energia, buon umore, diplomazia e spirito critico.

Grazie ad entrambi i Professori per aver creduto nelle mie potenzialità, dandomi l'opportunità di sviluppare un filone di ricerca nuovo, accompagnandomi passo a passo in questo percorso che ha trovato sviluppo in diverse attività e progetti, permettendomi di lavorare su un argomento decisamente stimolante, in un ambiente sereno, accogliente e funzionale. Grazie per i confronti costruttivi, gli stimoli, la pazienza, oltre che per la Vostra incredibile disponibilità mai venuta meno per l'intero arco di questo dottorato.

Spero che questo mio traguardo raggiunto, possa essere un motivo di orgoglio anche per Voi.

Ringrazio i Revisori della mia tesi di dottorato, la Prof.ssa Castoldi e la Prof.ssa Casari, per la cura con cui hanno esaminato il lavoro e per i suggerimenti ricevuti.

Derisero ringraziare coloro che hanno contribuito finanziando la ricerca per la sclerosi multipla e tutti i co-autori dei lavori pubblicati o ancora in revisione, contenuti in questa tesi. Vi sono riconoscente per la Vostra collaborazione, senza la quale questo lavoro di ricerca non sarebbe stato possibile. In particolare, un grazie speciale al mio supervisore presso il BNAC, il Prof. Zivadinov a cui devo una fantastica collaborazione scientifica che mi ha permesso di progredire nell'attività di ricerca sulla sclerosi multipla. Un grazie per tutte le opportunità, per l'occasione di mettermi in gioco e la spinta al superamento dei miei limiti che mi ha dato. Il lavoro nel suo team mi ha inoltre permesso di conoscere persone a cui sono particolarmente affezionata e che spero nonostante la distanza possano rivelarsi amicizie durature nel tempo.

Ringrazio inoltre il Prof. Schurgers e tutti i colleghi che ho incontrato durante il mio tirocinio presso il CARIM.

Un ringraziamento a tutti i componenti del mio laboratorio (Mirko, Alessio, Dario, Marcello, Mattia, Silvia P., Silvia L., Barbara e Paolo) per avermi fatto sentire parte di un gruppo di ricerca attivo, simpatico e dinamico.

Un grazie al Prof. Rispoli per esser stato sempre un punto di riferimento esterno.

Un ringraziamento affettuoso alla mia famiglia, con particolare rilievo a mia mamma che ogni giorno ha condiviso con me gioie, tristezze, sacrifici e successi. Un sincero grazie anche al suo compagno Yoris che insieme a lei è stato parte di questa condivisione.

Un grazie speciale agli amici di sempre, Marcella e Gianmaria, per non avermi mai abbandonata e per aver capito i miei silenzi che purtroppo a volte la distanza comporta.

Un grazie di cuore a Diana, Peppino, Luca, Sandra e alla Dr.ssa Ottobre per l'affetto e il sostegno che mi hanno dimostrato nei periodi più tristi, difficili, o dolorosi contrassegnati da un grande vuoto.

Ringrazio tutti i dottorandi, post-doc, specializzandi di medicina e gli amici professori italo-americani, conosciuti in questi anni che hanno contribuito a rendere piacevole questo percorso di dottorato e che, per motivi di spazio, non posso citare personalmente. Vi sono grata per la stima e l'amicizia che mi avete dimostrato.

Ringrazio tutti coloro che hanno condiviso con me, in questi anni di dottorato, momenti importanti della mia vita e che ci saranno ancora una volta il giorno del dottorato.

E infine ringrazio, soprattutto, me stessa per la determinazione, l'impegno e i sacrifici per raggiungere questo traguardo. Con l'augurio di non smettere mai di seguire la vocazione per la ricerca e lottare per quello in cui credo e per i miei sogni.